



Mass Production Cost Estimation of Direct H₂ PEM Fuel Cell Systems for Transportation Applications: 2013 Update

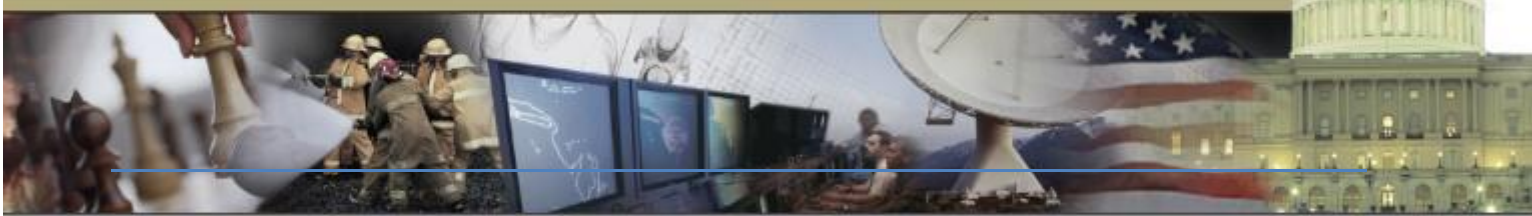
January 2014

Prepared By:

Brian D. James

Jennie M. Moton

Whitney G. Colella



CREATIVE
SOLUTIONS
FOR
TOMORROW'S
CHALLENGES

STRATEGIC ANALYSIS INC

Sponsorship and Acknowledgements

This material is based upon work supported by the Department of Energy under Award Number DE-EE0005236. The authors wish to thank Dr. Dimitrios Papageorgopoulos and Mr. Jason Marcinkoski of DOE's Office of Energy Efficiency and Renewable Energy (EERE) Fuel Cell Technologies (FCT) Program for their technical and programmatic contributions and leadership.

Disclaimer

This report was prepared as an account of work sponsored by an agency of the United States Government. Neither the United States Government nor any agency thereof, nor any of their employees, makes any warranty, express or implied, or assumes any legal liability or responsibility for the accuracy, completeness, or usefulness of any information, apparatus, product, or process disclosed, or represents that its use would not infringe privately owned rights. Reference herein to any specific commercial product, process, or service by trade name, trademark, manufacturer, or otherwise does not necessarily constitute or imply its endorsement, recommendation, or favoring by the United States Government or any agency thereof. The views and opinions of authors expressed herein do not necessarily state or reflect those of the United States Government or any agency thereof.

Authors Contact Information

Strategic Analysis Inc. may be contacted at:

Strategic Analysis Inc.
4075 Wilson Blvd, Suite 200
Arlington VA 22203
(703) 527-5410
www.sainc.com

The authors may be contacted at:

Brian D. James, BJames@sainc.com (703) 778-7114

Table of Abbreviations

ANL	Argonne National Laboratory
APTA	American Public Transportation Association
atm	atmospheres
BDI	Boothroyd Dewhurst Incorporated
BOL	beginning of life
BOM	bill of materials
BOP	balance of plant
C_{air}	Air Management System Cost (Simplified Cost Model)
C_{BOP}	Additional Balance of Plant Cost (Simplified Cost Model)
CC	capital costs
CCM	catalyst coated membrane
CEM	integrated compressor-expander-motor unit (used for air compression and exhaust gas expansion)
C_{Fuel}	Fuel Management System Cost (Simplified Cost Model)
C_{Humid}	Humidification Management System Cost (Simplified Cost Model)
CM	compressor motor
CNG	compressed natural gas
C_{stack}	Total Fuel Cell Stack Cost (Simplified Cost Model)
$C_{thermal}$	Thermal Management System Cost (Simplified Cost Model)
DFMA TM	design for manufacturing and assembly
DOE	Department of Energy
DOT	Department of Transportation
DTI	Directed Technologies Incorporated
EEC	electronic engine controller
EERE	DOE Office of Energy Efficiency and Renewable Energy
EOL	end of life
ePTFE	expanded polytetrafluoroethylene
FCT	EERE Fuel Cell Technologies Program
FCV	fuel cell vehicle
Ford	Ford Motor Company Inc.
FTA	Federal Transit Administration
FUDS	Federal Urban Driving Schedule
G&A	general and administrative
GDL	gas diffusion layer
GM	General Motors Inc.
H ₂	hydrogen
HFPO	hexafluoropropylene oxide
HDPE	high density polyethylene

ID	inner diameter
IR/DC	infra-red/direct-current
kN	kilo-Newtons
kW	kilowatts
kW _{e_net}	kilowatts of net electric power
LT	low temperature
MBRC	miles between road calls
MEA	membrane electrode assembly
mgde	miles per gallon of diesel equivalent
mpgge	miles per gallon of gasoline equivalent
mph	miles per hour
NREL	National Renewable Energy Laboratory
NSTF	nano-structured thin-film (catalysts)
OD	outer diameter
ODS	optical detection system
OPCO	over-pressure, cut-off (valve)
PEM	proton exchange membrane
PET	polyethylene terephthalate
Pt	platinum
PtCoMn	platinum-cobalt-manganese
QC	quality control
Q/ΔT	heat duty divided by delta temperature
R&D	research and development
RFI	request for information
SA	Strategic Analysis, Inc.
TIM	traction inverter module
TVS	Twin Vortices Series (of Eaton Corp. compressors)
V	volt

Foreword

Energy security is fundamental to the mission of the U.S. Department of Energy (DOE) and hydrogen fuel cell vehicles have the potential to eliminate the need for oil in the transportation sector. Fuel cell vehicles¹ can operate on hydrogen, which can be produced domestically, emitting less greenhouse gasses and pollutants than conventional internal combustion engine (ICE), advanced ICE, hybrid, or plug-in hybrid vehicles that are tethered to petroleum fuels. Transitioning from standard ICE vehicles to hydrogen-fueled fuel cell vehicles (FCVs) could greatly reduce greenhouse gas emissions, air pollution emissions, and ambient air pollution, especially if the hydrogen fuel is derived from wind-powered electrolysis or steam reforming of natural gas.^{2,3} A diverse portfolio of energy sources can be used to produce hydrogen, including nuclear, coal, natural gas, geothermal, wind, hydroelectric, solar, and biomass. Thus, fuel cell vehicles offer an environmentally clean and energy-secure pathway for transportation.

This research evaluates the cost of manufacturing transportation fuel cell systems (FCSs) based on low temperature (LT) proton exchange membrane (PEM) FCS technology. Fuel cell systems will have to be cost-competitive with conventional and advanced vehicle technologies to gain the market-share required to influence the environment and reduce petroleum use. Since the light duty vehicle sector consumes the most oil, primarily due to the vast number of vehicles it represents, the DOE has established detailed cost targets for automotive fuel cell systems and components. To help achieve these cost targets, the DOE has devoted research funding to analyze and track the cost of automotive fuel cell systems as progress is made in fuel cell technology. The purpose of these cost analyses is to identify significant cost drivers so that R&D resources can be most effectively allocated toward their reduction. The analyses are annually updated to track technical progress in terms of cost and to indicate how much a typical automotive fuel cell system would cost if produced in large quantities (up to 500,000 vehicles per year).

Bus applications represent another area where fuel cell systems have an opportunity to make a national impact on oil consumption and air quality. Consequently, beginning with year 2012, annually updated cost analyses have been conducted for PEM fuel cell passenger buses as well. Fuel cell systems for light duty automotive and buses share many similarities and indeed may even utilize identical stack hardware. Thus the analysis of bus fuel cell power plants is a logical extension of the light duty automotive power system analysis. Primary differences between the two applications include the installed power required (80 kilowatts of net electric power (kW_{e_net})⁴ for automotive vs. $\sim 160\text{kW}_{e_net}$ for

¹ Honda FCX Clarity fuel cell vehicle: <http://automobiles.honda.com/fcx-clarity/>; Toyota fuel cell hybrid vehicles: http://www.toyota.com/about/environment/innovation/advanced_vehicle_technology/FCHV.html

² Jacobson, M.Z., Colella, W.G., Golden, D.M. "Cleaning the Air and Improving Health with Hydrogen Fuel Cell Vehicles," *Science*, 308, 1901-05, June 2005.

³ Colella, W.G., Jacobson, M.Z., Golden, D.M. "Switching to a U.S. Hydrogen Fuel Cell Vehicle Fleet: The Resultant Change in Energy Use, Emissions, and Global Warming Gases," *Journal of Power Sources*, 150, 150-181, Oct. 2005.

⁴ Unless otherwise stated, all references to vehicle power and cost ($\$/\text{kW}$) are in terms of kW_{e_net} .

a 40 foot transit bus), desired power plant durability (nominally 5,000 hours lifetime for automotive vs. 25,000 hours lifetime for buses), and annual manufacturing rate (up to 500,000 systems/year for an individual top selling automobile model vs. ~4,000 systems/year for total transit bus sales in the US)⁵.

The capacity to produce fuel cell systems at high manufacturing rates does not yet exist, and significant investments will have to be made in manufacturing development and facilities in order to enable it. Once the investment decisions are made, it will take several years to develop and fabricate the necessary manufacturing facilities. Furthermore, the supply chain will need to develop which requires negotiation between suppliers and system developers, with details rarely made public. For these reasons, the DOE has consciously decided not to analyze supply chain scenarios at this point, instead opting to concentrate its resources on solidifying the tangible core of the analysis, i.e. the manufacturing and materials costs.

The DOE uses these analyses as tools for R&D management and tracking technological progress in terms of cost. Consequently, non-technical variables are held constant to elucidate the effects of the technical variables. For example, the cost of platinum is typically held constant to insulate the study from unpredictable and erratic platinum price fluctuations. Sensitivity analyses are conducted to explore the effects of non-technical parameters.

To maximize the benefit of our work to the fuel cell community, Strategic Analysis Inc. (SA) strives to make each analysis as transparent as possible. The transparency of the assumptions and methodology serve to strengthen the validity of the analysis. We hope that these analyses have been and will continue to be valuable tools to the hydrogen and fuel cell R&D community.

⁵ Total buses sold per year from American Public Transportation Association 2012 Public Transportation Fact Book, Appendix A Historical Tables, page 25, <http://www.apta.com/resources/statistics/Documents/FactBook/2012-Fact-Book-Appendix-A.pdf>. Note that this figure includes all types of transit buses: annual sales of 40' transit buses, as are of interest in this report, would be considerably lower.

Table of Contents

1	Overview	11
2	Project Approach	13
2.1	Integrated Performance and Cost Estimation	14
2.2	Cost Analysis Methodology.....	15
2.2.1	Stage 1: System Conceptual Design	17
2.2.2	Stage 2: System Physical Design	17
2.2.3	Stage 3: Cost Modeling	17
2.2.4	Stage 4: Continuous Improvement to Reduce Cost.....	19
2.3	Vertical Integration and Markups	19
3	Overview of the Bus System	23
4	System Schematics and Bills of Materials.....	26
4.1	2012 Automotive System Schematic	26
4.2	2012 Bus System Schematic.....	27
4.3	2013 Auto System Schematic.....	28
4.4	2013 Bus System Schematic.....	29
5	System Cost Summaries.....	30
5.1	Cost Summary of the 2013 Automotive System.....	31
5.2	Cost Summary of the 2013 Bus System	32
6	Automotive Power System Changes and Analysis since the 2012 Report.....	35
6.1	2013 ANL Polarization Model	36
6.1.1	Increase in the Stack Upper Pressure Limit	36
6.1.2	Temperature as an Independent Variable	36
6.1.3	2013 Polarization Model and Resulting Polarization Curves	37
6.2	Increase in Platinum Price.....	37
6.3	Imposition of $Q/\Delta T$ Radiator Constraint	37
6.4	Optimization of Stack Operating Conditions for Minimum System Cost	38
6.5	Plate Frame Humidifier	41
6.6	Low-Cost Gore MEA Manufacturing Process.....	42
6.7	Eaton-style Multi-Lobe Air Compressor-Expander-Motor (CEM) Unit.....	46
6.7.1	Design and Operational Overview	46
6.7.2	CEM Manufacturing Process.....	49

6.8	Revised Quality Control Procedures	54
6.9	Updated Material Prices	57
6.10	Alignment with DOE CEM Status Efficiencies	58
6.11	Update of Sizing and Cost Analysis Methodology for the Low Temperature Coolant Loop	58
7	Description of 2013 Automotive Fuel Cell System Manufacturing Assumptions and Cost Results ...	60
7.1	Fuel Cell Stack Materials, Manufacturing, and Assembly	60
7.1.1	Bipolar Plates	60
7.1.2	Membrane	66
7.1.3	Nanostructured Thin Film (NSTF) Catalyst Application.....	73
7.1.4	Catalyst Cost.....	77
7.1.5	Gas Diffusion Layer	78
7.1.6	MEA Sub-Gaskets	79
7.1.7	Subgasket Formation	83
7.1.8	MEA Crimping, Cutting, and Slitting.....	85
7.1.9	End Plates.....	87
7.1.10	Current Collectors	90
7.1.11	Coolant Gaskets/Laser-welding	91
7.1.12	End Gaskets.....	93
7.1.13	Stack Compression.....	96
7.1.14	Stack Assembly.....	96
7.1.15	Stack Housing.....	98
7.1.16	Stack Conditioning and Testing.....	99
7.2	Balance of Plant (BOP)	101
7.2.1	Air Loop	101
7.2.2	Humidifier & Water Recovery Loop	106
7.2.3	Coolant Loops.....	125
7.2.4	Fuel Loop.....	127
7.2.5	System Controller.....	128
7.2.6	Sensors	130
7.2.7	Miscellaneous BOP.....	132
7.2.8	System Assembly.....	136
7.2.9	System Testing	137

7.2.10	Cost Contingency	137
8	Bus Fuel Cell Power System	138
8.1	Bus Power System Overview and Comparison with Automotive Power System	138
8.2	Bus System Performance Parameters.....	139
8.2.1	Power Level.....	139
8.2.2	Polarization Performance Basis	139
8.2.3	Catalyst Loading	141
8.2.4	Operating Pressure	142
8.2.5	Stack Operating Temperature.....	142
8.2.6	Q/DT Radiator Constraint	143
8.2.7	Cell Active Area and System Voltage	143
8.3	Eaton-style Multi-Lobe Air Compressor-Motor (CM) Unit.....	144
8.3.1	Design and Operational Overview	144
8.3.2	Compressor Manufacturing Process.....	144
8.4	Bus System Balance of Plant Components	149
9	Capital Equipment Cost.....	151
10	Automotive Simplified Cost Model Function	153
11	Lifecycle Cost Analysis.....	157
12	Sensitivity Studies	164
12.1	Single Variable Analysis.....	164
12.1.1	Single Variable Automotive Analysis.....	164
12.1.2	Automotive Analysis at a Pt price of \$1100/troy ounce	165
12.1.3	Single Variable Bus Analysis	165
12.2	Monte Carlo Analysis	167
12.2.1	Monte Carlo Automotive Analysis	167
12.2.2	Monte Carlo Bus Analysis.....	169
13	Key Progress in the 2013 Automotive and Bus Analyses.....	171
14	Appendix A: 2013 Transit Bus Cost Results.....	174
14.1	Fuel Cell Stack Materials, Manufacturing, and Assembly Cost Results	174
14.1.1	Bipolar Plates	174
14.1.2	Membrane	174
14.1.3	Nanostructured Thin Film (NSTF) Catalyst Application.....	175

14.1.4	Catalyst Cost.....	175
14.1.5	Gas Diffusion Layer	175
14.1.6	MEA Sub-Gaskets Total	175
14.1.7	MEA Crimping, Cutting, and Slitting.....	176
14.1.8	End Plates.....	177
14.1.9	Current Collectors	177
14.1.10	Coolant Gaskets/Laser-welding	177
14.1.11	End Gaskets.....	178
14.1.12	Stack Assembly.....	178
14.1.13	Stack Housing.....	179
14.1.14	Stack Conditioning and Testing.....	179
14.2	2013 Transit Bus Balance of Plant (BOP) Cost Results	179
14.2.1	Air Loop	179
14.2.2	Humidifier & Water Recovery Loop	180
14.2.3	Coolant Loops.....	184
14.2.4	Fuel Loop.....	184
14.2.5	System Controller.....	184
14.2.6	Sensors	185
14.2.7	Miscellaneous BOP.....	185
14.2.8	System Assembly.....	186

1 Overview

This 2013 report covers fuel cell cost analysis of both light duty vehicle (automotive) and transit bus applications for only the current year (i.e. 2013). This report is the seventh annual update of a comprehensive automotive fuel cell cost analysis⁶ conducted by Strategic Analysis⁷ (SA), under contract to the US Department of Energy (DOE). The first report (hereafter called the “2006 cost report”) estimated fuel cell system cost for three different technology levels: a “current” system that reflected 2006 technology, a system based on projected 2010 technology, and another system based on projections for 2015. The 2007 update report incorporated technology advances made in 2007 and re-appraised the projections for 2010 and 2015. Based on the earlier report, it consequently repeated the structure and much of the approach and explanatory text. The 2008-2012, reports^{8,9,10,11,12} followed suit, and this 2013 report¹³ is another annual reappraisal of the state of technology and the corresponding costs. In the 2010 report, the “current” technology and the 2010 projected technology merged, leaving only two technology levels to be examined: the current status (then 2010) and the 2015 projection. In 2012, the 2015 system projection was dropped since the time frame between the current status and 2015 was so short. Also in 2012, analysis of a fuel cell powered 40 foot transit bus was added.

In this multi-year project, SA estimates the material and manufacturing costs of complete 80 kW_{e,net} direct-hydrogen Proton Exchange Membrane (PEM) fuel cell systems suitable for powering light-duty automobiles and 160 kW_{net} systems of the same type suitable for powering 40 foot transit buses. To assess the cost benefits of mass manufacturing, six annual production rates are examined for each automotive technology level: 1,000, 10,000, 30,000, 80,000, 100,000, and 500,000 systems per year. Since total U.S. 40 foot bus sales are currently ~4,000 vehicles per year, manufacturing rates of 200, 400, 800, and 1,000 systems/year are considered for cost analysis.

⁶ “Mass Production Cost Estimation for Direct H₂ PEM Fuel Cell Systems for Automotive Applications,” Brian D. James & Jeff Kalinoski, Directed Technologies, Inc., October 2007.

⁷ This project was contracted with and initiated by Directed Technologies Inc. (DTI). In July 2011, DTI was purchased by Strategic Analysis Inc. (SA) and thus SA has taken over conduct of the project.

⁸ James BD, Kalinoski JA, Baum KN. Mass production cost estimation for direct H₂ PEM fuel cell systems for automotive applications: 2008 update. Arlington (VA): Directed Technologies, Inc. 2009 Mar. Contract No. GS-10F-0099J. Prepared for the US Department of Energy, Energy Efficiency and Renewable Energy Office, Hydrogen Fuel Cells & Infrastructure Technologies Program.

⁹ James BD, Kalinoski JA, Baum KN. Mass production cost estimation for direct H₂ PEM fuel cell systems for automotive applications: 2009 update. Arlington (VA): Directed Technologies, Inc. 2010 Jan. Contract No. GS-10F-0099J. Prepared for the US Department of Energy, Energy Efficiency and Renewable Energy Office, Hydrogen Fuel Cells & Infrastructure Technologies Program.

¹⁰ “Mass Production Cost Estimation for Direct H₂ PEM Fuel Cell Systems for Automotive Applications: 2010 Update,” Brian D. James, Jeffrey A. Kalinoski & Kevin N. Baum, Directed Technologies, Inc., 30 September 2010.

¹¹ “Mass Production Cost Estimation for Direct H₂ PEM Fuel Cell Systems for Automotive Applications: 2011 Update,” Brian D. James, Kevin N. Baum & Andrew B. Spisak, Strategic Analysis, Inc., 7 September 2012.

¹² Personal communication with Leslie Eudy, National Renewable Energy Laboratory, 25 October 2012.

¹³ For previous analyses, SA was funded directly by the Department of Energy’s Energy Efficiency and Renewable Energy Office. For the 2010 and 2011 Annual Update report, SA was funded by the National Renewable Energy Laboratory. For the 2012 and 2013 Annual update reports, SA is funded by Department of Energy’s Energy Efficiency and Renewable Energy Office.

A Design for Manufacturing and Assembly (DFMATM) methodology is used to prepare the cost estimates. However, departing from DFMATM standard practice, a markup rate for the final system assembler to account for the business expenses of general and administrative (G&A), R&D, scrap, and profit, is not currently included in the cost estimates. However, markup is added to components and subsystems produced by lower tier suppliers and sold to the final system assembler. For the automotive application, a high degree of vertical integration is assumed for fuel cell production. This assumption is consistent with the scenario of the final system assembler (e.g. a General Motors (GM) or a Ford Motor Company (Ford)) producing virtually all of the fuel cell power system in-house, and only purchasing select stack or balance of plant components from vendors). Under this scenario, markup is not applied to most components (since markup is not applied to the final system assembly). In contrast, the fuel cell bus application is assumed to have a very low level of vertical integration. This assumption is consistent with the scenario where the fuel cell bus company buys the fuel cell power system from a hybrid system integrator who assembles the power system (whose components, in turn, are manufactured by subsystem suppliers and lower tier vendors). Under this scenario, markup is applied to most system components. (Indeed, multiple layers of markup are applied to most components as the components pass through several corporate entities on their way to the bus manufacturer.)

In general, the system designs do not change with production rate, but material costs, manufacturing methods, and business-operational assumptions do vary. Cost estimation at very low manufacturing rates (below 1,000 systems per year) presents particular challenges. Traditional low-cost mass-manufacturing methods are not cost-effective at low manufacturing rates due to high per-unit setup and tooling costs, and lower manufacturing line utilizations. Instead, less defined and less automated operations are typically employed. For some repeat parts within the fuel cell stack (e.g. the membrane electrode assemblies (MEAs) and bipolar plates), such a large number of pieces are needed for each system that even at low system production rates (1,000/year), hundreds of thousands of individual parts are needed annually. Thus, for these parts, mass-manufacturing cost reductions are achieved even at low system production rates. However, other fuel cell stack components (e.g. end plates and current collectors) and all FCS-specific balance of plant (BOP) equipment manufactured in-house do not benefit from this manufacturing multiplier effect, because there are fewer of these components per stack (i.e. two endplates per stack, etc.).

The 2013 system reflects the authors' best estimate of current technology and, with only a few exceptions, is not based on proprietary information. Public presentations by fuel cell companies and other researchers along with an extensive review of the patent literature are used as a primary basis for modelling the design and fabrication of the technologies. Consequently, the presented information may lag behind what is being done "behind the curtain" in fuel cell companies. Nonetheless, the current-technology system provides a benchmark against which the impact of future technologies may be compared. Taken together, the analysis of this system provides a good sense of the likely range of costs for mass-produced automotive and bus fuel cell systems and of the dependence of cost on system performance, manufacturing, and business-operational assumptions.

2 Project Approach

The overall goal of this analysis is to transparently and comprehensively estimate the manufacturing and assembly cost of PEM fuel cell power systems for light duty vehicle (i.e. automotive) and transit bus applications. The analysis is to be sufficiently in-depth to allow identification of key cost drivers. Systems are to be assessed at a variety of annual manufacturing production rates.

To accomplish these goals, a three step system approach is employed:

- 1) System conceptual design wherein a functional system schematic of the fuel cell power system is defined.
- 2) System physical design wherein a bill of materials (BOM) is created for the system. The BOM is the backbone of the cost analysis accounting system and is a listing and definition of subsystems, components, materials, fabrication and assembly processes, dimensions, and other key information.
- 3) Cost modeling where Design for Manufacturing and Assembly (DFMATM) or other cost estimation techniques are employed to estimate the manufacturing and assembly cost of the fuel cell power system. Cost modeling is conducted at a variety of annual manufacturing rates.

Steps two and three are achieved through the use of an integrated performance and cost analysis model. The model is Excel spreadsheet-based although outside cost and performance analysis software is occasionally used as inputs. Argonne National Laboratory models of the electrochemical performance at the fuel cell stack level are used to assess stack polarization performance.

The systems examined within this report do not reflect the designs of any one manufacturer but are intended to be representative composites of the best elements from a number of designs. The automotive system is normalized to a system output power of 80 kW_{e_net} and the bus system to 160 kW kW_{e_net}. System gross power is derived from the parasitic load of the BOP components.

The project is conducted in coordination with researchers at Argonne National Laboratory (ANL) who have independent configuration and performance models for similar fuel cell systems. Those models serve as quality assurance and validation of the project's cost inputs and results. Additionally, the project is conducted in coordination with researchers at the National Renewable Energy Laboratory (NREL) who are experts in manufacturing quality control, bus fuel cell power systems, and life-cycle cost modeling. Furthermore, the assumptions and results from the project are annually briefed to the US Car Fuel Cell Technology Team so as to receive suggestions and concurrence with assumptions. Finally, the basic approach of process based cost estimation is to model a complex system (eg. the fuel cell power system) as the summation of the individual manufacturing and assembly processes used to make each component of the system. Thus a complex system is defined as a series of small steps, each with a corresponding set of (small) assumptions. These individual small assumptions often have manufacturing existence proofs which can be verified by the manufacturing practitioners. Consequently, the cost analysis is further validated by documentation of all modeling assumptions and its source.

2.1 Integrated Performance and Cost Estimation

The fuel cell stack is the key component within the fuel cell system and its operating parameters effectively dictate all other system components. As stated, the systems are designed for a net system power. An integrated performance & cost assessment procedure is used to determine the configuration and operating parameters that lead to lowest system cost (on a \$/kW basis). Figure 1 lists the basic steps in the system cost estimation and optimization process and contains two embedded iterative steps. The first iterative loop seeks to achieve computational closure of system performance¹⁴ and the second iterative loop seeks to determine the combination of stack operational parameters that leads to lowest system cost.

- 1) Define system basic mechanical and operational configuration
- 2) Select target system net power production.
- 3) Select stack operating parameters (pressure, catalyst loading, cell voltage, air stoichiometry).
- 4) Estimate stack power density (W/cm^2 of cell active area) for those parameters.
- 5) Estimate system gross power (based on known net power target and estimation of parasitic electrical loads).
- 6) Compute required total active area to achieve gross power.
- 7) Compute cell active area (based on target system voltage).
- 8) Compute stack hydrogen and air flows based on stack and system efficiency estimates.
- 9) Compute size of stack and balance of plant components based on these flow rates, temperatures, pressures, voltages, and currents.
- 10) Compute actual gross power for above conditions.
- 11) Compare “estimated” gross power with computed actual gross power.
- 12) Adjust gross power and repeat steps 1-9.
- 13) Compute cost of power system.
- 14) Vary stack operating parameters and repeat steps 3-13.

Figure 1. Basic steps within the system cost estimation and optimization process

¹⁴ The term “computational closure” is meant to denote the end condition of an iterative solution where all parameters are internally consistent with one another.

Stack efficiency^{15,16} at rated power of the automotive systems was previously set at 55%, to match past DOE targets. However, in 2013, a radiator size constraint in the form of $Q/\Delta T$ was imposed (see Section 6.2), and stack efficiencies were allowed to fluctuate so as to achieve minimum system cost while also satisfying radiator constraints.

The main fuel cell subsystems included in this analysis are:

- Fuel cell stacks
- Air loop
- Humidifier and water recovery loop
- High-temperature coolant loop
- Low-temperature coolant loop
- Fuel loop (but not fuel storage)
- Fuel cell system controller
- Sensors

Some vehicle electrical system components explicitly excluded from the analysis include:

- Main vehicle battery or ultra-capacitor¹⁷
- Electric traction motor (that drives the vehicle wheels)
- Traction inverter module (TIM) (for control of the traction motor)
- Vehicle frame, body, interior, or comfort related features (e.g., driver's instruments, seats, and windows)

Many of the components not included in this study are significant contributors to the total fuel cell vehicle cost; however their design and cost are not necessarily dependent on the fuel cell configuration or stack operating conditions. Thus, it is our expectation that the fuel cell system defined in this report is applicable to a variety of vehicle body types and drive configurations.

2.2 Cost Analysis Methodology

As mentioned above, the costing methodology employed in this study is the Design for Manufacture and Assembly technique (DFMATM)¹⁸. Ford has formally adopted the DFMATM process as a systematic means for the design and evaluation of cost optimized components and systems. These techniques are powerful and flexible enough to incorporate historical cost data and manufacturing acumen that have been accumulated by Ford since the earliest days of the company. Since fuel cell system production requires some manufacturing processes not normally found in automotive production, the formal DFMATM process and SA's manufacturing database are buttressed with budgetary and price quotations

¹⁵ Stack efficiency is defined as voltage efficiency X H₂ utilization = Cell volts/1.229 X 100%.

¹⁶ Multiplying this by the theoretical open circuit cell voltage (1.229 V) yields a cell voltage of 0.676 V at peak power.

¹⁷ Fuel cell automobiles may be either "purebreds" or "hybrids" depending on whether they have battery (or ultracapacitor) electrical energy storage or not. This analysis only addresses the cost of an 80 kW fuel cell power system and does not include the cost of any peak-power augmentation or hybridizing battery.

¹⁸ Boothroyd, G., P. Dewhurst, and W. Knight. "Product Design for Manufacture and Assembly, Second Edition," 2002.

from experts and vendors in other fields. It is possible to identify low cost manufacturing processes and component designs and to accurately estimate the cost of the resulting products by combining historical knowledge with the technical understanding of the functionality of the fuel cell system and its component parts. This DFMA™-style methodology helps to evaluate capital cost as a function of annual production rate. This section explains the DFMA™ cost modelling methodology further and discusses FCS stack and balance of plant (BOP) designs and performance parameters where relevant.

The cost for any component analyzed via DFMA™ techniques includes direct material cost, manufacturing cost, assembly costs, and markup. Direct material costs are determined from the exact type and mass of material employed in the component. This cost is usually based upon either historical volume prices for the material or vendor price quotations. In the case of materials or devices not widely used at present, the manufacturing process must be analyzed to determine the probable high-volume price for the material or device. The manufacturing cost is based upon the required features of the part and the time it takes to generate those features in a typical machine of the appropriate type. The cycle time can be combined with the “machine rate,” the hourly cost of the machine based upon amortization of capital and operating costs, and the number of parts made per cycle to yield an accurate manufacturing cost per part. The assembly costs are based upon the amount of time to complete the given operation and the cost of either manual labor or of the automatic assembly process train. The piece cost derived in this fashion is quite accurate as it is based upon an exact physical manifestation of the part and the technically feasible means of producing it as well as the historically proven cost of operating the appropriate equipment and amortizing its capital cost. Normally (though not in this report), a percentage markup is applied to the material, manufacturing, and assembly cost to account for profit, general and administrative (G&A) costs, research and development (R&D) costs, and scrap costs. This percentage typically varies with production rate to reflect the efficiencies of mass production. It also changes based on the business type, on the amount of value that the manufacturer or assembler adds to the product, and on market conditions.

Cost analyses were performed for mass-manufactured systems at six production rates for the automotive FC power systems (1,000, 10,000, 30,000, 80,000, 100,000, and 500,000 systems per year) and four production rates for the bus systems (200, 400, 800, and 1,000 systems per year). System designs did not change with production rate, but material costs, manufacturing methods, and business-operational assumptions (such as markup rates) often varied. Fuel cell stack component costs were derived by combining manufacturers’ quotes for materials and manufacturing with detailed DFMA™-style analysis.

For some components (e.g. the bipolar plates and the coolant and end gaskets), multiple designs or manufacturing approaches were analyzed. The options were carefully compared and contrasted, and then examined within the context of the rest of the system. The best choice for each component was included in the 2013 baseline configuration. Because of the interdependency of the various components, the selection or configuration of one component sometimes affects the selection or configuration of another. To handle these combinations, the DFMA™ model was designed with switches for each option, and logic was built in that automatically adjusts variables as needed. As such, the reader should not assume that accurate system costs could be calculated by merely substituting the

cost of one component for another, using only the data provided in this report. Instead, data provided on various component options should be used primarily to understand the decision process used to select the approach for the baseline configurations.

The DFMA™-style methodology proceeds through four iterative stages: (1) System Conceptual Design, (2) System Physical Design, (3) Cost Modeling, and (4) Continuous Improvement to Reduce Cost.

2.2.1 Stage 1: System Conceptual Design

In the system conceptual design stage, a main goal is to develop and verify a chemical engineering process plant model describing the FCS. The FCSs consume hydrogen gas from a compressed hydrogen storage system or other hydrogen storage media. This DFMA™ modelling effort does not estimate the costs for either the hydrogen storage medium or the electric drive train. This stage delineates FCS performance criteria, including, for example, rated power, FCS volume, and FCS mass, and specifies a detailed drive train design. An Aspen HYSYS™ chemical process plant model is developed to describe mass and energy flows, and key thermodynamic parameters of different streams. This stage specifies required system components and their physical constraints, such as operating pressure, heat exchanger area, etc. Key design assumptions are developed for the PEM fuel cell vehicle (FCV) system, in some cases, based on a local optimization of available experimental performance data.

2.2.2 Stage 2: System Physical Design

The physical design stage identifies bills of materials (BOMs) for the FCS at a system and subsystem level, and, in some cases, at a component level. A BOM describes the quantity of each part used in the stack, the primary materials from which the part is formed, the feedstock material basic form (i.e. roll, coil, powder, etc.), the finished product basic form, whether a decision was made to make the part internally or buy it from an external machine shop (i.e. make or buy decision), the part thickness, and the primary formation process for the part. The system physical design stage identifies material needs, device geometry, manufacturing procedures, and assembly methods.

2.2.3 Stage 3: Cost Modeling

The cost modelling approach applied depends on whether (1) the device is a standard product that can be purchased off-the-shelf, such as a valve or a heat exchanger, or whether (2) it is a non-standard technology not yet commercially available in high volumes, such as a fuel cell stack or a membrane humidifier. Two different approaches to cost modeling pervade: (1) For standard components, costs are derived from industry price quotes and reasonable projections of these to higher or lower manufacturing volumes. (2) For non-standard components, costs are based on a detailed DFMA™ analysis, which quantifies materials, manufacturing, tooling, and assembly costs for the manufacturing process train.

2.2.3.1 Standardized Components: Projections from Industry Quotes

For standardized materials and devices, price quotations from industry as a function of annual order quantity form the basis of financial estimates. A learning curve formula is applied to the available data gathered from industry:

$$P_Q = P_I * F_{LC} \left(\frac{\ln(\frac{Q}{Q_I})}{\ln 2} \right) \quad (1)$$

where P_Q is the price at a desired annual production quantity $[Q]$ given the initial quotation price $[P_I]$ at an initial quantity Q_I and a learning curve reduction factor $[F_{LC}]$. F_{LC} can be derived from industry data if two sets of price quotes are provided at two different annual production quantities. When industry quotation is only available at one annual production rate, a standard value is applied to the variable F_{LC} .

2.2.3.2 Non-standard Components: DFMA™ Analysis

When non-standard materials and devices are needed, costs are estimated based on detailed DFMA™ style models developed for a specific, full physical, manufacturing process train. In this approach, the estimated capital cost $[C_{Est}]$ of manufacturing a device is quantified as the sum of materials costs $[C_{Mat}]$, the manufacturing costs $[C_{Man}]$, the expendable tooling costs $[C_{Tool}]$, and the assembly costs $[C_{Assy}]$:

$$C_{Est} = C_{Mat} + C_{Man} + C_{Tool} + C_{Assy} \quad (2)$$

The materials cost $[C_{Mat}]$ is derived from the amount of raw materials needed to make each part, based on the system physical design (material, geometry, and manufacturing method). The manufacturing cost $[C_{Man}]$ is derived from a specific design of a manufacturing process train necessary to make all parts. The manufacturing cost $[C_{Man}]$ is the product of the machine rate $[R_M]$ and the sum of the operating and setup time:

$$C_{Man} = R_M * (T_R + T_S) \quad (3)$$

where the machine rate $[R_M]$ is the cost per unit time of operating the machinery to make a certain quantity of parts within a specific time period, T_R is the total annual runtime, and T_S is the total annual setup time. The cost of expendable tooling $[C_{Tool}]$ is derived from the capital cost of the tool, divided by the number of parts that the tool produced over its life. The cost of assembly $[C_{Assy}]$ includes the cost of assembling non-standard components (such as a membrane humidifier) and also the cost of assembling both standard and non-standard components into a single system. C_{Assy} is calculated according to

$$C_{Assy} = R_{Assy} * \sum T_{Assy} \quad (4)$$

where R_{Assy} is the machine rate for the assembly train, i.e. the cost per unit time of assembling components within a certain time period and T_{Assy} is the part assembly time.

2.2.4 Stage 4: Continuous Improvement to Reduce Cost

The fourth stage of continuous improvement to reduce cost iterates on the previous three stages. This stage weighs the advantages and disadvantages of alternative materials, technologies, system conceptual design, system physical design, manufacturing methods, and assembly methods, so as to iteratively move towards lower cost designs and production methods. Feedback from industry and research laboratories can be crucial at this stage. This stage aims to reduce estimated costs by continually improving on the three-stages above.

2.3 Vertical Integration and Markups

Vertical integration describes the extent to which a single company conducts many (or all) of the manufacturing/assembly steps from raw materials to finished product. High degrees of vertical integration can be cost efficient by decreasing transportation costs and turn-around times, and reducing nested layers of markup/profit. However, at low manufacturing rates, the advantages of vertical integration may be overcome by the negative impact of low machinery utilization or poor quality control due to inexperience/lack-of-expertise with a particular manufacturing step.

For the 2012 analysis, both the automotive and bus fuel cell power plants were cost modeled as if they were highly vertically integrated operations. However for the 2013 analysis, the automotive fuel cell system retains the assumption of high vertical integration but the bus system assumes a non-vertically integrated structure. This is consistent with the much lower production rates of the bus systems (200 to 1,000 systems/year) compared to the auto systems (1,000 to 500,000 systems/year). Figure 2 graphically contrasts these differing assumptions. Per long standing DOE directive, markup (i.e. business cost adders for overhead, general & administrative expenses, profit, research and development expenses, etc.) are not included in the power system cost estimates for the final system integrator but are included for lower tier suppliers. Consequently, very little markup is included in the automotive fuel cell system cost because the final integrator performs the vast majority of the manufacture and assemble (i.e. the enterprise is highly vertically integrated). In contrast, bus fuel cell systems are assumed to have low vertical integration and thus incur substantial markup expense. Indeed, there are two layers of markup on most components (one for the actual manufacturing vendor and another for the hybrid system integrator).

Standard DFMATM practice, calls for a markup to be applied to a base cost to account for general and administrative (G&A) expenses, research and development (R&D), scrap, and company profit. While markup is typically applied to the total component cost (i.e. the sum of materials, manufacturing, and assembly), it is sometimes applied at different levels to materials and processing costs. The markup rate is represented as a percentage value and can vary substantially depending on business circumstances, typically ranging from as low as 10% for pass-thru components, to 100% or higher for small businesses with low sales volume.

Within this analysis, a set of standard markup rates is adopted as a function of annual system volume and markup entity. Portraying the markup rates as a function of actual sales revenue would be a better

correlating parameter as many expenses represented by the markup are fixed. However, that approach is more complex and thus a correlation with annual manufacturing rate is selected for simplicity. Generic markup rates are also differentiated by the entity applying the markup. Manufacturing markup represents expenses borne by the entity actually doing the manufacturing and/or assembly procedure. Manufacturing markup is assessed at two different rates: an “in-house” rate if the manufacture is done with machinery dedicated solely to production of that component and a “job-shop” rate if the work is sent to an outside vendor. The “in-house” rate varies with manufacturing rate because machine utilization varies directly (and dramatically) with manufacturing volume. The “job-shop” rate is held constant at 30% to represent the pooling of orders available to contract manufacturing businesses¹⁹. A pass-thru markup represents expenses borne by a company that buys a component from a sub-tier vendor and then passes it through to a higher tier vendor. Integrator’s markup represents expenses borne by the hybrid systems integrator than sets engineering specifications, sources the components, and assembles them into a power system (but does not actually manufacture the components). More than one entity may be involved in supply of the finished product. Per DOE directive, no markup is applied for the final system assembler.

Assumptions Regarding Extent of Vertical Integration

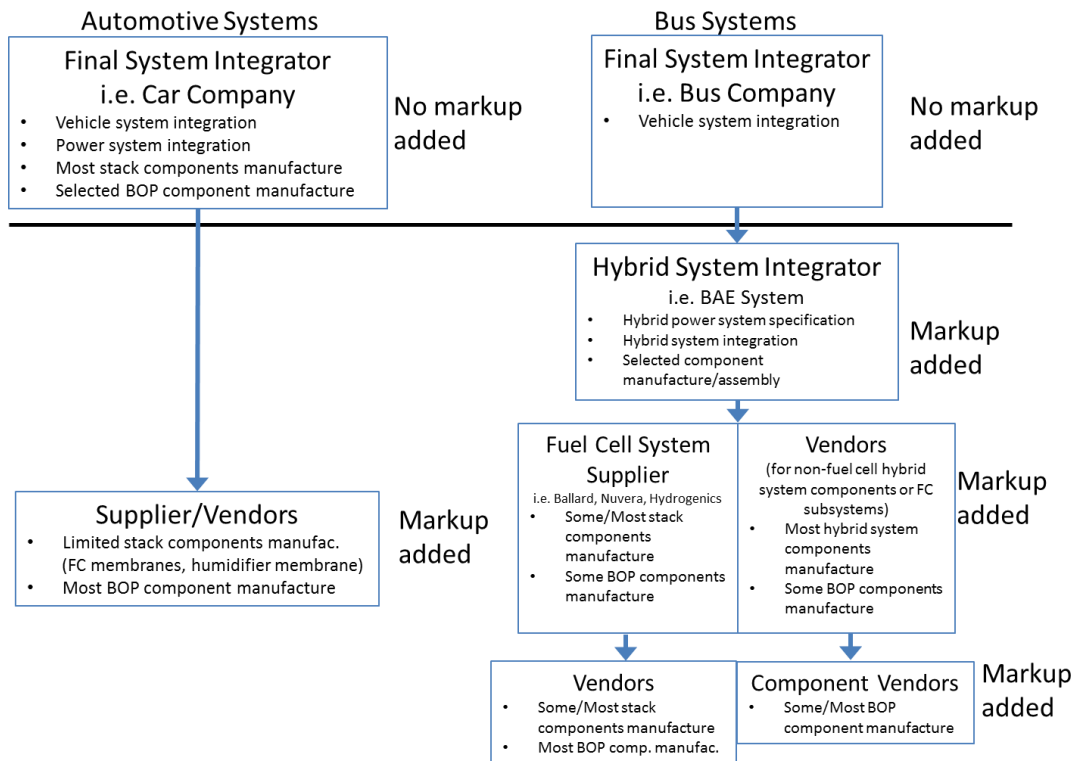


Figure 2: Comparison of bus and auto system vertical integration assumptions

¹⁹ The job-shop markup is not really constant as large orders will result in appreciable increases in machine utilization and thus a (potential) lowering of markup rate. However, in practice, large orders are typically produced in-house to avoid the job-shop markup entirely and increase the in-house “value added”. Thus in practice, job-shop markup is approximately constant.

Figure 3 lists the generic markup rates corresponding to each entity and production volume. When more than one markup is applied, the rates are additive. These rates are applied to each component of the automotive and bus systems as appropriate for that component’s circumstances and generally apply to all components except the fuel cell membrane, humidifier, and air compressor subsystem. Markup rates for those components are discussed individually in the component cost results below.

Business Entity	Annual System Production Rate								
	200	400	800	1000	10k	30K	80k	100k	500k
Manufacturer (in-house)	58.8%	54.3%	50.1%	48.9%	37.5%	33.0%	29.5%	28.8%	23.9%
Manufacturer (job-shop)	30%	30%	30%	30%	30%	30%	30%	30%	30%
Pass-Thru	20.2%	19.6%	19.1%	19.0%	17.3%	16.6%	16.0%	15.8%	14.9%
Integrator	20.2%	19.6%	19.1%	19.0%	17.3%	16.6%	16.0%	15.8%	14.9%

Figure 3. Generic markup rates for auto and bus cost analysis

The numeric levels of markup rates can vary substantially between companies and products and is highly influenced by the competitiveness of the market and the manufacturing and product circumstances of the company. For instance, a large established company able to re-direct existing machinery for short production runs would be expected to have much lower markup rates than a small, one-product company. Consequently, the selection of the generic markup rates in Figure 3 is somewhat subjective. However, they reflect input from informal discussions with manufacturers and are derived by postulating a power curve fit to key anchor markup rates gleaned from manufacturer discussions. For instance, a ~23% manufactures markup at 500k systems/year and a 100% markup at a few systems/year are judged to be reasonable. A power curve fit fills in the intervening manufacturing rates. Likewise, a 30% job shop markup rate is deemed reasonable based on conversations and price quotes from manufacturing shops. The pass-thru and integrator markups are numerically identical and much less than the manufacture’s rate as much less “value added” work is done. Figure 4 graphically displays the generic markup rates along with the curve fit models used in the analysis.

For the automotive systems, the application of markup rates is quite simple. The vast majority of components are modeled as manufactured by the final system integrator and thus no markup is applied to those components (by DOE directive, the final assembler applies no markup). The few automotive components produced by lower tier vendors (e.g. the CEM and the PEM membrane) receive a manufacturer’s markup.

For the bus systems, the application of markup rate is more complex. System production volume is much lower than for automotive systems, and thus it is most economical to have the majority of components produced by lower-tier job-shops. Consequently, the straight job-shop 30% markup is applied for job-shop manufacturing expenses. Additionally, a pass-thru markup is added for expenses of the fuel-cell-supplier/subsystem-vendor, and an integrator markup is added for expenses of the hybrid integrator. These markups are additive. Like the auto systems, no markup is applied for the final system integrator.

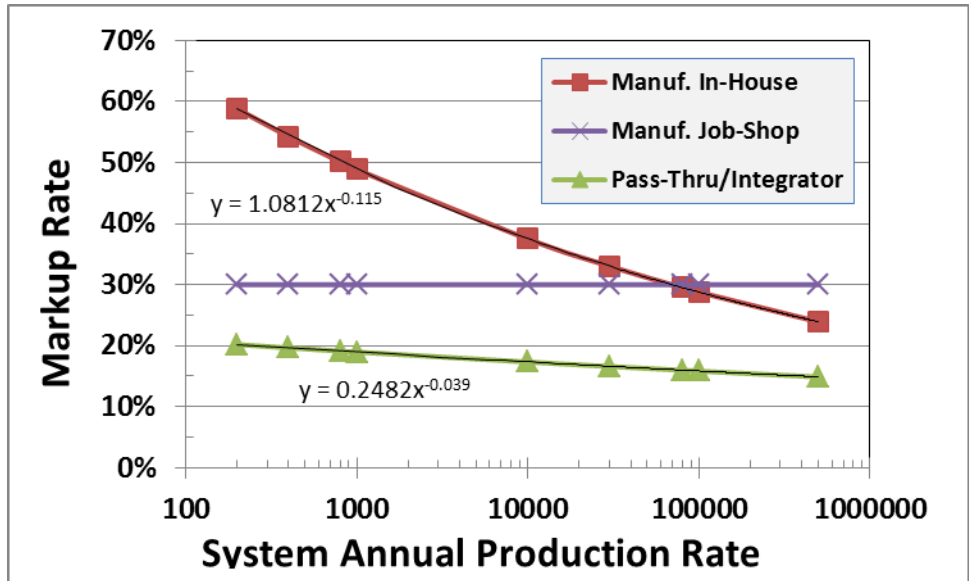


Figure 4. Graph of markup rates

Component level markup costs are reported in sections 0 and 0 of this report. Note that job-shop markup costs are included in the manufacturing cost line element, whereas all other markup costs (pass-thru and integrator) are included in the markup cost line element.

3 Overview of the Bus System

Fuel cell transit buses represent a growing market segment and a logical application of fuel cell technology. Fuel cell transit buses enjoy several advantages over fuel cell automobiles, particularly in the early stages of fuel cell vehicle integration, due to the availability of centralized refueling, higher bus power levels (which generally are more economical on a \$/kW basis), dedicated maintenance and repair teams, high vehicle utilization, (relatively) less cost sensitivity, and purchasing decision makers that are typically local governments or quasi-government agencies who are often early adopters of environmentally clean technologies.

Transit bus fuel cell power systems are examined in this report. The transit bus market generally consists of 40' buses (the common "Metro" bus variety) and 30' buses (typically used for Suburban/Commuter²⁰ to rail station routes). While the 30' buses can be simply truncated versions of 40' buses, they more commonly are based on a lighter and smaller chassis (often school bus frames) than their 40' counterparts. Whereas 40' buses typically have an expected lifetime of 500k to 1M miles, 30' buses generally have a lower expected lifetime, nominally 200k miles.

There are generally three classes of fuel cell bus architecture²¹:

- hybrid electric: which typically utilize full size fuel cells for motive power and batteries for power augmentation;
- battery dominant: which use the battery as the main power source and typically use a relatively small fuel cell system to "trickle charge" the battery and thereby extend battery range;
- plug-in: which operate primarily on the battery while there is charge, and use the fuel cell as a backup power supply or range extender.

In May 2011, the US Department of Energy issued a Request for Information (RFI) seeking input²² from industry stakeholders and researchers on performance, durability, and cost targets for fuel cell transit buses and their fuel cell power systems. A joint DOE-Department of Transportation (DOT)/Federal Transit Administration (FTA) workshop was held to discuss the responses, and led to DOE publishing fuel cell bus targets for performance and cost as shown in Figure 5. While not explicitly used in this cost analysis, these proposed targets are used as a guideline for defining the bus fuel cell power plant analyzed in the cost study.

The cost analysis in this report is based on the assumption of a 40' transit bus. Power levels for this class of bus vary widely based primarily on terrain/route and environmental loads. Estimates of fuel cell power plant required²³ net power can be as low as 75 kW for a flat route in a mild climate to 180+kW for a hillier urban route in a hot climate. Accessory loads on buses are much higher than on light duty passenger cars. Electric power is needed for climate control (i.e. cabin air conditioning and heating), opening and closing the doors (which also impacts climate control), and lighting loads. In a hot climate,

²⁰ Commuter buses are typically shorter in overall length (and wheel base) to provide ease of transit through neighborhoods, a tighter turning radius, and more appropriate seating for a lower customer user base.

²¹ Personal communication with Leslie Eudy, National Renewable Energy Laboratory, 25 October 2012.

²² "Fuel Cell Transit Buses", R. Ahluwalia, , X. Wang, R. Kumar, Argonne National Laboratory, 31 January 2012.

²³ Personal communication with Larry Long, Ballard Power Systems, September 2012.

such as Dallas Texas, accessory loads can reach 30-60 kW, although 30-40 kW is more typical²⁴. Industry experts²⁵ note that the trend may be toward slightly lower fuel cell power levels as future buses become more heavily hybridized and make use of high-power-density batteries (particularly lithium chemistries).

Parameter	Units	2012 Status	Ultimate Target
Bus Lifetime	years/miles	5/100,000 ^a	12/500,000
Power Plant Lifetime^{b,c}	hours	12,000	25,000
Bus Availability	%	60	90
Fuel Fills^d	per day	1	1 (<10 min)
Bus Cost^e	\$	2,000,000	600,000
Power Plant Cost^{b,e}	\$	700,000	200,000
Road Call Frequency (Bus/Fuel-Cell System)	miles between road calls (MBRC)	2,500/10,000	4,000/20,000
Operating Time	hours per day/days per week	19/7	20/7
Scheduled and Unscheduled Maintenance Cost^f	\$/mile	1.20	0.40
Range	miles	270	300
Fuel Economy	mgde ^g	7	8

a Status represents NREL fuel cell bus evaluation data. New buses are currently projected to have 8 year/300,000 mile lifetime.

b The power plant is defined as the fuel cell system and the battery system. The fuel cell system includes supporting subsystems such as the air, fuel, coolant, and control subsystems. Power electronics, electric drive, and hydrogen storage tanks are excluded.

c According to an appropriate duty cycle.

d Multiple sequential fuel fills should be possible without increase in fill time.

e Cost projected to a production volume of 400 systems per year. This production volume is assumed for analysis purposes only, and does not represent an anticipated level of sales.

f Excludes mid-life overhaul of power plant.

g Miles per gallon diesel equivalent (mgde)

Figure 5. Proposed DOE targets for fuel cell-powered transit buses (From US DOE²⁶)

The cost analysis in this report is based on a 160 kW_{net} fuel cell bus power plant. This power level is within the approximate range of existing fuel cell bus demonstration projects²⁷ as exemplified by the 150 kW Ballard fuel cell buses²⁸ used in Whistler, Canada for the 2010 winter Olympics, and the 120kW UTC power PureMotion fuel cell bus fleets in California²⁹ and Connecticut. Selection of a 160 kW_{net} power level is also convenient because it is twice the power of the nominal 80kW_{net} systems used for the

²⁴ Personal communication with Larry Long, Ballard Power Systems, September 2012.

²⁵ Personal communication with Peter Bach, Ballard Power Systems, October 2012.

²⁶ "Fuel Cell Bus Targets", US Department of Energy Fuel Cell Technologies Program Record, Record # 12012, March 2, 2012. http://www.hydrogen.energy.gov/pdfs/12012_fuel_cell_bus_targets.pdf

²⁷ "Fuel Cell Transit Buses", R. Ahluwalia, X. Wang, R. Kumar, Argonne National Laboratory, 31 January 2012.

²⁸ The Ballard bus power systems are typically referred to by their gross power rating (150kW). They deliver approximately 140kW net.

²⁹ "SunLine Unveils Hydrogen-Electric Fuel Cell Bus: Partner in Project with AC Transit", article at American Public Transportation Association website, 12 December 2005, http://www.apta.com/passengertransport/Documents/archive_2251.htm

light duty automotive analysis, thereby easily facilitating comparisons to the use of two auto power plants.

The transit bus driving schedule is expected to consist of much more frequent starts and stops, low fractional time at idle power (due to high and continuous climate control loads), and low fractional time at full power compared to light-duty automotive drive cycles³⁰. While average bus speeds depend on many factors, representative average bus speeds³¹ are 11-12 miles per hour (mph), with the extremes being a New York City type route (~6 mph average) and a commuter style bus route (~23 mph average). No allowance has been made in the cost analysis to reflect the impact of a particular bus driving schedule.

There are approximately 4,000 forty-foot transit buses sold each year in the United States³². However, each transit agency typically orders its own line of customized buses. Thus while orders of identical buses may reach 500 vehicles at the high end, sales are typically much lower. Smaller transit agencies sometimes pool their orders to achieve more favorable pricing. Of all bus types³³ in 2011, diesel engine power plants are the most common (63.5%), followed by CNG/LNG/Blends (at 18.6%), and hybrids (electrics or other) (at only 8.8%). Of hybrid electric 40' transit bus power plants, BAE Systems and Alison are the dominant power plant manufacturers. These factors combine to make quite small the expected annual manufacturing output for a particular manufacturer of bus fuel cell power plants. Consequently, 200, 400, 800, and 1,000 buses per year are selected as the annual manufacturing rates to be examined in the cost study. This is considered a representative estimates for near-term fuel cell bus sales, perhaps skewed towards the upper end of production rates to facilitate the general DFMATM cost methodology employed in the analysis. However, these production rates could alternately be viewed as a low annual production estimate if foreign fuel cell bus sales are considered.

³⁰ Such as the Federal Urban Drive Schedule (FUDS), Federal Highway Drive Schedule (FHDS), Combined Urban/Highway Drive Cycle, LA92, or US06.

³¹ Personal communication with Leslie Eudy, National Renewable Energy Laboratory, 25 October 2012.

³² Personal communication with Leslie Eudy, National Renewable Energy Laboratory, 25 October 2012.

³³ 2012 Public Transportation Fact Book, American Public Transportation Association (APTA), 63rd Edition September 2012. Accessed February 2013 at http://www.apta.com/resources/statistics/Documents/FactBook/APTA_2012_Fact%20Book.pdf

4 System Schematics and Bills of Materials

System schematics are a useful method of identifying the main components within a system and how they interact. System flow schematics for each of the systems in the current report are shown below. Note that for clarity, only the main system components are identified in the flow schematics. As the analysis has evolved throughout the course of the annual updates, there has been a general trend toward system simplification. This reflects improvements in technology to reduce the number of parasitic supporting systems and thereby reduce system cost. The path to system simplification is likely to continue, and, in the authors' opinion, remains necessary to achieve or surpass cost parity with internal combustion engines.

The authors have conducted annually updated DFMA™ analysis of automotive fuel cell systems since 2006. Side by side comparison of annually updated system diagrams is a convenient way to assess important changes/advances. Consequently, the 2012 and 2013 auto and bus system diagrams are displayed below to highlight configuration changes.

4.1 2012 Automotive System Schematic

The system schematic for the 2012 light duty vehicle (auto) fuel cell power system appears in Figure 6.

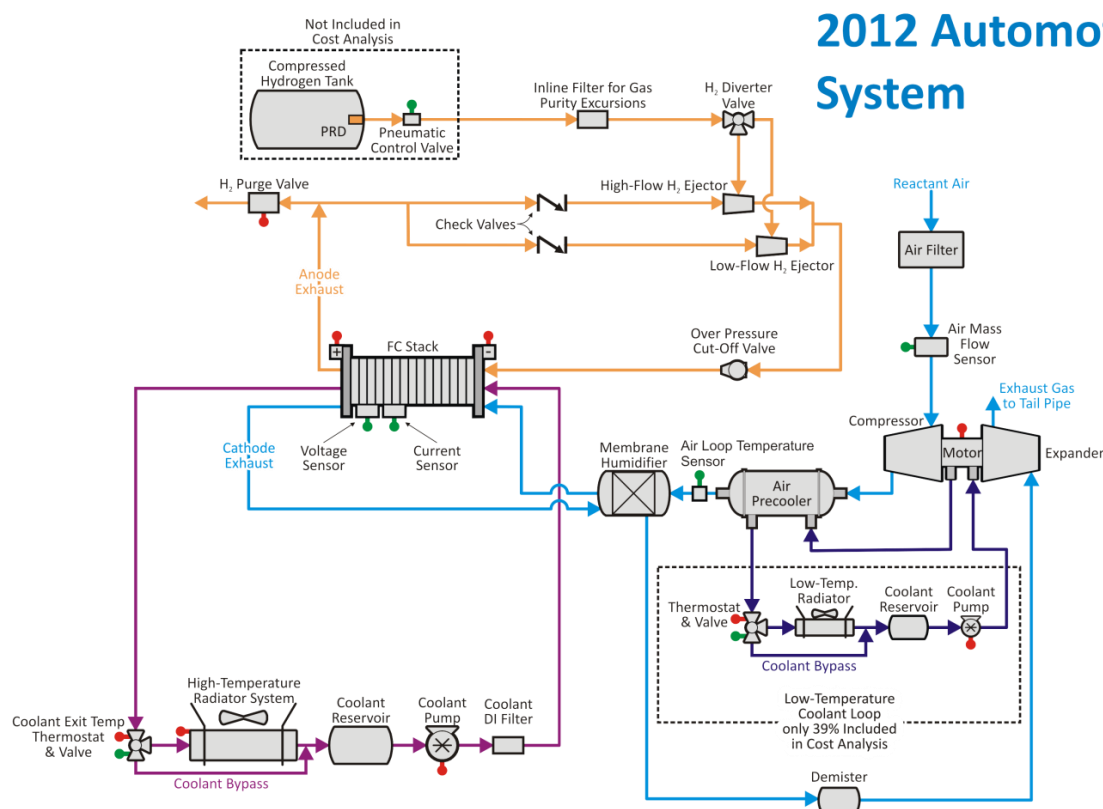


Figure 6. Flow schematic for the 2012 automotive fuel cell system

4.2 2012 Bus System Schematic

The system schematic for the 2012 bus fuel cell power system appears in Figure 7. The power system is directly analogous to the 2012 automotive system with the exception that there are two stacks instead of one, and certain stack-related components are duplicated.

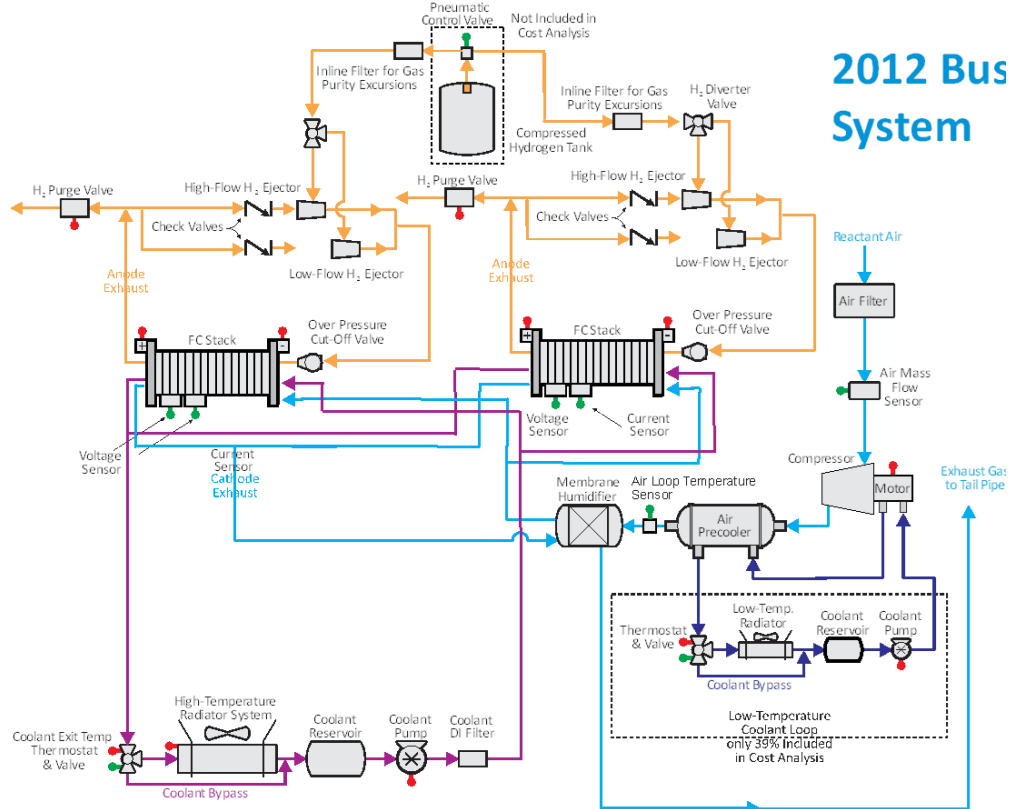


Figure 7. Flow schematic for the 2012 bus fuel cell system

4.3 2013 Auto System Schematic

The system schematic for the 2013 automotive fuel cell power system appears in Figure 8. Power system hardware and layout are directly analogous to the 2012 automotive system with the minor exception that the low temperature loop is now modeled as dedicated strictly to the fuel cell system as opposed to being shared with the traction motor system.

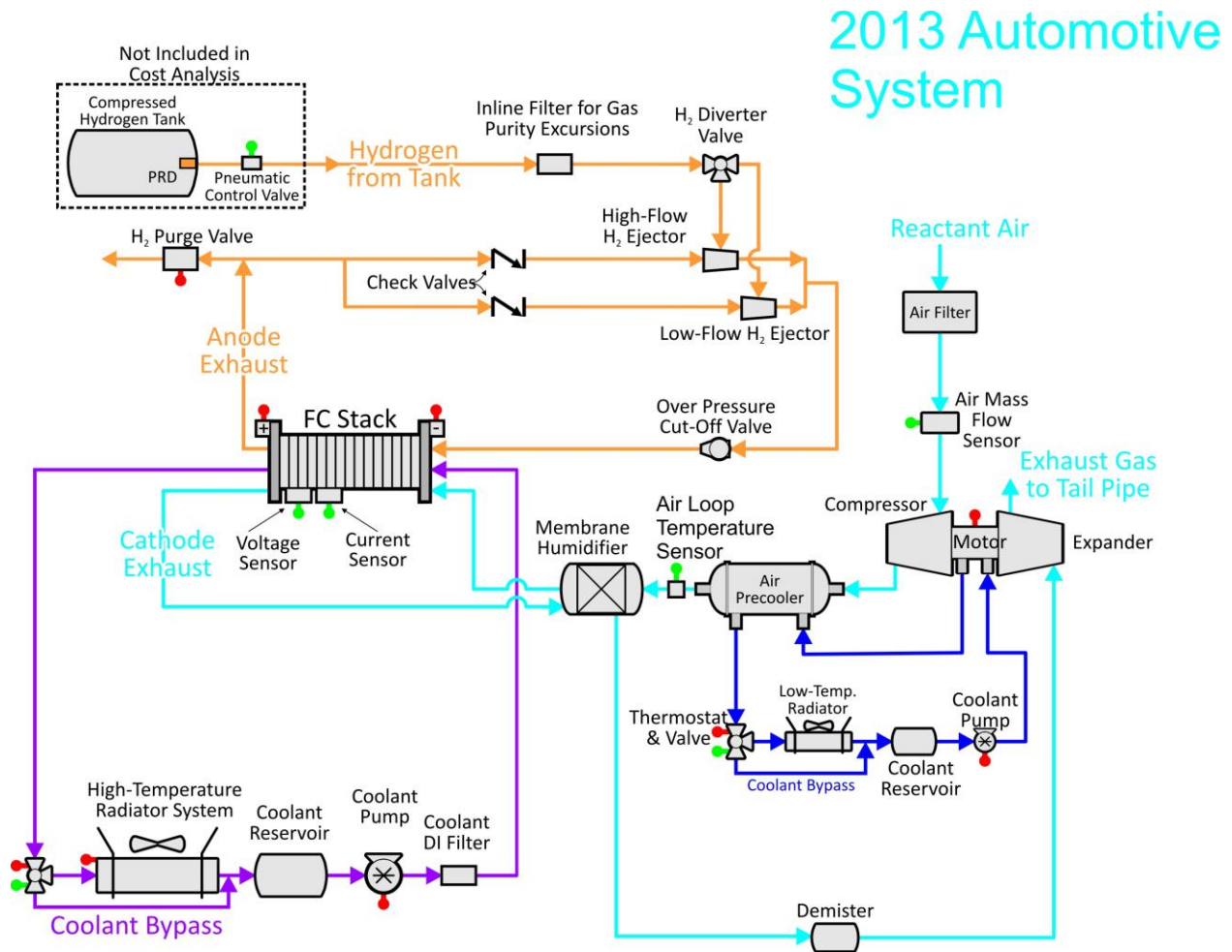


Figure 8. Flow schematic for the 2013 automotive fuel cell system

4.4 2013 Bus System Schematic

The system schematic for the 2013 bus fuel cell power system appears in Figure 9. Power system hardware and layout are directly analogous to the 2013 auto system with the exception of two key differences. 1) The automotive system contains one 80kW fuel cell stack as opposed to the bus system which contains two 80kW stacks, and 2) the automotive system operates at a higher pressure than the bus system, leading to the automotive system's air supply subsystem employing a compressor, motor, and expander (CEM) unit while the bus system uses only a compressor and motor unit.

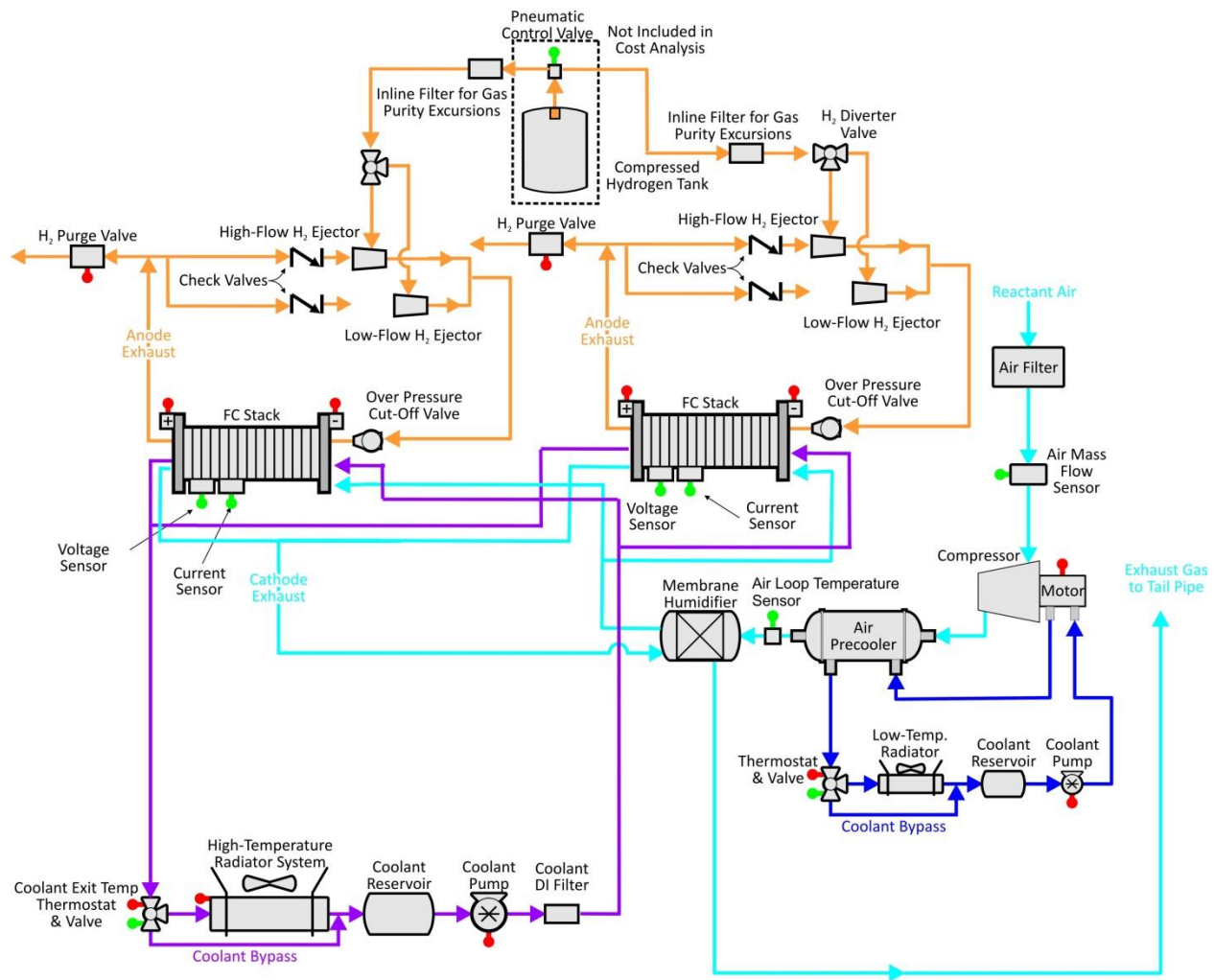


Figure 9. Flow schematic for the 2013 bus fuel cell system

5 System Cost Summaries

Complete fuel cell power systems are configured to allow assembly of comprehensive system Bills of Materials, which in turn allow comprehensive assessments of system cost. Key parameters for the 2013 automotive and bus fuel cell power systems are shown in Figure 10 below, with cost result summaries detailed in subsequent report sections.

	2012 Auto Technology System	2013 Auto Technology System	2012 Bus Technology System	2013 Bus Technology System
Power Density (mW/cm ²)	984	692	716	601
Total Pt loading (mgPt/cm ²)	0.196	0.153	0.4	0.4
Net Power (kW _{net})	80	80	160	160
Gross Power (kW _{gross})	88.2	89.4	177.1	186.2
Cell Voltage (V)	0.676	0.695	0.676	0.676
Operating Pressure (atm)	2.5	2.5	1.8	1.8
Stack Temp. (Coolant Exit Temp) (°C)	82	92.3	69.4	74
Q/ΔT (kW _{th} /°C)	1.7	1.45	5.12	2.60
Active Cells	369	359	739	739
Membrane Material	Nafion on 25-micron ePTFE	No change from 2012	Nafion on 25-micron ePTFE	No change from 2012
Radiator/ Cooling System	Aluminum Radiator, Water/Glycol Coolant, DI Filter, Air Precooler	No change from 2012	Aluminum Radiator, Water/Glycol Coolant, DI Filter, Air Precooler	No change from 2012
Bipolar Plates	Stamped SS 316L with TreadStone Coating	No change from 2012	Stamped SS 316L with TreadStone Litecell™ Coating	No change from 2012
Air Compression	Centrifugal Compressor, Radial-Inflow Expander	No change from 2012	Centrifugal Compressor, Without Expander	Eaton-Style Multi-Lobe Compressor, Without Expander
Gas Diffusion Layers	Carbon Paper Macroporous Layer with Microporous Layer (Ballard Cost)	No change from 2012	Carbon Paper Macroporous Layer with Microporous Layer (Ballard Cost)	No change from 2012
Catalyst Application	3M Nanostructured Thin Film (NSTF™)	No change from 2012	3M Nanostructured Thin Film (NSTF™)	No change from 2012
Air Humidification	Tubular Membrane Humidifier	Plate Frame Membrane Humidifier	Tubular Membrane Humidifier	Plate Frame Membrane Humidifier
Hydrogen Humidification	None	None	None	None
Exhaust Water Recovery	None	None	None	None
MEA Containment	Screen Printed Seal on MEA Subgaskets, GDL crimped to CCM	No change from 2012	Screen Printed Seal on MEA Subgaskets, GDL crimped to CCM	No change from 2012
Coolant & End Gaskets	Laser Welded(Cooling)/ Screen-Printed Adhesive Resin (End)	No change from 2012	Laser Welded (Cooling), Screen-Printed Adhesive Resin (End)	No change from 2012
Freeze Protection	Drain Water at Shutdown	No change from 2012	Drain Water at Shutdown	No change from 2012
Hydrogen Sensors	2 for FC System 1 for Passenger Cabin (not in cost estimate) 1 for Fuel System (not in cost estimate)	No change from 2012	2 for FC System 1 for Passenger Cabin (not in cost estimate) 1 for Fuel System (not in cost estimate)	No change from 2012
End Plates/ Compression System	Composite Molded End Plates with Compression Bands	No change from 2012	Composite Molded End Plates with Compression Bands	No change from 2012
Stack Conditioning (hrs)	5	No change from 2012	5	No change from 2012

Figure 10. Summary chart of the 2012 and 2013 fuel cell systems

The bus stack design differs from the automotive stack design in that (1) bus stacks are assumed to operate at a lower pressure and thereby have a lower stack power density; and (2) bus stacks are assumed to operate with a higher Pt catalyst loading so as to meet the greater longevity requirements for buses compared with cars. With a general correlation between Pt loading and stack durability, the bus system, in comparison with the automotive system, has a much higher platinum (Pt) loading due to an assumed longer lifetime. Also, the coolant stack exit temperature is much lower for the bus than for the automotive system primarily due to the typically very low part power operation of the bus stacks. In other words, the bus stacks are typically operating a greater percentage of the time at a lower percentage of their maximum power, compared with passenger cars. As a result, the bus exhaust temperature is lower. A bus is assumed to have a greater surface area available for radiator cooling and therefore is not subject to a Q/ΔT constraint. A more detailed discussion of the key differences between the automotive and bus systems appears in Section 8.1.

5.1 Cost Summary of the 2013 Automotive System

Results of the cost analysis for the 2013 automotive technology system at each of the six annual production rates are shown below. Figure 11 details the cost of the stacks, Figure 12 details the cost of the balance of plant components, and Figure 13 details the cost summation for the system.

While the cost results, particularly the \$/kW results, are presented to the penny level, this should not be construed to indicate that level of accuracy in all cases. Rather, results are presented to a high level of monetary discretization to allow discernment of the direction and approximate magnitude of cost changes. Those impacts might otherwise be lost to the reader due to rounding and rigid adherence to rules for significant digits, and might be misconstrued as an error or as having no impact.

		2013 Automotive System					
Annual Production Rate	Sys/yr	1,000	10,000	30,000	80,000	100,000	500,000
System Net Electric Power (Output)	kWnet	80	80	80	80	80	80
System Gross Electric Power (Output)	kWgross	89.44	89.44	89.44	89.44	89.44	89.44
Stack Components							
Bipolar Plates (Stamped)	\$/stack	\$1,976	\$572	\$506	\$489	\$489	\$486
MEAs							
Membranes	\$/stack	\$4,530	\$1,251	\$757	\$500	\$455	\$236
Catalyst Ink & Application (NSTF)	\$/stack	\$2,242	\$1,168	\$1,126	\$1,080	\$1,082	\$1,051
GDLs	\$/stack	\$2,661	\$795	\$447	\$267	\$238	\$102
M & E Cutting & Slitting	\$/stack	\$533	\$55	\$20	\$9	\$8	\$4
MEA Frame/Gaskets	\$/stack	\$1,493	\$265	\$146	\$137	\$145	\$130
Coolant Gaskets (Laser Welding)	\$/stack	\$219	\$43	\$43	\$33	\$31	\$31
End Gaskets (Screen Printing)	\$/stack	\$153	\$15	\$5	\$2	\$2	\$0
End Plates	\$/stack	\$177	\$70	\$60	\$52	\$51	\$45
Current Collectors	\$/stack	\$57	\$14	\$10	\$9	\$8	\$7
Compression Bands	\$/stack	\$10	\$9	\$8	\$6	\$6	\$5
Stack Housing	\$/stack	\$63	\$11	\$8	\$6	\$6	\$5
Stack Assembly	\$/stack	\$76	\$32	\$32	\$32	\$32	\$32
Stack Conditioning	\$/stack	\$176	\$58	\$55	\$48	\$42	\$29
Total Stack Cost	\$/stack	\$14,368	\$4,361	\$3,224	\$2,672	\$2,594	\$2,164
Total Stacks Cost (Net)	\$/kWnet	\$179.60	\$54.51	\$40.31	\$33.40	\$32.42	\$27.05
Total Stacks Cost (Gross)	\$/kWgross	\$160.65	\$48.76	\$36.05	\$29.87	\$29.00	\$24.20

Figure 11. Detailed stack cost for the 2013 automotive technology system

		2013 Automotive System					
Annual Production Rate	Sys/yr	1,000	10,000	30,000	80,000	100,000	500,000
System Net Electric Power (Output)	kWnet	80	80	80	80	80	80
System Gross Electric Power (Output)	kWgross	89.44	89.44	89.44	89.44	89.44	89.44
BOP Components							
Air Loop	\$/system	\$1,818	\$1,108	\$1,106	\$963	\$933	\$903
Humidifier & Water Recovery Loop	\$/system	\$2,915	\$441	\$252	\$180	\$170	\$133
High-Temperature Coolant Loop	\$/system	\$512	\$420	\$420	\$365	\$345	\$323
Low-Temperature Coolant Loop	\$/system	\$97	\$88	\$88	\$78	\$74	\$70
Fuel Loop	\$/system	\$350	\$304	\$295	\$265	\$255	\$241
System Controller	\$/system	\$171	\$151	\$137	\$103	\$96	\$82
Sensors	\$/system	\$1,755	\$1,190	\$921	\$680	\$625	\$231
Miscellaneous	\$/system	\$292	\$170	\$161	\$147	\$143	\$138
Total BOP Cost	\$/system	\$7,909	\$3,872	\$3,380	\$2,781	\$2,640	\$2,121
Total BOP Cost	\$/kW (Net)	\$98.87	\$48.40	\$42.24	\$34.76	\$33.00	\$26.52
Total BOP Cost	\$/kW (Gross)	\$88.43	\$43.29	\$37.79	\$31.09	\$29.52	\$23.72

Figure 12. Detailed balance of plant cost for the 2013 automotive technology system

		2013 Automotive System					
Annual Production Rate	Sys/yr	1,000	10,000	30,000	80,000	100,000	500,000
System Net Electric Power (Output)	kWnet	80	80	80	80	80	80
System Gross Electric Power (Output)	kWgross	89.44	89.44	89.44	89.44	89.44	89.44
Component Costs/System							
Fuel Cell Stacks	\$/system	\$14,368	\$4,361	\$3,224	\$2,672	\$2,594	\$2,164
Balance of Plant	\$/system	\$7,909	\$3,872	\$3,380	\$2,781	\$2,640	\$2,121
System Assembly & Testing	\$/system	\$149	\$103	\$102	\$101	\$101	\$101
Cost/System	\$/system	\$22,426	\$8,336	\$6,706	\$5,554	\$5,335	\$4,387
Total System Cost	\$/kWnet	\$280.33	\$104.20	\$83.82	\$69.42	\$66.68	\$54.83
Cost/kWgross	\$/kWgross	\$250.74	\$93.20	\$74.97	\$62.10	\$59.65	\$49.05

Figure 13. Detailed system cost for the 2013 automotive technology system

5.2 Cost Summary of the 2013 Bus System

Results of the cost analysis of the 2013 bus technology system at 200, 400, 800, and 1,000 systems per year production rates are shown below. Figure 14 details the cost of the stacks, Figure 15 details the cost of the balance of plant components, and Figure 16 details the cost summation for the system.

		2013 Bus System			
Annual Production Rate	Sys/yr	200	400	800	1,000
System Net Electric Power (Output)	kWnet	160	160	160	160
System Gross Electric Power (Output)	kWgross	186.22	186.22	186.22	186.22
Stack Components					
Bipolar Plates (Stamped)	\$/stack	\$1,155	\$1,086	\$1,027	\$1,008
MEAs					
Membranes	\$/stack	\$10,884	\$6,974	\$4,603	\$4,051
Catalyst Ink & Application (NSTF)	\$/stack	\$4,852	\$4,739	\$4,653	\$4,625
GDLs	\$/stack	\$8,399	\$5,674	\$3,839	\$3,386
M & E Cutting & Slitting	\$/stack	\$15	\$13	\$12	\$12
MEA Gaskets (Frame or Sub-Gasket)	\$/stack	\$769	\$695	\$675	\$625
Coolant Gaskets (Laser Welding)	\$/stack	\$207	\$175	\$135	\$194
End Gaskets (Screen Printing)	\$/stack	\$1	\$1	\$1	\$1
End Plates	\$/stack	\$143	\$133	\$124	\$121
Current Collectors	\$/stack	\$15	\$14	\$14	\$14
Compression Bands	\$/stack	\$17	\$16	\$15	\$14
Stack Insulation Housing	\$/stack	\$274	\$145	\$81	\$69
Stack Assembly	\$/stack	\$155	\$139	\$129	\$127
Stack Conditioning	\$/stack	\$797	\$389	\$371	\$296
Total Stack Cost	\$/stack	\$27,680	\$20,194	\$15,679	\$14,545
Total Cost for all 2 Stacks	\$/2 stacks	\$55,361	\$40,387	\$31,358	\$29,089
Total Stacks Cost (Net)	\$/kWnet	\$346.01	\$252.42	\$195.99	\$181.81
Total Stacks Cost (Gross)	\$/kWgross	\$297.29	\$216.89	\$168.40	\$156.21

Figure 14. Detailed stack cost for the 2013 bus technology system

		2013 Bus System			
Annual Production Rate	Sys/yr	200	400	800	1,000
System Net Electric Power (Output)	kWnet	160	160	160	160
System Gross Electric Power (Output)	kWgross	186.22	186.22	186.22	186.22
BOP Components					
Air Loop	\$/system	\$6,689	\$5,995	\$5,433	\$5,274
Humidifier & Water Recovery Loop	\$/system	\$1,420	\$1,170	\$1,007	\$966
High-Temperature Coolant Loop	\$/system	\$1,741	\$1,685	\$1,631	\$1,614
Low-Temperature Coolant Loop	\$/system	\$213	\$207	\$201	\$199
Fuel Loop	\$/system	\$1,006	\$959	\$914	\$900
System Controller	\$/system	\$584	\$533	\$488	\$474
Sensors	\$/system	\$4,545	\$4,155	\$3,771	\$3,649
Miscellaneous	\$/system	\$1,117	\$908	\$792	\$765
Total BOP Cost	\$/system	\$17,316	\$15,614	\$14,238	\$13,841
Total BOP Cost	\$/kW (Net)	\$108.22	\$97.58	\$88.98	\$86.51
Total BOP Cost	\$/kW (Gross)	\$92.99	\$83.85	\$76.46	\$74.33

Figure 15. Detailed balance of plant cost for the 2013 bus technology system

		2013 Bus System			
Annual Production Rate	Sys/yr	200	400	800	1,000
System Net Electric Power (Output)	kWnet	160	160	160	160
System Gross Electric Power (Output)	kWgross	186.22	186.22	186.22	186.22
Component Costs/System					
Fuel Cell Stacks	\$/system	\$55,361	\$40,387	\$31,358	\$29,089
Balance of Plant	\$/system	\$17,316	\$15,614	\$14,238	\$13,841
System Assembly & Testing	\$/system	\$464	\$339	\$275	\$262
Cost/System	\$/system	\$73,141	\$56,340	\$45,870	\$43,192
Total System Cost	\$/kWnet	\$457.13	\$352.12	\$286.69	\$269.95
Cost/kWgross	\$/kWgross	\$392.77	\$302.55	\$246.33	\$231.94

Figure 16. Detailed system cost for the 2013 bus technology system

6 Automotive Power System Changes and Analysis since the 2012 Report

This report represents the seventh annual update of the 2006 SA fuel cell cost estimate report³⁴ under contract to the DOE. The 2006 report (dated October 2007) documented cost estimates for fuel cell systems based on projected 2006, 2010, and 2015 technologies. Like the other five updates before it, this annual report updates the previous work to incorporate advances made over the course of 2013. These advances include new technologies, improvements and corrections made in the cost analysis, and alterations of how the systems are likely to develop. This 2013 analysis closely matches the methodology and results formatting of the 2012 analysis³⁵.

Like the 2012 update, the substantive changes in 2013 revolve around stack components. Argonne National Laboratory (ANL) provided updated 2013 stack polarization modeling results of 3M nanostructured thin film (NSTF) catalyst membrane electrode assemblies (MEA's). These results are used to re-optimize the stack operating conditions and catalyst loading for the 2013 cost estimation. Additional changes to the stack and BOP components involve updating the design and manufacturing methods to involve a handful of new technologies and the most up-to-date feedback from industry. These changes include re-examination of NSTF catalyst and platinum (Pt) material recycle, materials cost changes for the membrane and stack components, substitution of previously used tubular membrane air humidifier with a plate frame humidifier, and updates to quality control systems used in the manufacturing lines.

Noteworthy changes since the 2012 update report and the corresponding effects on system cost are listed in Figure 17 below.

³⁴ "Mass Production Cost Estimation for Direct H₂ PEM Fuel Cell Systems for Automotive Applications", Brian D. James, Jeff Kalinoski, Directed Technologies Inc., October 2007.

³⁵ "Mass Production Cost Estimation of Direct H₂ PEM Fuel Cell Systems for Transportation Applications: 2012 Update," Brian D. James, & Andrew B. Spisak, Strategic Analysis, Inc., 18 October 2012.

Change	Reason	Change from previous value	Cost (500k sy/year, \$/kW)
2012 Final Cost Estimate		NA	46.95
Plate Frame Humidifier	Switch to a much lower volume plate frame humidifier (as opposed to previous membrane tube humidifier).	\$0.51	\$47.46
Improved Catalyst Deposition Modeling	Re-examination of NSTF application including wastage and Pt recycling.	(\$0.20)	\$47.26
Realigned Compressor and Expander Efficiencies	Adjusted the air compressor (75% to 71%), exh. gas expander (80% to 73%), and motor (85% to 80%) efficiencies to match the status values modeled by ANL.	\$1.87	\$49.13
Updated Material Costs	Obtained new stainless steel and other material price quotations.	\$0.13	\$49.26
Updated Quality Control System	Re-examined quality control systems to ensure full functionality and improve cost realism.	\$0.00	\$49.26
Increased Platinum Cost	Increase in Pt base cost from \$1100/troy ounce to \$1500/troy ounce.	\$3.19	\$52.45
Other Misc. Changes	Updates made to improve and correct model i.e. LT and HT loop, CEM, and membrane adjustments.	(\$0.86)	\$51.59
Updated Polarization Data, Stack Operating Condition Optimization, and Imposition of Radiator Area Constraints	Improved membrane electrode assembly (MEA) performance data based on expanded 3M NSTF experimental results. Performed stack condition optimization to achieve lowest system cost. Limited radiator Q/DT for volume management within the auto.	\$3.24	\$54.83
Final 2013 Value		\$7.88	\$54.83

Figure 17. Changes in automotive power system costs since 2012 update

6.1 2013 ANL Polarization Model

Each analysis year, stack performance is re-examined to incorporate any improvements or refinements over the previous year. For 2013, Argonne National Laboratory revisited their stack polarization models based on first principal modeling of membrane electrode assemblies using 3M nanostructured thin film (NSTF) catalysts. Two new elements were added to the 2013 polarization model: 1) an increase of the upper stack pressure limit (from the 2.5 atm to 3.0 atm) based on incorporation of additional polarization data, and 2) a re-examination of stack temperature dependence.

6.1.1 Increase in the Stack Upper Pressure Limit

The stack pressure increase was fairly simple to implement as it entailed parameter verification at elevated temperatures and subsequent validation against 3M single cell experimental measurements at those conditions. Exploration of a higher upper pressure limit was deemed desirable as the 2012 analysis showed the lowest system cost occurred at conditions of peak pressure (at that time 2.5atm), thereby opening the possibility of even lower system cost if the pressure was allowed to further increase.

6.1.2 Temperature as an Independent Variable

Re-examining the temperature dependence of the stack proved more complex. The water balance within the MEA is highly sensitive to cell temperature as the air and hydrogen streams are at, or at least very close to, water saturation conditions, thus lower stack temperature typically correlates with greater amounts of liquid water production and higher stack temperature with vapor water production. The balance of water not only affects polarization but also the amount of waste heat that needs to be transferred to the coolant to maintain a target temperature: the greater the liquid water production, the greater the radiator heat load. As will be discussed below, radiator sizing is an area of particular

focus for 2013 and thus it was necessary to fully track cell temperature as it affects both radiator heat load and cell performance. The polarization performance used in the 2012 analysis used an “optimal temperature” determined by ANL in separate modeling analysis and thus did not allow independent variation of temperature as part of cost optimization. Consequently for the 2013 analysis, the polarization model was expanded to incorporate temperature as an independent parameter (in addition to cathode platinum loading, pressure, air stoichiometry, and cell voltage) and thus to better assess the effect of temperature on electrochemical performance and on radiator size.

6.1.3 2013 Polarization Model and Resulting Polarization Curves

The full ANL polarization model was used to create a data base of expected 2013 polarization performance with clearly defined stack conditions in the expected range for automotive fuel cell operation. Each run of the model was defined by stack pressure, catalyst loading, air stoichiometry, cell voltage, temperature, and power density. Temperature was defined as the coolant temperature exiting the stack. Based on this data base of operating points, a simplified polarization model was developed to allow rapid assessment of stack power density based on input of the other five variables. The simplified polarization model uses empirical curve fit coefficients to assess polarization performance at a designated reference temperature (T_{upper} , a function of pressure and air stoichiometric ratio, defined as the maximum temperature permissible due to water balance and membrane dry out constraints), with subsequent iterative adjustment of current density to correspond to operation at other temperatures. While temperature is an independent variable in the simplified model, its upper limit is bounded at T_{upper} and its lower limit is bounded by (T_{upper} minus 10°C) (selected as a practical limitation to maintain accuracy within simplified analysis framework).

Figure 18 plots the 2013 ANL voltage and power density modeling results compared to the 2012 results. As immediately seen, the power density is down considerably compared to 2012.³⁶ Handling of water within the cells is suspected to be a main factor in the performance difference although a full explanation requires additional analysis and is planned as part of the 2014 cost analysis.

6.2 Increase in Platinum Price

The year to year price of Platinum is generally held constant to insulate the system cost analysis from arbitrary market price fluctuations. However, over the last several years, the price of Pt bullion has increased and has seemingly reached a new plateau price. Consequently, the price of Pt is raised from its previous \$1,100/troy ounce value to a new 2013 analysis value of \$1,500/troy ounce.

6.3 Imposition of Q/Δ T Radiator Constraint

As directed by DOE and as consistent with DOE’s 2012 MYRD&D plan, a radiator Q/ΔT constraint was placed on the system for the first time in 2013. Q/ΔT is a measure of radiator size where Q is the main fuel cell radiator’s heat rejection duty and is a function of the temperatures and mass flows of the stack inlet and outlet streams, stack efficiency (i.e. how much heat is generated within the stack), and the extent of liquid product water produced (i.e. how much energy goes into changing the product water

³⁶ Although stack operating conditions differ between 2012 and 2013, even at the same conditions, 2013 polarization performance is lower than 2012 polarization.

from liquid to vapor). ΔT is the delta (i.e. difference) between the stack coolant exit temperature (typically 80-94°C) and the worst case ambient air temperature (assumed to be 40°C). A large value of $Q/\Delta T$ signifies the need for a large radiator and conversely, a small value of $Q/\Delta T$ signifies a small radiator. The DOE 2017 target for $Q/\Delta T$ is $<1.45 \text{ kW}_{\text{th}}/\text{°C}$ and consequently this limit was imposed on the 2013 automotive analysis. Previous analysis did not impose a $Q/\Delta T$ limit and the 2012 value was $\sim 1.7 \text{ kW}_{\text{th}}/\text{°C}$ implying a larger radiator than the automotive community (and DOE) feels is reasonable to incorporate into a light duty automobile.

While the computation of $Q/\Delta T$ appears simple (as it is merely the ratio of two easily understood parameters), in practice it is more complex. $Q/\Delta T$ is quite sensitive to both Q and ΔT and Q varies considerably depending on the extent of cell production water condensation. Water condensation is a function of temperature and gas flows within the cell and is more accurately analyzed within the ANL full polarization model than within a cost model. Consequently, as will be discussed below, stack conditions leading to the $Q/\Delta T$ constraint are assessed by ANL rather than within the SA cost model.

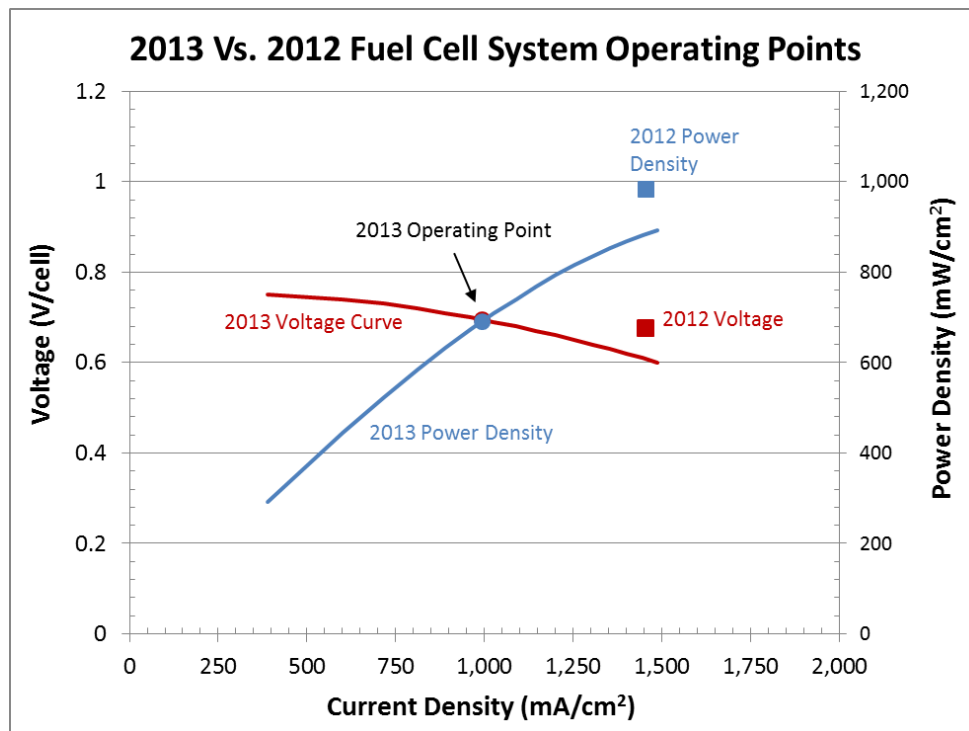


Figure 18. 2013 vs. 2012 ANL voltage and power density modeling results.
 (2012 System Operating Point: 0.676V at 1,456 mA/cm² with 243cm²/cell active area,
 2013 System Operating Point: 0.695V at 995 mA/cm² with 360.3cm²/cell active area)

6.4 Optimization of Stack Operating Conditions for Minimum System Cost

To select stack operating conditions at system design rated power (80 kWe), five parameters were simultaneously varied with system cost recorded for each set of operating conditions. In this manner, stack conditions leading to the lowest system cost were determined.

Five variables were varied over the ranges listed in Figure 19. Only stack operating conditions consistent with acceptable cell water balance and membrane hydration conditions were considered as the polarization model inherently applied that constraint. However, an additional constraint of $Q/\Delta T \leq 1.45$ kW_{th}/°C was applied to maintain a radiator size acceptable for integration within a light duty vehicle (as mentioned in Section 6.2).

Variable	Parameter Range
Stack inlet pressure	1.5 - 3.0 atm
Cell voltage	0.6 - 0.8 volts
Cathode catalyst loading	0.10 - 0.25 mg Pt/cm ²
Air stoichiometric ratio	1.5 – 2.5
Coolant stack exit temperature	~75°C - ~95°C

Figure 19. Stack operating conditions varied as part of system cost optimization

In past light duty automotive fuel cell system analysis, the optimization was conducted by applying a Monte Carlo analysis using the At-Risk™ Excel add-in for the DFMA™ cost model. However for 2013, system optimization was conducted by ANL as their computation of $Q/\Delta T$ was judged to be more accurate. Thus, ANL ran their full polarization model coupled with a simplified SA-supplied cost model (see Section 0) to determine stack operating conditions leading to lowest overall system cost contingent on constraints for cell water balance, membrane dry-out, and radiator size ($Q/\Delta T$). Based on this optimization, the 2013 automotive system beginning-of-life (BOL) stack design conditions at peak power are:

- 0.695 volts/cell
- 995 mA/cm² current density
- 692 mW/cm² power density
- 2.5 atm stack inlet pressure
- 92.3°C (outlet coolant temperature)
- 0.153 mgPt/cm² total catalyst loading

To corroborate these findings, an optimization was also conducted using the previously applied methodology i.e. At-Risk™ Monte Carlo analysis based on the full cost model and simplified polarization model. Although the full cost model contains a lower precision $Q/\Delta T$ computation compared to the full ANL polarization model, the results are similar and comparison of results allows corroboration of the ANL optimal stack parameters. The montage of graphs in Figure 20 and Figure 21 show system cost plotted against each of the stack operating parameters. Each blue dot corresponds to an individual Monte Carlo simulation run. Only points within the constraint limits are plotted³⁷. The red trend lines connecting the lower limits of the iterations show the general cost trend for each variable. Thus we observe that cost generally increases with rising catalyst loading, air stoichiometry, system efficiency, and cell voltage. Cost generally decreases with rising coolant temperature and $Q/\Delta T$. Stack pressure shows an unusually double minimum that is not fully understood but will be explored in greater detail in

³⁷ Only points leading to total system costs at or below \$80/kW are plotted. There are many additional combinations of parameters that lead to higher system cost.

future years of the analysis. However, overall there is very high agreement between the ANL and SA cost optimizations.

SA Monte Carlo Optimization of Operating Conditions

(at 500k systems/year)

(Very similar but not exactly the same as ANL optimization.
ANL optimization used for final parameter selection since Q/ΔT computation was more accurate.)

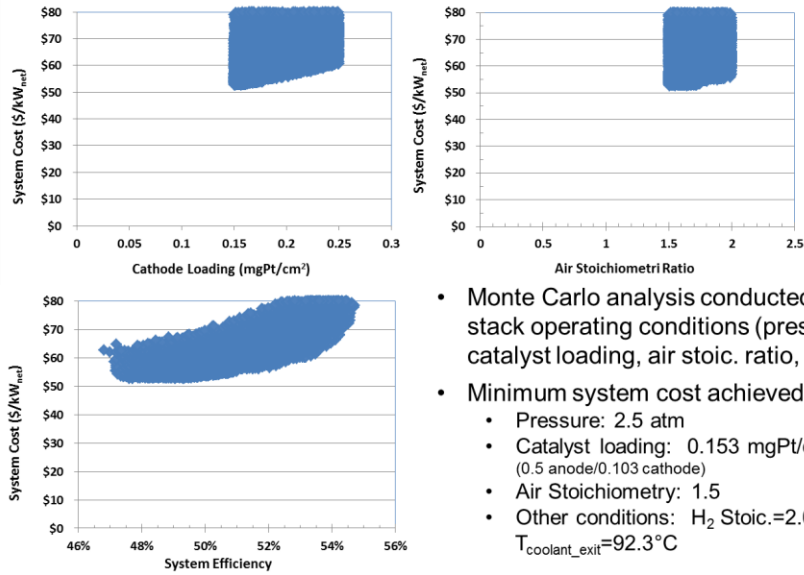
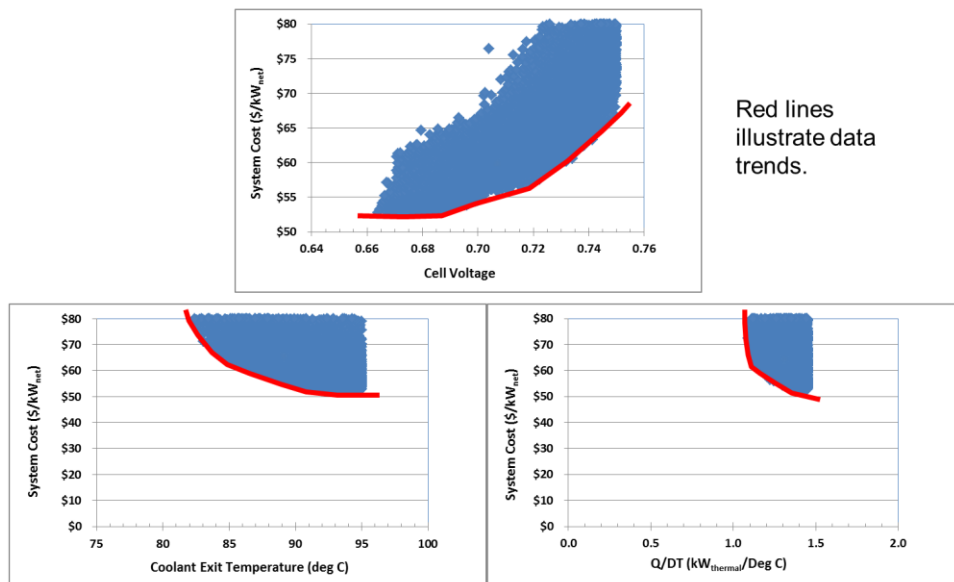


Figure 20. Monte Carlo results for catalyst loading, air stoichiometry, and system efficiency

SA Monte Carlo Optimization of Operating Conditions

(at 500k systems/year)

(Very similar but not exactly the same as ANL optimization)



20

Figure 21. Monte Carlo results for cell voltage, coolant exit temperature, and Q/ΔT

6.5 Plate Frame Humidifier

A full DFMA™ analysis of a plate frame humidifier system has been incorporated into the 2013 auto and bus fuel cell systems. The plate frame air humidifier was examined as a potentially lower cost and smaller volume alternative to the previously modeled tubular membrane humidifier from the 2012 fuel cell system design. Compared to tubular membrane designs, the plate frame membrane humidifiers allow a thinner membrane (5 microns) to be used. Since membrane thickness correlates with required membrane area for a given amount of water transport, plate frame humidifiers are expected to be more compact and lower cost than tubular humidifiers.

The design and projected manufacturing methods for the 2013 plate frame humidifier are based on publicly available information from W.L Gore & Associates, Inc. and DPoint Technologies Inc.³⁸ Both companies were consulted and provided input during the cost analysis process but information transfer was entirely public domain and non-proprietary. The resulting design is thus a Strategic Analysis Inc. interpretation of the Gore/DPoint Technologies unit, and may differ in design and manufacturing process from the actual unit. However, it is expected that the key cost influencing aspects have been adequately captured in the cost analysis.

The modeled Gore plate frame humidifier design is composed of multiple stacked cell pouches made of a 4-layer composite membrane with stainless steel flow fields inside the pouch and stainless steel rib spacers between each pouch in the stack. The total process consists of eight steps:

1. Fabrication of Composite Membranes
2. Fabrication of Stainless Steel Flow Fields and Separators
3. Pouch Formation
4. Stainless Steel Rib Formation
5. Stack Formation
6. Formation of the Housing
7. Assembly of the Composite Membrane and Flow Fields into the Housing
8. System Testing

The cost for the membrane humidifier is estimated to be about \$95 for an 80-cell pouch stack (sized for an 80-kWe automotive fuel cell system) including housing, assembly, and testing at 500,000 systems per year. Over 50% of the total cost is attributed to materials, primarily the composite membrane.

These cost results are based on a humidifier containing 1.6 m² of membrane area. Much discussion surrounded selection of this membrane area. Separately funded experimental testing was conducted at Ford on the Gore/DPoint humidifier and showed very good correlation with ANL modeling predictions³⁹. Both experimental and modeling results showed that ~2m² of humidifier membrane area was required for an 80kWe fuel cell system at DOE specified operating conditions. However, when ANL applied their

³⁸ Johnson, William B. "Materials and Modules for Low-Cost, High Performance Fuel Cell Humidifiers," W.L. Gore & Associates, Inc., presentation at the 2012 DOE Hydrogen and Fuel Cell Program Annual Merit Review, Washington, DC, 17 May 2012.

³⁹ Ahluwalia, R., K., Wang, X., , *Fuel Cells Systems Analysis*, Presentation to the Fuel Cell Tech Team, Southfield, MI, 14 August, 2013.

performance model at the SA/ANL specified system operating conditions, the required membrane area dropped to 0.5m². This significant membrane area reduction is due primary to higher pressure, lower air flow, and higher temperature conditions included in the model. Additionally, Gore raised a concern that membrane performance degradation was not factored into any of the modeled estimates. Consequently, a value of 1.6m² humidifier membrane area was selected for SA cost modeling to reflect both a deliberate humidifier oversizing (to offset the expected but quantitatively unknown rate of degradation) and a conservative estimate. DPoint was consulted on this area selection and expressed acceptance. Gore continues to prefer the use of 2 m² membrane area (or even greater).

Section 7.2.2.3 contains additional details of each humidifier processing step, individual component cost estimates, and a single-variable sensitivity analysis to investigate the impact membrane area requirements and other key parameters.

6.6 Low-Cost Gore MEA Manufacturing Process

To explore potential cost reduction of the catalyst coated membranes (CCMs) for the fuel cell system, a novel low-cost catalyzed membrane fabrication method⁴⁰ developed by W.L. Gore & Associates was analyzed using a full DFMATM cost analysis methodology. The Gore MEA manufacturing approach is based on roll-to-roll MEA fabrication methods being developed by Gore under DOE funding. Even though the Gore MEA method was analyzed, the polarization performance of the Gore MEAs has not been sufficiently characterized to allow incorporation in the 2013 cost analysis. Thus the 2012 MEA fabrication method (i.e. 3M nanostructured thin film (NSTF) catalyst application onto an ePTFE-supported ionomer membrane) is used for the 2013 baseline system so as to be consistent with available polarization data. However, a comparison was made between the NSTF and Gore MEA fabrication methods, assuming equal polarization performance, and is shown later in this section.

The Gore MEA modeled system draws exclusively from non-proprietary input and is based on an SA interpretation of open-literature sources for composite membrane fabrication. The modeled MEA is composed of three sequential die-slot coating roll-to-roll fabrication steps:

1. **Cathode Formation:** Carbon-supported platinum cathode catalyst ink deposited onto a reusable Mylar substrate via die-slot coating followed by a moderate temperature drying furnace (6.5µm finished (dry) thickness). Ink composition derived from Umicore US Patent #7,141,270.
2. **ePTFE Supported Ionomer Electrolyte Formation:** Die-slot coating of a Nafion® ionomer onto the cathode layer followed by unrolling and lowering of an expanded polytetrafluoroethylene (ePTFE) layer onto the wet ionomer, followed by furnace drying (15µm finished (dry) thickness). Composition and application parameters derived from DuPont US Patent #7,648,660 B2.
3. **Anode Formation:** Die-slot coating of carbon-supported platinum anode catalyst ink onto the electrolyte layer followed by furnace drying (3µm finished (dry) thickness). Ink composition derived from Umicore US Patent #7,141,270.

⁴⁰ Busby, F. Colin. "Manufacturing of Low-Cost, Durable Membrane Electrode Assemblies Engineered for Rapid Conditioning," W.L. Gore & Associates, Inc., presentation at the 2012 DOE Hydrogen and Fuel Cell Program Annual Merit Review, Washington, DC, 16 May 2012.

Figure 22 schematically details these three processes. The DFMA™ cost analysis of each step is based on the capital cost of the equipment, processing speed, material usage, expected yields, labor usage, and electric utility consumption. Unlike most other components within the automotive fuel cell system (also see bus vertical integration description in Section 2.3), the catalyzed MEA is modeled as if purchased from a lower tier parts supplier rather than fabricated in-house by the fuel cell system integrator. As such, markup for profit, research and development, and other general and administrative expenses is added to the material and manufacturing cost to derive an overall CCM cost projection.

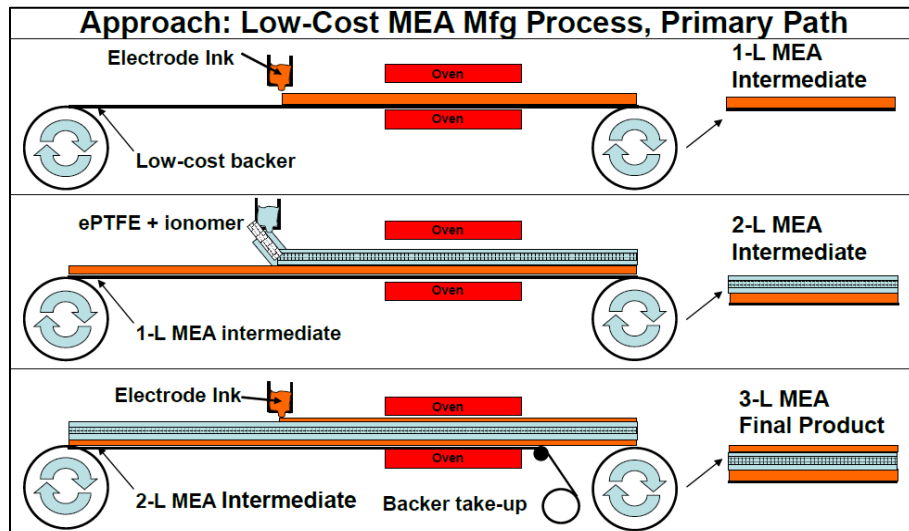


Figure 22. W.L.Gore MEA 3-step manufacturing process. Source: Busby, F. Colin. “Manufacturing of Low-Cost, Durable Membrane Electrode Assemblies Engineered for Rapid Conditioning,” W.L. Gore & Associates, Inc., presentation at the 2012 DOE Hydrogen and Fuel Cell Program Annual Merit Review, Washington, DC, 16 May 2012.

Cost results for the Gore MEAs are shown in Figure 23. The anode and cathode processes have similar manufacturing costs with material costs being higher for the cathode than the anode (logically reflecting the higher platinum loading needed on the cathode). DFMA™ cost analysis was originally planned to assess the cost of the expanded polytetrafluoroethylene (ePTFE) substrate used as a support in the electrolyte layer. However, investigation concluded that the critical processing steps associated with ePTFE manufacture (particularly those steps for optimal fuel cell performance) are largely maintained as trade secrets rather than open literature or patented information. Consequently, a quote-based approach was used to evaluate ePTFE cost. Details of ePTFE pricing appear in section 7.1.2.2.

Annual Production Rate	1,000	10,000	30,000	80,000	100,000	500,000
Material (\$/stack)	\$349	\$332	\$327	\$323	\$322	\$317
Manufacturing (\$/stack)	\$1,045	\$101	\$34	\$25	\$20	\$12
Tooling (Mylar Web) (\$/stack)	\$1.08	\$0.90	\$0.89	\$0.87	\$0.85	\$0.74
Total Cost (1395.59672379935)	\$1,396	\$433	\$362	\$349	\$343	\$330
Total Cost (17.4449590474918)	\$17.44	\$5.42	\$4.52	\$4.36	\$4.29	\$4.12

Figure 23. Cost breakdown for the Gore MEA anode application

Annual Production Rate	1,000	10,000	30,000	80,000	100,000	500,000
Material (\$/stack)	\$988	\$603	\$463	\$351	\$327	\$194
Manufacturing (\$/stack)	\$1,586	\$152	\$51	\$37	\$30	\$18
Total Cost (\$/stack)	\$2,574	\$754	\$514	\$389	\$357	\$212
Total Cost (\$/kWnet)	\$32.17	\$9.43	\$6.42	\$4.86	\$4.47	\$2.65

Figure 24. Cost breakdown for the Gore MEA electrolyte application

Annual Production Rate	1,000	10,000	30,000	80,000	100,000	500,000
Material (\$/stack)	\$669	\$660	\$657	\$655	\$654	\$651
Manufacturing (\$/stack)	\$1,043	\$100	\$34	\$13	\$20	\$12
Total Cost (\$/stack)	\$1,713	\$759	\$691	\$668	\$674	\$663
Total Cost (\$/kWnet)	\$21.41	\$9.49	\$8.63	\$8.35	\$8.43	\$8.28

Figure 25. Cost breakdown for the Gore MEA cathode application

A single-variable sensitivity was applied to the Gore MEA fabrication process to identify the largest suspected cost driven parameters. The Tornado Chart in Figure 26 displays this sensitivity and results indicate that ePTFE costs can have a significant impact on MEA costs. Other possible cost drivers include the MEA line speed, ionomer cost, and equipment capital cost, however MEA uncertainty is a maximum of +/- 7% for each parameter. The parameter values used in the sensitivity analysis are shown in Figure 27.

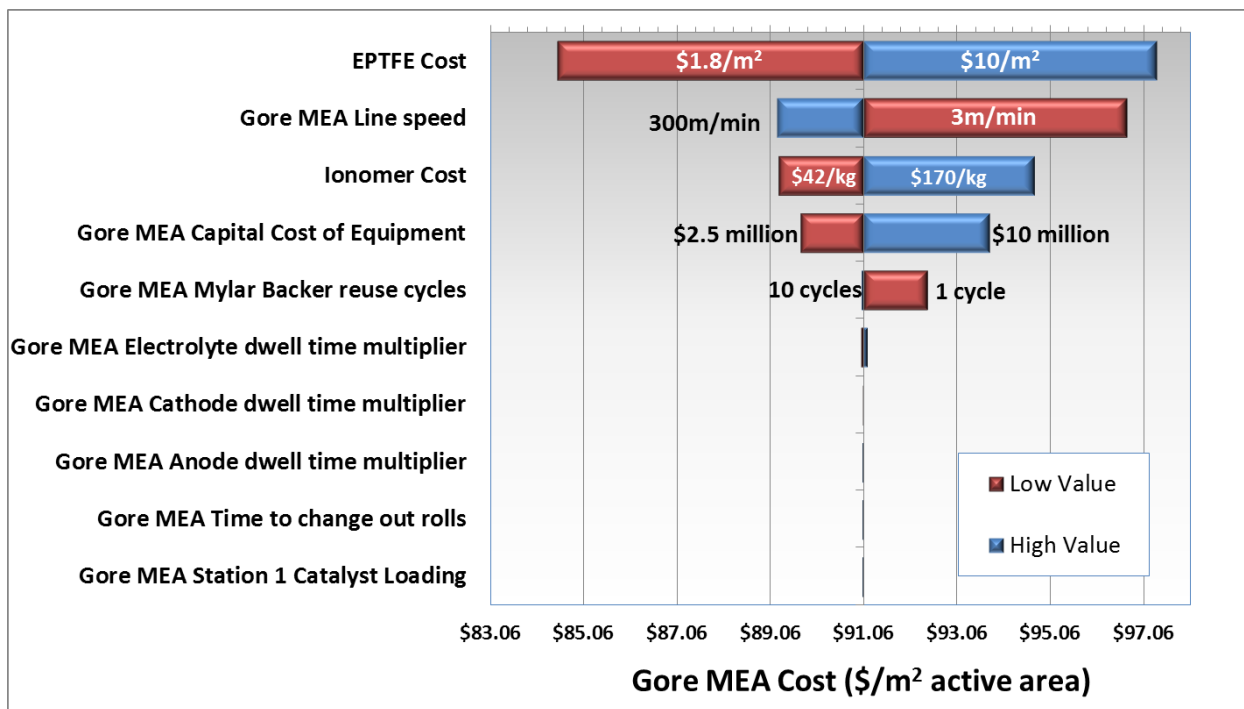


Figure 26. Single-variable sensitivity Tornado Chart for Gore low-cost MEA

Gore MEA Sensitivity Limits for Tornado Chart					
Parameter	Units	Low Value	Base Value	High Value	Rationale
EPTFE Cost	\$/m ²	1.8	6	10	Price of EPTFE gathered from multiple sources suggesting a range based on quality of PTFE, national origin, and quality/grade (fuel cell grade vs. textile grade).
Gore MEA Line speed	m/min	3	10	300	DuPont Patent US 7,648,660 B2 states 3 m/min to be the upper end of the most preferred line speed. However, companies experienced in converting machinery suggest as high as 300m/min.
Ionomer Cost	Multiplier (\$/kg)	0.5 (\$42.44)	1 (\$84.89)	2 (\$169.77)	Membrane material costs vary significantly.
Gore MEA Capital Cost of Equipment	Multiplier (\$)	0.5 (\$2.5 mil)	1 (\$5 mil)	2 (\$10 mil)	Base value based on summation of individual manufacturing equipment components.
Gore MEA Mylar Backer reuse cycles	cycles	1	5	10	Engineering judgement to capture range of potential reuse cycles.
Gore MEA Electrolyte dwell time multiplier	Multiplier (min)	0.5 (3)	1 (6)	2 (12)	From DuPont Patent US 7,648,660 B2: oven drying times are between 1 and 3 minutes for each of the three heating zones for a hot air convection oven. At the "base value" the dwell time is ~6 minutes .
Gore MEA Cathode dwell time multiplier	Multiplier (min)	0.5 (0.3)	1 (0.6)	2 (1.3)	Oven drying times for cathode were calculated based on the energy needed to remove a typical solvent composition. The "base value" corresponds to a dwell time of 0.6 min.
Gore MEA Anode dwell time multiplier	Multiplier (min)	0.5 (0.1)	1 (0.2)	2 (0.4)	Oven drying times for anode were calculated based on the energy needed to remove a typical solvent composition. The "base value" corresponds to a dwell time of 0.2 min
Gore MEA Time to change out rolls	min	1	10	-	Discussions with converting machinery users suggests a range of 1 to 10 min for roll change-out.
Gore MEA Station 1 Catalyst Loading	mg/cm ²	-	0.05	0.13	The "base value" of 0.05 mgPt/cm ² considers the Gore MEA station 1 to be the application of the anode, while the catalyst loading of 0.13 mgPt/cm ² considers the Gore MEA station 1 to be the application of the cathode.
2013 Gore MEA Cost at 500,000 systems per year (\$/m²)				\$91.06	

Figure 27. Single-variable sensitivity limits used in the Gore low-cost MEA Tornado Chart.

Figure 28 compares the projected costs of the Gore CCM manufacturing method described previously with those of the 3M NSTF fabrication method used in the current 2013 baseline system cost analysis. (The Gore low-cost MEA manufacturing technique was not adopted into the baseline 2013 cost analysis because performance data is not available.) The NSTF fabrication method is based on a catalyst application to an ePTFE-supported Nafion® ionomer membrane. Catalyst application is modeled as vacuum magnetron sputtering of Pt/Co/Mn catalyst onto a high-surface-area substrate of PR-149 whiskers grown by sublimation followed by annealing. Membrane fabrication is modeled as occlusion of ePTFE in Nafion® ionomer solution within a separate factory setting. Refer to Section 7.1.3 for a full description of 3M NSTF CCM manufacturing process.

As shown in Figure 28, the capital cost of both CCMs is seen to decrease with increasing automotive system annual production rate. While the material costs for both Gore and 3M CCMs are similar (as is to be expected since material cost is dominated by platinum and both approaches have equal catalyst loading), the processing costs for the 3M CCM are greater than for the Gore CCM (also to be expected since the Gore approach uses non-vacuum chamber technology and is capable of higher liner speeds). Overall, the Gore CCM is estimated to be slightly less expensive than the 3M CCM. As production rate increases, the cost differential between the two different CCMs decreases in absolute terms. At the highest production rates considered (500,000 automotive systems per year), the Gore CCM processing costs are projected to approach just a few dollars per m² active area. Note that this analysis compares CCM costs on a per-square-meter of membrane basis, assuming the exact same engineering performance of the CCMs; the analysis does not capture potential differences in polarization performance and durability between the two CCMs.

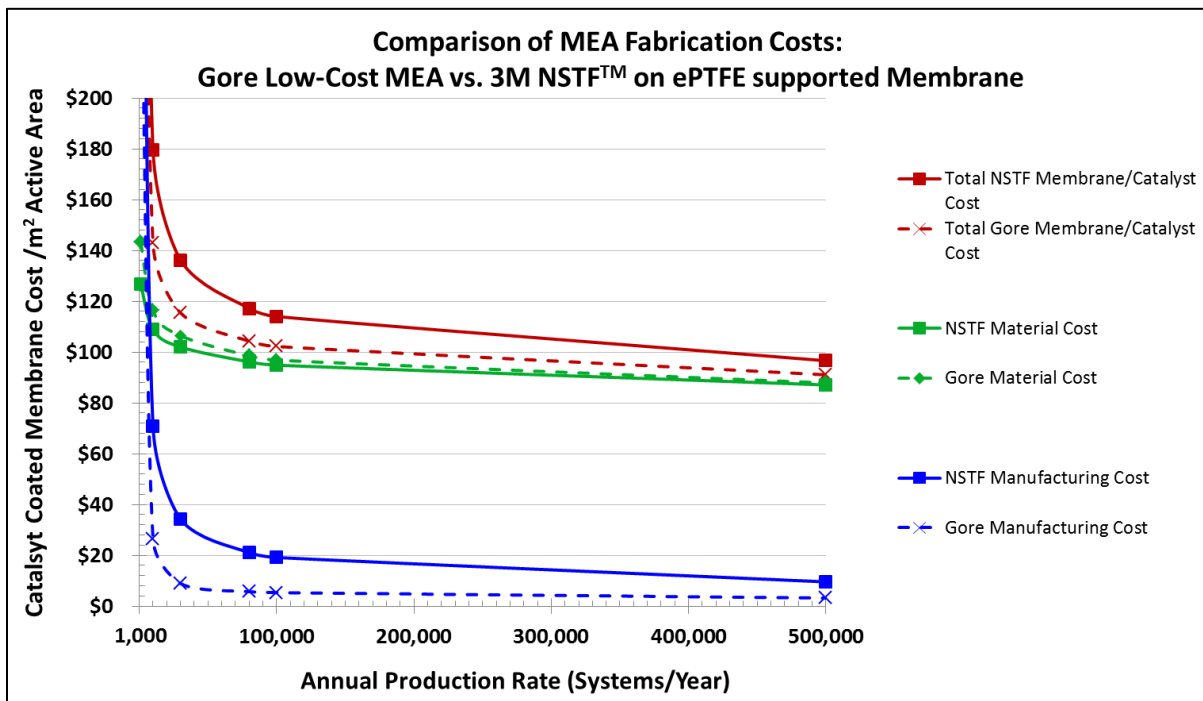


Figure 28. Comparison of the Gore low-cost MEA and 3M NSTF™/Membrane Catalyst Coated Membrane manufacture processes

6.7 Eaton-style Multi-Lobe Air Compressor-Expander-Motor (CEM) Unit

6.7.1 Design and Operational Overview

The air compression system for the automotive power system is based on a Honeywell-designed centrifugal air compressor mated to a radial inflow exhaust gas expander and a 165,000 rpm permanent magnet motor. In search for alternative and less expensive CEM units, a twin vortex, Roots-type air compressor, expander, motor was also analyzed in 2013. The modeled twin-vortex CEM is based on non-proprietary design and concept details from Eaton Corporation and combines public literature

relating to existing commercial turbocharger products with details from Eaton’s DOE funded CEM project⁴¹. The basis for the cost analysis is thus SA’s interpretation of a future Eaton technology CEM and is thus referred to as an “Eaton-style” CEM. A complete DFMATM analysis of the Eaton-style CEM was conducted based on a 5-shaft design. The auto Eaton-style air compressor unit (including motor and motor controller) is estimated at \$816 at 500,000 units per year.

The baseline compressor is modeled on Eaton’s R340 supercharger which is in Eaton's Twin Vortices Series (TVS). The unit is a Roots-type supercharger featuring 2 four-lobed rotors, high-flow inlet and outlet ports, and the capability to achieve high efficiency over a wide air flow range. The isentropic efficiency map of the R340 unit is shown in Figure 29. The compressor is mechanically mated to a 24,000 rpm (max) high efficiency brushless motor as shown in Figure 30. Intermeshing of the counter-rotating vortices is shown in Figure 31.

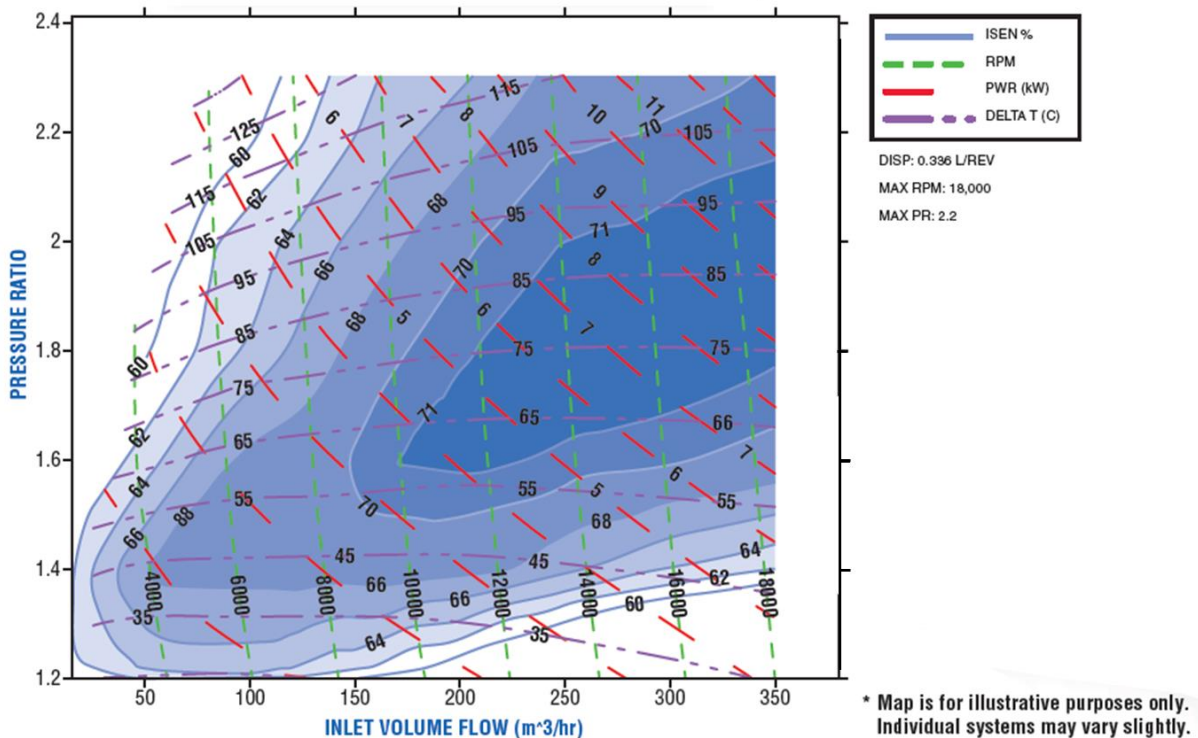


Figure 29. Isentropic efficiency map of the Eaton R340 supercharger⁴² (figure courtesy of Eaton)

⁴¹ “Roots Air Management System with Integrated Expander”, Dale Stretch, William Eybergen, Brad Wright, Eaton Corporation, FY 2013 Annual Progress Report, under DOE Contract Number: DE-EE0005665.

⁴² Figure downloaded from: <http://www.rousfuelcell.com/pdf/roush-recharging-brochure.pdf>



Figure 30. Exterior view of the Eaton R340 supercharger (figure courtesy of Eaton)



Figure 31. Interior view of the R340 supercharger vortices⁴³ (figure courtesy of Eaton)

The Eaton R340 has a peak compression ratio of ~ 2.5 but peak efficiency occurs around a compression ratio of 1.8. Thus the Eaton compressor is potentially applicable to both the auto system (stack pressure ~ 2.5 atm) and the bus system (stack pressure ~ 1.8 atm). Details of the Eaton compressor as it applies to the automotive system appear in Figure 32. Updates to efficiencies since the 2012 analysis are reviewed in Section 6.10. Note however, that Eaton compressor efficiencies are target values: measured efficiencies will be used in the cost analysis as they become available.

⁴³ Figure downloaded from <http://www.roughfuelcell.com/pdf/rough-echarging-brochure.pdf>

Parameter	Value
Compressor Type	Roots (twin vortices)
Compression Ratio at Design Point	2.67
Air Flow Rate at Design Point	244 kg/hour (68 g/s)
Compression Efficiency ⁴⁴ at Design Point	71%
Expander Type	Multi-Lobe
Expander Efficiency at Design Point	73%
Combined Motor and Motor Controller Efficiency ⁴⁵	80%

Figure 32. Details of the Eaton auto air compressor

6.7.2 CEM Manufacturing Process

The Eaton-style CEM unit analyzed is based on a 5-shaft design (2 compressor drive shafts, 2 expander drive shafts, and a motor shaft), as seen in Figure 33, and consists of a motor, motor controller, compressor rotors, expander rotors, drive shafts, couplings, bearings, housing, and other components. A schematic of the SA conceptual design is shown in Figure 34.

On the expander side, the motor shaft contains a timing gear that drives speed reducing gears on the expander drive shafts. The expander drive shafts are made of high carbon steel and precision machined with a key slot to capture the expander rotors. The expander rotors have an aluminum core (extruded with a twist) that is surrounded by an overmold of fiberglass filled high density polyethylene (HDPE). The expander housing and manifold are injection molded fiberglass filled HDPE (the expander sees lower temperatures than the compressor and can be made out of less expensive plastic materials). Ball bearings and needle bearings are used to suspend and capture the rotors inside the expander housing between the bearing plate and the expander manifold.

On the compressor side, the motor shaft is attached to a torsional coupling that attaches to one of the compressor drive shafts with multiple dowels for alignment. Two timing gears drive the second compressor shaft at the same rotation speed. Each shaft has a key slot where the rotor slides on and attaches. Each rotor-shaft assembly has both ball bearings and needle bearings that hold it in place against a bearing plate and the compressor housing.

Shaft seals are required to isolate oil within the gear housing and maintain pressure within the compressor and expander. Figure 35 and Figure 36 contain a complete list of compressor/motor unit components along with selected material, type of manufacturing process used in the analysis, dimensions, quantity, mass, and estimated cost. Additional details on manufacturing processes are discussed in Section 8.3 (bus air compressor section).

⁴⁴ Compression efficiency is defined as isentropic efficiency.

⁴⁵ Combined efficiency is defined as the product of motor efficiency and motor controller efficiency.

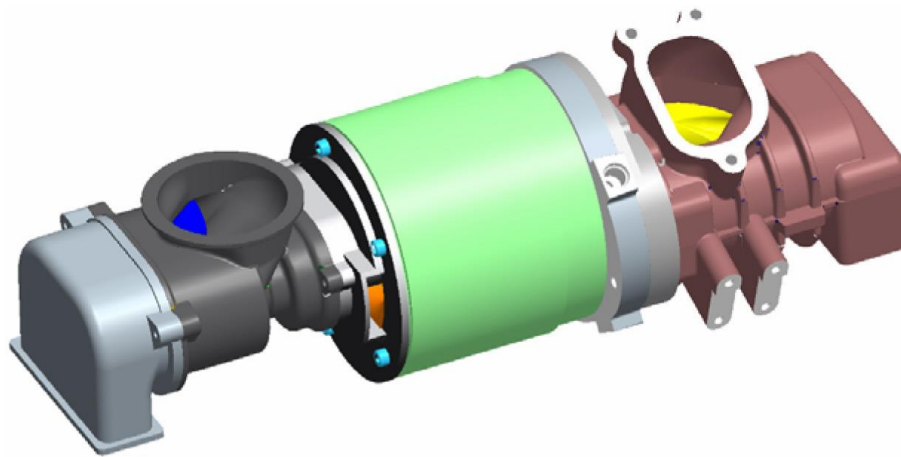


Figure 33. Image of Eaton 5-shaft CEM design. Source: 2013 Annual Progress Report, *Roots Air Management System with Integrated Expander*, Eaton Corporation.

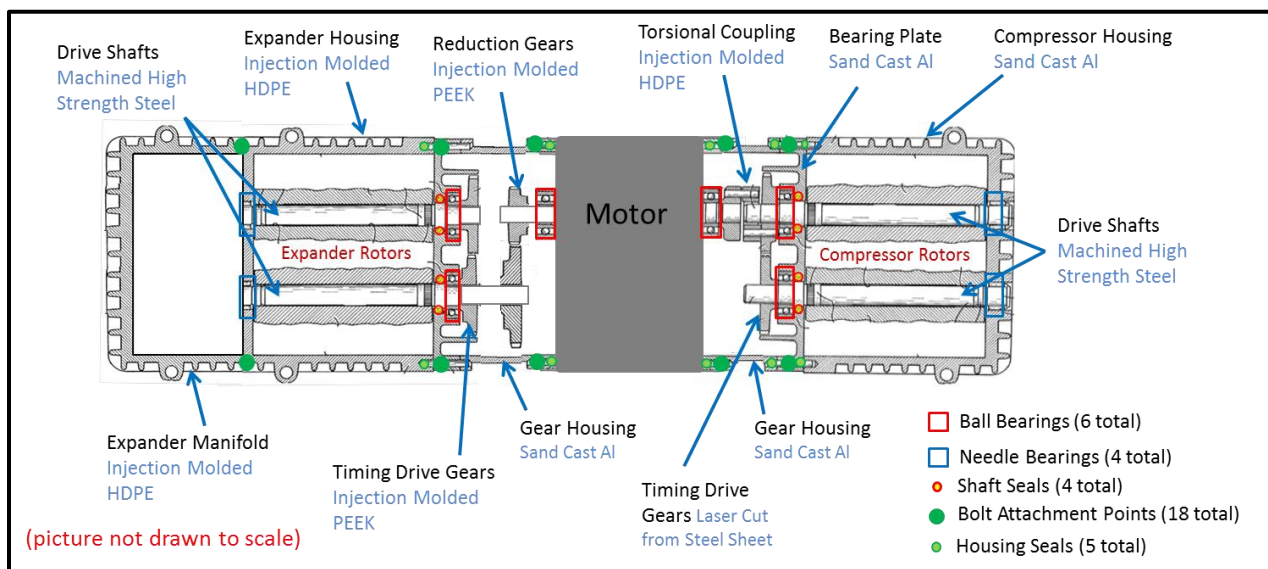


Figure 34. Schematic of cross-sectional view of SA's concept for Eaton 5-shaft CEM design. Source: Drawing derivation from US patent 4,828,467: Richard J. Brown, Marshall, Mich. "Supercharger and Rotor and Shaft Arrangement Therefor", Eaton Corporation, Cleveland, Ohio, May 9, 1989.

Cost results in Figure 35 and Figure 36 were estimated at manufacturing rates of 1,000 and 500,000 systems per year. These results were not included in the 2013 auto final values, but were used as a comparison to the Honeywell-style design currently modeled. The 2013 auto cost analysis encompasses six manufacturing rates, however the cost results for the Eaton-style CEM were only estimated for two manufacturing rates so as to compare to Eaton cost estimates as part of their DOE project.

Assembly and manufacturing markup are included in the SA cost estimate, and assume a 15% markup on all the compressor and expander components and a 10% markup for the motor and motor controller components. The most expensive part of the CEM is the motor controller and motor. A full DFMATM analysis was completed for the motor controller in the 2012 analysis and is also used in the Eaton-style

CEM analysis after appropriate scaling for input power. The electric motor for the CEM was considered a purchased component with its cost based on a quotation obtained by Eaton under their DOE project⁴⁶. A full DFMATM analysis of the electric motor was not conducted. Section 8.3 further discusses issues related to the Eaton compressor.

⁴⁶ Eaton/DOE Contract Number DE-EE0005665.

SA Cost Summary for Eaton 5-Shaft Compressor/Expander/Motor Unit							Annual Production Rate (systems/year)	
							1,000	500,000
	Material	Manufacturing Method	Qty/sys	Dimensions	kg/part	kg/sys	\$/system	
Compressor Components								
Compressor Rotors	6061-T1 Aluminum	Extrusion w/twist	2	15cm x 7cm max OD	0.70	1.40	\$76.39	\$32.24
Compressor Housing	6061 Aluminum	Sand Casting	1	25cm (width) x 15cm (height) x 17cm (length) x 1cm (aver. Thickness)	3.778	3.778	\$26.93	\$18.38
Compressor Bearing Plate	6061-T1 Aluminum	Sand casting	1	17cm (width) x 15cm (height) x 1cm (aver. Thickness)	0.716	0.716	\$16.58	\$10.22
Compressor Shaft Seals	O-ring seal, polymer	Purchased	4	1.9cm (ID), 5cm (OD)	0.005	0.02	\$8.00	\$6.00
Timing Drive Gears (compressor: steel)	Stainless Steel	Laser cut from sheet	2	5cm max OD, 1cm thick	0.144	0.288	\$12.93	\$5.08
Total						6.20	\$140.83	\$71.92
								\$116.34
Expander Components								
Expander Rotor	6061-T1 Aluminum and fiberglass filled HDPE overmold	Extrusion w/twist	2	15cm x 7cm max OD	0.57	1.14	\$47.47	\$18.15
Expander Manifold	Fiberglass filled HDPE	Injection molded	1	12cm (width) x 15cm (height) x 17cm (length) x 0.6cm (aver. Thickness)	0.67	0.67	\$11.66	\$2.11
Expander Housing	Fiberglass filled HDPE	Injection molded	1	25cm (width) x 15cm (height) x 17cm (length) x 1cm (aver. Thickness)	1.782	1.782	\$19.27	\$6.04
Timing Drive Gear (expander: plastic)	PEEK	Injection molded	2	5cm max OD, 1cm thick	0.017	0.034	\$9.74	\$3.30
Down Speed Gears	PEEK	Injection molded	2	5cm max OD, 1cm thick	0.017	0.034	\$9.74	\$3.30
Total						3.66	\$97.88	\$32.90
								\$77.32
Compressor/Expander Combined Components								
Housing/motor Seals	O-ring seal, PET	Injection molded	5	17cm (width) x 15cm (height) x 0.2cm (diameter round X-section)	0.07	0.35	\$8.20	\$1.55
Housing Screws	316 Stainless Steel	Purchased	18		0.005	0.09	\$7.20	\$3.60
Front Bearing	Steel ball bearings, self lubricated	Purchased	6	5cm (diameter), 1.9cm (ID)	0.322	1.932	\$12.96	\$6.00
Rear Bearing	Steel needle bearings, self lubricated	Purchased	4	5cm (diameter), 1.9cm (ID)	0.322	1.288	\$12.48	\$4.00
Rotor Drive Shafts	High carbon Steel Alloy	Rod, machined	4	1.9cm (diameter) x 18cm (length)	0.769	3.076	\$22.80	\$22.52
Torsionally Flexed Coupling	Fiberglass filled HDPE	Injection molded	1	3cm max OD, 1cm thick	0.004	0.004	\$5.54	\$0.37
Coupling Dowels	Steel	Rod, machined	6	0.25cm diameter, 3cm length	0.001	0.006	\$2.04	\$1.98
Gear Housing/motor end plates	6061-T1 Aluminum	Sand casting	2	17cm (width) x 15cm (height) x 7cm (length) x 1cm (aver. Thickness)	1.71	3.42	\$24.36	\$14.48
Contingency (5% of total cost to account of any missing parts or errors in cost assumptions)							\$58.27	\$34.33
Total						10.17	\$153.85	\$88.83

Figure 35. List of compressor and expander components for SA concept of Eaton-style CEM unit. Cost results are not included in the final auto 2013 cost results, but used as a comparison to currently studied CEM systems.

<i>SA Cost Summary for Eaton 5-Shaft Compressor/Expander/Motor Unit</i>							Annual Production Rate (systems/year)	
							1,000	500,000
	Material	Manufacturing Method	Qty/sys	Dimensions	kg/part	kg/sys	\$/system	
<i>Motor Components</i>								
Motor		Purchased	1		est 30	est 30	\$338.00	\$160.00
Motor Shaft Seal	Formed seal	Purchased	1		0.01	0.01	\$2.50	\$2.25
Drive Shaft (next to motor)	High carbon Steel Alloy	Rod, machined	1	1.9cm (diameter) x 6cm (length)	0.39	0.39	\$4.64	\$4.44
Total						30.40	\$345.14	\$166.69
								\$166.69
<i>Motor Controller Components</i>								
Controller		Purchased	1		2.00	2.00	\$485.88	\$360.49
Total						2.00	\$485.88	\$360.49
								\$360.49
Totals for Compressor, Expander, Motor, and Motor Controller								
Total Materials and Fabrication (not including assembly, testing, and markup)						> 53	\$1,223.57	\$720.84
Final System Assembly							\$17.00	\$11.33
15% Tier 1 Manufacturer/Assembler Markup on Compressor components (including final assy)							\$62.50	\$31.75
10% Tier 1 Manufacturer/Assembler Markup on Motor/Controller components							\$82.39	\$52.05
Total							\$1,385.47	\$815.97

Figure 36. List of motor and motor controller components and total cost for SA concept of Eaton-style CEM unit. (Cost results are not tallied in the final auto 2013 cost summation, but rather are used as a comparison to the currently studied CEM systems.)

When comparing to the Honeywell-style CEM, used as the baseline in both the 2012 and 2013 cost analyses, the Eaton-style CEM comes in less expensive at 1,000 systems/year and slightly more expensive at 500k systems/year. Figure 37 shows a side-by-side comparison of the Eaton and Honeywell-style designs with a breakdown in cost for the compressor, expander, motor, CEM markup, motor controller, and motor controller markup.

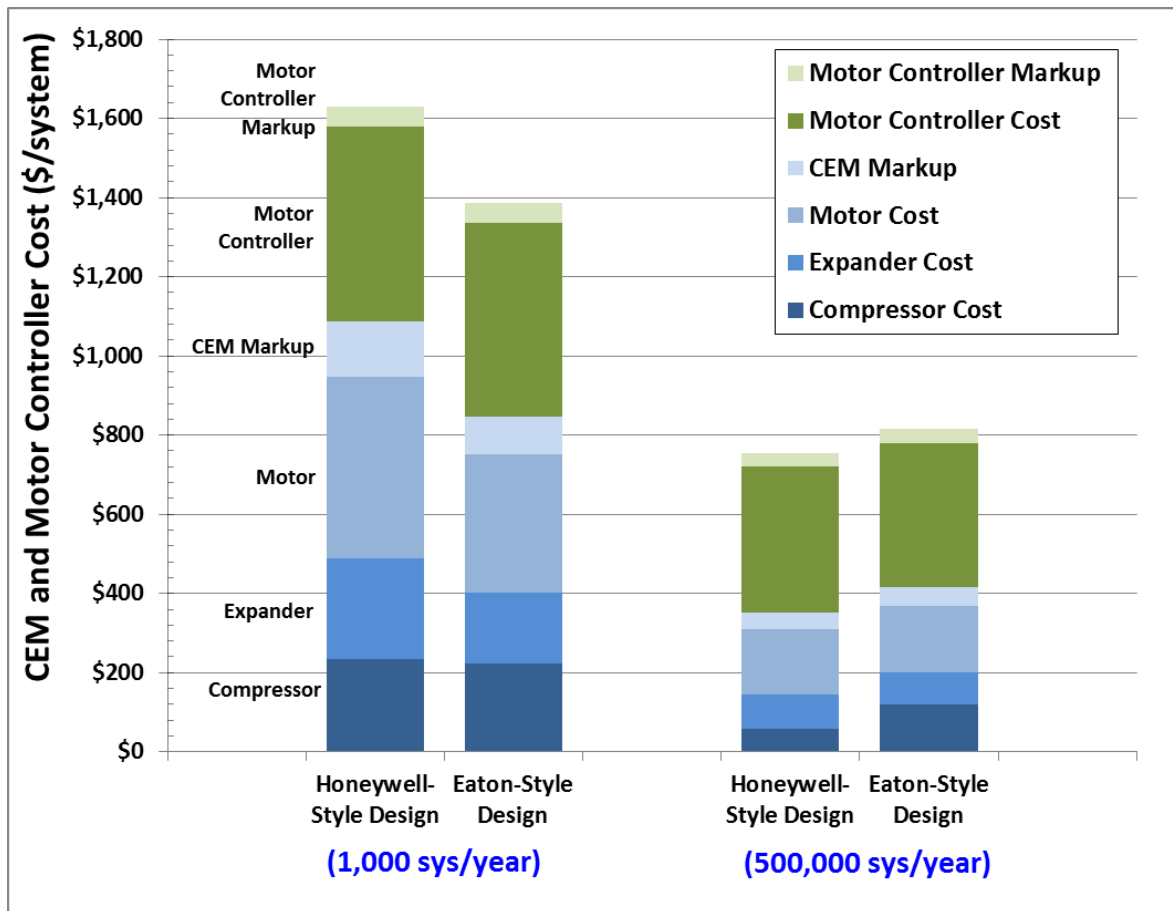


Figure 37. Cost breakdown for the Honeywell-style and Eaton-style CEM designs.

6.8 Revised Quality Control Procedures

The quality control (QC) systems were updated for the 2013 DFMA™ analysis and reflect further review and analysis by QC expert Mike Ulsh of NREL. Overall, a more rigorous definition of the quality control systems was established. The general approach for defining the new QC systems was to:

1. Postulate the required resolution for defect identification.
2. Specify equipment needed to achieve desired resolution at specified line speed.
3. Ensure QC system equipment is not the pacing component.

The more rigorous 2013 analysis led to higher cost QC system than in 2012, however the QC cost impact is still relatively low, especially considering the high cost of not developing high rate QC systems⁴⁷. Figure 38 and Figure 39 contain details of the updated QC systems. QC equipment costs are based on vendor quotations or estimates made by the authors in consultation with experts at NREL. Figure 38 shows the QC systems used for most of the stack component processes and Figure 39 showing the new

⁴⁷ Ulsh, M. "Fuel Cell MEA Manufacturing R&D", National Renewable Energy Laboratory Presentation at the US Department of Energy Fuel Cell Technologies Office Annual Merit Review, May 15, 2013.

QC equipment for the newly modeled plate frame humidifier. Year to year, the most significant change in QC approach relate to Gore MEA fabrication, bipolar plate processes, and plate frame membrane humidifier fabrication.

The Gore MEA fabrication process was not used in the 2013 final cost values for the bus or auto system, but a cost study was completed for the Gore MEA (Section 6.6) to allow comparison to the NSTF type membrane fabrication used in the 2013 baseline analysis. The Gore MEA consists of three processes (application of two electrodes and the electrolyte), each with an attendant QC procedure. An infrared/direct current (IR/DC) system⁴⁸ is used to send an electric current down the length of the electrode layer (anode and cathode). An IR camera mounted above the electrode and peering down onto the moving web is used to visually assess the temperature signature of the electrode and detect anomalies that would be indicative of electrode thickness variation. For QC of the electrolyte layer, an optical detection system is used to visually detect pinholes in the ionomer and/or layer discoloration (an indication of electrolyte thickness variation).

The QC system for the bipolar plates includes a NIST non-contact laser triangulation probe and a commercial optical detection system from Keyence. The laser triangulation system checks for flow field depth and flatness of the bipolar plate. Probe speed is generally insufficient to keep up with the fast moving web. Consequently, only a few passes across the plate are conducted with this being judged to be adequate to detect anomalies anywhere on the plate. Additionally, an optical system is used to ensure completeness of manifold apertures and to check the in-plane dimensions of the part (i.e. length, width, and aperture openings).

The plate frame membrane humidifier contains multiple processing steps with QC systems installed for membrane fabrication stations, the flow field plates, membrane pouch fabrication, stack formation and assembly. The membrane stations use an optical detection system to locate pinholes in the ePTFE and for discoloration due to thickness variation. The flow fields, pouch fabrication, and stack formation processes use a commercial vision system from Keyence to visually inspect and guarantee completeness of the process. After the assembly of the humidifier stack, a conveyor mass scale is used to ensure assembly of all components.

⁴⁸ Niccolo V. Aieta, Prodip K. Das, Andrew Perdue, Guido Bender, Andrew M. Herring, Adam Z. Weber, Michael J. Ulsh, "Applying infrared thermography as a quality-control tool for the rapid detection of polymer-electrolyte-membrane-fuel-cell catalyst-layer-thickness variations", *Journal of Power Sources*, Volume 211, 1 August 2012, Pages 4-11.

Part Tested	2011/2012 Diagnostic System	2013 Diagnostic System	Comment on Change	Detection Resolution	Total QC Cost (at 500k sys/yr)	Fault/Parameters Tested
Membrane Station 1 (electrode of Gore MEA)	X-Ray Fluorescence (XRF) (point measurement only) OR IR/DC	Infrared/Direct Current (IR/DC)	Applied to Gore MEA manufacturing process. (Gore MEA not used in 2013 Final Values)	2mm x 2mm	\$190k	Unevenness of electrode conductivity as indicator of electrode thickness variation.
Membrane Station 2 (ePTFE/Ionomer of Gore MEA)	Optical Detection System	Optical Detection System (ODS)	Applied to Gore MEA manufacturing process. Compute # of cameras needed based on pixels per line, field of view, target resolution. (Gore MEA not used in 2013 Final Values)	20 micron	\$392k	Visual inspection to locate pinholes in ionomer, discolorations that would indicate thickness variation or other problems.
Membrane Station 3 (electrode of Gore MEA)	XRF (point measurement only) OR IR/DC	Infrared/Direct Current (IR/DC)	Applied to Gore MEA manufacturing process. (Gore MEA not used in 2013 Final Values)	2mm x 2mm	\$190k	Unevenness of electrode conductivity as indicator of electrode thickness variation.
Gasketed MEA (Subgasket)	Optical Thickness and Surface Topology System	Optical Detection System (ODS) (commercial system from Keyence)	Nanovea system provides more capability than is needed. Switched to a more basic optical detection system.	0.6mm	\$80k	Misalignment of subgasket and membrane. Folds, bends, tears, scratches in subgasket or membrane.
Bipolar Plate	NIST Non-Contact Laser Triangulation Probe	NIST Non-Contact Laser Triangulation Probe, Optical Detection System (commercial system from Keyence)	Triang. Probes (3) used in a single pass (or possible two passes) to detect minute anomalies in flow field channel formation and out of flatness. Single pass only provides small fraction of areal inspection. Optical system used to scan entire plate to detect gross anomalies.	~30 micron over 3 scan lines (one side of plate, 3 probes, single pass), 0.6 mm for Optical Camera (entire plate, one side)	\$100k	Triangulation: flow field depth, plate flatness. Optical System: general dimensions, completeness of manifold apertures.
End Plate	Conveyor Mass Scale and Human Visual Inspection	Commercial vision system (from Keyence)	Switch to ODS rather than human visual inspection. Inspect both sides (with flip in between). Mass measurement is eliminated as it is judged to not be needed.	0.6mm	\$100k	Completeness of injection molding
NSTF Catalyst	Previously IR/DC.	IR/DC	Same			Catalyst loading, particle size, defects, general Pt uniformity
MEA (after cutting/slitting)	XRF (point measurement only)	Not used.	Not needed (since 2013 analysis uses 3M subgasketing approach).			Thickness, cracks, delamination
GDL (Microporous Layer)	Mass Flow Meter	Mass Flow Meter	Same			Proper layer coverage
GDL (Microporous Layer)	Viscometer	Viscometer	Same			Proper layer coverage
GDL (Final Product)	Inline Vision System	Optical Detection System (ODS) (based on Ballard)	Based on Ballard custom system.	<=0.5mm	\$100k	Cracks, improper layer coverage, defects
Laser Welding for Bipolar Plates	Optical Seam Inspection System	Optical Seam Inspection System	Same			Completeness of laser weld

Figure 38. Summary of quality control systems used in stack manufacture

Part Tested	2013 Diagnostic System	QC Operation	Detection Resolution	Total Cost	Cost Notes	Fault/Parameters Tested
Membrane Station A (inspection of ePTFE web)	Optical Detection System	Line camera to optically detect pinholes or other anomalies in ePTFE layer.	350 micron	\$36k	For 1m web width: Requires 1 line cameras (12k pixels each). Total cost = \$36k.	Visual inspection to locate pinholes in ePTFE, discolorations that would indicate thickness variation or other problems.
Membrane Station B (inspection of ePTFE web)	Optical Detection System	Set of line cameras to optically detect pinholes or other anomalies of top surface of ePTFE/ionomer membrane.	20 micron	\$392k	For 1m web width: Requires 17 line cameras (12k pixels each). Total cost = \$392k.	Visual inspection to locate pinholes in ionomer, discolorations that would indicate thickness variation or other problems.
Membrane Station C (inspection of ePTFE web)	Optical Detection System	Line camera to optically detect pinholes or other anomalies in top surface of ePTFE/ionomer/ePTFE composite membrane.	350 micron	\$36k	For 1m web width: Requires 1 line cameras (12k pixels each). Total cost = \$36k.	Visual inspection to locate pinholes in ePTFE, discolorations that would indicate thickness variation or other problems.
Humidifier Flowfield Plates	Commercial vision system (from Keyence)	Commercial areal (not line) camera to view top surface of flow field to detect gross etching problems.	350 micron	\$60k	\$20k for complete optical system able to view single 10cm x 10cm flowfield based on 1600x1200 pixel camera. Plus \$10k misc. for fixturing, extra cabling, etc. Plus \$30k conveyerized stacking to place plates into parts magazines. Total cost = \$60k.	Completeness of etching.
Membrane Pouches	Commercial vision system (from Keyence)	Commercial areal (not line) camera to view top surface of flow field pouch to detect incorrect membrane bonding and/or misalignment of membrane wrap around flow field.	350 micron	\$60k	\$20k for complete optical system able to view single 10cm x 10cm flowfield based on 1600x1200 pixel camera. Plus \$10k misc. for fixturing, extra cabling, etc. Plus \$30k to move camera down line of 10 pouches coming off line. Total cost = \$60k.	Completeness of bonding.
Forming Stack	Commercial vision system (from Keyence)	Commercial areal (not line) camera to view top surface of flow field pouch to detect missing ribs and misplaced adhesive		\$20k	A rough estimate for each camera is \$10k including camera, cabling, and (portion of) computer. Since only one camera is used and multiple pictures will be taken at different times in the cycle, the cap cost is hit with a factor of 2 to reflect full purchase of software and computer. Cost modeled: 2x \$10k=\$20k.	Visual Inspection of alignment of adhesive and ensuring ribs are not missing
Humidifier Assembly	Conveyor Mass Scale	Measure mass of completed cell to detect any missing/additional internal components.	~2 grams	\$23k	Based on ThermoFischer Scientific CheckWare. \$18k plus \$5k of accessories and bottom-drop out for rejected parts.	Mass of assembled system to detect missing components.

Figure 39. Summary of quality control systems for new plate frame membrane humidifier

6.9 Updated Material Prices

Material costs were updated in 2013 to allow an accurate projection of system cost and improve the validity of the DFMA™ model. However, it is unnecessary to update all material cost each year, instead emphasis is placed on updating quotes more than 3 years old. Consequently, all material quotes prior to 2010 were updated. Figure 40 lists these newly updated material costs. Section 7.1.2.2 contains a discussion of ePTFE price as quotations received from ePTFE suppliers had quite a large range and therefore merits special attention. Additionally, surcharges on stainless steel were found to be of note.

Material prices are in constant flux based on many factors including supply and demand and market changes. The pricing of stainless steel in the world market is based on a base price augmented by a monthly changing surcharge to reflect individual fluctuations in the commodity price for each element within the steel (i.e. nickel, iron, manganese, etc.) For example, stainless steel (SS) 316L contains nickel, chrome, molybdenum, and iron and each have a different added surcharge amount to compensate for the fluctuation in that element's cost. Price quotations typically reflect only the base price (as a \$/kg for a specific grade, width, weight, finish, etc.) Surcharges must be (eventually) paid but are only assessed at time of shipment. These surcharges can be significant, amounting to 25% (for <0.38mm thickness SS) to >90% (for >0.38mm thick SS) of the total base value of the SS. The thicker SS sheeting is less expensive due to less processing, but the surcharge is a greater percentage of the base value for the material. Surcharges for SS used in the 2013 analysis were taken from an ATI website (\$/kg)⁴⁹ for August 2013 delivery. AK Steel also provides their surcharges online⁵⁰. It should be noted that there is a slight difference in surcharge between companies, depending on the month the quote is received.

Material	Component	Cost Basis	Production Rate: 1k sys/year		Production Rate: 500k sys/year	
			Volume	Price	Volume	Price
Stainless Steel Sheeting (Grade 316L) (0.076mm)	Bipolar Plates	Quote from Allegheny Steel (ATI) (5/24/2013)	20.8 tonnes/yr	\$11.37/kg	10,377 tonnes/yr	\$11.10/kg
Stainless Steel Sheeting (Grade 316L) (0.6mm) with 2B finish	Plate Frame Membrane Humidifier	Quote from AK Steel (7/30/2013)	3.8 tonnes/yr	\$3.93/kg	1,923 tonnes/yr	\$3.93/kg
Vulcan XC-72	Gore MEA Station 1 and 3	Quote from McCullough&Associates (supplier of Cabot) (6/10/2013)	53.3 kg/yr	\$9.17/kg	17.5 tonnes/yr	\$9.17/kg
Methanol	Gore MEA Station 1 and 3	Methanex (5/15/2013):	183 kg/ys	\$0.53/kg	77.6 tonnes/yr	\$0.53/kg
DI water	Gore MEA Station 1 and 3	ChemWorld (6/10/2013)	183 kg/ys	\$1.75/kg	77.6 tonnes/yr	\$1.75/kg
Type A Resin	Screen Printed Subgasket Seal	Quotes from BASF, Coating Resins, Momentive Materials (5/2013)	268 kg/yr	\$15.19/kg	133.8 tonnes/yr	\$15.19/kg
LYTEX 9063	End Plates	Quote from Quantum Composites (6/12/2013)	2.2 tonnes/yr	\$31.49/kg	1,093 tonnes/yr	\$19.51/kg
Copper Sheeting (1.1cm thick)	Current Collector	Quote from Chris Industries (6/7/2013)	83 m ² /yr	\$90.87/m ²	37,830 m ² /yr	\$82.96/m ²
Polypropylene	Stack Housing	The Plastics Exchange (4/26/2013)	3.5 tonnes/yr	\$1.33/kg	1,760 tons/yr	\$1.33/kg
ePTFE (10-25 microns thick)	MEA	See Section 7.1.2.2 of report	22k m ² /yr	\$17/m ²	7.7 million m ² /yr	\$6.00/m ²

Figure 40. List of material costs updated in 2013 DFMA™ analysis.

⁴⁹ ATI Surcharges Website, November 29, 2013. <http://www.atimetals.com/businesses/business-units/ludlum/Resources/surcharge-calculator/Pages/default.aspx>

⁵⁰ AK Steel Surcharges Website http://www.aksteel.com/markets_products/surcharges/stainless.aspx

6.10 Alignment with DOE CEM Status Efficiencies

Assumed component efficiencies (at full rated power conditions) for the compressor, expander, and combined motor/motor-controller were altered from previous year levels to bring them in line with 2013 estimates from Argonne National Laboratory. Previous efficiencies were based on input from Honeywell for their future model centrifugal-compressor/radial-inflow-expander/permanent-magnet unit but were aspirational rather than experimentally demonstrated, and largely mimicked the DOE technical targets. In contrast, the efficiencies used in the 2013 analysis are meant to reflect currently demonstrated or “status” performance. The updated values are shown in Figure 41.

(all efficiencies at rated power)	2012 Values	2013 Values
Compressor Efficiency (isentropic)	75%	71%
Expander Efficiency (isentropic)	80%	73%
Combined Motor/Motor-Controller Efficiency	85%	80%

Figure 41. Assumed CEM Efficiency

6.11 Update of Sizing and Cost Analysis Methodology for the Low Temperature Coolant Loop

As shown in Figure 8, both high temperature and low temperature coolant loops are utilized within the fuel cell system. The high temperature loop (peak coolant temperature ~90°C) is used to cool the relatively high temperature fuel cell stacks. The low temperature loop (peak coolant temperature ~83°C) is used to cool the cathode air stream down to the relatively cool temperature (~80°) needed in the membrane humidifier. The low temperature loop is also used to cool the CEM motor and controller which operate most efficiently at cool temperatures. In past SA cost studies, the low temperature loop was also used to cool the traction inverter module (TIM) which was a substantially higher cooling load than that used in the air precooler. Consequently, for those past studies, the cost of the low temperature loop was split between the fuel cell power system and powertrain system, ratioed by heat duty, and only ~39% of the total low temperature loop was included in the fuel cell summary. For 2013, the traction inverter load was excluded from the low temperature loop and 100% of the low temperature loop cost was including in the cost summation. This change was enacted to simplify the analysis and more closely align with modeling efforts at Argonne National Laboratory.

Additional analysis by Argonne National Laboratory has identified 80°C as the optimal humidifier air inlet temperature to minimize humidifier membrane area requirements. Additional temperature parameters for the 2013 low temperature loop are shown in Figure 42 with a system schematic in Figure 43.

Low Temperature Loop 2013 Values		
Location in Schematic Diagram	Stream	Temperature (°C)
1	Coolant Precooler inlet temperature	61°C
2	Coolant Precooler exit temperature	65°C
3	Air Precooler inlet temperature	182°C
4	Air Precooler outlet temperature	80°C
5	Coolant Motor/Motor-Controller inlet temperature	60°C
6	Outside Air Temperature	40°C

Figure 42. Low Temperature Loop Temperatures

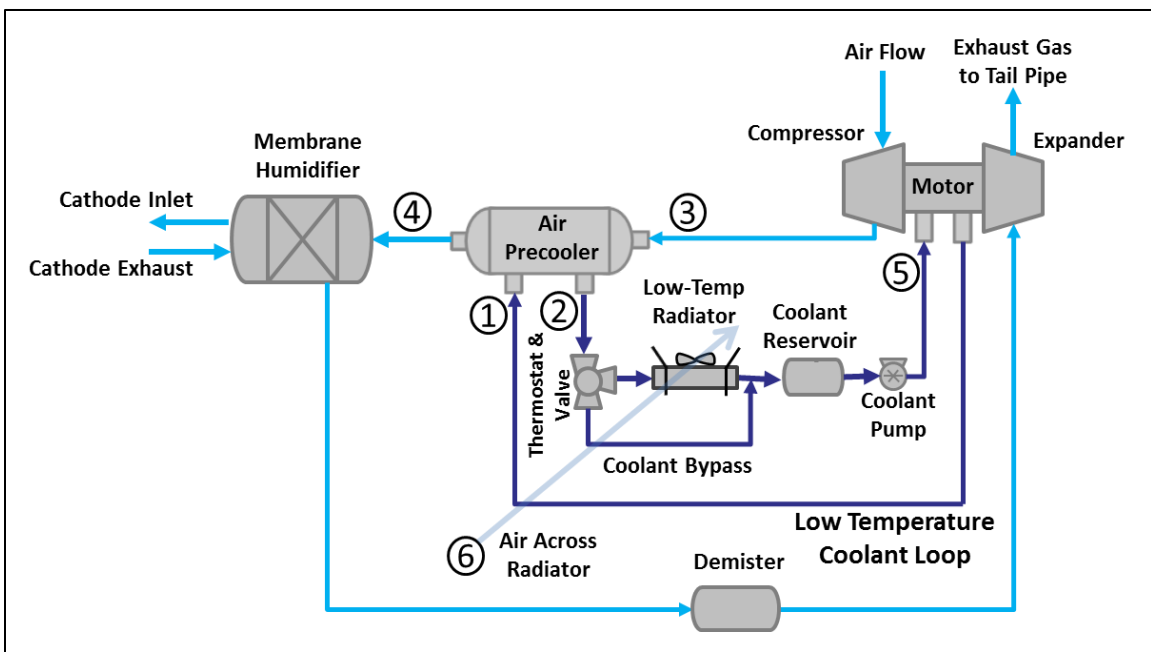


Figure 43. Low Temperature Loop Schematic

7 Description of 2013 Automotive Fuel Cell System Manufacturing Assumptions and Cost Results

7.1 Fuel Cell Stack Materials, Manufacturing, and Assembly

7.1.1 Bipolar Plates

Each stack in the system consists of hundreds of active cells, each of which contains two bipolar plates. A one-to-one (1:1) ratio of active cells to cooling cells is assumed, to facilitate better temperature uniformity throughout the stack. Consequently, one side of the bipolar plate is a cooling cell flow field and the other side is an active cell flow field. In previous estimates, the cathode and anode flow field sides of the bipolar plates were envisioned as having identical flow patterns and being symmetrical. Consequently, only one bipolar plate design was needed and the cells could be flipped 180 degrees to alternate between cathode flow fields and anode flow fields. However, based on feedback from Ballard Power Systems Inc., different designs were assumed for the anode plates compared with the cathode plates. At the very end of each stack on either side, an extra bipolar plate sits and is not part of the repeating cell unit. This extra bipolar plate is only half-used, as it does only cooling. Specially-designed end gaskets are used to block off the flow into the gas channel side of those plates. Because each system contains hundreds of bipolar plates, hundreds of thousands of plates are needed even at the lowest production rate. This high level of production of a repeating component even at low system production levels means that bipolar plate mass-manufacturing techniques are applicable across a wide range of system production rates.

The stamped metal plates were selected because of consistent industry feedback suggesting that this material and manufacturing method is the most common approach currently implemented with success.

7.1.1.1 Progressive Die Stamping of the Bipolar Plates

Sheet metal stamping is selected for production of the bipolar plates and is inferred to be employed by GM for their fuel cell stacks⁵¹. Since ~700 plates are needed per system and multiple features are required on each plate (flow fields, manifolds, etc.), progressive die stamping is a logical choice for manufacturing method. In progressive die stamping, coils of sheet metal are fed into stamping presses having a series of die stations, each one sequentially imparting one or more features into the part as the coil advances. The parts move through the stationary die stations by indexing and a fully formed part emerges from the last station. As shown in Figure 44, the four main sequential die stations envisioned are (1) shearing of the intake manifolds, (2) shearing of the exhaust manifolds, (3) shallow forming of the flow field paths, and (4) shearing off of the part.

⁵¹ The composition and manufacturing method for production of GM bipolar plates is a trade secret and is not known to the authors. However, a review of GM issued patents reveals that they are actively engaged in metallic plate research.

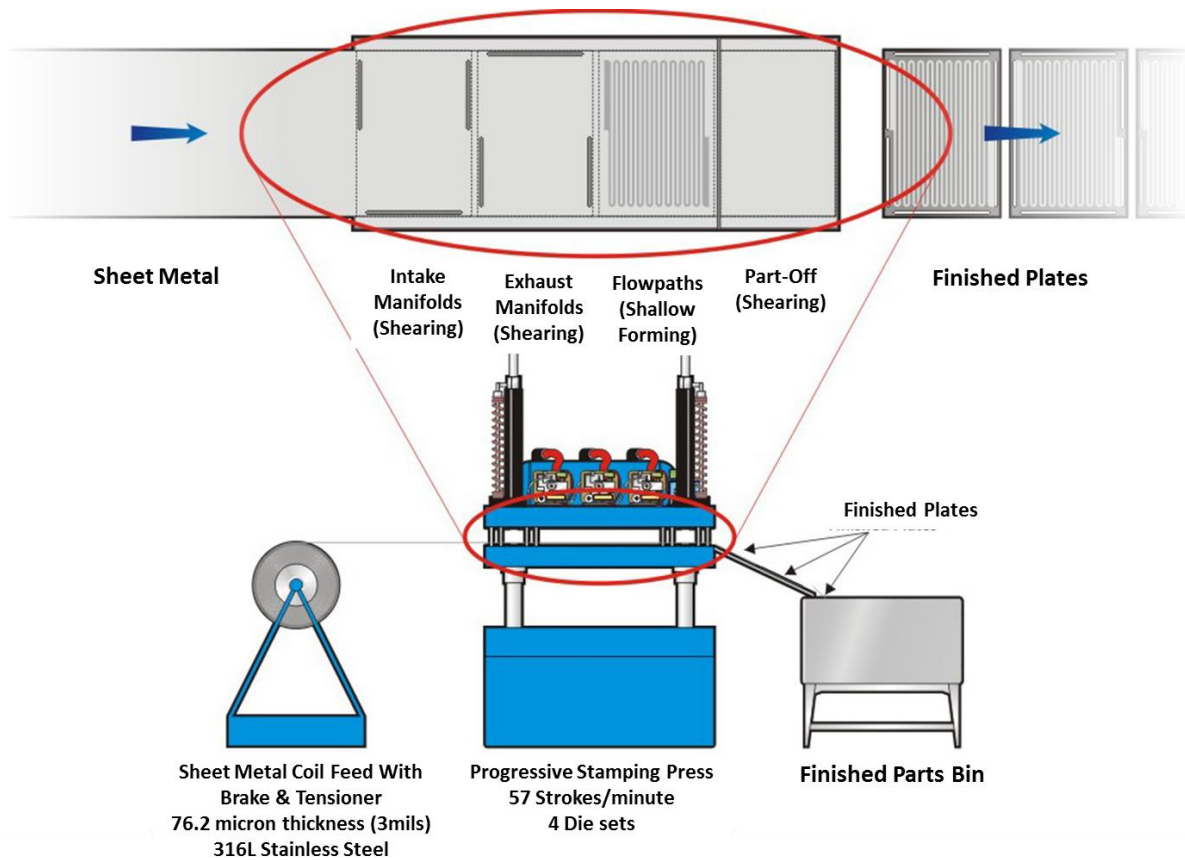


Figure 44. Bipolar plate stamping process diagram

Costs for bipolar plate progressive die stamping were obtained following the standard SA methodology described above. In summary, capital costs, maintenance costs, and electric power requirements were derived from manufacturer price quotes and also survey data supplied within Boothroyd Dewhurst Inc. (BDI) proprietary software. These data were then used to estimate true annual operating costs when the manufacturing line is operated at less than full capacity and 100% utilization. The cost estimation process and assumptions are described more fully below.

Capital Cost and Press Tonnage: Press clamping force is the primary factor influencing both the size and cost of a metal forming press. Price quotes and performance data for AIRAM Press Co. Ltd pneumatic presses ranging from 50 tons to 210 tons of clamping force were analyzed to develop a function describing the approximate purchase cost as a function of clamping force. The cost of supporting equipment required for press operation was then added to the base press cost. Some of the supporting equipment has a fixed cost regardless of press size, while other supporting equipment costs scale with press size. A sheet metal coil feeder was judged necessary and its cost was found to be largely independent of press size. To ensure part accuracy, a sheet metal straightener was added, although it may prove to be ultimately unnecessary due to the thin material used (76.2 microns, or 3 mils).

Press force needed in the progressive die is a function of the material thickness, the material tensile strength, the perimeter of cutting, and the perimeter and depth of bending or other forming. In early

modeling efforts, the press force was computed based on the assumption that the channels in the plate active area were merely formed by bending. Thus, in the 2006 report⁵², it was estimated that a 65-ton press was necessary to produce the bipolar plates. However, it was noted that there was disagreement in the bipolar plate stamping community regarding the necessary press tonnage to form the plates, for example, with one practitioner stating that a 1,000-ton press was needed. This particularly high press tonnage being quoted may be due to the metal in the flow field channels being swaged⁵³ rather than bent in this particular manufacturer’s case. Subsequent review by Ballard suggested that the previous 2006 SA estimate for total stamping system capital cost was substantially too low either due to a discrepancy with the required press tonnage or with the supporting equipment, or both. Consequently, in this revised analysis, the estimated capital cost is increased five-fold to better reflect industry feedback and to better approximate the higher cost of a larger tonnage press.

Press Speed: The speed of the press (in strokes per minute) varies with press size (kilo-Newtons (kN)): a small press is capable of higher sustained operating speeds than a large press. Press speed is a function of press size, and this relationship is shown in Figure 45.

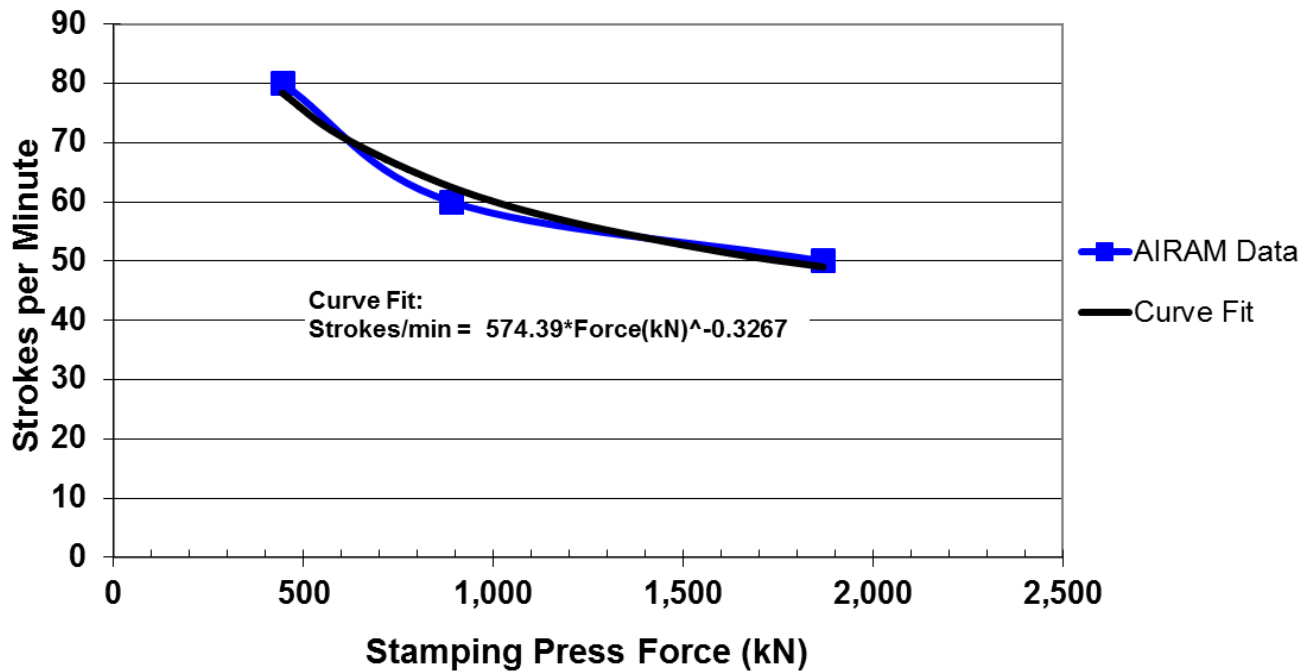


Figure 45. Press speed vs. press force

Quality Control System: A non-contact laser triangulation probe developed by NIST provides detailed information concerning flow field depth, plate size, thickness and defects for the stamped bipolar plate. As shown in Figure 46, the sensor must be able to scan three plates at a time in order to match the speed of the stamping press, which is producing nearly three plates every two seconds. The

⁵² “Mass Production Cost Estimation for Direct H₂ PEM Fuel Cell Systems for Automotive Applications,” Brian D. James & Jeff Kalinoski, Directed Technologies, Inc., October 2007.

⁵³ Use of the word “swaged” is meant to denote a more substantial lateral movement of metal during the process than is typically observed within bending or stamping operations.

measurement area for each sensor is 600 mm by 300 mm, significantly larger than the size of a single plate. The line speed has been proven at roughly 300 mm/second but further R&D could increase the effective speed to an estimated maximum of 2 m/sec. Since the probes are inexpensive, they add little additional capital cost; consequently, three sensors are envisioned for the system to ensure adequate measurement overlap for each plate and to match the stamping speed.

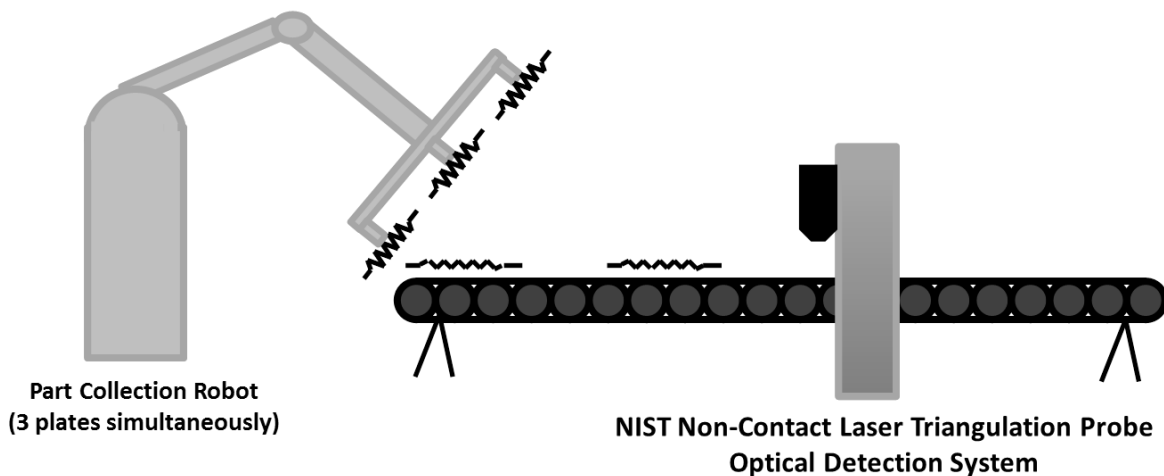


Figure 46. Bipolar plate part collection and quality control: NIST Non-Contact Laser Triangulation Probe, Optical Detection System

Maintenance: The same press operated at higher speeds tends to require maintenance more frequently. Based on discussion with industry vendors, the minimum life of a set of these stamping machine wear parts was estimated to be 10 million cycles, with a total replacement cost estimated to be 20 to 25% of complete press initial capital cost depending on machine size. Since the above cycle life is the minimum number of cycles, but could be substantially more, an approximation is applied to this latest modelling iteration such that the maintenance cost of the press is estimated to be 15% of initial press capital cost every 10 million cycles. This approach deviates from SA’s historically-implemented methodology, which estimates maintenance costs as a percentage of initial capital costs per year rather than per cycle. Applying a similar cycle-based lifetime criterion, feeder equipment maintenance is estimated to be 5% of initial feeder capital cost every 10 million cycles.

Utilities: The principal sources of demand for electricity in the progressive die process train are the air compressor for the pneumatic press and the electric motor for turning the coil feeder. Compressor power is a function of the volumetric airflow requirement of each press size and was estimated to vary between 19 kW at the low end (50-ton press) and 30 kW at the high end (210-ton press)⁵⁴. Based on available data, a mathematical relationship was developed to describe electric power consumption as a function of press size.

⁵⁴ Information provided through conversations with AIRAM (<http://www.airam.com/>)

Machine Rate: Using the above information for total line capital, maintenance, and utilities costs, mathematical expressions can be generated that relate machine rates with various size presses at varying utilization. Basic input parameters are summarized in Figure 48 and Figure 49.

Die Cost: Die costing is estimated according to the equations outlined in the Boothroyd and Dewhurst section on sheet metal stamping. As expected, complex stamping operations require more intricate, and therefore more expensive, dies. The first two, and final, press steps are simple punching and sheering operations and therefore do not require expensive dies. The flowpath-forming step involves forming a complex serpentine shape, which requires a highly complex die that is significantly more expensive than the dies for other steps in the process. This step also requires the majority of press force. The die cost figures are listed below in Figure 47 (under “Tooling”). Note that “secondary operations” refers to the coating process that will be further discussed in Section 7.1.1.2.

Annual Production Rate	1,000	10,000	30,000	80,000	100,000	500,000
Materials (\$/stack)	\$236	\$232	\$230	\$230	\$230	\$230
Manufacturing (\$/stack)	\$224	\$49	\$34	\$30	\$32	\$30
Tooling (\$/stack)	\$106	\$94	\$93	\$92	\$93	\$92
Secondary Operations: Coating (\$/stack)	\$1,410	\$196	\$148	\$137	\$134	\$134
Total Cost (\$/stack)	\$1,976	\$572	\$506	\$489	\$489	\$486
Total Cost (\$/kWnet)	\$24.70	\$7.15	\$6.32	\$6.12	\$6.11	\$6.08

Figure 47. Cost breakdown for stamped bipolar plates

Die Lifetime: Over time, the repetitive use of the dies to form the metallic bipolar plates will cause these tools to wear and lose form. Consequently, the dies require periodic refurbishing or replacement depending on the severity of the wear. Based on communication with 3-Dimensional Services, Inc., dies for progressive bipolar plate stampings are estimated to last between 400,000 and 600,000 cycles before refurbishment, and may be refurbished 2 to 3 times before replacement. Thus, a die (tooling) lifetime of 1.8 million cycles (3 x 600,000) is specified, with a die cost of \$228,154 (\$100,000 of which is from the two refurbishments, at \$50,000 each).

Annual Production Rate	1,000	10,000	30,000	80,000	100,000	500,000
Equipment Lifetime (years)	15	15	15	15	15	15
Interest Rate	10%	10%	10%	10%	10%	10%
Corporate Income Tax Rate	40%	40%	40%	40%	40%	40%
Capital Recovery Factor	0.175	0.175	0.175	0.175	0.175	0.175
Equipment Installation Factor	1.4	1.4	1.4	1.4	1.4	1.4
Maintenance/Spare Parts (% of CC)	13%	13%	13%	13%	13%	13%
Miscellaneous Expenses (% of CC)	2%	2%	2%	2%	2%	2%
Power Consumption (kW)	34	34	34	34	34	34

Figure 48. Machine rate parameters for bipolar plate stamping process

Annual Production Rate	1,000	10,000	30,000	80,000	100,000	500,000
Capital Cost (\$/line)	\$555,327	\$555,327	\$555,327	\$555,327	\$555,327	\$555,327
Costs per Tooling Set (\$)	\$228,154	\$228,154	\$228,154	\$228,154	\$228,154	\$228,154
Tooling Lifetime (cycles)	1,800,000	1,800,000	1,800,000	1,800,000	1,800,000	1,800,000
Simultaneous Lines	1	2	4	9	12	56
Laborers per Line	0.25	0.25	0.25	0.25	0.25	0.25
Line Utilization	11.0%	55.1%	82.7%	98.0%	91.8%	98.4%
Cycle Time (s)	1.05	1.05	1.05	1.05	1.05	1.05
Effective Total Machine Rate (\$/hr)	\$605	\$132	\$93	\$81	\$85	\$80
Stainless Steel Cost (\$/kg)	\$11.37	\$11.20	\$11.10	\$11.10	\$11.10	\$11.10

Figure 49. Bipolar plate stamping process parameters

7.1.1.2 Alloy Selection and Corrosion Concerns

One of the challenges presented by using metallic plates is that they are more susceptible to corrosion than carbon-based plates. For this reason, alloy selection is very important. There is much uncertainty in the fuel cell community as to which alloy and surface treatments are needed to provide adequate corrosion resistance. Although some believe that suitable stainless steel alloys exist that adequately address this problem, others insist that protective coatings are necessary. If the right coating method were selected, it may be possible to use a cheaper and/or lighter (but less corrosion-resistant) material for the plates, which could help offset the cost of coating. In determining the coating method and/or plate material, consideration must be given to the different corrosion environments each plate will encounter: hydrogen and coolant for the anode plates, and oxygen and coolant for the cathode plates.

Literature and patent reviews and conversations with researchers indicate that coatings/surface treatments may not be needed and that 316L stainless steel (or another commercial alloy of similar cost) is appropriate. However, further input from the USCAR Fuel Cell Technical Team suggested that coatings *are* necessary. At the direction of the Fuel Cell Tech Team, coatings were included in the system cost and are based on a 76.2-micron (3-mil) stainless steel 316L alloy metallic bipolar plates coated using a proprietary process from TreadStone Technologies, Inc.

An anti-corrosion coating is applied to both sides of the bipolar plates based on TreadStone's proprietary LiteCell process. A DFMATM analysis was conducted based on information from TreadStone's patent US 7,309,540, as well as information transferred under a non-disclosure agreement, with close collaboration with C.H. Wang and Gerry DeCuollo of TreadStone Technologies, Inc.

According to the patent, the coating consists of "one or more resistant layers, comprising conductive vias through the resistant layer(s)" (see Figure 50). The resistant layer provides excellent corrosion protection, while the vias provide sufficient electrical conduction to improve overall conductivity through the plate.

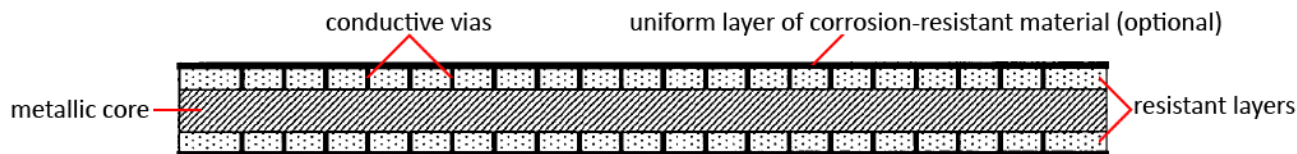


Figure 50. Conductive vias shown in US patent 7,309,540 for TreadStone Technologies, Inc. anti-corrosion coating

The resistant layer is applied via a physical vapor deposition process. Details of the manufacturing process are considered proprietary, so only limited explanation is provided here.

The postulated coating application follows a three-step process. The major step is the deposition of a non-continuous layer of gold dots (~1% surface coverage) via a patented low-cost process designed to impart low contact resistance. The plate coating is applied after bipolar plate stamping. The gold layer is only applied to one side of the plates because only one side requires low contact resistance.

The cost breakdown for the TreadStone process is shown in Figure 51. The coating cost is observed to be primarily a function of annual production rate, with cost spiking at low quantities of only 1,000 systems per year. This is a reflection of low utilization of the coating system, and the application cost could perhaps be reduced with an alternate application technique.

Annual Production Rate	1,000	10,000	30,000	80,000	100,000	500,000
Materials (\$/stack)	\$50	\$50	\$50	\$50	\$50	\$50
Manufacturing (\$/stack)	\$1,360	\$146	\$98	\$87	\$84	\$84
Total Cost (\$/stack)	\$1,410	\$196	\$148	\$137	\$134	\$134
Total Cost (\$/kWnet)	\$17.62	\$2.45	\$1.85	\$1.71	\$1.68	\$1.68

Figure 51. Cost breakdown for TreadStone LiteCell bipolar plate coating process

7.1.2 Membrane

The total cost of the fuel cell membrane (uncatalyzed) is estimated as the summation of three components:

1. ionomer (input material cost)
2. ePTFE substrate (input material cost)
3. manufacturing cost of casting into membrane form

Each component is described in detail below.

7.1.2.1 Ionomer Cost

Ionomer cost is based upon a 2010 Dow Chemical reference report⁵⁵ on high-volume manufacture of Nafion-like long side chain perfluorosulfonic acid proton exchange membranes from hexafluoropropylene oxide (HFPO) raw material. In this report, ionomer material and manufacturing

⁵⁵ "High Volume Cost Analysis of Perfluorinated Sulfonic Acid Proton Exchange Membranes," Tao Xie, Mark F. Mathias, and Susan L. Bell, GM, Inc., May 2010.

costs are analyzed at extremely high volumes: as high as 6,000 MT/year (although only ~400MT/year of material is suitable for 500k vehicles/year). The combination of extremely high production volume and simpler manufacturing process—the industry report models membrane casting rather than application to an ePTFE substrate—results in reported finished membrane cost much lower than calculated by the SA model. Rather than using the direct results of the Dow cost report, the 2012 Fuel Cell Tech Team recommended that the membrane continue to be modeled as an ePTFE-supported membrane and that we adopt the Dow ionomer price at plant sizes more in line with expected annual demand. Consequently for the 2012 and 2013 analyses, a production-volume-dependent scaling relationship was derived from the Dow report data and used to estimate ionomer price at various fuel cell system annual production rates. This ionomer price curve is shown in Figure 52. Data points on the graph correspond to the six annual system manufacturing rates analyzed in the study.

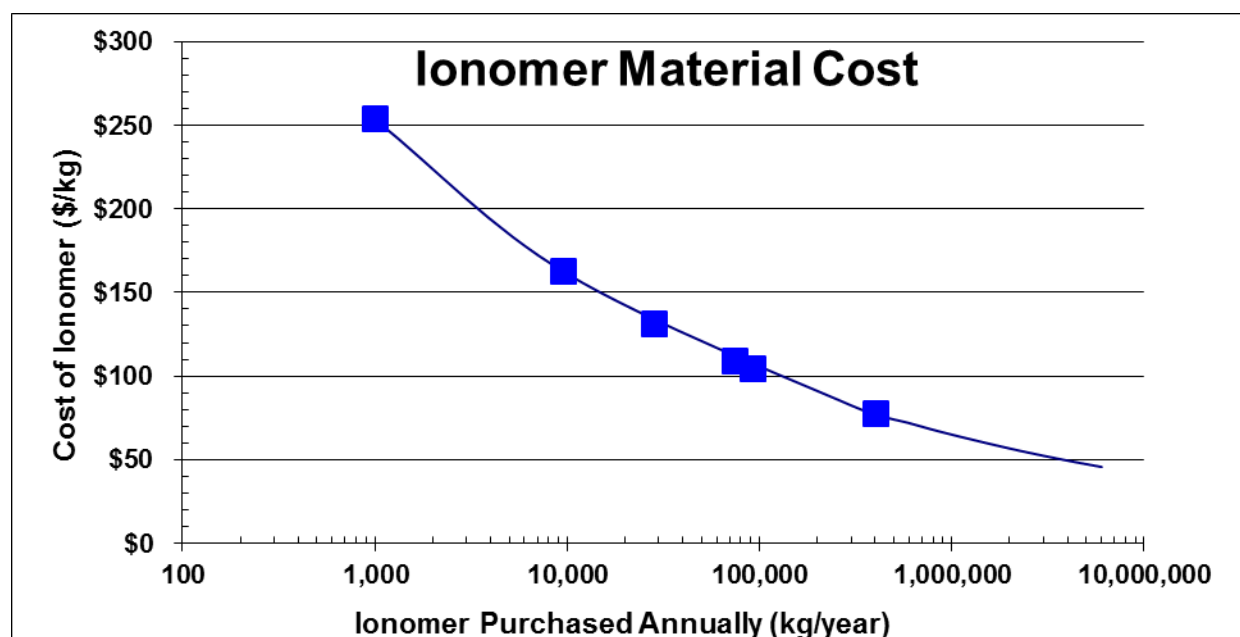


Figure 52. Ionomer material cost curve

7.1.2.2 ePTFE Cost

An expanded polytetrafluoroethylene (ePTFE) porous layer is modeled as a mechanical substrate for the ionomer membrane. Use of an ePTFE supported fuel cell membrane is well documented in the literature and is a continuation of past SA cost analysis practice. A ground-up DFMA™ cost analysis of ePTFE was initiated but it soon became evident that such an analysis was impractical as the specific (and crucial) processing steps⁵⁶ were closely guarded industry secrets unavailable as inputs into the cost analysis. While ePTFE is manufactured in high production volume for the textiles industry (eg. Gore-Tex), there are different qualities available and also potentially different processing steps for fuel cell applications. For this reason, a quote base cost estimated is used within the 2013 report.

⁵⁶ ePTFE uses a particular grade of non-expanded PTFE as a precursor material and then applies a multi-stage, presumably bi-axially, mechanical stretching regiment to attain an optimized node and fibril end structure of the 95+% porous ePTFE. Exact parameters of those stretching steps, along with proprietary heat treatments or other non-disclosed steps, are highly confidential to W.L. Gore and other fuel cell ePTFE manufacturers.

Quotes from multiple ePTFE manufacturers were obtained, all on the basis of confidentiality. These cost quotes (without attribution to their source) are shown in Figure 53. W.L. Gore & Associates, Inc., the predominant supplier of ePTFE to the fuel cell industry did not provide a cost quotation, although they did review this cost analysis.

A wide range of prices is observed in Figure 53 due to both differences between manufacturers and uncertainty in projection to high manufacturing volumes. ePTFE prices are affected by the quality and cost of the starting PTFE material and one manufacturer suggested that only the better quality “fuel cell grade” of PTFE was suitable for fuel cell applications. The lower red curve in Figure 53 represents an ePTFE price quote from a Chinese supplier of textile grade ePTFE which probably isn’t well suited to fuel cell applications but is included in the graph to illustrate the ePTFE price floor. The other price quotations are from US suppliers. Price quotes were obtained for both 10 micron and 25 micron ePTFE thickness but prices did not vary appreciably, indicating that the majority of cost was in the processing steps. A mid-range price of ePTFE is used in the cost analysis, with the upper and lower bound price quotes used as limits in the sensitivity analysis.

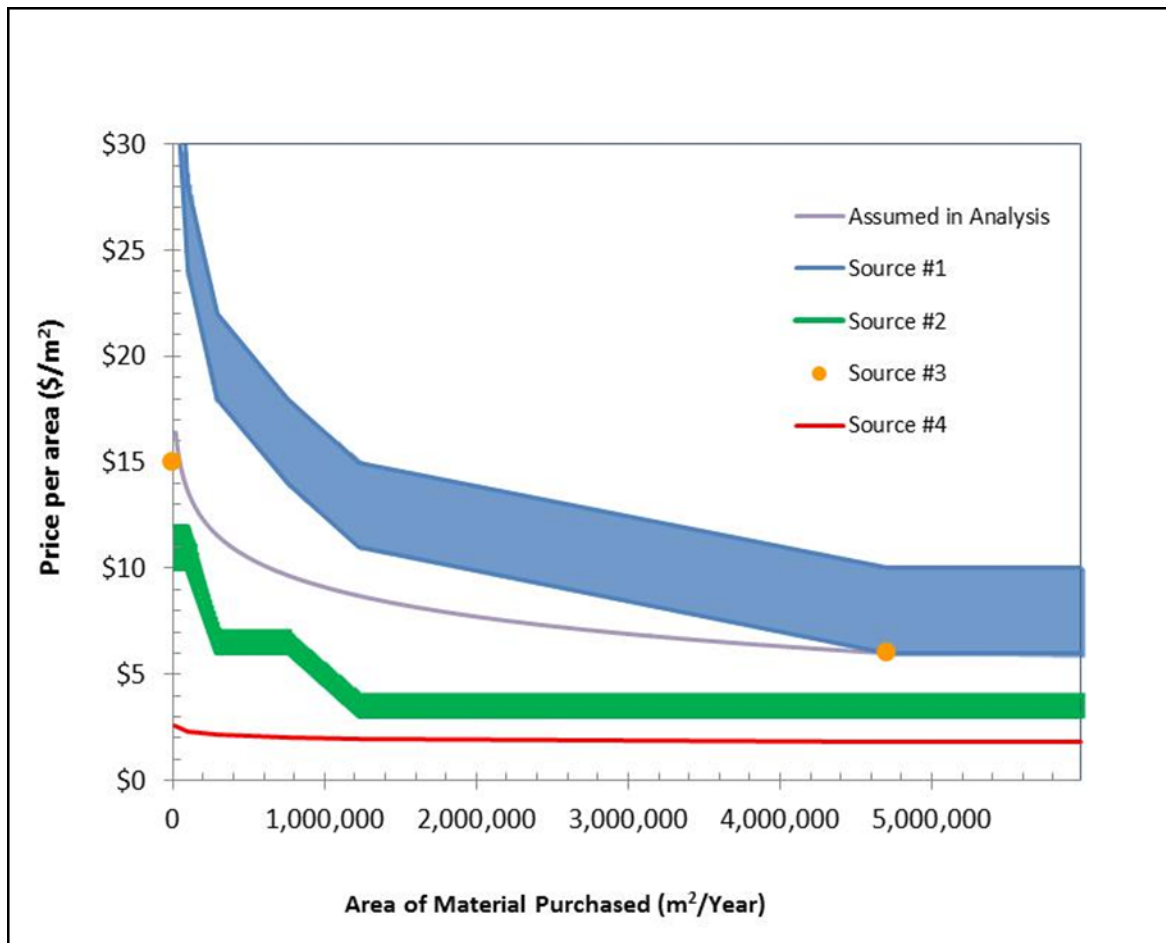


Figure 53. ePTFE price quotations and data selected for use in SA DFMA™ models

7.1.2.3 Membrane Manufacturing Cost

The membrane manufacturing method for 2013 is modeled as factory-based roll-to-roll processing, unchanged from previous SA analyses. The analysis is not based on a detailed enumeration of capital costs but rather uses industry supplied approximate plant cost estimates combined with estimated yield rates, labor requirements, line speeds, and markup rates to derive a simplified cost curve representing manufacturing cost as a function of membrane annual production rate.

As schematically detailed in Figure 54, the membrane fabrication process consists of eight main steps:

Unwinding: An unwind stand with tensioners is used to feed the previously procured ePTFE substrate into the process line. A web width of ~ 1m is deemed feasible for both the membrane fabrication line and the subsequent catalyzation.

First Ionomer Bath: The ePTFE substrate is dipped into an ionomer/solvent bath to partially occlude the pores.

First Infrared Oven Drying: The web dries via infrared ovens. A drying time of 30 seconds is postulated. Since the web is traveling quickly, considerable run length is required. The ovens may be linear or contain multiple back-and-forth passes to achieve the total required dwell time.

Second Ionomer Bath: The ionomer bath dipping process is repeated to achieve full occlusion of the ePTFE pores and an even thickness, pinhole-free membrane.

Second Infrared Oven Drying: The web is dried with a second bank of infra-red ovens after the second ionomer bath.

Boiling Water Hydration: The web is held in boiling water for 5 minutes to fully hydrate the ionomer. Optimal selection of the ionomer may reduce or eliminate this boiling step.

Air Dryer: High velocity air is used to dry the web after the hydration step.

Rewind: The finished membrane is wound onto a spool for transport to the catalyzation process line.

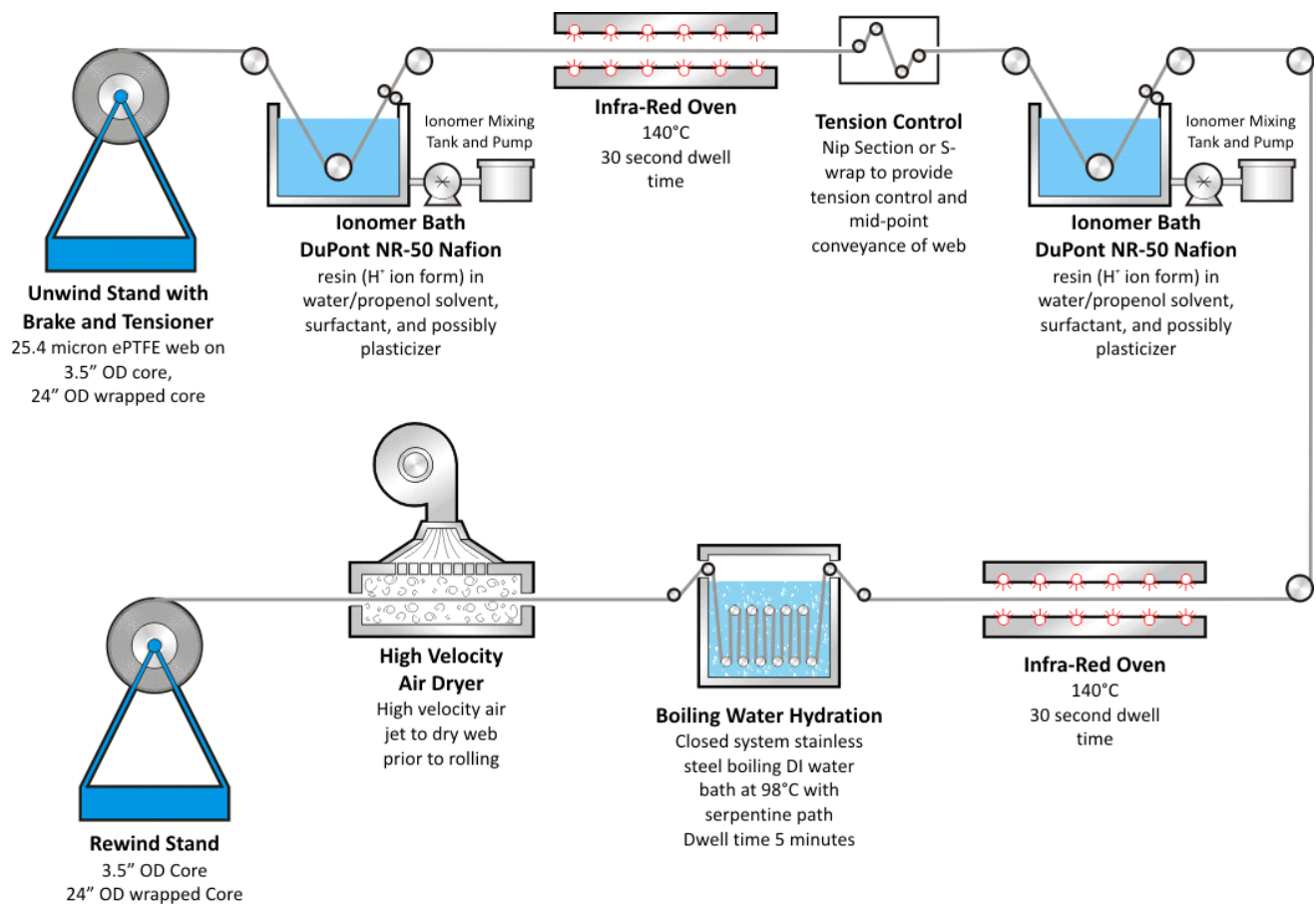


Figure 54. Membrane fabrication process diagram

Details of the simplified membrane fabrication cost analysis are shown in Figure 55. Two roll-to-roll plants are postulated: a “low-speed plant” (5 m/min) and a “high-speed” plant (35 m/min). Run at part load, they cover the full span of membrane production requirements (1,000 to 500,000 vehicles/year).

Key assumptions are noted below.

Capital Cost: Capital costs are coarsely estimated based on industry input and are significantly greater than previous element-by-element summations based on component price quotes.

Web speed: Even the “high-speed” web (35 m/min) is very slow by converting machinery standards where speeds of 100 m/min are often achieved. This is a nod toward cost conservativeness and a reflection that the upper bound of membrane web speed is not known at this time.

Discount Rate: The discount rate is increased to 20% to reflect the increased business risk of a membrane production line⁵⁷.

⁵⁷ While all fuel cell system manufactured components share similar market risk in that the demand for fuel cell vehicles is uncertain, some components (e.g. the membrane manufacturing line) utilize specialized equipment that

Production for Simultaneous Product Lines: In virtually all other components of the automotive fuel cell stack, it is assumed that there is vertical integration and dedicated component production for a single vehicle product. For the membrane however, it is likely that a separate company would fabricate the membrane for multiple car companies or, at least, that the membrane plant would produce membrane for more than one line of vehicles. Consequently, a multiplier on the yearly membrane demand is included to reflect supply to multiple vehicle product lines. This multiplier is not constant as production rate increases since the plant is at some point limited by capacity. The non-constant nature of the multiplier leads to unevenness in the resulting \$/m² cost projections.

Peak Equipment Utilization: Input from a membrane supplier raised the point that average plant utilization would be significantly affected under scenarios of rapid demand growth. Consequently, utilization (at most manufacturing rates) is limited to 67% to reflect the five-year average utilization assuming 25% per year demand growth. For the 500,000 vehicles per year case, plant utilization is allowed to increase to 80% to reflect a more stable production scenario.

Production/Cutting Yield: There are appreciable cutting losses associated with the roll-to-roll manufacturing process, which directly affect the membrane material costs. ePTFE yield was assessed at 77% to 98%. It is assumed that a portion of ionomer in the scrap membrane is able to be recycled. Consequently, it is assumed for costing purposes that the ionomer material wastage rate is half that of the overall membrane areal scrap rate (making the ionomer yield 89% to 99%). Manufacturing yield is assessed at the same yield as ePTFE.

Workdays and Hours: The maximum plant operating hours are assumed to be 20 hours per day, 240 days per year. Actual hours vary based on actual plant utilization.

Cost Markup: The standard methodology throughout the analysis has been not to apply manufacturer markups, in keeping with the vertically integrated manufacturing assumption, and the directives of the DOE on this costing project. However, since it is likely that the membrane producer will not be vertically integrated, a markup is included in our membrane cost estimate. Furthermore, because the membrane is a critical component of the stack, significantly higher margins are allocated than are typical to the automotive industry where there is a large supplier base with virtually interchangeable products competing solely on price. Markup on the manufacturing process varies from 40% to 70%. A constant 25% markup rate is applied to the materials (ePTFE and ionomer) in keeping with auto industry practice of the auto company supplying high cost materials to the vendor rather than paying a full markup for the vendor to procure the materials.

Revenue: Annual membrane fabricator revenue is not an input in the analysis. Rather it is an output. However, it is worth noting that even at high membrane production rates, company revenues are still only about \$35M per year. This is a modest company size and supports the notion of allowing higher-than-average markups as a means to entice people into the business.

can't be resold or repurposed for other markets. Furthermore, the membrane manufacturing line is one of the largest capital investments thereby amplifying the consequences of missing production projections.

Simplified Computation of Membrane Manufacturing Cost							
Annual Veh Prod. (1 product line)	vehicle/year	1,000	10,000	30,000	80,000	130,000	500,000
Capital Amortization							
Capital Cost (Membrane Fabrication)	\$	\$15,000,000	\$15,000,000	\$15,000,000	\$35,000,000	\$35,000,000	\$35,000,000
Machine Lifetime	years	10	10	10	10	10	10
Discount Rate	%	20%	20%	20%	20%	20%	20%
Corporate Income Tax Rate	%	40%	40%	40%	40%	40%	40%
Capital Recovery Factor (CRF)		0.331	0.331	0.331	0.331	0.331	0.331
Labor Costs							
Min. Mfg. Labor Staff (Simul. on 1 Shift)	FTE	5	25	25	50	50	50
Labor Rate	\$/min	1	1	1	1	1	1
Machine Costs							
Maintenance/Spare Parts (% of installed C.C./year)	%	5%	5%	5%	5%	5%	5%
Miscellaneous Expenses	%	5%	5%	5%	5%	5%	5%
Total Power Consumption	kW	200	200	250	350	350	350
Electrical Utility Cost	\$/kWh	0.07	0.07	0.07	0.07	0.07	0.07
Membrane Production Parameters							
Simul. Product Lines to Which Memb. is Supplied		5	3.25	2.2	2	1.75	1.5
Vehicle Annual Production	veh/year	5,000	32,500	66,000	160,000	227,500	750,000
m ² per Vehicle	m ² /vehicle	13.00	13.00	13.00	13.00	13.00	13.00
Peak Equipment Utilization Due to Growth	%	67%	67%	67%	67%	67%	100%
Production/Cutting Yield	%	77%	84%	88%	91%	93%	97.956%
Gross Production @ 100% Utilization (plant)	m ² /year	1,440,000	1,440,000	1,440,000	10,080,000	10,080,000	10,080,000
Gross Production (plant)	m ² /year	83,927	500,053	974,185	2,275,706	3,176,927	9,953,438
Net Production (plant)	m ² /year	65,000	422,500	858,000	2,080,000	2,957,500	9,750,000
Net Production of 1 Line	m ² /year	13,000	130,000	390,000	1,040,000	1,690,000	6,500,000
Design Web Speed	m/min	5	5	5	35	35	35
Web Width	m	1	1	1	1	1	1
Work Days per Year	days/year	240	240	240	240	240	240
Plant Utilization	% of 20hr days	5.8%	34.7%	67.7%	22.6%	31.5%	98.7%
Hours per Year of Production	hrs/year	280	1,667	3,247	1,084	1,513	4,740
Hours per Day of Production	hrs/day	1.17	6.95	13.53	4.52	6.30	19.75
Annual Cost Summation							
Capital Recovery Cost	\$/year	\$4,963,069	\$4,963,069	\$4,963,069	\$11,580,494	\$11,580,494	\$11,580,494
Labor Cost	\$/year	\$576,000	\$2,880,000	\$4,870,927	\$5,760,000	\$5,760,000	\$14,219,197
Maintenance/Spares Cost	\$/year	\$750,000	\$750,000	\$750,000	\$1,750,000	\$1,750,000	\$1,750,000
Miscellaneous Expenses	\$/year	\$750,000	\$750,000	\$750,000	\$1,750,000	\$1,750,000	\$1,750,000
Utility Cost	\$/year	\$3,917	\$23,336	\$56,827	\$26,550	\$37,064	\$116,123
Effective Machine Rate	\$/min	\$420	\$94	\$58	\$321	\$230	\$103
Total Manufacturing Cost (\$/net m2, pre-markup)							
From computations	\$/m ²	\$108.35	\$22.17	\$13.28	\$10.03	\$7.06	\$3.02
From simplified curve fit	\$/m ²	\$ 93.83	\$ 25.84	\$ 13.97	\$ 8.06	\$ 6.15	\$ 2.89
Manufacturing Cost Markup %	%	70%	59%	54%	49%	47%	40%
Gross Margin	%	41%	37%	35%	33%	32%	29%
Annual Revenue (on manufacturing only)	\$/year	\$10,368,358	\$17,348,407	\$18,407,310	\$24,970,418	\$26,626,707	\$39,451,822
Total Manufacturing Cost (\$/net m2, post-markup)							
From computations	\$/m ²	\$184.21	\$35.22	\$20.39	\$14.93	\$10.34	\$4.22
From simplified curve fit	\$/m ²	\$ 159.51	\$ 41.06	\$ 21.45	\$ 12.01	\$ 9.00	\$ 4.05

Figure 55. Simplified membrane manufacturing cost analysis assumptions

Membrane manufacturing cost is plotted against membrane annual volume in Figure 56 below. Note that membrane material costs (ionomer and ePTFE) are not included. Membrane manufacturing costs are computed using the multiple production line assumption. To aid in numerical calculation, a power curve was curve-fit to the cost computations.

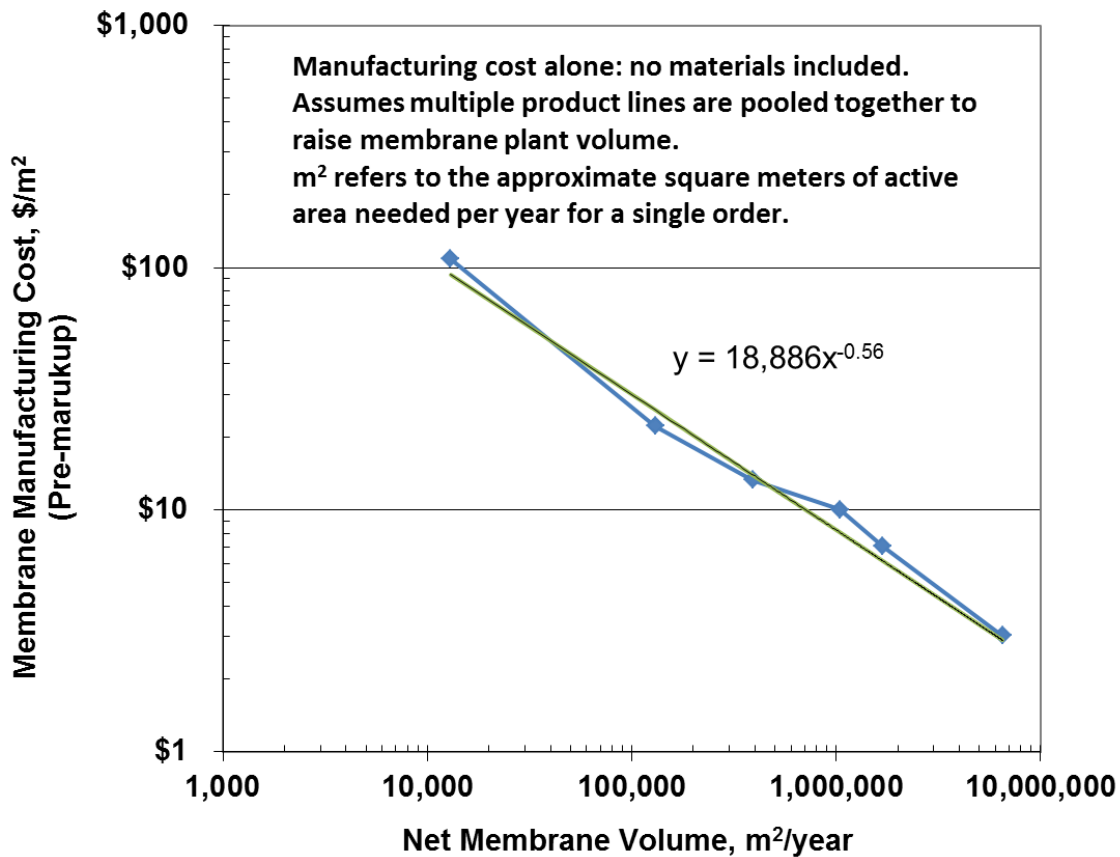


Figure 56. Membrane manufacturing cost vs. annual membrane manufacturing volume

7.1.2.4 Total Membrane Cost

Figure 57 summarized cost results for the un-catalyzed ePTFE supported membrane.

Annual Production Rate	1,000	10,000	30,000	80,000	100,000	500,000
Materials (\$/m ²)	\$44	\$29	\$23	\$18	\$17	\$12
Manufacturing (\$/m ²)	\$224	\$45	\$22	\$12	\$10	\$4
Total Cost (\$/m² (total) total)	\$268	\$74	\$45	\$30	\$27	\$16
Total Cost (\$/stack)	\$4,530	\$1,251	\$757	\$500	\$455	\$236
Total Cost (\$/kWnet)	\$56.63	\$15.64	\$9.47	\$6.24	\$5.68	\$2.95

Figure 57. Cost breakdown for the membrane (un-catalyzed)

7.1.3 Nanostructured Thin Film (NSTF) Catalyst Application

Over the years, SA has conducted cost analysis of two general types of catalyst application methods:

- Ink-based application
- Vapor deposition application

SA analysis from 2006 to 2010 was based on ink-based application (specifically die slot coating of the catalyst ink directly onto a moving membrane web via a Coatema VertiCoater system). Such an approach had the advantage of being one of the least costly application techniques judged adequate for high production rates and reasonably high MEA performance.

In 2010, SA switched to a new method of catalyst deposition that has shown significant improvements in power density and reported durability at low Pt loadings. Developed at 3M, the Nanostructured Thin Film Catalyst (NSTF) deposition process begins with vapor sublimation of a layer of crystalline finger-like projections, or “whiskers”, to create a high surface area substrate on which the active catalysts may be deposited. Next, vapor deposition methods are utilized to deposit a very thin layer of a ternary Platinum-Cobalt-Manganese (PtCoMn) catalyst onto the whiskers in a very precise and uniform manner. The resulting catalyst coated whiskers can then be pressed into the fuel cell membrane to form a porous mat electrode intimately bonded to the membrane. This NSTF catalyst application method continues to be used for the 2013 cost analysis.

In 2013, a Gore low cost membrane fabrication and catalyst application method was analyzed. Details of the Gore approach appear in Section 6.6. While not selected for inclusion in the 2013 baseline system, the Gore approach will be further explored in future analysis years.

The NSTF application process involves four main steps as identified by a review of non-proprietary open source literature from 3M^{58,59}. 3M representatives have reviewed and critiqued the analysis not for 100% accuracy as to how they would specifically carry out the production, but rather to vet the general approach and major elements affecting cost. They judge the process and resulting cost estimate to be consistent with internal proprietary projections of resulting catalyst cost.

7.1.3.1 NSTF Application Process

The main steps of the modeled NSTF catalyst application process are listed below and shown in Figure 58:

- **Deposition:** Physical Vapor Deposition(PVD) of PR-149 (Perylene Red pigment 149) onto a DuPont Kapton® polyamide web (a temporary deposition substrate)
- **Annealing:** Vacuum annealing of the PR-149, resulting in the formation of crystalline nanostructures through a screw dislocation growth process
- **Catalyst Sputtering:** Ternary PtCoMn catalyst is magnetron-sputtered into the nanostructures
- **Catalyst Transfer:** Roll-to roll transfer of the catalyst coated nanostructures from the Kapton® substrate to the PEM membrane

⁵⁸ US Patent #4,812,352 titled “Article having surface layer of uniformly oriented, crystalline, organic microstructures”.

⁵⁹ Advanced Cathodes and Supports for PEM Fuel Cell”, presented by Mark Debe of 3M at the 2009 DOE Hydrogen Program Annual Review Meeting, Arlington, VA, 20 May 2009.

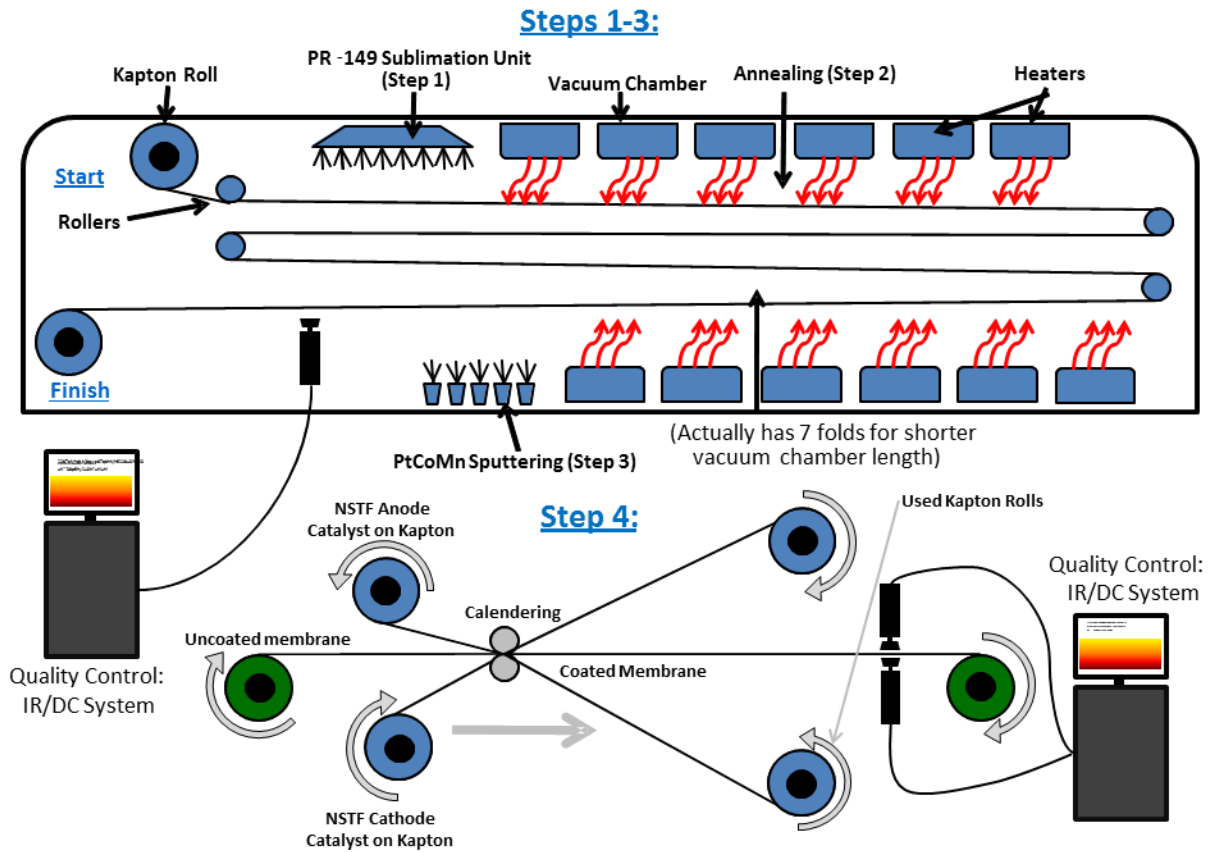


Figure 58. NSTF production process diagram

7.1.3.2 Cost and Performance Assumptions

Cost and performance assumptions concerning the NSTF catalyst creation system are listed below.

Capital Cost: The capital costs of the manufacturing machinery were based on conversations with industry representatives or are derived from previous SA work involving similar components. A complete list of capital cost is shown in Figure 59.

Component	Cost
Evacuation Chamber 1	\$81,256
Evacuation Chamber 2	\$152,355
Sublimation Unit	\$104,206
Cylindrical Magnetron Sputtering Unit	\$220,466
64 m (effective length) Vacuum Annealing Oven	\$446,597
Re-Pressurization Chamber 1	\$132,041
Re- Pressurization Chamber 2	\$81,256
Unwind and Rewind Stand w/ Tensioner	\$56,140
Hot Calender Decal Application (Step 4)	\$104,206
IR/DC Quality Control System	\$630,000
Total Capital Cost per Line	\$2,008,523

Figure 59. Capital costs of NSTF manufacturing line

Line Speed: The line speed calculation is based on a balance between the vacuum chamber length and the time needed for the sublimation, annealing, and sputtering operations and is set at 5.84 m/min. It is not cost effective to draw and release a vacuum for separate operations: thus all three are postulated to occur within the same vacuum chamber. The bulk of the chamber will be devoted to annealing, which, at the given line speed, requires approximately 58 m of length. Creating a vacuum chamber this long would be prohibitively expensive, and thus the web is assumed to travel in a serpentine pattern folding back on itself 7 times, so the annealing chamber itself will be ~8.5 m in total length. An additional ~3.5 m of sublimation and ~1.5m of sputtering chamber will be on either end of the annealing chamber. A minimum of ten minutes of annealing time is required for nanostructure formation. In addition to the annealing time, ~17 seconds is needed for catalyst deposition and 40 seconds is needed for PR-149 sublimation onto the substrate. These times are based on the thickness of the coatings (100nm for the PR-149 and 44nm for the catalyst coating) as indicated by 3M and an approximate deposition rate of 2.5 nm/sec. as indicated by representatives of Vergason Technology, Inc.

Catalyst Loading: 3M has demonstrated that high performance can be achieved at catalyst loadings of 0.15 mgPt/cm² in this configuration⁶⁰. The assumed mole fraction for the ternary catalyst was assumed to be 73% Platinum, 24% Cobalt, and 2% Manganese.

Web Roll Assumptions: We have assumed a roll length of 1500 m, with a loading time of ~16 minutes per roll⁶¹.

IR/DC Quality Control System: An infra-red (IR)/direct-current (DC) system is used to assess the uniformity of the electrode layers at three locations within the NSTF production sequence. The IR/DC system⁶² operates by placing two conductive rollers across the width of the web a short distance from one another. An electric current is fed to one of the roller, and then down the length of the electrode layer (anode and cathode) to be collected by the other roller. An IR camera mounted above the electrode and peering down onto the moving web is used to visually assess the temperature signature of the electrode and detect anomalies that would be indicative of electrode thickness variation, improper catalyst loading, improper particle size, non-uniform platinum distribution, or other general defects⁶³. Due to the simplicity of the signal processing required, IR camera systems can easily match the line speed of the catalyst deposition (5.84 m/min). To achieve appropriate resolution, six IR cameras are needed at each analysis site to achieve a 1m total field of view (the web width) at a 5.84 m/min web speed. Three systems are needed (at 500k systems/year) and correspond to viewing of 1) the catalyst layer after sputtering, 2) the anode after calendaring, and 3) the cathode after calendaring. Only one

⁶⁰ "Advanced Cathodes and Supports for PEM Fuel Cell", presented by Mark Debe of 3M at the 2009 DOE Hydrogen Program Annual Review Meeting, Arlington, VA, 20 May 2009.

⁶¹ The 16 minute total time includes times for loading and unloading the Kapton rolls as well as pressurizing and drawing a vacuum.

⁶² Niccolo V. Aieta, Prodip K. Das, Andrew Perdue, Guido Bender, Andrew M. Herring, Adam Z. Weber, Michael J. Ulsh, "Applying infrared thermography as a quality-control tool for the rapid detection of polymer-electrolyte-membrane-fuel-cell catalyst-layer-thickness variations", Journal of Power Sources, Volume 211, 1 August 2012, Pages 4-11.

⁶³ Private conversation with Michael Ulsh, NREL.

system is needed at 1k systems/year as it is assumed that the IR/DC equipment is re-used for all three webs.

7.1.3.3 NSTF Cost Results

Machine rate and process parameters are show in Figure 51 and Figure 52. The overall cost breakdown at various system values and technology levels is shown in Figure 53.

Annual Production Rate	1,000	10,000	30,000	80,000	100,000	500,000
Equipment Lifetime (years)	13	13	13	13	13	13
Interest Rate	10%	10%	10%	10%	10%	10%
Corporate Income Tax Rate	40%	40%	40%	40%	40%	40%
Capital Recovery Factor	0.183	0.182	0.181	0.181	0.181	0.181
Equipment Installation Factor	1.4	1.4	1.4	1.4	1.4	1.4
Maintenance/Spare Parts (% of CC)	10%	10%	10%	10%	10%	10%
Miscellaneous Expenses (% of CC)	7%	7%	7%	7%	7%	7%
Power Consumption (kW)	751	751	752	752	752	752

Figure 60. NSTF application process parameters

Annual Production Rate	1,000	10,000	30,000	80,000	100,000	500,000
Capital Cost (\$/Line)	\$1,588,523	\$1,798,523	\$2,008,523	\$2,008,523	\$2,008,523	\$2,008,523
Simultaneous Lines	1	1	2	3	4	17
Laborers per Line	2	2	2	2	2	2
Line Utilization	4.3%	39.1%	56.2%	96.3%	89.5%	99.1%
Effective Total Machine Rate (\$/hr)	\$4,859	\$732	\$601	\$413	\$433	\$406
Line Speed (m/s)	0.097	0.097	0.097	0.097	0.097	0.097

Figure 61. Machine rate parameters for NSTF application process

Annual Production Rate	1,000	10,000	30,000	80,000	100,000	500,000
Material (\$/stack)	\$1,014	\$997	\$993	\$989	\$988	\$973
Manufacturing (\$/stack)	\$1,188	\$153	\$116	\$75	\$77	\$64
Tooling (\$/stack)	\$40	\$18	\$17	\$16	\$16	\$14
Total Cost (\$/stack)	\$2,242	\$1,168	\$1,126	\$1,080	\$1,082	\$1,051
Total Cost (\$/kWnet)	\$28.03	\$14.60	\$14.08	\$13.50	\$13.52	\$13.14

Figure 62. Cost breakdown for NSTF application process

7.1.4 Catalyst Cost

As described in the previous section, a PtCoMn catalyst is used for the NSTF catalyst system and is applied via a physical vapor deposition method (modeled as magnetron sputtering). Consistent with PVD, the metal is supplied in the form of a pure sputtering target for each metal. The cost of each target is estimated to be:

Platinum: \$1,500/troy ounce

Cobalt: \$2.74/troy ounce

Manganese: \$ 0.15/troy ounce

The raw material cost of platinum is the major cost element of the catalyst ink. At the direction of the DOE, a platinum cost of \$1,500 per troy ounce is selected and is a price increase from the \$1,100/troy

ounce used in previous SA analysis. As shown in Figure 63, the newly updated \$1,500/troy ounce Pt price is a good match to the price of Platinum over the last several years.

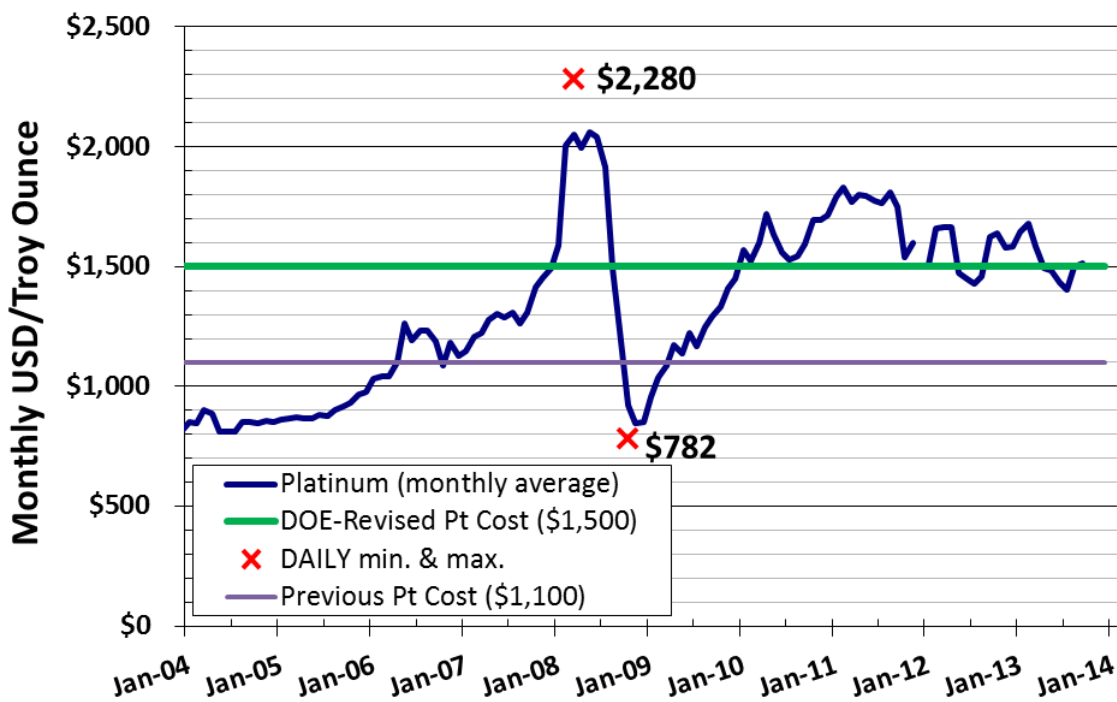


Figure 63. Ten-year graph of monthly platinum prices

7.1.5 Gas Diffusion Layer

The gas diffusion layer (GDL) costs for 2011 and previous analyses were based upon a price quote for a vendor macroporous layer combined with a DFMATM analysis of a microporous layer addition. This resulted in a GDL cost of ~\$11/m² at 500k systems/year (\$2.54/kWnet).

The 2012 and 2013 GDL cost estimates are based on recent DOE-funded research by Ballard Power Systems for cost reduction of a teflonated ready-to-assemble GDL consisting of a non-woven carbon base layer with two microporous layers⁶⁴. The Ballard analysis⁶⁵ estimates a cost of ~\$4.45/m² at 10M m²/year (approximately equivalent to 500k systems/year) and a cost of \$56/m² at less than 100k m²/year (approximately equivalent to 5k systems/year). Based upon these data points, a learning curve exponent of 0.6952 was derived and used to estimate the GDL cost at intermediate production rates. Figure 64 graphically portrays GDL cost used in the analysis as a function of annual GDL production.

⁶⁴ "Reduction in Fabrication Costs of Gas Diffusion Layers," Jason Morgan, Ballard Power Systems, DOE Annual Merit Review, May 2011.

⁶⁵ Personal communication with Jason Morgan of Ballard Power Systems, 24 July 2012.

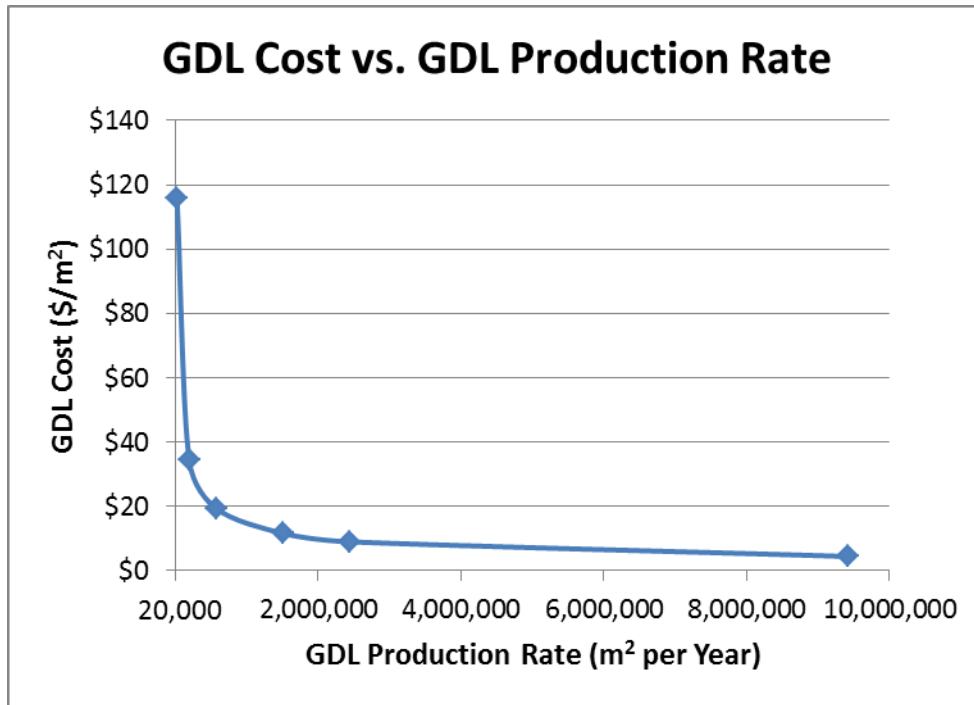


Figure 64. GDL cost as a function of production rate

The overall cost breakdown at various system values and technology levels is shown in Figure 65.

Annual Production Rate	1,000	10,000	30,000	80,000	100,000	500,000
GDL Cost (\$/stack)	\$2,661	\$795	\$447	\$267	\$238	\$102
Total Cost (\$/stack)	\$2,661	\$795	\$447	\$267	\$238	\$102
Total Cost (\$/kWnet)	\$33.26	\$9.94	\$5.59	\$3.34	\$2.97	\$1.28

Figure 65. Cost breakdown for GDL

7.1.6 MEA Sub-Gaskets

Prior to 2012, the fuel cell systems analyzed by SA were assumed to use MEA frame gaskets for gas and liquid sealing between the membrane and the bipolar plate⁶⁶. The frame gaskets were insertion-molded around the periphery of the MEA and added substantial cost due to high cycle time and the relatively high cost of custom injection-moldable sealant. Consequently, during the 2012 analysis, an examination was conducted of fuel cell manufacturer processes and patents to identify an alternative lower cost sealing approach. The use of sub-gaskets was identified as a promising alternative and was selected for both the 2012 and 2013 fuel cell systems.

The sub-gasket sealing approach consists of thin layers of PET gasketing material, judiciously cut into window-frame shapes and laminated to themselves and the periphery of the MEA to form a contiguous and flat sealing surface against the bipolar plate. A thin bead of adhesive sealing material is screen-printed onto the bipolar plates to form a gas- and liquid-tight seal between the bipolar plate and the sub-gasket material. The bipolar plate design has been changed to incorporate a raised surface at the

⁶⁶ "Mass Production Cost Estimation for Direct H2 PEM Fuel Cell Systems for Automotive Applications: 2010 Update," Brian D. James, Jeffrey A. Kalinoski & Kevin N. Baum, Directed Technologies, Inc., 30 September 2010.

gasket bead location to minimize the use of the gasket material. Screen printing of the gasket bead onto the bipolar plates is a well-understood and demonstrated process. The sub-gasket layers are bonded to the MEA in a roll-to-roll process, shown in Figure 66, based upon a 3M patent application⁶⁷. While the construction is relatively simple in concept, fairly complex machinery is required to handle and attain proper placement and alignment of the thin sub-gasket and MEA layers. This sub-gasket process has four main steps:

1. Formation of a catalyst coated membrane (CCM) web
2. Attachment of membranes to the first half of the sub-gasket ladder web
3. Attachment of the second half of the sub-gasket ladder web to the half sub-gasketed membrane
4. Attach GDLs to sub-gasketed membrane and cut to form individual five-layer MEAs

⁶⁷ "Fuel Cell Subassemblies Incorporating Subgasketed Thrifted Membranes," US2011/0151350A1

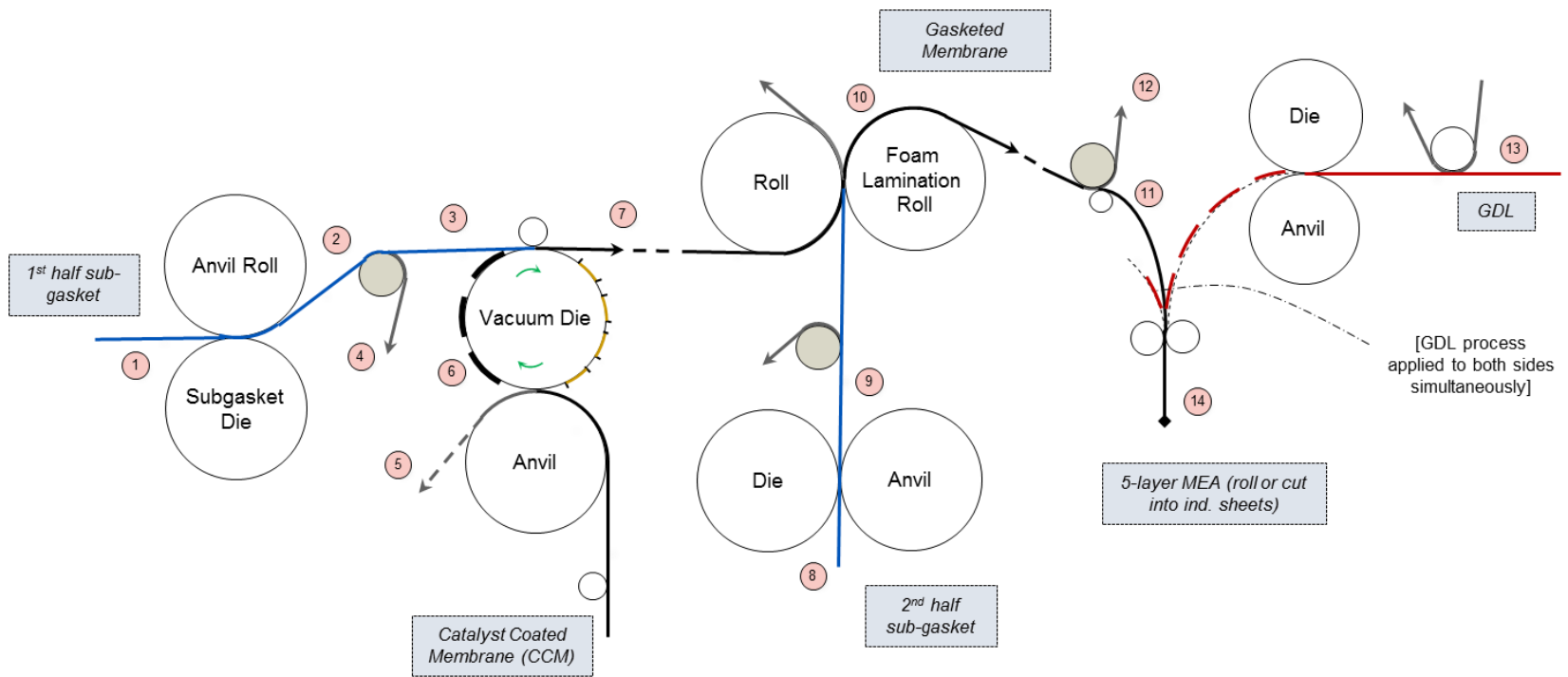


Figure 66. Roll-to-roll subgasket application process

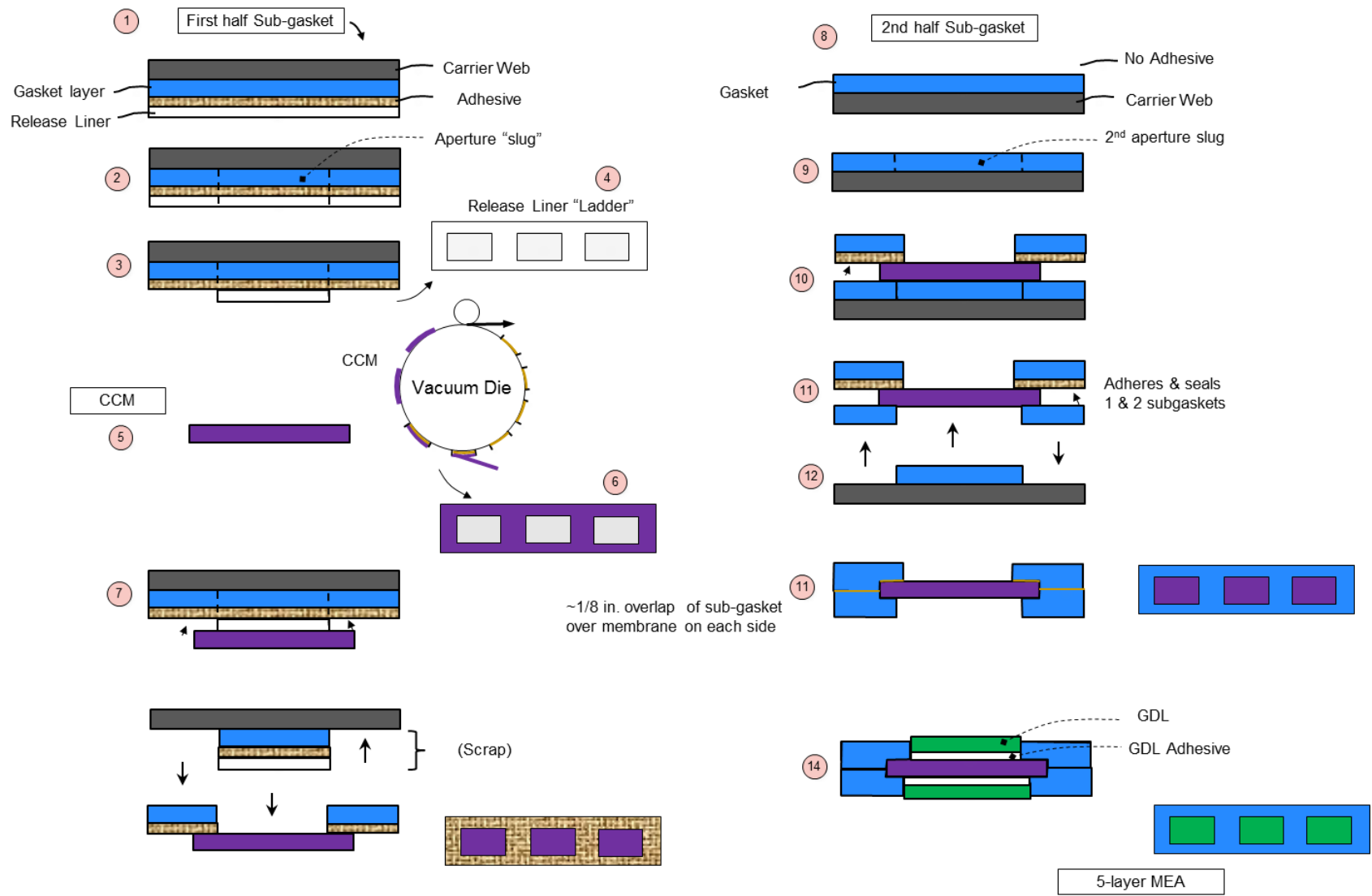


Figure 66. Continued...

The process uses a proprietary 3M “pressure sensitive adhesive,” which is modeled at a notional \$20/kg based on high end generic adhesive surrogates. The sub-gasket layer consists of two layers of 0.1mm PET film at \$1.67/m² based on a high-volume internet price quote. These materials experience significant waste using this process, as the center section of both the sub-gasket layers (corresponding to the fuel cell active area) and the adhesive liner is scrapped. The process capital equipment is based on component analogy to membrane web processing units and is assumed to operate at a line speed of 30m/min with five line workers.

A thin bead of sealing material is screen printed onto the bipolar plates to form a gas and liquid tight seal between the bipolar plate and the sub-gasket material. This process is directly analogous to the screen-printed coolant gaskets analyzed in past cost analyses⁶⁸. The cost of this screen printing step is combined with that of the sub-gasket procedure described above, and presented as a single cost result in Figure 11.

7.1.7 Subgasket Formation

Details of the MEA subgasket formation process appear in Figure 67 and Figure 68 with cost results shown in Figure 69.

Annual Production Rate	1,000	10,000	30,000	80,000	100,000	500,000
Equipment Lifetime (years)	13	13	13	13	13	13
Interest Rate	10%	10%	10%	10%	10%	10%
Corporate Income Tax Rate	40%	40%	40%	40%	40%	40%
Capital Recovery Factor	0.186	0.186	0.186	0.186	0.186	0.186
Equipment Installation Factor	1.4	1.4	1.4	1.4	1.4	1.4
Maintenance/Spare Parts (% of CC)	10%	10%	10%	10%	10%	10%
Miscellaneous Expenses (% of CC)	7%	7%	7%	7%	7%	7%
Power Consumption (kW)	101	101	101	101	101	101

Figure 67. MEA Subgasket process parameters

Annual Production Rate	1,000	10,000	30,000	80,000	100,000	500,000
Capital Cost (\$/Line)	\$2,848,600	\$2,848,600	\$2,848,600	\$2,848,600	\$2,848,600	\$2,848,600
Simultaneous Lines	1	1	1	2	3	11
Laborers per Line	5	5	5	5	5	5
Line Utilization	2.6%	23.7%	68.3%	87.8%	72.5%	93.0%
Effective Total Machine Rate (\$/hr)	\$14,328	\$1,774	\$771	\$652	\$740	\$629
Line Speed (m/s)	0.50	0.50	0.50	0.50	0.50	0.50
Kapton Tooling Cost (\$/m2)	\$7.12	\$3.92	\$3.68	\$3.60	\$3.59	\$3.57
Subgasket Material Cost (\$/m2)	\$1.67	\$1.67	\$1.67	\$1.67	\$1.67	\$1.67

Figure 68. MEA Subgasket machine parameters

⁶⁸ The reader is directed to section 4.4.9.3 of the 2010 update of the auto fuel cell cost analysis for a more detailed discussion. “Mass Production Cost Estimation for Direct H₂ PEM Fuel Cell Systems for Automotive Applications: 2010 Update,” Brian D. James, Jeffrey A. Kalinoski & Kevin N. Baum, Directed Technologies, Inc., 30 September 2010.

Annual Production Rate	1,000	10,000	30,000	80,000	100,000	500,000
Material (\$/stack)	\$54	\$54	\$54	\$54	\$54	\$54
Manufacturing (\$/stack)	\$1,247	\$141	\$59	\$48	\$54	\$43
Tooling (Kapton Web) (\$/stack)	\$19	\$9	\$9	\$8	\$8	\$8
Total Cost (\$/stack)	\$1,320	\$205	\$122	\$110	\$116	\$106
Total Cost (\$/kWnet)	\$16.50	\$2.56	\$1.52	\$1.38	\$1.46	\$1.32

Figure 69. Cost breakdown for MEA Subgasket

7.1.7.1 Screenprinted Subgasket Seal

Details of the screenprinted subgasket seal application step appear in Figure 70 and Figure 71 with cost results shown in Figure 72.

Annual Production Rate	1,000	10,000	30,000	80,000	100,000	500,000
Screen Printing Machine	DEK Horizon	DEK PV 1200				
Equipment Lifetime	15	15	15	15	15	15
Interest Rate	10%	10%	10%	10%	10%	10%
Corporate Income Tax Rate	40%	40%	40%	40%	40%	40%
Capital Recovery Factor	0.175	0.175	0.175	0.175	0.175	0.175
Equipment Installation Factor	1.4	1.4	1.4	1.4	1.4	1.4
Maintenance/Spare Parts (% of CC)	3%	1%	1%	1%	1%	1%
Miscellaneous Expenses (% of CC)	12%	12%	12%	12%	12%	12%
Power Consumption (kW)	61	166	166	166	166	166

Figure 70. Screenprinted Subgasket process parameters

Annual Production Rate	1,000	10,000	30,000	80,000	100,000	500,000
Screen Printing Machine	DEK Horizon	DEK PV 1200				
Capital Cost (\$/Line)	\$393,281	\$1,460,784	\$1,460,784	\$1,460,784	\$1,460,784	\$1,460,784
Simultaneous Lines	1	1	1	3	4	16
Laborers per Line	0.25	0.25	0.25	0.25	0.25	0.25
Line Utilization	29.1%	30.9%	92.7%	82.4%	77.3%	96.6%
Effective Total Machine Rate (\$/hr)	\$173	\$547	\$199	\$220	\$233	\$192
Line Speed (m/s)	1.00	1.00	1.00	1.00	1.00	1.00
Index Time (s)	\$9.62	\$4.00	\$4.00	\$4.00	\$4.00	\$4.00
Resin Cost (\$/kg)	\$15.19	\$15.19	\$15.19	\$15.19	\$15.19	\$15.19

Figure 71. Screenprinted subgasket machine parameters

Annual Production Rate	1,000	10,000	30,000	80,000	100,000	500,000
Material (\$/stack)	\$4	\$4	\$4	\$4	\$4	\$4
Manufacturing (\$/stack)	\$169	\$57	\$21	\$23	\$24	\$20
Total Cost (\$/stack)	\$173	\$61	\$25	\$27	\$28	\$24
Total Cost (\$/kWnet)	\$2.17	\$0.76	\$0.31	\$0.34	\$0.35	\$0.30

Figure 72. Cost breakdown for screenprinted subgasket

7.1.7.2 Total MEA Subgasket & Seal Cost'

The total cost of the subgasket (subgasket formation plus screenprinted seal) appears in Figure 73.

MEA Gasketing - Total Cost						
Annual Production Rate	1,000	10,000	30,000	80,000	100,000	500,000
Material (\$/stack)	\$58	\$58	\$58	\$58	\$58	\$58
Manufacturing (\$/stack)	\$1,416	\$198	\$80	\$71	\$78	\$63
Tooling (Kapton Web) (\$/stack)	\$19	\$9	\$9	\$8	\$8	\$8
Total Cost (\$/stack)	\$1,493	\$265	\$146	\$137	\$145	\$130
Total Cost (\$/kWnet)	\$18.67	\$3.32	\$1.83	\$1.72	\$1.81	\$1.62

Figure 73. Cost breakdown for total MEA subgasket

7.1.8 MEA Crimping, Cutting, and Slitting

Industry feedback⁶⁹ confirmed that the previous modeled procedure of hot pressing the membrane and GDL to bond the parts was incompatible with the NSTF catalyst layer⁷⁰. Bonding of the three layers of the MEA (the catalyst-coated membrane plus GDL on either side) is desirable for proper alignment of the parts as well as ease of subsequent MEA handling. Consequently for both the 2012 and 2013 cost analyses, the layers of the MEA are crimped together periodically along the edges after the MEA gasketing process and before the cutting and slitting process, to an extent sufficient to hold the assembly together. Cost of the operation is very low, as it merely requires an extra roller assembly in the cutting and slitting process line.

(The crimping process arguably should be viewed as a final processing stage of the gasketing process so that rolls of bonded GDL/CCM/gasket emerge from that process train. However, since crimping replaces hot pressing which was previously grouped with cutting and slitting, that organization of the cost results is preserved.)

As shown in Figure 74, the rolls of crimped MEA are fed through cutters and slitters to trim to the desired dimensions for insertion into the stack. The 50-cm-wide input roll is slit into ribbon streams of the appropriate width (again, depending on cell geometry). The streams continue through to the cutters, which turn the continuous material into individual rectangles. These rectangles are then sorted into magazine racks.

⁶⁹ Personal communication with Mark Debe of 3M, November 2011.

⁷⁰ Previous cost analysis postulated bonding of the GDL and catalyst coated membrane through a hot pressing procedure since the ionomer within the catalyst ink composition could serve as a bonding agent for the GDL. However, there is no ionomer in the NSTF catalyst layer and thus hot pressing would not be effective for NSTF MEA's.

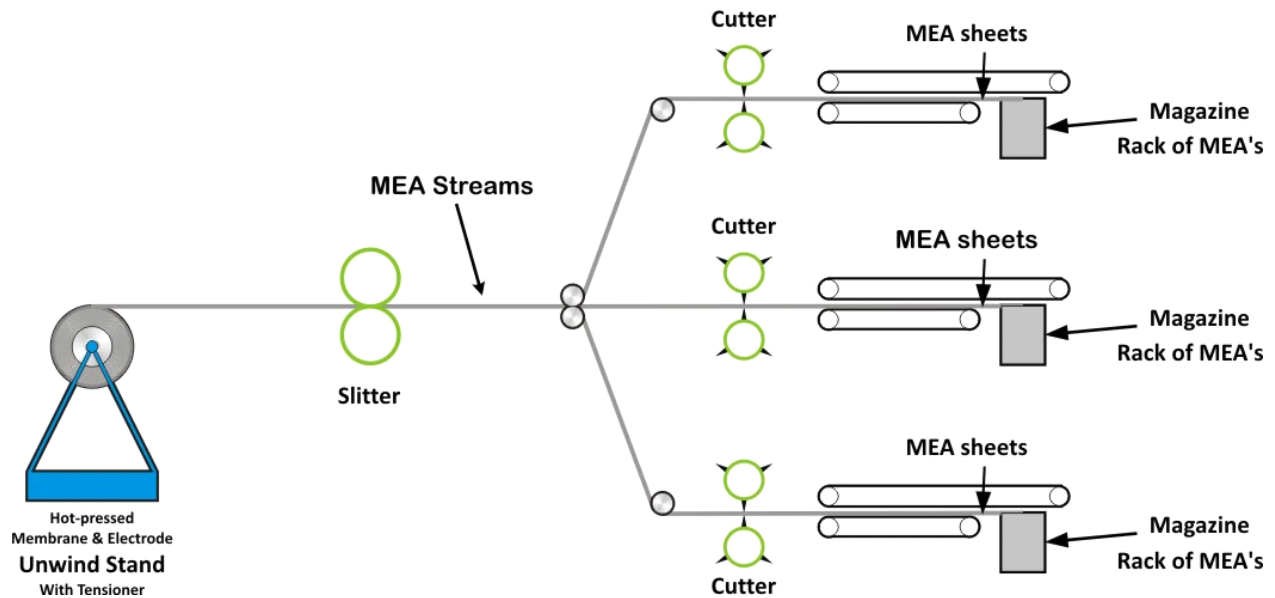


Figure 74. Cutting & slitting process diagram

Figure 75 and Figure 76 further detail the process parameters. Machine utilization at 1,000 systems per year is extremely poor (as low as 0.18%). However, costs associated with manual cutting are comparable to the automated system running at poor utilization. Consequently, for simplicity this process is presented as being automated at all production rates. Figure 77 summarizes the overall cost of the crimping, cutting, and slitting operation.

Annual Production Rate	1,000	10,000	30,000	80,000	100,000	500,000
Equipment Lifetime (years)	14	14	14	14	14	14
Interest Rate	10%	10%	10%	10%	10%	10%
Corporate Income Tax Rate	40%	40%	40%	40%	40%	40%
Capital Recovery Factor	0.177	0.177	0.177	0.177	0.177	0.177
Equipment Installation Factor	1.4	1.4	1.4	1.4	1.4	1.4
Maintenance/Spare Parts (% of CC)	10%	10%	10%	10%	10%	10%
Miscellaneous Expenses (% of CC)	7%	7%	7%	7%	7%	7%
Power Consumption (kW)	18.7	18.7	18.7	18.7	18.7	18.7

Figure 75. Cutting & Slitting process parameters

Annual Production Rate	1,000	10,000	30,000	80,000	100,000	500,000
Capital Cost (\$/line)	\$1,266,839	\$1,266,839	\$1,266,839	\$1,266,839	\$1,266,839	\$1,266,839
Costs per Tooling Set (\$)	\$5,614	\$5,614	\$5,614	\$5,614	\$5,614	\$5,614
Tooling Lifetime (cycles)	200,000	200,000	200,000	200,000	200,000	200,000
Simultaneous Lines	1	1	1	1	1	2
Laborers per Line	0.25	0.25	0.25	0.25	0.25	0.25
Line Utilization	0.3%	2.8%	8.3%	21.9%	27.3%	68.3%
Effective Total Machine Rate (\$/hr)	\$50,801	\$5,583	\$1,915	\$735	\$591	\$244
Line Speed (m/s)	1.07	1.22	1.29	1.33	1.33	1.33

Figure 76. Machine rate parameters for Cutting & Slitting process

Annual Production Rate	1,000	10,000	30,000	80,000	100,000	500,000
Manufacturing (\$/stack)	\$530	\$53	\$18	\$7	\$5	\$2
Tooling (\$/stack)	\$2	\$2	\$2	\$2	\$2	\$2
Total Cost (\$/stack)	\$533	\$55	\$20	\$9	\$8	\$4
Total Cost (\$/kWnet)	\$6.66	\$0.69	\$0.25	\$0.11	\$0.09	\$0.05

Figure 77. Cost breakdown for Cutting & Slitting process

7.1.9 End Plates

In a typical PEM fuel cell stack, the purposes of an end plate are threefold:

- Evenly distribute compressive loads across the stack
- Cap off and protect the stack
- Interface with the current collector

Typically there is also a separate insulator plate at each end to electrically insulate the stack from the rest of the vehicle. However the SA end plate design, based on a UTC patent (see Figure 78), eliminates the need for separate insulators. Thus, the SA modeled end plates also serve a fourth function: electrical insulation of the ends of the stack.

The end plate is made from a compression-molded composite (LYTEX 9063), is mechanically strong (455 MPa) to withstand the compressive loading, and is sufficiently electrically non-conductive (3×10^{14} ohm-cm volume resistivity). Use of this material allows for an end plate with lower cost and lower thermal capacity than the typical metal end plates, with the additional benefit of having very low corrosion susceptibility. The benefits of lower cost and corrosion resistance are obvious, and the low thermal capacity limits the thermal energy absorbed during a cold start, effectively accelerating the startup period.

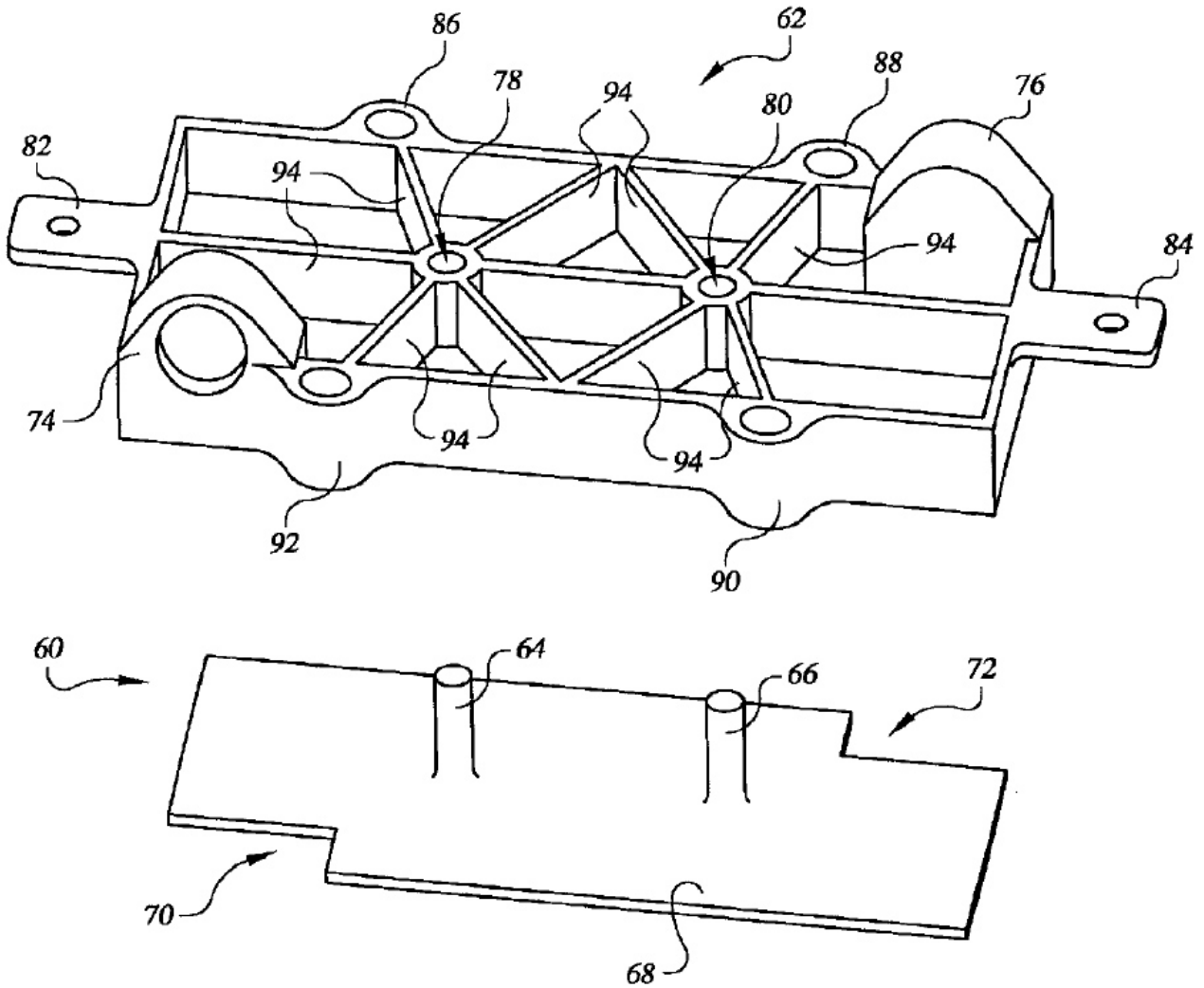


Figure 78. End plate concept (Figure courtesy of US patent 6,764,786)

LYTEX 9063 is a high performance engineered structural composite (ESC) molding compound consisting of epoxy and glass fiber reinforcement. It is designed for military and aerospace structural applications requiring excellent mechanical properties, retention of properties at elevated temperatures, good chemical resistance and excellent electrical properties. For all of these reasons, it is ideally suited for this application.

The end plates are manufactured via compression molding. A summary of the procedure is as follows⁷¹:

- Remove enough LYTEX from cold storage for one day's usage. Allow it to warm to room temperature.
- Clean mold thoroughly. Apply a uniform thin coating of a mold release. (Note: Once the mold is conditioned for LYTEX, only periodic reapplications are required.)

⁷¹ Based on Quantum Composites recommended procedures for LYTEX molding.

- Adjust mold temperature to 300°F (148°C).
- Adjust molding pressure on the material to 1,500 psi (105 kg/cm).
- Remove protective film completely from both sides of the LYTEX.
- Cut mold charge so the LYTEX covers approximately 80% of the mold area and is about 105% of the calculated part weight.
- Dielectrically preheat the LYTEX quickly to 175°F (80°C).
- Load material into mold and close the mold.
- Cure for 3 minutes
- Remove part from mold. Because of low shrinkage and high strength, the part may fit snugly in the mold.
- Clean up mold and begin again.
- Re-wrap unused LYTEX and return to cold storage.

Details of the end plate processing parameters are shown in Figure 79 and Figure 80.

Annual Production Rate	1,000	10,000	30,000	80,000	100,000	500,000
Equipment Lifetime (years)	15	15	15	15	15	15
Interest Rate	10%	10%	10%	10%	10%	10%
Corporate Income Tax Rate	40%	40%	40%	40%	40%	40%
Capital Recovery Factor	0.175	0.175	0.175	0.175	0.175	0.175
Equipment Installation Factor	1.4	1.4	1.4	1.4	1.4	1.4
Maintenance/Spare Parts (% of CC)	10%	10%	10%	10%	10%	10%
Miscellaneous Expenses (% of CC)	12%	12%	12%	12%	12%	12%
Power Consumption (kW)	28	28	57	60	60	65

Figure 79. End plate compression molding process parameters

As seen in Figure 81, the material represents the majority of the end plate costs, ranging from 38% to 95%, depending on the production rate.

Annual Production Rate	1,000	10,000	30,000	80,000	100,000	500,000
Capital Cost (\$/line)	\$223,882	\$223,882	\$419,958	\$447,969	\$447,969	\$503,991
Costs per Tooling Set (\$)	\$25,837	\$25,837	\$74,045	\$79,713	\$79,713	\$90,564
Tooling Lifetime (cycles)	300,000	300,000	300,000	300,000	300,000	300,000
Simultaneous Lines	1	1	1	1	1	3
Laborers per Line	0.5	0.5	0.5	0.5	0.5	0.5
Line Utilization	2.6%	25.7%	19.1%	46.4%	58.0%	82.9%
Cycle Time (s)	310.16	310.16	345.72	350.80	350.80	360.96
Cavities/Platen	2	2	9	10	10	12
Effective Total Machine Rate (\$/hr)	\$1,220	\$146	\$332	\$161	\$134	\$112
LYTEX Cost (\$/kg)	\$31.49	\$26.37	\$24.23	\$22.47	\$22.09	\$19.51

Figure 80. Machine rate parameters for compression molding process

Annual Production Rate	1,000	10,000	30,000	80,000	100,000	500,000
Material (\$/stack)	\$69	\$58	\$53	\$49	\$48	\$43
Manufacturing (\$/stack)	\$106	\$13	\$7	\$3	\$3	\$2
Tooling (\$/stack)	\$1.72	\$0.17	\$0.16	\$0.07	\$0.05	\$0.07
Total Cost (\$/stack)	\$176.75	\$70.39	\$60.23	\$52.33	\$50.96	\$44.60

Figure 81. Cost breakdown for end plates

7.1.10 Current Collectors

The function of the current collectors is to channel the electrical current that is distributed across the active area of the stack down to the positive and negative terminals. In the SA modeled design, based on the UTC patent (Figure 78) and shown in Figure 82, two copper current studs protrude through the end plates to connect to a copper sheet in contact with the last bipolar plate.

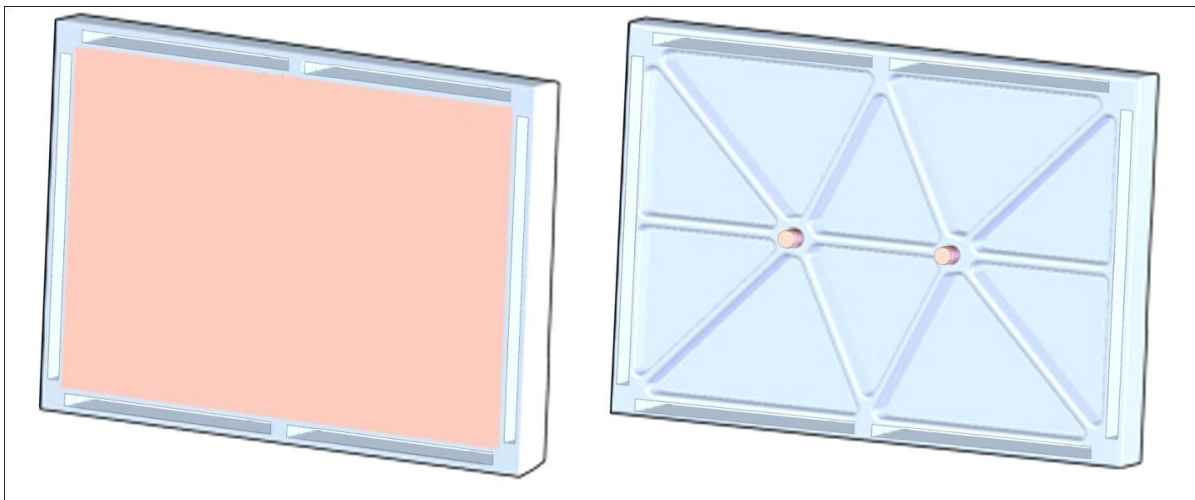


Figure 82. End plate and current collector⁷²

The current collectors were designed to fit snugly within the end plate. A shallow (0.3 mm) cavity in the end plate provides room for the 1 mm thick copper sheet, sized to the active area of the cells. The remaining 0.7 mm of the sheet thickness protrudes from the end plate, and the end plate gasket seals around the edges.

The face of the current collector is pressed against the coolant side of the last bipolar plate in the stack. With the compression of the stack, it makes solid electrical contact with the bipolar plate, and thus can collect the current generated by the stack.

The other side of the current collector is flush against the inner face of the end plate. Two copper studs protrude through their corresponding holes in the end plate, where they are brazed to the current collector sheet. On the outside of the end plate, these studs serve as electrical terminals to which power cables may be attached.

⁷² Some details of the port connections are not shown in the illustration.

Manufacturing the current collectors is a fairly simple process. A roll of 1 mm thick copper sheeting is stamped to size, and 8 mm diameter copper rod is cut to 2.43 cm lengths. The ends of the rods are then brazed to one face of the sheet. At low production (1,000 systems per year), a manual cutting process is used. All other manufacturing rates use an automated process that cuts parts from a roll of copper sheet stock.

Details of current collector processing parameters are shown in Figure 83 and Figure 84. Cost results are shown in Figure 85.

Annual Production Rate	1,000	10,000	30,000	80,000	100,000	500,000
Equipment Lifetime (years)	15	15	15	15	15	15
Interest Rate	10%	10%	10%	10%	10%	10%
Corporate Income Tax Rate	40%	40%	40%	40%	40%	40%
Capital Recovery Factor	0.175	0.175	0.175	0.175	0.175	0.175
Equipment Installation Factor	1.4	1.4	1.4	1.4	1.4	1.4
Maintenance/Spare Parts (% of CC)	13%	13%	13%	13%	13%	13%
Miscellaneous Expenses (% of CC)	2%	2%	2%	2%	2%	2%
Power Consumption (kW)	23	23	23	23	23	23

Figure 83. Current collector manufacturing process parameters

Annual Production Rate	1,000	10,000	30,000	80,000	100,000	500,000
Costs per Tooling Set (\$)	\$1,973	\$1,973	\$1,973	\$1,973	\$1,973	\$1,973
Tooling Lifetime (cycles)	400,000	400,000	400,000	400,000	400,000	400,000
Capital Cost (\$/line)	\$122,574	\$157,393	\$168,313	\$168,313	\$168,313	\$168,313
Simultaneous Lines	1	1	1	1	1	1
Laborers per Line	1.00	0.25	0.25	0.25	0.25	0.25
Line Utilization	0.1%	0.2%	0.5%	1.2%	1.5%	7.4%
Effective Total Machine Rate (\$/hr)	\$25,154	\$12,308	\$4,400	\$1,679	\$1,342	\$280
Index Time (s)	3.00	0.55	0.55	0.55	0.55	0.55
Copper Cost (\$/kg)	\$11.23	\$10.11	\$10.11	\$8.98	\$8.42	\$7.86

Figure 84. Machine rate parameters for current collector manufacturing process

Annual Production Rate	1,000	10,000	30,000	80,000	100,000	500,000
Material (\$/stack)	\$8.12	\$7.36	\$7.36	\$7.31	\$7.28	\$6.65
Manufacturing (\$/stack)	\$48.45	\$6.22	\$2.22	\$0.84	\$0.67	\$0.14
Tooling (\$/stack)	\$0.13	\$0.01	\$0.01	\$0.01	\$0.01	\$0.01
Secondary Operations (\$/stack)	\$0.53	\$0.53	\$0.53	\$0.53	\$0.53	\$0.53
Total Cost (\$/stack)	\$57.23	\$14.11	\$10.12	\$8.68	\$8.48	\$7.33
Total Cost (\$/kWnet)	\$0.72	\$0.18	\$0.13	\$0.11	\$0.11	\$0.09

Figure 85. Cost breakdown for current collector manufacturing process

7.1.11 Coolant Gaskets/Laser-welding

Coolant gaskets seal between the facing coolant-flow sides of the bipolar plates, around the perimeter of the flow fields, and thus prevent coolant from leaking into the air or hydrogen manifolds. There is a coolant gasket in every repeat unit, plus an extra at the end of the stack. Thus each stack has hundreds of coolant gaskets.

Three methods coolant gaskets methods have been previously analyzed:

- insertion molding to apply the coolant gasket

- screen printing of the coolant gasket
- laser welding

Laser welding of the bipolar plate edges (to eliminate the need of a separate coolant) has been selected for every system analyzed since 2008 and is also selected for the 2013 design.

Laser welding is an option that only applies to use with metallic bipolar plates. The idea of welding two plates together to form a seal is a popular approach in the fuel cell industry, an alternative to injection-molding with potential for increased production rates. Conversations with Richard Trillwood of Electron Beam Engineering of Anaheim, California indicate that grade 316L stainless steel is exceptionally well-suited to laser welding. Additionally, the thinness of the plates allows welding from the plate face, which is significantly quicker and thus less expensive than edge welding around the perimeter. Figure 86 details key process parameters.

Annual Production Rate	1,000	10,000	30,000	80,000	100,000	500,000
Equipment Lifetime (years)	15	15	15	15	15	15
Interest Rate	10%	10%	10%	10%	10%	10%
Corporate Income Tax Rate	40%	40%	40%	40%	40%	40%
Capital Recovery Factor	0.175	0.175	0.175	0.175	0.175	0.175
Equipment Installation Factor	1.4	1.4	1.4	1.4	1.4	1.4
Maintenance/Spare Parts (% of CC)	10%	10%	10%	10%	10%	10%
Miscellaneous Expenses (% of CC)	12%	12%	12%	12%	12%	12%
Power Consumption (kW)	35	35	35	35	35	35

Figure 86. Coolant gasket laser welding process parameters

Laser welding provides a number of distinct advantages compared to traditional gasketing methods. The welds are extremely consistent and repeatable, and do not degrade over time as some gaskets do. It also has extremely low power requirements, and very low maintenance and material costs. Consumables include argon gas, compressed air and a cold water supply. Maintenance involves lamp replacement every three months, lens cleaning, and general machine repair. Trillwood suggests that the welding speed is limited to a range of 60 to 100 inches per minute, with a maximum of three parts being welded simultaneously. However, according to *Manufacturing Engineering & Technology*,⁷³ laser welding speeds range from 2.5m/min to as high as 80 m/min. A welding speed of 15 m/min (0.25m/s) is selected as a conservative middle value.

Figure 87 shows the machine rate parameters, and Figure 88 shows the cost breakdown.

⁷³ *Manufacturing Engineering & Technology*, by Kalpakjian & Schmid (5th edition), p. 957.

Annual Production Rate	1,000	10,000	30,000	80,000	100,000	500,000
Capital Cost (\$/line)	\$451,281	\$857,562	\$857,562	\$857,562	\$857,562	\$857,562
Gaskets Welded Simultaneously	1	3	3	3	3	3
Runtime per Gasket (s)	0.50	0.50	0.50	0.50	0.50	0.50
Simultaneous Lines	1	1	3	6	7	35
Laborers per Line	0.25	0.25	0.25	0.25	0.25	0.25
Line Utilization	20%	68%	68%	91%	98%	98%
Effective Total Machine Rate (\$/hr)	\$319	\$188	\$188	\$144	\$136	\$136
Material Cost (\$/kg)	\$0.00	\$0.00	\$0.00	\$0.00	\$0.00	\$0.00

Figure 87. Machine rate parameters for gasket laser-welding process

Annual Production Rate	1,000	10,000	30,000	80,000	100,000	500,000
Material (\$/stack)	\$0.00	\$0.00	\$0.00	\$0.00	\$0.00	\$0.00
Manufacturing (\$/stack)	\$219.37	\$43.08	\$43.08	\$33.12	\$31.13	\$31.13
Tooling (\$/stack)	\$0.00	\$0.00	\$0.00	\$0.00	\$0.00	\$0.00
Total Cost (\$/stack)	\$219.37	\$43.08	\$43.08	\$33.12	\$31.13	\$31.13
Total Cost (\$/kWnet)	\$2.74	\$0.54	\$0.54	\$0.41	\$0.39	\$0.39

Figure 88. Cost breakdown for coolant gasket laser welding

7.1.12 End Gaskets

The end gaskets are very similar to the coolant gaskets but are sandwiched between the last bipolar plate and the end plate, rather than between two bipolar plates. This means that welding is not an option, as the end plates are non-metallic. They also have a slightly different geometry than the coolant gaskets, due to their function as a seal against reactant gasses rather than the coolant. Like the coolant gaskets, they were initially modeled using insertion molding, but were switched to a screen printing approach beginning in 2008. The largest difference between coolant gaskets and end gaskets is simply the quantity needed; with only two end gaskets per stack, there are far fewer end gaskets than coolant gaskets. Screen printing of the end gaskets is selected for the 2013 design.

Conversations with DEK International confirmed initial SA assumptions and various screen printers were examined for their efficacy at five production levels. To screen print a seal onto a bipolar plate, a single plate, or a pallet holding several plates, is first fed into the machine by conveyor. Once in the screen printer, it is locked into place and cameras utilize fiducial markers on either the plate itself or the pallet for appropriate alignment. A precision emulsion screen is placed over the plates, allowing a wiper to apply the sealing resin. After application, the resin must be UV cured to ensure adequate sealing.

Two different scenarios were examined in the screen printing process. In the first, one plate would be printed at a time, reducing costs by halving the need for handling robots to align plates. It would also avoid the necessity of a pallet to align multiple plates in the screen printer. The second scenario requires two handling robots to place four plates onto prefabricated self-aligning grooves in a pallet, ensuring proper alignment in the screen printer. The advantage of this technique is reduced cycle time per plate. However, it would result in increased capital costs due to more expensive screen printers, increased necessity for handling robots and precise mass-manufacture of pallets. Small variations in the grooves of pallets would lead to failure of the screen printer to align properly or apply the resin appropriately.

Printers: Three different screen printer models were examined as recommended by representatives from the DEK Corporation. The Horizon 01i machine was suggested for one-plate printing. The Europa VI and the PV-1200 were both evaluated for four plate printing. Comparison of the screen printers can be seen in Figure 89. After cost-analysis, it was determined that, despite the reduced cycle time (12.26 second to 4 seconds), the PV-1200 and Europa VI machines were more expensive, even at higher volumes. The Horizon was cheapest at all production levels.

		Screen Printers (DEK)		
Machine		Horizon	Europa VI	PV-1200
Cycle Time	s	9.63	12.26	4
Cost	\$	\$150,000	\$200,000	\$1,000,000
Power Consumption	kW	3.5	3.5	0.7
Print Area	in ²	400	841	841

Figure 89. Screen printer comparison

Resin: The selected resin formula is based upon information gleaned from the Dana Corporation US patent 6,824,874. The patent outlines several resins that would be suitable to provide an effective seal between bipolar plates and resin “A” was selected for its formulaic simplicity. However, any of the other recommended resins could be substituted with negligible changes in cost and performances.

UV Curing: Following printing, a short conveyor is needed to transfer the printed plate to a UV curing system. Consultation with representatives from UV Fusion Systems Inc. of Gaithersburg, Maryland, along with information from the Dana Corporation resin patent indicated that the VPS 1250 lamp carrying 350 watt type D and type H+ bulbs⁷⁴ would be adequate to cure the resin. If it is only necessary to cure a single plate, then one seven inch type D, and one seven inch type H+ bulb should be used. In order to ensure full UV coverage, for a 24 inch pallet holding four plates, three side-by-side ten inch bulbs of both types would be employed.

Patent research indicates that roughly two seconds of exposure for each type of lamp is sufficient for curing. When using the PV-1200 screen printer the curing time for both lamps matches the cycle time for the screen printer. If using the Horizon printer, the cure time is less than half the cycle time for the printer, yet in both situations the plates could be indexed to match the screen printer cycle time. A shutter would be built into the lamp to block each bulb for half of the time the plate is within the system to ensure adequate exposure of both light types. Rapidly turning the bulbs on and off is more destructive to the bulb life than continuous operation, making a shutter the preferred method of alternating light sources.

Cost estimation for UV curing system includes cost of lamps, bulbs, power supply rack, light shield to protect operators, and blowers for both lamp operation and heat reduction.

⁷⁴ Type D and Type H+ bulbs refer to the specific light wavelength emitted. Both wavelengths are needed for curing.

Maintenance: Communication with DEK has indicated that, if properly cared for, the screen printers have a lifetime of twenty years, but on average are replaced after only eight years due to poor maintenance practices. The modeled lifetime is specified as ten years. Regular maintenance, including machine repair, cleaning, and replacement of screens every 10,000 cycles costs an estimated \$10,000 per year.

Utilities: Relatively little power is used by the printers. A belt-drive system that collects and releases parts is the primary power consumer of the screen printers. Additional consumption comes from the alignment system, the wiper blade and the screen controls. Depending on the specifications of the individual printer, power consumption varies from 0.7 to 3.5 kW. On the other hand, the UV curing system has higher power demand. The total power usage, ranging from 61 to 166 kW, is primarily consumed by the lamps, but also by the exhaust blowers and the modular blowers for the lamps.

Figure 90 shows the key process parameters, as selected for the model. The capital cost includes the cost of the screen printer, plus a UV curing system, plate handling robots, and a conveyor belt. Figure 91 shows the assumed machine rate parameters and Figure 92 the cost breakdown.

Annual Production Rate	1,000	10,000	30,000	80,000	100,000	500,000
Equipment Lifetime (years)	15	15	15	15	15	15
Interest Rate	10%	10%	10%	10%	10%	10%
Corporate Income Tax Rate	40%	40%	40%	40%	40%	40%
Capital Recovery Factor	0.175	0.175	0.175	0.175	0.175	0.175
Equipment Installation Factor	1.4	1.4	1.4	1.4	1.4	1.4
Maintenance/Spare Parts (% of CC)	3%	3%	3%	3%	3%	3%
Miscellaneous Expenses (% of CC)	12%	12%	12%	12%	12%	12%
Power Consumption (kW)	61.4	61.4	61.4	61.4	61.4	61.4

Figure 90. End gasket screen printing process parameters

Annual Production Rate	1,000	10,000	30,000	80,000	100,000	500,000
Capital Cost (\$/line)	\$393,281	\$393,281	\$393,281	\$393,281	\$393,281	\$393,281
Gaskets Printed Simultaneously	1	1	1	1	1	1
Runtime per Gasket (s)	9.62	9.62	9.62	9.62	9.62	9.62
Simultaneous Lines	1	1	1	1	1	1
Laborers per Line	0.25	0.25	0.25	0.25	0.25	0.25
Line Utilization	0.2%	1.6%	4.9%	12.9%	16.2%	80.9%
Effective Total Machine Rate (\$/hr)	\$28,104	\$2,836	\$957	\$369	\$299	\$73
Material Cost (\$/kg)	\$15.19	\$15.19	\$15.19	\$15.19	\$15.19	\$15.19

Figure 91. Machine rate parameters for end gasket screen printing process

Annual Production Rate	1,000	10,000	30,000	80,000	100,000	500,000
Material (\$/stack)	\$0.03	\$0.03	\$0.03	\$0.03	\$0.03	\$0.03
Manufacturing (\$/stack)	\$153.46	\$15.43	\$5.20	\$2.01	\$1.62	\$0.40
Tooling (\$/stack)	\$0	\$0	\$0	\$0	\$0	\$0
Total Cost (\$/stack)	\$153.49	\$15.45	\$5.23	\$2.03	\$1.65	\$0.42
Total Cost (\$/kWnet)	\$1.92	\$0.19	\$0.07	\$0.03	\$0.02	\$0.01

Figure 92. Cost breakdown for end gasket screen printing

7.1.13 Stack Compression

Traditional PEM fuel cells use tie-rods, nuts and Belleville washers to supply axial compressive force to ensure fluid sealing and adequate electrical connectivity. However, the use of metallic compression bands is assumed, as used by Ballard Power Systems and described in US Patent 5,993,987 (Figure 93). Two stainless steel bands of 2 cm width are wrapped axially around the stack and tightened to a pre-determined stack compressive loading, and then the ends of the bands are tack welded to each other. The end plates' low conductivity allows them to act as insulators, to prevent shorting of the stack. Custom recesses in the end plates are used to provide a convenient access to the lower surface of the bands to enable welding. The edges of the bipolar plates do not contact the compressive bands. The costs are reported as part of the stack assembly section, as shown in Figure 97.

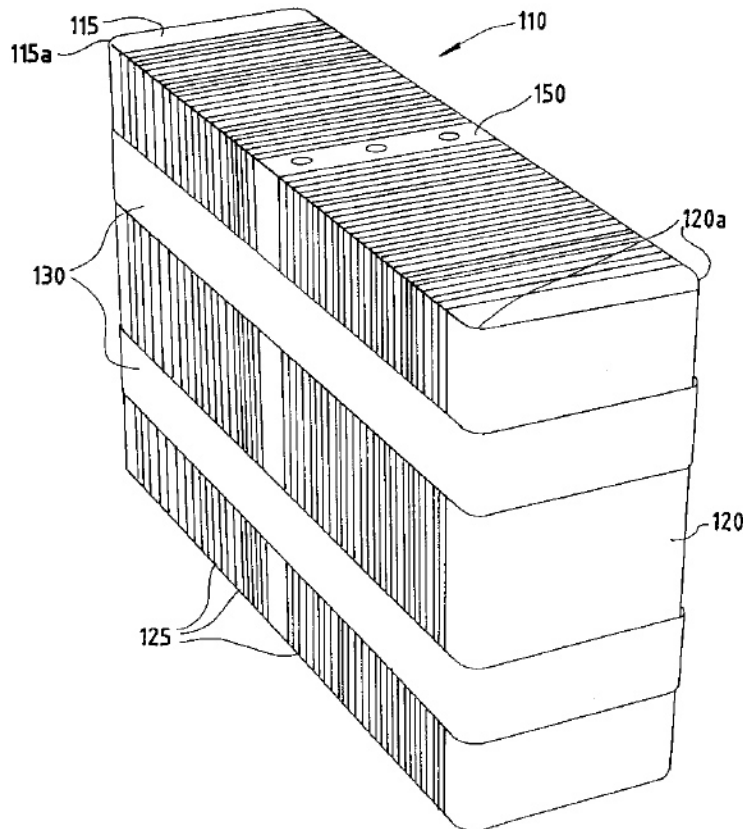


Figure 93. Stack compression bands concept (Figure courtesy of US patent 5,993,987)

7.1.14 Stack Assembly

Stack assembly costs were based on the amortized workstation costs and the estimated times to perform the required actions. Two methods of stack assembly were analyzed: manual and semi-automated.

At the lowest production rate of 1,000 systems per year, manual assembly was selected. Manual assembly consists of workers using their hands to individually acquire and place each element of the stack: end plate, insulator, current collector, bipolar plate, gasketed MEA, bipolar plate, and so on. An

entire stack is assembled at a single workstation. The worker sequentially builds the stack (vertically) and then binds the cells with metallic compression bands. The finished stacks are removed from the workstation by conveyor belt.

At higher production levels, stack assembly is semi-automatic, requiring less time and labor and ensuring superior quality control. This is termed “semi-automatic” because the end components (end plates, current conductors, and initial cells) are assembled manually but the ~369 active cell repeat units are assembled via automated fixture. Figure 94 details the layout of the assembly workstations and Figure 95 and Figure 96 list additional processing parameters.

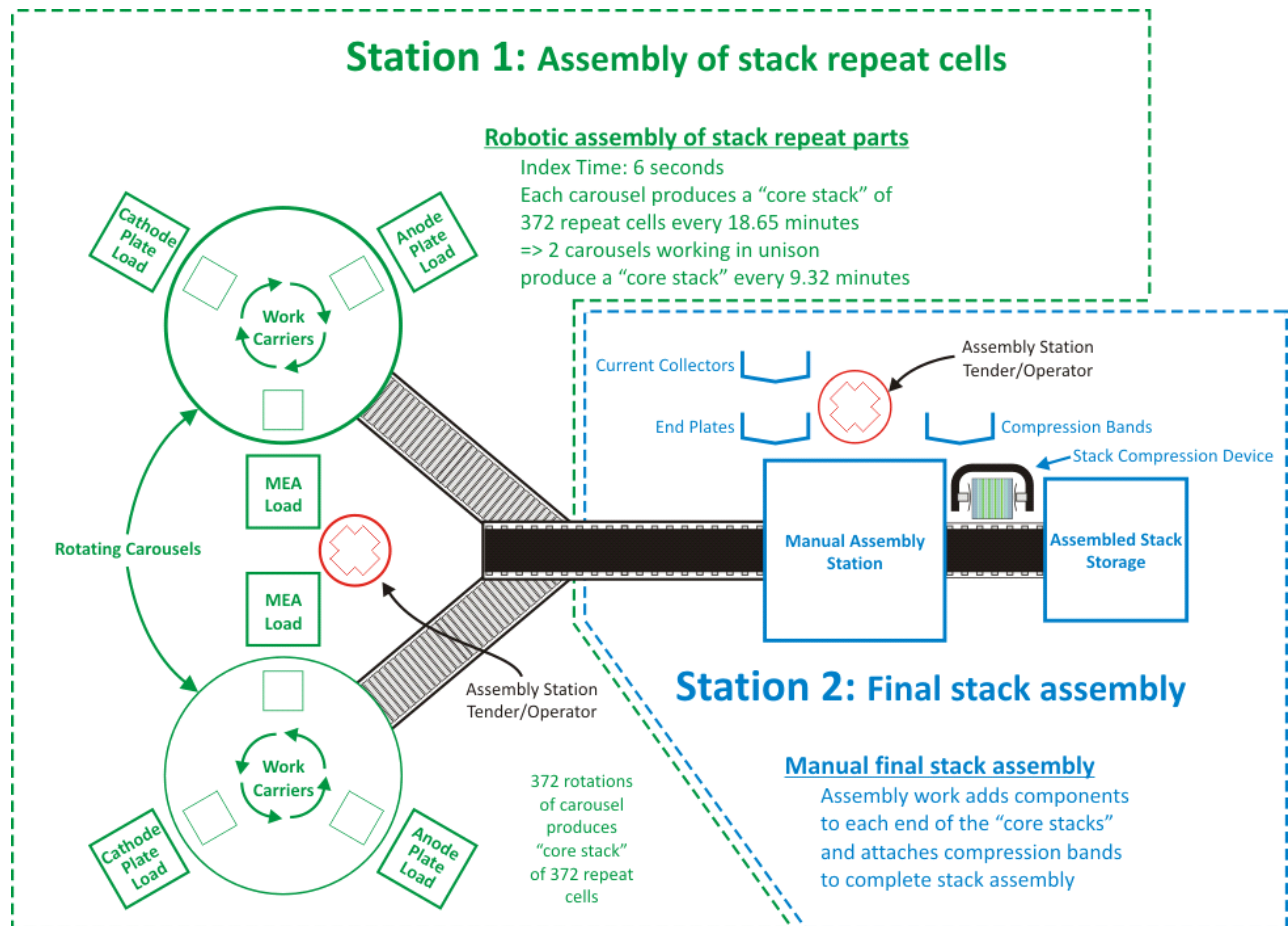


Figure 94. Semi-automated stack assembly work flow diagram

Following assembly, each stack is transported to a leak-check station where the three sets of fluid channels (hydrogen, air, and coolant) are individually pressurized with gas and monitored for leaks. This test is very brief and meant only to verify gas and liquid sealing. Full performance testing of the stack will occur during stack conditioning.

As shown in Figure 97, stack assembly is quite inexpensive, ranging from \$0.95/kW_{net} at the most to only \$0.40/kW_{net}. The only material costs are those of the compressive metal bands.

Annual Production Rate	1,000	10,000	30,000	80,000	100,000	500,000
Equipment Lifetime (years)	5	15	15	15	15	15
Interest Rate	10%	10%	10%	10%	10%	10%
Corporate Income Tax Rate	40%	40%	40%	40%	40%	40%
Capital Recovery Factor	0.306	0.175	0.175	0.175	0.175	0.175
Equipment Installation Factor	1.4	1.4	1.4	1.4	1.4	1.4
Maintenance/Spare Parts (% of CC)	10%	10%	10%	10%	10%	10%
Miscellaneous Expenses (% of CC)	7%	7%	7%	7%	7%	7%
Power Consumption (kW)	1	7	7	7	7	7

Figure 95. Stack assembly process parameters

Annual Production Rate	1,000	10,000	30,000	80,000	100,000	500,000
Assembly Method	Manual	Semi-Auto	Semi-Auto	Semi-Auto	Semi-Auto	Semi-Auto
Capital Cost (\$/line)	\$11,228	\$822,481	\$822,481	\$822,481	\$822,481	\$822,481
Simultaneous Lines	1	1	3	8	10	50
Laborers per Line	1.00	0.25	0.25	0.25	0.25	0.25
Line Utilization	46.4%	98.6%	98.5%	98.5%	98.5%	98.5%
Effective Total Machine Rate (\$/hr)	\$49.21	\$97.54	\$97.62	\$97.62	\$97.62	\$97.62
Index Time (min)	\$93.10	\$19.86	\$19.86	\$19.86	\$19.86	\$19.86

Figure 96. Machine rate parameters for stack assembly process

Annual Production Rate	1,000	10,000	30,000	80,000	100,000	500,000
Compression Bands (\$/stack)	\$0.00	\$0.00	\$0.00	\$0.00	\$0.00	\$0.00
Assembly (\$/stack)	\$76.36	\$32.29	\$32.31	\$32.31	\$32.31	\$32.31
Total Cost (\$/stack)	\$76.36	\$32.29	\$32.31	\$32.31	\$32.31	\$32.31
Total Cost (\$/kWnet)	\$0.95	\$0.40	\$0.40	\$0.40	\$0.40	\$0.40

Figure 97. Cost breakdown for stack assembly

7.1.15 Stack Housing

The stack insulation housing is a plastic housing that encases the stack. It is meant primarily for protection from physical damage caused by road debris and liquids, as well as for protection from electrical shorting contacts and a small amount of thermal insulation. It is modeled as vacuum-thermoformed polypropylene. It is 0.5 cm thick, and is separated from the stack by a 1 cm gap. At high production rate, the cycle time is seven seconds: three for insertion, and four for the vacuum thermoforming. Processing parameters are shown in Figure 98 and Figure 99. A cost breakdown of the stack housing production is shown below in Figure 100.

Annual Production Rate	1,000	10,000	30,000	80,000	100,000	500,000
Equipment Lifetime (years)	8	8	8	15	15	15
Interest Rate	10%	10%	10%	10%	10%	10%
Corporate Income Tax Rate	40%	40%	40%	40%	40%	40%
Capital Recovery Factor	0.229	0.229	0.229	0.175	0.175	0.175
Equipment Installation Factor	1.4	1.4	1.4	1.4	1.4	1.4
Maintenance/Spare Parts (% of CC)	5%	5%	5%	5%	5%	5%
Miscellaneous Expenses (% of CC)	6%	6%	6%	6%	6%	6%
Power Consumption (kW)	30	30	30	35	35	40

Figure 98. Stack housing vacuum thermoforming process parameters

Annual Production Rate	1,000	10,000	30,000	80,000	100,000	500,000
Capital Cost (\$/line)	\$50,000	\$50,000	\$50,000	\$250,000	\$250,000	\$656,281
Costs per Tooling Set (\$)	\$96,620	\$96,620	\$96,620	\$96,620	\$96,620	\$96,620
Tooling Lifetime (years)	3	3	3	3	3	3
Cavities per platen	1	1	1	1	1	1
Total Cycle Times (s)	71	71	71	15	15	7
Simultaneous Lines	1	1	1	1	1	1
Laborers per Line	1.00	1.00	1.00	1.00	1.00	0.25
Line Utilization	0.6%	5.9%	17.7%	10.1%	12.6%	28.9%
Effective Total Machine Rate (\$/hr)	\$1,137	\$157	\$84	\$311	\$258	\$254
Material Cost (\$/kg)	\$1.33	\$1.33	\$1.33	\$1.33	\$1.33	\$1.33

Figure 99. Machine rate parameters for stack housing vacuum thermoforming process

Annual Production Rate	1,000	10,000	30,000	80,000	100,000	500,000
Material (\$/stack)	\$4.68	\$4.68	\$4.68	\$4.68	\$4.68	\$4.68
Manufacturing (\$/stack)	\$22.49	\$3.10	\$1.67	\$1.31	\$1.09	\$0.49
Tooling (\$/stack)	\$36.23	\$3.62	\$1.21	\$0.40	\$0.32	\$0.06
Total Cost (\$/stack)	\$63.40	\$11.41	\$7.56	\$6.39	\$6.09	\$5.24
Total Cost (\$/kWnet)	\$0.79	\$0.14	\$0.09	\$0.08	\$0.08	\$0.07

Figure 100. Cost breakdown for stack housing

7.1.16 Stack Conditioning and Testing

PEM fuel cell stacks have been observed to perform better in polarization tests if they first undergo “stack conditioning.” Consequently, a series of conditioning steps are modeled based on a regulation scheme discussed in UTC Fuel Cell’s US patent 7,078,118. The UTC Fuel Cell patent describes both a voltage variation and a fuel/oxidant variation regime for conditioning. The voltage variation method is selected since it requires marginally less fuel consumption and allows easier valving of reactants. The conditioning would occur immediately after stack assembly at the factory. Because the conditioning is effectively a series of controlled polarization tests, the conditioning process also serves a stack quality control purpose and no further system checkout is required.

Figure 101 details the stack conditioning steps. The UTC patent states that while prior-art conditioning times were 70+ hours, the UTC accelerated break-in methodology is able to achieve 95% of the performance benefit in 5 hours and typically achieve maximum performance in 13.3 hours⁷⁵. Five hours of conditioning time is selected for cost modeling.

⁷⁵ The UTC Fuel Cell patents does not overtly state 13.3 hours to maximum performance but that duration is suggested by their specification of test procedure, 10 cycles of polarization testing for maximum performance, 100mA/cm² increments, and 5 minute increment hold times.

	Step	DC Power Supply					Current Density
		Gas on Anode	Gas on Cathode	Primary Load Switch	Positive Terminal	Electrode Potential	
Cathode Filling Cycles	1	4% H ₂ -N ₂	N ₂	Open	Connected to Cathode	Cathode 0.04V to 1.04V	Low
	2	4% H ₂ -N ₂	N ₂	Open	Connected to Cathode	Cathode 0.04V to 1.04V	Low
	3	Repeat Step #1					Low
	4	Repeat Step #2					Low
	5	Repeat Step #1					Low
	6	Repeat Step #2					Low
Anode Filling Cycles	7	N ₂	4% H ₂ -N ₂	Open	Connected to Anode	Anode 0.04V to 1.04V	Low
	8	N ₂	4% H ₂ -N ₂	Open	Connected to Anode	Anode 0.04V to 1.04V	Low
	9	Repeat Step #7					Low
	10	Repeat Step #8					Low
	11	Repeat Step #7					Low
	12	Repeat Step #8					Low
Performance Calibrations	13	H ₂	Air	Closed	Not Connected	Depends on Current Density	0-1600 mA/cm ²
	14	Repeat step #13 up to 10 times					

Figure 101. Stack conditioning process based on US patent 7,078,118 (“Applied Voltage Embodiment”)

Conditioning cost is calculated by estimating the capital cost of a programmable load bank to run the stacks up and down the polarization curve according to the power-conditioning regimen. The fuel cells load banks are assumed to condition three stacks simultaneously. Since the three stacks can be staggered in starting time, peak power can be considerably less than 3 times the individual stack rated power of ~89 kW_{gross}. It is estimated that simultaneous peak power would be approximately 150 kW and cost approximately \$152,000 at 500,000 fuel cell systems/year⁷⁶. Hydrogen usage is estimated based on 50% fuel cell efficiency and \$3/kg hydrogen. SA’s standard machine rate methodology yields machine rates as low as \$0.29/min for each load bank. Process parameters are shown in Figure 102 and Figure 103. Total costs for stack conditioning are shown in Figure 104. Note that considerable power is generated, and rather than dumping the load to a resistor bank, it may be advantageous to sell the electricity back to the grid. This would require considerable electrical infrastructure and is expected to provide only a relatively small benefit; sale of electricity to the grid is not included in our cost estimates.

⁷⁶ The costs of the programmable load banks are modeled on systems from FuelCon Systems Inc. for which a ROM price quote of \$210,000 to \$280,000 per bank was obtained for production quantities of 10-20.

Annual Production Rate	1,000	10,000	30,000	80,000	100,000	500,000
Equipment Lifetime (years)	10	10	10	10	10	10
Interest Rate	10%	10%	10%	10%	10%	10%
Corporate Income Tax Rate	40%	40%	40%	40%	40%	40%
Capital Recovery Factor	0.205	0.205	0.205	0.205	0.205	0.205
Equipment Installation Factor	1.4	1.4	1.4	1.4	1.4	1.4
Maintenance/Spare Parts (% of CC)	10%	10%	10%	10%	10%	10%
Miscellaneous Expenses (% of CC)	7%	7%	7%	7%	7%	7%
Power Consumption (kW)	1	1	1	1	1	1

Figure 102. Stack conditioning process parameters

Annual Production Rate	1,000	10,000	30,000	80,000	100,000	500,000
Capital Cost (\$/line)	\$436,236	\$409,610	\$383,005	\$321,755	\$275,713	\$151,751
Simultaneous Lines	1	3	9	24	29	145
Laborers per Line	0.1	0.1	0.1	0.1	0.1	0.1
Line Utilization	28.9%	96.5%	96.5%	96.5%	99.8%	99.8%
Effective Total Machine Rate (\$/hr)	\$105.38	\$34.96	\$33.17	\$29.04	\$25.32	\$17.24
Test Duration (hrs)	5	5	5	5	5	5

Figure 103. Machine rate parameters for stack conditioning process

Annual Production Rate	1,000	10,000	30,000	80,000	100,000	500,000
Conditioning/Testing (\$/stack)	\$175.66	\$58.28	\$55.29	\$48.41	\$42.20	\$28.73
Total Cost (\$/stack)	\$175.66	\$58.28	\$55.29	\$48.41	\$42.20	\$28.73
Total Cost (\$/kWnet)	\$2.20	\$0.73	\$0.69	\$0.61	\$0.53	\$0.36

Figure 104. Cost breakdown for stack conditioning

7.2 Balance of Plant (BOP)

While the stack is the heart of the fuel cell system, many other components are necessary to create a functioning system. In general, our cost analysis utilizes a DFMATM-style analysis methodology for the stack but a less detailed methodology for the balance of plant (BOP) components. Each of the BOP components is discussed below along with its corresponding cost basis.

7.2.1 Air Loop

The air loop of the fuel cell power system consists of five elements:

- Air Compressor, Expander and Motor (CEM) Unit
- Air Mass Flow Sensor
- Air Filter and Housing
- Air Ducting

These components are described in the subsections below. The cost breakdown is show below in Figure 105.

Annual Production Rate	1,000	10,000	30,000	80,000	100,000	500,000
Filter and Housing (\$/system)	\$56	\$51	\$51	\$51	\$51	\$51
Compressor, Expander & Motor (\$/system)	\$1,629	\$933	\$933	\$800	\$776	\$754
Mass Flow Sensor (\$/system)	\$21	\$17	\$17	\$13	\$12	\$10
Air Ducting (\$/system)	\$101	\$98	\$97	\$93	\$88	\$84
Air Temperature Sensor (\$/system)	\$10	\$8	\$8	\$6	\$6	\$5
Total Cost (\$/system)	\$1,818	\$1,108	\$1,106	\$963	\$933	\$903
Total Cost (\$/kW_{net})	\$22.72	\$13.85	\$13.83	\$12.04	\$11.66	\$11.29

Figure 105. Cost breakdown for air loop

7.2.1.1 Compressor-Expander-Motor Unit & Motor Controller

The air compression system is envisioned as an integrated air compressor, exhaust gas expander, and permanent magnet motor. An electronic CEM controller is also included in the system. For the 2013 system analysis, the CEM is based on a Honeywell design for a high rpm, centrifugal compressor, radial inflow expander integrated unit.

In the 2008 and prior year system cost analyses, the fuel cell CEM unit was based on a multi-lobe compressor and expander from Opcon Autorotor of Sweden with cost based on a simplified DFMA™ analysis in which the system was broken into seven cost elements: wheels/lobes, motor, controller, case, bearings, variable geometry, and assembly/test.

For the 2009 analysis, an all-new, extremely detailed CEM cost estimate was conducted in collaboration with Honeywell. It is a bottom-up cost analysis based directly on the blueprints from an existing Honeywell design, which pairs a centrifugal compressor and a radial-inflow expander, with a permanent-magnet motor running on air bearings at 100,000 rpm. After analyzing the base design, engineers from both SA and Honeywell simplified and improved the design to increase its performance and lower cost, to better-reflect a mass-production design. Ultimately, six different configurations were examined; three main configurations, plus a version of each without an expander.

The six different configurations examined are listed in Figure 106. “Design #1” is based on an existing Honeywell design, which runs at 100,000 rpm. Design #2 is an optimized version of Design #1 running at 165,000 rpm, in order to reduce its size. Design #3 is a further-optimized future system, based on Design #2 but with slightly more aggressive design assumptions. Designs #4, 5, and 6 are identical to Designs #1, 2, and 3 respectively, but with the expander removed.

	Current (100k rpm)	Near Future (165k rpm)	Future (165k rpm)
With Expander	Design 1	Design 2 (2010 tech)	Design 3
Without Expander	Design 4	Design 5	Design 6 (2015 tech)

Figure 106. Matrix of CEM design configurations

The cost estimate utilizes a combination of DFMA™ methodology and price quotes from established Honeywell vendors. Excluding repeat parts, the existing Honeywell turbocompressor design (Design #1) has 104 different components and assemblies. Each of these components is categorized into one of three different tiers. “Tier 1” consists of the 26 largest/most-significant components in need of the most careful cost analysis. “Tier 2” corresponds to the 42 mid-level components for which a vendor quote is sufficient. The “Tier 3” components are the minor components such as screws and adhesives that are insignificant enough that educated guesses are sufficient in lieu of vendor quotes. Honeywell engineers solicited price quotes from their existing supplier base for components in the top two tiers, as well as for some of the components in Tier 3, and supplied these values to SA for review and analysis.

In some cases, the high-volume quotes were judged to be inappropriate, as they were merely based on repeated use of low-production-rate manufacturing methods rather than low-cost, high-manufacturing-rate production and assembly methods. Consequently, these quotes were replaced with cost estimates based on a mix of DFMA™ techniques and our best judgment.

After having completed the initial cost summation for Design #1, the unit costs seemed prohibitively high. Consequently, Honeywell engineers reviewed their design and created a list of potential improvements. SA augmented the list with some DFMA™-based suggestions, the list was vetted by both parties, and the design changes incorporated into the cost model. Changes deemed reasonable to describe as “current technology” were applied to Design #2, and the more aggressive improvements were used to define Design #3. The most important of these improvements is the switch from 100,000 to 165,000 rpm, which facilitates a reduction in the size of the CEM by roughly 35%, thereby saving greatly on material (and to a lesser extent, manufacturing) costs, while also providing the intrinsic benefits of reduced size. These improvements are listed in Figure 107.

Each of the six CEM designs was analyzed across the range of five production rates (1,000 to 500,000 systems per year): this yields 30 different cost estimates for each of the 100+ components. Summed together, they provide 30 different estimates for the CEM cost. The five Design #2 estimates provide the compressor costs across the range of production rates.

For the 2010 update, the CEM cost model was fully integrated into the fuel cell system cost model, and adjusted to scale dynamically based on the pressure and power requirements of the system. This was achieved via a complex system of multipliers that are applied differently for almost every different component, since there are a wide variety of combinations and permutations for costing methods across the range of components, and not everything scales at the same rate. For example, as the pressure ratio increases and the CEM increases in size, the diameter of the turbine wheel increases, and its volume increases at a rate proportional to the square of its diameter. The diameter of the compressor wheel scales at a different rate than that of the turbine (expander) wheel, and the shaft length and motor mass each scale at yet another rate. The geometric scaling factors were derived from data that Honeywell provided showing dimensions of key components across a range of performance parameters such as pressure ratio, mass flow rate, and shaft power.

Design #	2010					2015
	1	2	3	4	5	6
	With Expander			Without Expander		
	Current (100k rpm)	Future (165k rpm)	Future (165k rpm)	Current (100k rpm)	Future (165k rpm)	Future (165k rpm)
Removed Turbine (Expander)				x	x	x
Increased speed from 100,000 to 165,000 rpm	x		x		x	x
Improved turbine wheel design	x		x		x	x
Improved variable nozzle technology	x		x		x	x
Lower cost electrical connectors	x		x		x	x
Design change to integrate housing into single casting			x			x
Integrate/eliminate mounting bosses on main housing			x			x
Compressor housing design change to re-route cooling air over motor			x			x
Improved foil bearing design			x			x
Back-to-back compressor wheel			x			x
Removed washers/face bolts			x			x
Improved bearing installation/design			x			x
Improved labyrinth seal			x			x
Changed fasteners to more common, inexpensive design			x			x
Changed threaded inserts to more common, inexpensive design			x			x
Reduced testing of machined/cast parts			x			x
Aluminum turbine wheel			x			

Figure 107. List of Improvements for the 6 compressor configurations

The materials cost of each component increases proportionately with the volume of material needed, and the manufacturing costs scale separately, at rates dependent on the manufacturing processes involved and the specifics of each process.

For components whose cost estimates are derived partially or completely from price quotes rather than full DFMA™ analysis (such as those in Tier 2 and Tier 3), assumptions were made about the fractional split between the component's material and manufacturing costs, so that each fraction can be scaled independently.

With this new scaling and integration into the main fuel cell system cost model, the size and cost of the CEM now scale dynamically based on the performance requirements of the system. So if a new electrical component is added to the BOP that increases the parasitic load (and thus increases the gross power required), the CEM will automatically scale to accommodate.

The SA/Honeywell CEM analysis also examined the motor controller, for which the same design was deemed applicable to control all six compressor designs. Unlike with the custom parts involved in the compressor, the motor controller uses almost exclusively off-the-shelf parts that are already manufactured at high volume. As such, there is limited value in conducting a detailed DFMA™ analysis,

so the cost analysis is primarily based on vendor quotation. The original Honeywell controller design was a standalone unit with its own air or water cooling. However, in order to cut costs, it is now assumed that the CEM controller is integrated into the water-cooled electronics housing for the overall fuel cell system controller. Thirty percent of the controller base cost is assumed to correspond to logic functions, with the remaining 70% corresponding to power management. Accordingly, to scale the controller cost for different input powers (as is necessary when varying stack operating parameters to determine the lowest possible system cost), the 30% of the baseline controller cost (i.e. the portion for logic circuitry) is held at a constant cost, the remaining 70% of baseline cost (i.e. the portion for power management) is assumed to scale linearly with input power.

The CEM and motor controller costs for the various configurations are shown below in Figure 108 for the various 2013 system CEM options. Design 2 is selected for the 2013 cost analysis. Note that the costs at 10k and 30k systems per year are reported as identical values. This is a slight inaccuracy based on not scaling the 10k/year cost estimates.

7.2.1.2 Air Mass Flow Sensor

A high-performance (~2% signal error) automotive hot-wire mass flow sensor is used for measuring the air flow rate into the fuel cell system. Since these devices are already produced in very high quantities, little change in cost is expected between high and low production rates.

7.2.1.3 Air Ducting

The air ducting is modeled as conformal polymer tubes to guide the cathode air in and out of the stack.

7.2.1.4 Air Filter and Housing

Some fuel cell manufacturers filter inlet air both for particles and for volatile organic compounds. However, while particle filters are needed, it is not clear that VOC filters are necessary. Consequently, a standard automotive air particle filter and polymer filter housing are assumed.

Design	Sys/yr	2013 CEM			2013 Motor Controller			2013 Total
		Cost	Assy	Markup	Cost	Assy	Markup	Cost
Design 1 Existing Tech. 100,000 RPM	1,000	\$1,311.19			\$485.88			\$2,077.21
	10,000	\$580.69			\$404.11			\$1,147.20
	30,000	\$580.69	\$23.00	15%	\$404.11	\$7.67	10%	\$1,147.20
	80,000	\$453.84			\$390.84			\$986.72
	100,000	\$446.45			\$373.37			\$959.00
	500,000	\$435.13			\$360.49			\$931.82
Design 2 "Near Future" 165,000 RPM	1,000	\$921.26			\$485.88			\$1,628.80
	10,000	\$394.72			\$404.11			\$933.34
	30,000	\$394.72	\$23.00	15%	\$404.11	\$7.67	10%	\$933.34
	80,000	\$291.91			\$390.84			\$800.50
	100,000	\$287.13			\$373.37			\$775.78
	500,000	\$280.15			\$360.49			\$753.60
Design 3 "Future" 165,000 RPM	1,000	\$782.11			\$485.88			\$1,468.78
	10,000	\$344.52			\$404.11			\$875.61
	30,000	\$344.52	\$23.00	15%	\$404.11	\$7.67	10%	\$875.61
	80,000	\$249.62			\$390.84			\$751.87
	100,000	\$245.46			\$373.37			\$727.87
	500,000	\$239.38			\$360.49			\$706.72
Design 4 Existing Tech. 100,000 RPM No Expander	1,000	\$1,074.15			\$772.44			\$2,119.84
	10,000	\$494.36			\$642.46			\$1,310.10
	30,000	\$494.36	\$23.00	15%	\$642.46	\$7.67	10%	\$1,310.10
	80,000	\$376.17			\$621.35			\$1,150.96
	100,000	\$371.85			\$593.58			\$1,115.45
	500,000	\$365.82			\$573.11			\$1,085.99
Design 5 "Near- Future" 165,000 RPM No Expander	1,000	\$836.69			\$772.44			\$1,846.76
	10,000	\$353.93			\$642.46			\$1,148.61
	30,000	\$353.93	\$23.00	15%	\$642.46	\$7.67	10%	\$1,148.61
	80,000	\$255.78			\$621.35			\$1,012.51
	100,000	\$252.79			\$593.58			\$978.52
	500,000	\$248.30			\$573.11			\$950.84
Design 6 "Future" 165,000 RPM No Expander	1,000	\$702.32			\$772.44			\$1,692.24
	10,000	\$306.55			\$642.46			\$1,094.12
	30,000	\$306.55	\$23.00	15%	\$642.46	\$7.67	10%	\$1,094.12
	80,000	\$216.31			\$621.35			\$967.12
	100,000	\$213.92			\$593.58			\$933.83
	500,000	\$210.27			\$573.11			\$907.11

Figure 108. CEM cost results

7.2.2 Humidifier & Water Recovery Loop

The humidifier and water recovery loop consists of three components:

- Air precooler
- Demister
- Humidifier

Total subsystem cost is shown in Figure 109. Further details of each subsystem component appear below.

Annual Production Rate	1,000	10,000	30,000	80,000	100,000	500,000
Air Precooler (\$/system)	\$32.26	\$32.26	\$32.26	\$32.26	\$32.26	\$32.26
Demister (\$/system)	\$119.21	\$21.58	\$13.48	\$8.88	\$8.11	\$6.30
Membrane Air Humidifier (\$/system)	\$2,690.72	\$380.34	\$204.11	\$138.26	\$128.76	\$94.36
Total Cost (\$/system)	\$21.25	\$17.00	\$17.00	\$12.75	\$11.90	\$10.20
Total Cost (\$/kW_{net})	\$0.09	\$0.07	\$0.07	\$0.05	\$0.05	\$0.04

Figure 109. Cost breakdown for humidifier & water recovery loop

7.2.2.1 Air Precooler

The air precooler sits between the air compressor and the membrane humidifier, where it cools the hot compressed air to the humidifier’s optimal inlet temperature. The design is based on the ANL-supplied key parameters for a compact liquid/air cross-flow intercooler, and the dimensions are scaled based on the specific heat transfer requirements. The unit is 100% aluminum and uses an array of 0.4-mm-thick tubes with 0.08-mm-thick fins spaced at 24 fins per inch, which cool the air with a very minimal pressure drop (0.1 psi). Because the cost impact of the precooler is small, a full DFMA™ analysis was not conducted. Instead, the mass and volume of the radiator core were determined by heat transfer calculations conducted at ANL, and the materials cost of the unit was estimated based on detailed geometry assumptions and the cost of aluminum (\$6.82/kg). The materials cost was then simply doubled to account for the cost of manufacturing. As a result of this simplified costing methodology, air precooler cost does not vary with annual production rate.

Further details of the air precooler coolant and air temperatures are discussed in Section 6.11. Air precooler cost is detailed in Figure 110.

Annual Production Rate	1,000	10,000	30,000	80,000	100,000	500,000
Material (\$/system)	\$16	\$16	\$16	\$16	\$16	\$16
Manufacturing (\$/system)	\$16	\$16	\$16	\$16	\$16	\$16
Total Cost (\$/system)	\$32	\$32	\$32	\$32	\$32	\$32
Total Cost (\$/kW_{net})	\$0.40	\$0.40	\$0.40	\$0.40	\$0.40	\$0.40

Figure 110. Cost breakdown for air precooler

7.2.2.2 Demister

The demister removes liquid water droplets from the cathode exhaust stream and thereby prevents erosion of the turbine blades. Designed by SA, the demister’s housing consists of two threaded, hollow 2-mm-thick polypropylene frustums that unscrew from one another to allow access to the filter inside. The filter is a nylon mesh Millipore product designed for water removal and cost \$5.84 each at high volume (assuming 81 cm² per demister). The polypropylene adds only ~10 cents of material cost per part, and at high volume, the injection molding process is only 15 cents per part. Because the housing is so inexpensive, the filter dominates the total demister cost (\$6.30/demister, or \$0.08/kW_{net} at 500,000 systems per year).

Figure 111 and Figure 112 show demister processing parameters. Figure 113 details demister cost results.

Annual Production Rate	1,000	10,000	30,000	80,000	100,000	500,000
Equipment Lifetime (years)	15	15	15	15	15	15
Interest Rate	10%	10%	10%	10%	10%	10%
Corporate Income Tax Rate	40%	40%	40%	40%	40%	40%
Capital Recovery Factor	0.175	0.175	0.175	0.175	0.175	0.175
Equipment Installation Factor	1.4	1.4	1.4	1.4	1.4	1.4
Maintenance/Spare Parts (% of CC)	5%	5%	5%	5%	5%	5%
Miscellaneous Expenses (% of CC)	6%	6%	6%	6%	6%	6%
Power Consumption (kW)	21	21	21	21	21	21

Figure 111. Demister injection molding process parameters

Annual Production Rate	1,000	10,000	30,000	80,000	100,000	500,000
Capital Cost (\$/line)	\$288,923	\$288,923	\$288,923	\$288,923	\$288,923	\$288,923
Costs per Tooling Set (\$)	\$16,215	\$16,215	\$16,215	\$16,215	\$16,215	\$16,215
Tooling Lifetime (cycles)	1,000,000	1,000,000	1,000,000	1,000,000	1,000,000	1,000,000
Cavities per platen	1	1	1	1	1	1
Total Cycle Time (s)	6	6	6	6	6	6
Simultaneous Lines	1	1	1	1	1	1
Laborers per Line	0.50	0.50	0.50	0.50	0.50	0.50
Line Utilization	0.1%	0.6%	1.6%	4.3%	5.4%	26.5%
Effective Total Machine Rate (\$/hr)	\$27,163	\$5,226	\$1,899	\$758	\$617	\$162
Material Cost (\$/kg)	\$1.33	\$1.33	\$1.33	\$1.33	\$1.33	\$1.33

Figure 112. Machine rate parameters for demister injection molding process

Annual Production Rate	1,000	10,000	30,000	80,000	100,000	500,000
Material (\$/system)	\$12.27	\$10.81	\$9.84	\$7.41	\$6.92	\$5.95
Manufacturing (\$/system)	\$102.62	\$10.34	\$3.50	\$1.37	\$1.11	\$0.29
Tooling (\$/system)	\$4.32	\$0.43	\$0.14	\$0.11	\$0.09	\$0.07
Total Cost (\$/system)	\$119.21	\$21.58	\$13.48	\$8.88	\$8.11	\$6.30
Total Cost (\$/kWnet)	\$1.49	\$0.27	\$0.17	\$0.11	\$0.10	\$0.08

Figure 113. Cost breakdown for demister

7.2.2.3 Membrane Humidifier

The 2012 and prior year cost analyses were based on a tubular membrane design from Perma Pure LLC (model FC200-780-7PP) as shown in Figure 114.

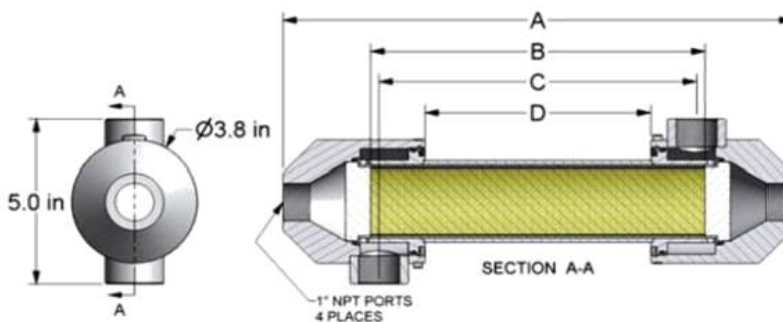


Figure 114. Perma Pure FC200-780-7PP humidifier

However, the 2013 analysis is based on use of a plate frame membrane humidifier design for both the auto and bus DFMA™ analyses. As further detailed in Section 6.5, the plate frame humidifier is based on a W.L. Gore and DPoint Technologies Inc. design. For the automotive application, the modeled design is composed of 80 “cell pouches” where each cell pouch is a loop of membrane with a metal spacer within the loop. The dimension of each cell pouch is 10cm by 10cm, summing to a total humidifier membrane area of 1.6 m². The cell pouches allow dry primary inlet air to flow through the inside of the pouch and humid secondary outlet oxygen-depleted air from the cathode to flow cross-wise over the outside of the pouch (as seen in Figure 115). Stamped metal “ribs” are used to separate the pouches and thus enable gas flow between the pouches. The cell pouches are arranged in a simple aluminum cast-metal housing to direct the gas flows.

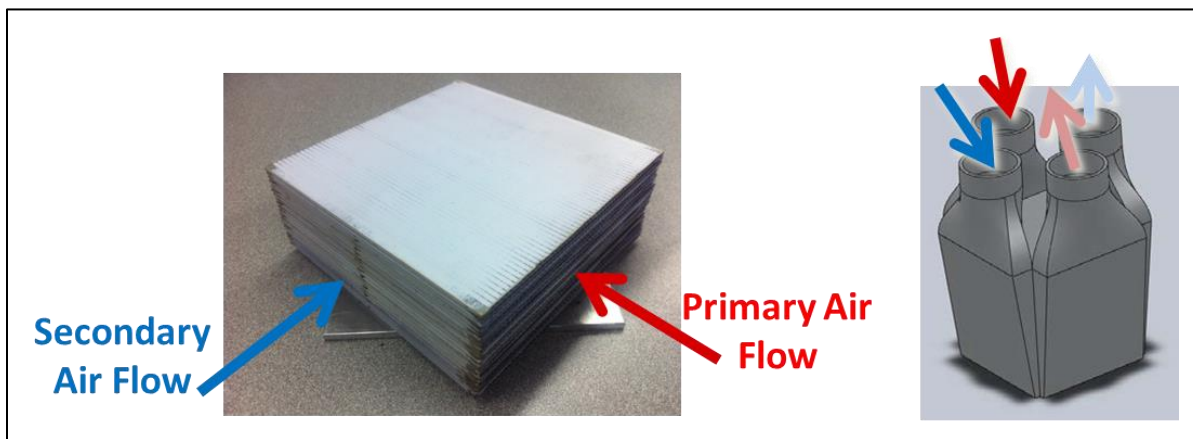


Figure 115. Images from W.L. Gore & Associates presentation⁷⁷ showing (Left) stack of cell pouches with primary flow (dry air) flowing through the cell pouches and secondary flow (wet air) flowing over/under and between pouches and (Right) humidifier housing with four ports: primary and secondary flow inlet and outlet ports.

7.2.2.3.1 Membrane Humidifier Manufacturing Process

The manufacturing process for the plate frame membrane humidifier is modeled as eight steps:

1. Fabrication of Composite Membranes
2. Fabrication of Etched Stainless Steel Flow Fields
3. Pouch Formation
4. Stainless Steel Rib Formation
5. Stack Formation
6. Formation of the Housing
7. Assembly of the Composite Membrane and Flow Fields into the Housing
8. Humidifier System Testing

Manufacturing details and cost components for each process are described in the following sections.

⁷⁷ Johnson, William B. “Materials and Modules for Low-Cost, High Performance Fuel Cell Humidifiers,” W.L. Gore & Associates, Inc., presentation at the 2012 DOE Hydrogen and Fuel Cell Program Annual Merit Review, Washington, DC, 17 May 2012.

Fabrication of Composite Humidifier Membranes

The postulated process for manufacture of the composite humidifier membrane is based on a die-slot coating roll-to-roll system and is very similar to that of the Gore MEA (Section 6.6).

- A 10 μm thick ePTFE layer is unrolled onto a Mylar backer.
- A 5 μm thick die-slot coated layer of Nafion[®] ionomer is laid on top of the ePTFE.
- A second layer of 10 μm thick ePTFE is unrolled onto the ionomer layer.
- The stacked layers are passed through a continuous curing oven.
- In the final step, all three layers are hot laminated to a 180 μm polyethylene terephthalate (PET) non-woven porous layer, also known as a gas diffusion layer (GDL).

The ePTFE layers bracket and mechanically support the very thin, and thus high water flux, ionomer layer and are arranged in a symmetrical orientation to minimize stresses during thermal cycling and thereby enhance lifetime. The much thicker PET layer provides additional mechanical support and abrasion resistance. Figure 116 shows a schematic of the postulated fabrication process inspired by a Ballard patent for composite membrane manufacturing⁷⁸ and a Gore patent for integral composite membranes⁷⁹.

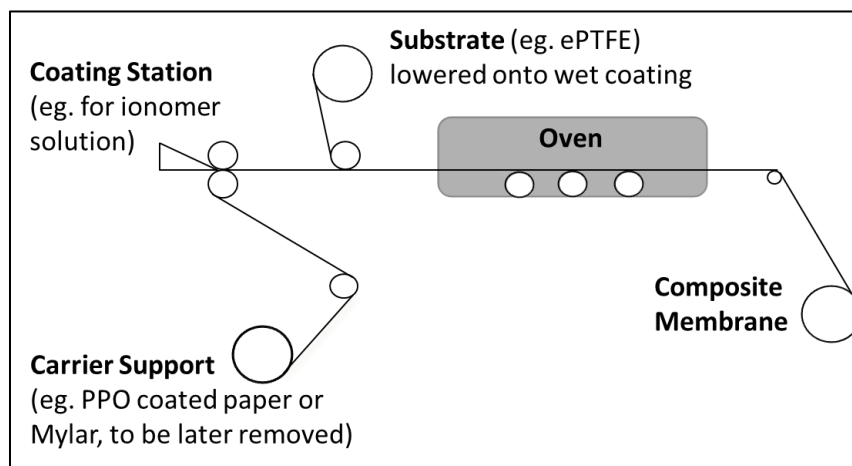


Figure 116. Design for ionomer addition to ePTFE, followed by oven drying to form a composite membrane from combination of Ballard Patent (U.S. Patent 6,689,501 B2) and Gore patent (U.S. Patent 5,599,614).

Key elements of composite membrane fabrication process include:

- Adding a porous substrate (eg. ePTFE) onto a wet impregnate solution (eg. ionomer) (shown in Figure 116).
- Coating ionomer directly onto a porous substrate (eg. die slot coating onto the top of the ePTFE) (not shown in Figure 116).

⁷⁸ Ballard Patent: U.S. Patent 6,689,501 B2

⁷⁹ Gore Patent: "Integral composite Membrane" U.S. Patent 5,599,614.

- Adding a second porous substrate (eg. ePTFE) onto the top of a wet solution layer (eg. ionomer) (not shown in Figure 116).

The process is modeled using a 1m web width at a baseline speed of 10m/min (based on Dupont patent⁸⁰). Curing oven residence time is a total of 9 minutes (3 minutes at 40°C, 3 minutes at 60°C and 3 minutes at 90°C), also based on the DuPont patent. The total capital cost of manufacturing equipment for the composite membrane is approximately \$3M with the cost breakdown and cost basis listed in Figure 117. Figure 118 and Figure 119 show membrane processing parameters. Cost results are shown Figure 120 and reveal that (at 500,000 systems/year) material cost is the largest cost contributor, with ePTFE cost being the dominating cost element. Consequently, ePTFE cost was carefully assessed and found to vary substantially vendor to vendor, partly due to variations in ePTFE precursor materials and processing steps (together referred to as ePTFE “quality”). A discussion of the range of ePTFE costs used within the cost analysis appears in Section 7.1.2.2.

Component	Capital Cost	Basis
Web Casting Operation		
Base slot die coating system	\$700k	Frontier Industrial Technology Inc. ROM quote (with 100% cost margin to reflect custom eng.)
Additional pump cart	\$25k	Frontier Industrial Technology Inc. ROM quote (with 100% cost margin to reflect custom eng.)
ePTFE Unwind stands	2 x \$60k	Machine Works Inc. quote (with 100% cost margin to reflect custom eng.)
Customization Adder	2x	Conservatism for custom machinery
Total Web Casting Capital Cost	\$1.7M	
Additional heating zones	\$37k	Modified Wisconsin Ovens quote
Tensioner for laminator	\$60k	Estimate based on similar machinery
Laminator	\$684k	Modified Andritz Kuster quote
Clean Room	\$125k	Industrial ROM estimate
Quality Control Equipment	\$464k	Line cameras to provide 20micron anomaly resolution after ionomer addition and 350 micron resolution of each ePTFE layer.
Total Capital Cost (uninstalled)	\$3M	

Figure 117. Capital cost of manufacturing equipment required for the composite membrane fabrication process.

⁸⁰ DuPont Patent US 7,648,660 B2

Annual Production Rate	1,000	10,000	30,000	80,000	100,000	500,000
Equipment Lifetime (years)	15	15	15	15	15	15
Interest Rate	10%	10%	10%	10%	10%	10%
Corporate Income Tax Rate	40%	40%	40%	40%	40%	40%
Capital Recovery Factor	0.175	0.175	0.175	0.175	0.175	0.175
Equipment Installation Factor	1.4	1.4	1.4	1.4	1.4	1.4
Maintenance/Spare Parts (% of CC)	10%	10%	10%	10%	10%	10%
Miscellaneous Expenses (% of CC)	7%	7%	7%	7%	7%	7%
Power Consumption (kW)	248	248	248	248	248	248

Figure 118. Fabrication of composite membranes process parameters

Annual Production Rate	1,000	10,000	30,000	80,000	100,000	500,000
Capital Cost (\$/line)	\$3,061,631	\$3,061,631	\$3,061,631	\$3,061,631	\$3,061,631	\$3,061,631
Simultaneous Lines	1	1	1	1	1	1
Laborers per Line	0.67	0.67	0.67	0.67	0.67	0.67
Line Utilization	0.1%	1.2%	3.5%	9.0%	11.2%	52.7%
Casting Line Rate (m/s)	0.17	0.17	0.17	0.17	0.17	0.17
Effective Total Machine Rate (\$/hr)	\$272,606	\$30,852	\$10,795	\$4,228	\$3,422	\$767
Backer Cost (\$/m ²)	\$0.96	\$0.96	\$0.96	\$0.96	\$0.96	\$0.96

Figure 119. Machine rate parameters for fabrication of composite membranes

Annual Production Rate	1,000	10,000	30,000	80,000	100,000	500,000
Materials (\$/stack)	\$91.61	\$65.00	\$53.81	\$44.56	\$42.55	\$29.01
Manufacturings (\$/stack)	\$1,290.49	\$129.23	\$43.21	\$16.32	\$13.09	\$2.76
Toolings (\$/stack)	\$0.16	\$0.16	\$0.16	\$0.16	\$0.16	\$0.16
Markups (\$/stack)	\$552.90	\$68.04	\$34.01	\$18.31	\$15.07	\$7.98
Total Costs (\$/stack)	\$1,935.16	\$262.42	\$131.18	\$79.35	\$70.86	\$39.90
Total Costs (\$/kWnet)	\$24.19	\$3.28	\$1.64	\$0.99	\$0.89	\$0.50

Figure 120. Cost breakdown for fabrication of composite membranes

Fabrication of Etched Stainless Steel Flow Fields

The humidifier flow field plates serve to separate the sides of the cell pouch and open a channel through which the air may pass. The plates are fabricated by electrochemical etching of 0.6mm stainless steel 316L sheet. Etching is selected as it grants the design flexibility and dimensional tolerance critical to achieving low pressure drop and high membrane water transport performance. To reduce the cost of the etching process, multiple flow fields are etched from a single large panel of SS. The process includes the following stages:

- **Stage 1 (Add Photoresist):** Photoresist is first laminated to both sides of a 0.6mm (24mils) SS316 metal coil and cut to 1m by 2m panel size (holding 180 parts).
- **Stage 2 (Illuminate with light):** Two SS/photoresist panels are manually loaded into a light chamber, covered with stencils (one stencil on each side of each panel), exposed to light simultaneously on each side of panel for 7.5 minutes to activate the photoresist not covered by the stencil, and then the panels are removed from the light chamber. The photoresist has now been selectively removed from the panel in the exact pattern desired for etching.
- **Stage 3 (Stripping):** Ten panels are loaded into a vertical fixture, simultaneously lowered into a stripping tank of alkaline solution (sodium carbonate), the exposed portions of photoresist are striped/dissolved by the alkaline solution over a 5 minutes submersion, the panel are then lifted from the tank.

- **Stage 4 (Etching):** The ten panels fixture is moved to an electrochemically etching bath, electrodes are connected to each panel, the panels are simultaneously lowered into the etching tank, an electric current is applied to electrochemically etch the exposed SS surface. The electrochemical etching rate is estimated at 6.7 μm per minute, taking a total of 45 minutes to etch 600 microns (300 microns from each side simultaneously). Perforations are also etched into the material to allow for easy flow field separation using a low force stamping machine. The average power consumption estimated is approximately 1.2kW per 100cm² part (2.16MW for 10 panels).
- **Stage 5 (Cleaning):** After the etching is complete, the panels are lowered into a wash tank of alkaline solution (sodium hydroxide) for 4 minutes to remove the remaining photoresist.

Additionally, the etched plates are anodized for corrosion resistance, separated by stamping into 10cm by 10cm pouch cell sizes, and packaged into magazines for robotic assembly. Anodizing cost is estimated at 1.6 cents per 50cm² of anodizing surface (\$3 for a 100 cell stack) with the parts being anodized while in panel form before separated. Figure 121 and Figure 122 show flow field processing parameters. Cost results for the etching process are shown in Figure 123.

Annual Production Rate	1,000	10,000	30,000	80,000	100,000	500,000
Equipment Lifetime	15	15	15	15	15	15
Interest Rate	10%	10%	10%	10%	10%	10%
Corporate Income Tax Rate	40%	40%	40%	40%	40%	40%
Capital Recovery Factor	0.175	0.175	0.175	0.175	0.175	0.175
Equipment Installation Factor	1.4	1.4	1.4	1.4	1.4	1.4
Maintenance/Spare Parts (% of CC)	13%	13%	13%	13%	13%	13%
Miscellaneous Expenses (% of CC)	2%	2%	2%	2%	2%	2%
Power Consumption (kWhr/year)	73,223	724,115	2,170,724	5,786,434	7,233,043	36,161,969

Figure 121. Fabrication of etched stainless steel flow fields process parameters

Annual Production Rate	1,000	10,000	30,000	80,000	100,000	500,000
Capital Cost (\$/line)	\$1,018,927	\$1,018,927	\$1,018,927	\$1,018,927	\$1,268,927	\$2,968,927
Stage 1 Simultaneous Lines	1	1	1	1	1	1
Stage 2 Simultaneous Lines	1	1	1	1	1	5
Stage 3 Simultaneous Lines	1	1	1	1	1	1
Stage 4 Simultaneous Lines	1	1	1	1	2	6
Stage 5 Simultaneous Lines	1	1	1	1	1	1
Stage 1 Line Utilization	0.0%	0.2%	0.7%	1.8%	2.2%	11.0%
Stage 2 Line Utilization	0.9%	8.8%	26.5%	70.5%	88.2%	88.2%
Stage 3 Line Utilization	0.1%	1.2%	3.6%	9.7%	12.1%	60.6%
Stage 4 Line Utilization	1.0%	10.2%	30.4%	81.2%	50.7%	84.5%
Stage 5 Line Utilization	0.1%	1.1%	3.3%	8.8%	11.0%	55.1%
Stage 1 Laborers per Line	1	1	1	1	1	1
Stage 2 Laborers per Line	2	2	2	2	2	2
Stage 3 Laborers per Line	1	1	1	1	1	1
Stage 4 Laborers per Line	0	0	0	0	0	0
Stage 5 Laborers per Line	1	1	1	1	1	1
Stage 1 Cycle Time (s)	6	6	6	6	6	6
Stage 2 Cycle Time (s)	480	480	480	480	480	480
Stage 3 Cycle Time (s)	330	330	330	330	330	330
Stage 4 Cycle Time (s)	2,761	2,761	2,761	2,761	2,761	2,761
Stage 5 Cycle Time (s)	300	300	300	300	300	300
Effective Total Machine Rate (\$/hr)	\$11,121.30	\$1,337.58	\$604.65	\$375.43	\$374.92	\$304.75
Stainless Steel Cost (\$/kg)	\$3.93	\$3.93	\$3.93	\$3.93	\$3.93	\$3.93

Figure 122. Machine rate parameters for fabrication of etched stainless steel flow fields

Annual Production Rate	1,000	10,000	30,000	80,000	100,000	500,000
Materials (\$/stack)	\$15	\$15	\$15	\$15	\$15	\$15
Manufacturings (\$/stack)	\$411	\$49	\$22	\$14	\$14	\$11
Total Costs (\$/stack)	\$426	\$64	\$37	\$29	\$29	\$26
Total Costs (\$/kWnet)	\$5.32	\$0.80	\$0.46	\$0.36	\$0.36	\$0.33

Figure 123. Cost breakdown for fabrication of etched stainless steel flow fields

Pouch Formation

The cell pouches are formed using custom machinery to wrap a flow field with composite membrane and apply adhesive to seal the ends of the membrane and form a membrane loop. An image of a complete single cell pouch is shown in Figure 124. The process order used to fabricate these cell pouches is as follows:

- a. Composite humidifier membrane material is unrolled on to a cutting deck.
- b. The custom machine cuts the composite membrane to a 20cm length.
- c. A flow field is placed in the center of the membrane.
- d. One end of the membrane is wrapped around the flow field.
- e. A bead of silicone adhesive is applied to the membrane end wrapped around the flow field.
- f. The other end of the membrane is wrapped around the flow field and onto the adhesive bead. The ends are held in place until bonded.
- g. A vision quality control system is used to verify alignment of the cell pouch.
- h. The cell pouch is removed and stacked in a magazine to be used in the next stack assembly process.

A schematic of the process steps is shown in Figure 125. (The schematic does not show the quality control system.) The complete system is estimated at \$413,000 and able to simultaneously prepare 10 pouches with a 9 second cycle time (i.e. 9 seconds per 10 pouches).



Figure 124. Plate Frame Membrane Humidifier single cell pouch (Source: Johnson, William B. "Materials and Modules for Low-Cost, High Performance Fuel Cell Humidifiers," W.L. Gore & Associates, Inc., presentation at the 2012 DOE Hydrogen and Fuel Cell Program Annual Merit Review, Washington, DC, 17 May 2012.)

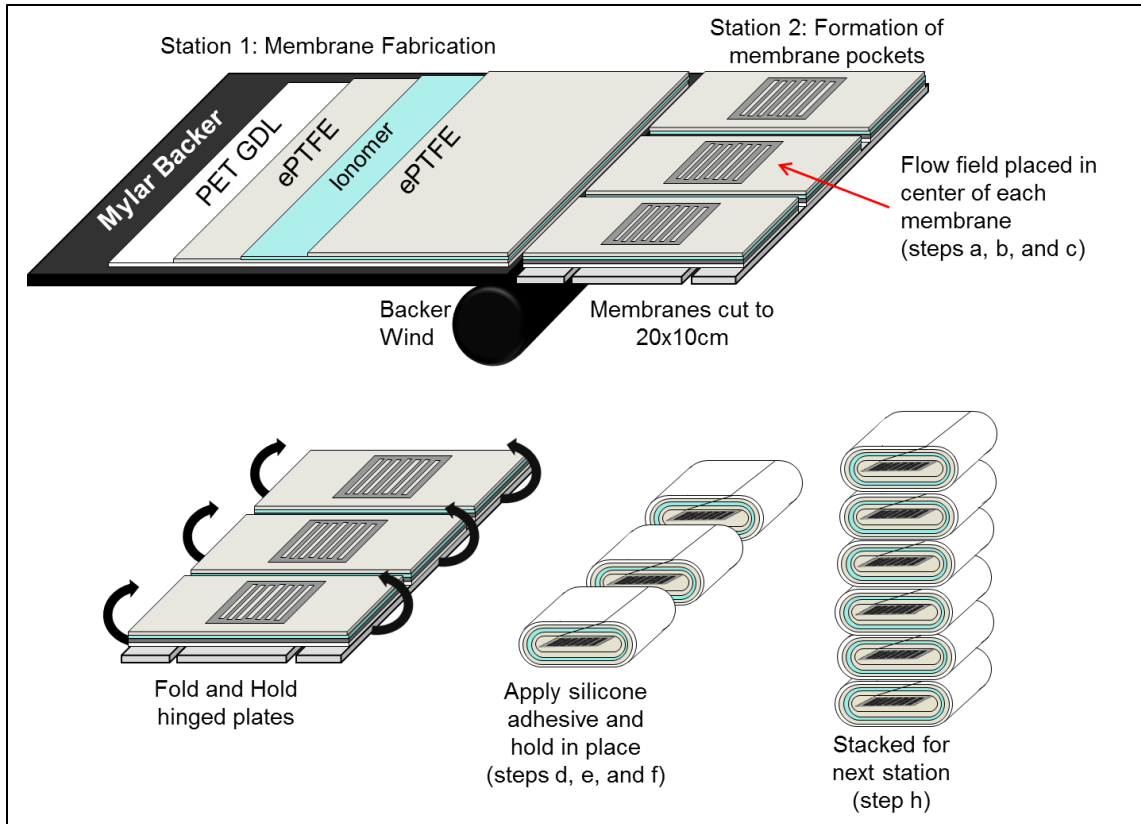


Figure 125. Process steps used in DFMA™ analysis for humidifier cell pouch formation.

Figure 126 and Figure 127 show cell pouch formation processing parameters. Cost results for the cell pouch formation process are in Figure 128.

Annual Production Rate	1,000	10,000	30,000	80,000	100,000	500,000
Equipment Lifetime (years)	15	15	15	15	15	15
Interest Rate	10%	10%	10%	10%	10%	10%
Corporate Income Tax Rate	40%	40%	40%	40%	40%	40%
Capital Recovery Factor	0.175	0.175	0.175	0.175	0.175	0.175
Equipment Installation Factor	1.4	1.4	1.4	1.4	1.4	1.4
Maintenance/Spare Parts (% of CC)	10%	10%	10%	10%	10%	10%
Miscellaneous Expenses (% of CC)	7%	7%	7%	7%	7%	7%
Power Consumption (kW)	27	27	27	27	27	27

Figure 126. Pouch formation process parameters

Annual Production Rate	1,000	10,000	30,000	80,000	100,000	500,000
Capital Cost (\$/line)	\$413,179	\$413,179	\$413,179	\$413,179	\$413,179	\$413,179
Costs per Tooling Set (\$)	\$1,259	\$1,259	\$1,135	\$648	\$571	\$228
Costs per Tooling Set 2 (\$)	1,400	1,400	1,400	1,400	1,400	977
Tooling Lifetime (cycles)	2,000,000	2,000,000	2,000,000	2,000,000	2,000,000	2,000,000
Simultaneous Lines	1	1	1	1	1	3
Laborers per Line	0.25	0.25	0.25	0.25	0.25	0.25
Line Utilization	0.6%	6.0%	17.9%	47.6%	59.5%	99.2%
Cycle Time (s)	0.875	0.875	0.875	0.875	0.875	0.875
Effective Total Machine Rate (\$/hr)	\$8,521.92	\$868.05	\$298.69	\$120.53	\$99.14	\$64.90
Silicon Adhesive Cost (\$/kg)	\$12.05	\$12.05	\$12.05	\$12.05	\$12.05	\$12.05

Figure 127. Machine rate parameters for pouch formation

Annual Production Rate	1,000	10,000	30,000	80,000	100,000	500,000
Materials (\$/stack)	\$0.44	\$0.44	\$0.44	\$0.44	\$0.44	\$0.44
Manufacturings (\$/stack)	\$171.56	\$17.40	\$5.98	\$2.41	\$1.98	\$1.30
Toolings (\$/stack)	\$0.11	\$0.11	\$0.10	\$0.08	\$0.08	\$0.05
Total Costs (\$/stack)	\$172.10	\$17.95	\$6.52	\$2.93	\$2.50	\$1.79
Total Costs (\$/kWnet)	\$2.15	\$0.22	\$0.08	\$0.04	\$0.03	\$0.02

Figure 128. Cost breakdown for pouch formation

Stainless Steel Rib Formation

Metal ribs are used to create air passageways between the cell pouches of the plate frame humidifier. The ribs are stamped from 0.6mm thick stainless steel 316L sheeting and formed into 10cm by 0.25cm by 0.6mm ribs. Plate handling robots are used to collect and stack the ribs into magazines to be used during stack assembly. The capital cost of the stamping press is \$165,000 and the cycle time is approximately 0.67 seconds per rib (90 stamps per minute).

Figure 129 and Figure 130 show rib formation processing parameters. Cost results for rib formation are shown in Figure 131.

Annual Production Rate	1,000	10,000	30,000	80,000	100,000	500,000
Equipment Lifetime (years)	15	15	15	15	15	15
Interest Rate	10%	10%	10%	10%	10%	10%
Corporate Income Tax Rate	40%	40%	40%	40%	40%	40%
Capital Recovery Factor	0.175	0.175	0.175	0.175	0.175	0.175
Equipment Installation Factor	1.4	1.4	1.4	1.4	1.4	1.4
Maintenance/Spare Parts (% of CC)	13%	13%	13%	13%	13%	13%
Miscellaneous Expenses (% of CC)	2%	2%	2%	2%	2%	2%
Power Consumption (kW)	18	18	18	18	18	18

Figure 129. Stainless steel rib formation process parameters

Annual Production Rate	1,000	10,000	30,000	80,000	100,000	500,000
Capital Cost (\$/line)	\$158,710	\$158,710	\$158,710	\$158,710	\$158,710	\$158,710
Costs per Tooling Set (\$)	\$6,000	\$6,000	\$6,000	\$6,000	\$6,000	\$6,000
Tooling Lifetime (cycles)	400,000	400,000	400,000	400,000	400,000	400,000
Simultaneous Lines	1	1	1	2	2	7
Laborers per Line	0.25	0.25	0.25	0.25	0.25	0.25
Line Utilization	1%	13%	40%	53%	66%	94%
Cycle Time (s)	0.66	0.66	0.66	0.66	0.66	0.66
Effective Total Machine Rate (\$/hr)	\$1,422	\$1,422	\$1,422	\$1,422	\$1,422	\$1,422
BPP Pre-Coating Cost (\$/kg)	\$3.93	\$3.93	\$3.93	\$3.93	\$3.93	\$3.93

Figure 130. Machine rate parameters for stainless steel rib formation

Annual Production Rate	1,000	10,000	30,000	80,000	100,000	500,000
Materials (\$/stack)	\$1.19	\$1.19	\$1.19	\$1.19	\$1.19	\$1.19
Manufacturings (\$/stack)	\$63.19	\$6.83	\$2.66	\$2.13	\$1.82	\$1.45
Toolings (\$/stack)	\$3.60	\$3.60	\$3.60	\$3.60	\$3.60	\$3.60
Total Costs (\$/stack)	\$67.98	\$11.62	\$7.44	\$6.92	\$6.61	\$6.23
Total Costs (\$/kWnet)	\$0.85	\$0.15	\$0.09	\$0.09	\$0.08	\$0.08

Figure 131. Cost breakdown for stainless steel rib formation

Stack Formation

The plate frame membrane humidifier stack is assembled by “pick and place” robots. The following steps are used for assembly.

1. Repeated robotic steps for the number of pouches required in the stack (80 cell pouches for automotive system).
 - a. Robot acquires and places pouch cell with flow field insert
 - b. Apply silicone gasket/adhesive bead on three sealing lines
 - c. Acquire and place three parallel SS rib spacers onto the sealing lines
 - d. Apply additional silicone gasket/adhesive beads on three sealing lines on rib spacers
2. Compress stack in an assembly jig and hold for 24 hours in a humidified warm enclosure. (72 hours curing time would be required if left at room temperature.)
3. Use optical quality control system to detect membrane misalignment in stack.

The total capital cost of the pick and place robots and other equipment required for the system is \$203,000. The cycle time is 9 seconds for each pouch (~12 min for an 80 cell pouch stack).

Figure 132 and Figure 133 show stack formation processing parameters. Cost results for stack formation process are in Figure 134.

Annual Production Rate	1,000	10,000	30,000	80,000	100,000	500,000
Equipment Lifetime (years)	15	15	15	15	15	15
Interest Rate	10%	10%	10%	10%	10%	10%
Corporate Income Tax Rate	40%	40%	40%	40%	40%	40%
Capital Recovery Factor	0.175	0.175	0.175	0.175	0.175	0.175
Equipment Installation Factor	1.4	1.4	1.4	1.4	1.4	1.4
Maintenance/Spare Parts (% of CC)	10%	10%	10%	10%	10%	10%
Miscellaneous Expenses (% of CC)	7%	7%	7%	7%	7%	7%
Power Consumption (kW)	22	22	22	22	22	22

Figure 132. Stack formation process parameters

Annual Production Rate	1,000	10,000	30,000	80,000	100,000	500,000
Capital Cost (\$/line)	\$185,000	\$185,000	\$185,000	\$185,000	\$185,000	\$185,000
Simultaneous Lines	1	1	2	5	6	30
Laborers per Line	0.25	0.25	0.25	0.25	0.25	0.25
Line Utilization	6%	60%	89%	95%	99%	99%
Cycle Time (s)	9	9	9	9	9	9
Effective Total Machine Rate (\$/hr)	\$397	\$52	\$39	\$37	\$36	\$36
Silicon Adhesive Cost (\$/kg)	12.05	12.05	12.05	12.05	12.05	12.05

Figure 133. Machine rate parameters for stack formation

Annual Production Rate	1,000	10,000	30,000	80,000	100,000	500,000
Materials (\$/stack)	\$4	\$4	\$4	\$4	\$4	\$4
Manufacturings (\$/stack)	\$79	\$10	\$8	\$7	\$7	\$7
Total Costs (\$/stack)	\$84	\$15	\$12	\$12	\$12	\$12
Total Costs (\$/kWnet)	\$1.05	\$0.18	\$0.15	\$0.15	\$0.14	\$0.14

Figure 134. Cost breakdown for stack formation

Formation of the Housing

The humidifier aluminum housing is formed using a 900 ton cold chamber die casting machine to form two separate parts (body and upper lid). Boothroyd Dewhurst Inc. (BDI) software was used for the cost estimate. The housing walls are 2.5mm thick and have approximate dimensions of 22cm tall by 11cm length and width. The volume is less than 5 liters and the mass of the housing about 1kg. Four bolts/nuts are used to connect the body to the lid with an elastomer O-ring for sealing. A CAD drawing of the complete housing is shown in Figure 135. Process steps used in DFMA analysis for humidifier cell pouch formation along with the corresponding cost results are displayed in Figure 136.

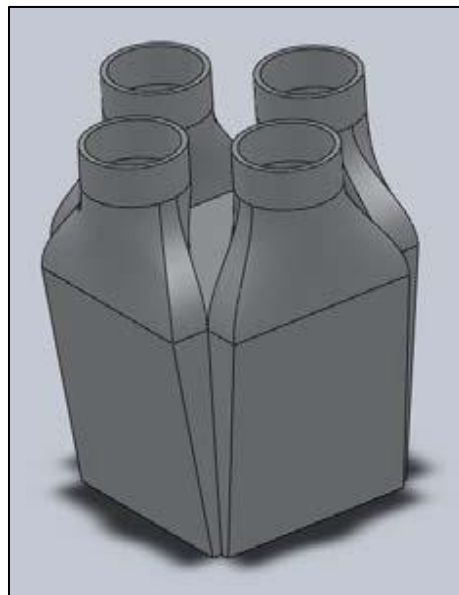


Figure 135. Process steps used in DFMA™ analysis for humidifier cell pouch formation (Source: Johnson, William B. “Materials and Modules for Low-Cost, High Performance Fuel Cell Humidifiers,” W.L. Gore & Associates, Inc., presentation at the 2012 DOE Hydrogen and Fuel Cell Program Annual Merit Review, Washington, DC, 17 May 2012.)

Annual Production Rate	1,000	10,000	30,000	80,000	100,000	500,000
Material (\$/stack)	\$5.05	\$5.05	\$5.05	\$5.05	\$5.05	\$5.05
Manufacturing (\$/stack)	\$17.63	\$3.73	\$1.25	\$0.66	\$0.58	\$0.50
Tooling (\$/stack)	\$30.60	\$3.06	\$2.36	\$1.44	\$1.34	\$1.21
Total Cost (\$/stack)	\$53.28	\$11.84	\$8.66	\$7.15	\$6.97	\$6.76
Total Cost (\$/kWnet)	\$0.67	\$0.15	\$0.11	\$0.09	\$0.09	\$0.08

Figure 136. Cost breakdown for formation of the Housing

Assembly of the Composite Membrane and Flow Fields into the Housing

Complete manual assembly of the plate frame humidifier is performed at a custom work stand using the following sequence:

- a. Acquire housing body and insert into fixture.
- b. Acquire pouch stack and load stack into housing.
- c. Acquire and insert gasket into housing body.
- d. Acquire upper lid and place onto gasket/housing-body.
- e. Acquire, insert and fasten 4 bolts/nuts.
- f. Acquire finished housing and move to cart.
- g. Weigh finished unit to detect missing/additional parts. (Quality control step.)

The cycle time is approximately 2 minutes per system. Figure 137 and Figure 138 show assembly process parameters. Cost results for assembly are shown in Figure 139.

Annual Production Rate	1,000	10,000	30,000	80,000	100,000	500,000
Equipment Lifetime (years)	10	10	10	10	10	10
Interest Rate	10%	10%	10%	10%	10%	10%
Corporate Income Tax Rate	40%	40%	40%	40%	40%	40%
Capital Recovery Factor	0.205	0.205	0.205	0.205	0.205	0.205
Equipment Installation Factor	1.4	1.4	1.4	1.4	1.4	1.4
Maintenance/Spare Parts (% of CC)	10%	10%	10%	10%	10%	10%
Miscellaneous Expenses (% of CC)	7%	7%	7%	7%	7%	7%
Power Consumption (kW)	18	18	18	18	18	18

Figure 137. Assembly of the composite membrane and flow fields into the housing process parameters

Annual Production Rate	1,000	10,000	30,000	80,000	100,000	500,000
Assembly Method	Manual	Manual	Manual	Manual	Manual	Manual
Capital Cost (\$/line)	\$34,228	\$34,228	\$34,228	\$34,228	\$34,228	\$34,228
Simultaneous Lines	1	1	1	1	1	5
Laborers per Line	1	1	1	1	1	1
Line Utilization	1.0%	9.9%	29.8%	79.4%	99.2%	99.2%
Index Time (min)	2	2	2	2	2	2
Effective Total Machine Rate (\$/hr)	\$430	\$86	\$60	\$52	\$51	\$51

Figure 138. Machine rate parameters for assembly of the composite membrane and flow fields into the housing

Annual Production Rate	1,000	10,000	30,000	80,000	100,000	500,000
Manufacturings (\$/stack)	\$14.33	\$2.85	\$2.00	\$1.73	\$1.70	\$1.70
Total Costs (\$/stack)	\$14.33	\$2.85	\$2.00	\$1.73	\$1.70	\$1.70
Total Costs (\$/kWnet)	\$0.18	\$0.04	\$0.02	\$0.02	\$0.02	\$0.00

Figure 139. Cost breakdown for assembly of the composite membrane and flow fields into the housing

Humidifier System Testing

A simple functionality test is completed for each completed humidifier system. It includes testing for air flow pressure drop and air leakage. These tests require an air compressor, gas manifolding, and a diagnostic measurement system. The steps considered in this testing process are:

- a. Acquire unit and insert into fixture.
- b. Connect 4 inlet and outlet air manifolds.
- c. Sequentially flow gas (as appropriate) to test:
 - Pressure drop in primary flow (20 seconds)
 - Pressure drop in secondary flow (20 seconds)
 - Air leakage (primary to secondary) (20 seconds)
- d. Disconnect inlet and outlet air manifolds.
- e. Remove unit from fixture.

The estimated capital cost is:

- \$30,000 for a 1-system test fixture (used at low production levels)
- \$40,000 for a 3-system test fixture (used at high production levels)

The cycle time for testing is about 83 seconds per cycle.

- 83 seconds per system for a 1-system test fixture and 1 worker
- 23 seconds per system for a 3-system test fixture and 1 worker

Figure 140 and Figure 141 show humidifier system testing process parameters. Cost results are displayed in Figure 142.

Annual Production Rate	1,000	10,000	30,000	80,000	100,000	500,000
Equipment Lifetime (years)	15	15	15	15	15	15
Interest Rate	10%	10%	10%	10%	10%	10%
Corporate Income Tax Rate	40%	40%	40%	40%	40%	40%
Capital Recovery Factor	0.175	0.175	0.175	0.175	0.175	0.175
Equipment Installation Factor	1.4	1.4	1.4	1.4	1.4	1.4
Maintenance/Spare Parts (% of CC)	10%	10%	10%	10%	10%	10%
Miscellaneous Expenses (% of CC)	7%	7%	7%	7%	7%	7%
Power Consumption (kW)	2	2	2	5	5	5

Figure 140. Humidifier system testing process parameters

Annual Production Rate	1,000	10,000	30,000	80,000	100,000	500,000
Capital Cost (\$/line)	\$30,000	\$30,000	\$30,000	\$40,000	\$40,000	\$40,000
Simultaneous Lines	1	1	1	1	1	1
Laborers per Line	1	1	1	1	1	1
Line Utilization	0.7%	6.9%	20.6%	15.2%	19.0%	95.1%
Systems partially connected at any one time	1	1	1	3	3	3
Selected Effective Test time per System	1.38	1.38	1.38	0.38	0.38	0.38
Effective Total Machine Rate (\$/hr)	\$492.13	\$90.67	\$60.81	\$73.07	\$67.68	\$50.42

Figure 141. Machine rate parameters for humidifier system testing

Annual Production Rate	1,000	10,000	30,000	80,000	100,000	500,000
Manufacturings (\$/stack)	\$11.40	\$2.09	\$1.40	\$0.47	\$0.43	\$0.32
Total Costs (\$/stack)	\$11.40	\$2.09	\$1.40	\$0.47	\$0.43	\$0.32
Total Costs (\$/kWnet)	\$0.14	\$0.03	\$0.02	\$0.01	\$0.01	\$0.00

Figure 142. Cost breakdown for humidifier system testing

7.2.2.3.2 Combined Cost Results for Plate Frame Membrane Humidifier

Cost results for the Gore plate frame membrane humidifier are summarized in Figure 143 at 500,000 systems per year and in Figure 144 for all manufacturing rates, with costs further subdivided into materials, manufacturing, tooling, markup, and total costs. The greatest cost drivers are the material costs, particularly for the membrane materials at ~\$29/humidifier. Costs are strongly impacted by the quantity of membrane material needed for the humidifier. The largest processing cost for the humidifier is the flow field fabrication due to the innate details of the flow field design which are deemed to require a (relatively) expensive etching process. Membrane and flow fields make up approximately 2/3rds of the total cost and materials are about half the total humidifier cost (at 500,000 systems per year), as seen in Figure 145.

Component Costs per Humidifier System			All at 500k systems per year					
			Materials	Manuf.	Tools	Secondary Operations	Markup	Total
Station 1: Membrane Fabrication	\$/stack		\$29.01	\$2.76	\$0.16	\$0.00	\$7.98	\$39.90
Station 2: Humidifier Etching (Flow Field Plates)	\$/stack		\$15.09	\$11.13	\$0.00	\$0.00	\$0.00	\$26.21
Station 3: Pouch Forming	\$/stack		\$0.44	\$1.30	\$0.05	\$0.00	\$0.00	\$1.79
Station 4: Stamp SS ribs	\$/stack		\$1.19	\$1.45	\$3.60	\$0.00	\$0.00	\$6.23
Station 5: Stack Forming	\$/stack		\$4.33	\$7.23	\$0.00	\$0.00	\$0.00	\$11.57
Station 6: Stack Housing	\$/stack		\$5.05	\$0.50	\$1.21	\$0.00	\$0.00	\$6.76
Station 7: Assembly of Stack into Housing	\$/stack		\$0.00	\$1.70	\$0.00	\$0.00	\$0.00	\$1.70
Station 8: System Test	\$/stack		\$0.00	\$0.32	\$0.00	\$0.00	\$0.00	\$0.32
Totals =			\$55.11	\$26.38	\$5.02	\$0.00	\$7.98	\$94.49

Figure 143. Membrane humidifier system cost results: ~\$95 at 500k systems/year

Annual Production Rate	1,000	10,000	30,000	80,000	100,000	500,000
Materials (\$/stack)	\$118	\$91	\$80	\$71	\$69	\$55
Manufacturings (\$/stack)	\$2,059	\$221	\$86	\$45	\$41	\$26
Toolings (\$/stack)	\$34	\$7	\$6	\$5	\$5	\$5
Markups (\$/stack)	\$553	\$68	\$34	\$18	\$15	\$8
Total Costs (\$/stack)	\$2,764	\$387	\$206	\$139	\$129	\$94
Total Costs (\$/kWnet)	\$34.55	\$4.84	\$2.58	\$1.74	\$1.62	\$1.18

Figure 144. Combined cost results for all plate frame humidifier processes.

Markup is typically applied to the sum of materials, manufacturing, and tooling to capture the real business costs associated with overhead, general administrative (G&A), scrap, R&D, and profit. Per previous DOE directive, markup is only applied to lower-tier suppliers and is NOT applied to the system assembler. A high degree of vertical integration for the overall auto fuel cell power system is assumed. (As discussed in more detail in Section 2.3, a lower level of vertical integration is assumed for the bus fuel cell system, therefore markup is applied to the humidifier.) For the plate frame membrane humidifier, markup is not applied to the auto humidifier assembler. However, markup is included in the costs of the ePTFE, PET, and composite humidifier membrane as those components are assumed to be manufactured by lower tier suppliers. (Markup on the manufacturing process for the composite membrane appears in the markup column in Figure 143.)

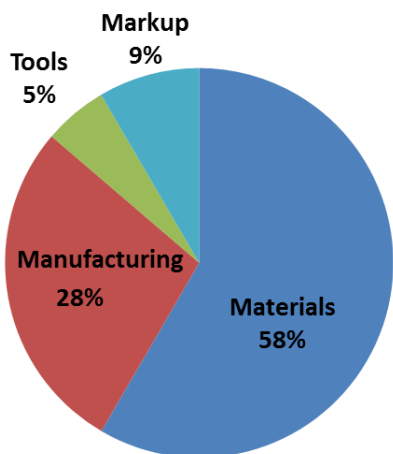


Figure 145. Humidifier membrane cost dominated by material cost at 500k systems/year

In cost analysis of fuel cell system components, it is beneficial to benchmark results with currently developed systems. Figure 146 compares SA’s cost estimate to Gore’s cost estimate and shows good agreement at medium and high production rates. SA estimates are much higher than Gore’s at low manufacturing rates due to poor utilization of expensive equipment (i.e. composite membrane fabrication). At low utilization of equipment, a business may decide to “job shop” or outsource the work to a company that has higher utilization of similar equipment. Such “job shopping” is not assumed for the humidifier in the 2013 analysis although a more detailed scale-down of the manufacturing equipment may lead to a lower cost estimate at 1,000 systems per year.

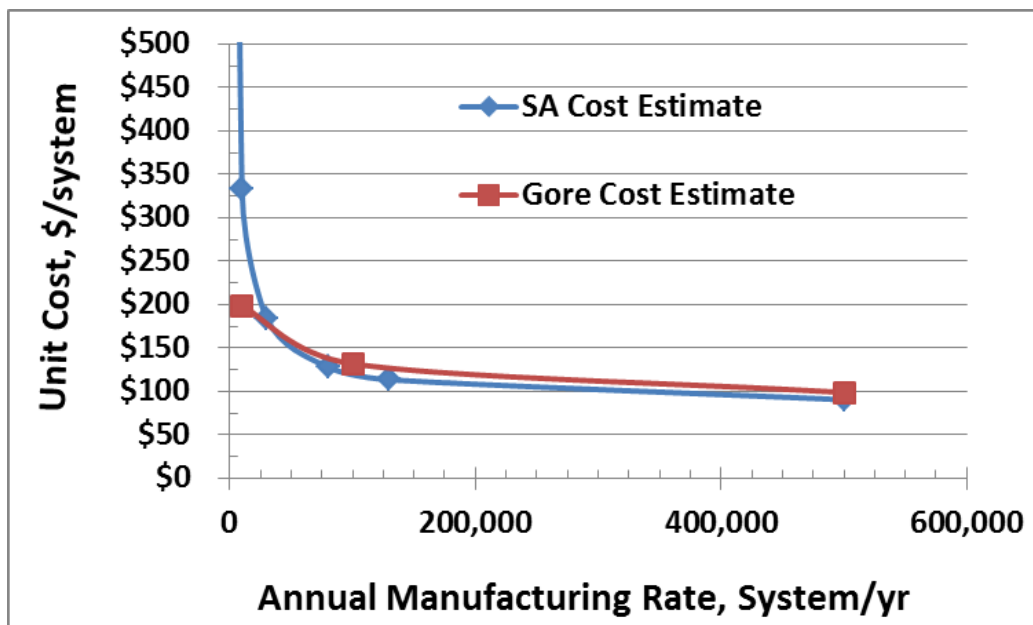


Figure 146. Comparison of Gore and SA cost estimates for the plate frame membrane humidifier.

A sensitivity analysis of multiple parameters at 500,000 systems per year (Tornado Chart in Figure 147 with sensitivity limits in Figure 148) shows that the most important cost driver for the humidifier is the quantity of membrane material required. This indicates that between 0.5m² and 2.6m² of membrane

area (based on discussion in Section 6.5), the plate frame humidifier would cost between \$40/system and \$137/system. The second most important cost driver is the price of the ePTFE material used in the membrane. Both the fuel cell stack MEA and humidifier manufactured costs are quite sensitive to the cost of ePTFE. While plate frame humidifier uncertainty is high (-57%/+46%), the overall humidifier cost is low compared to the total auto fuel cell power system cost.

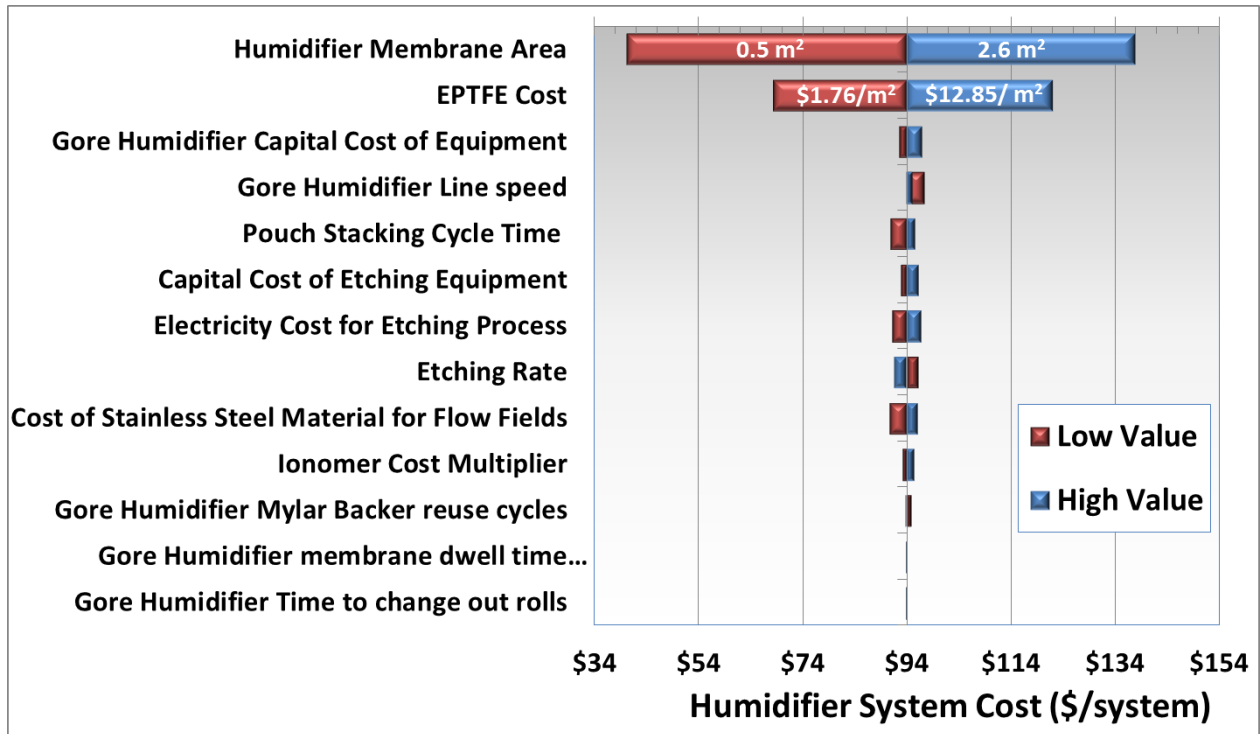


Figure 147. Single-variable sensitivity Tornado Chart of plate frame membrane humidifier cost per system.

Gore MEA Sensitivity Limits for Tornado Chart				
Parameter	Units	Low Value	Base Value	High Value
Humidifier Membrane Area	m ² (cells)	0.5 (24 cells)	1.6 (80 cells)	2.6 (130 cells)
EPTFE Cost	\$/m ²	1.76	7.05	12.85
Gore Humidifier Capital Cost of Equipment	Multiplier	0.5	1	2
Gore Humidifier Line speed	m/min	3	10	300
Pouch Stacking Cycle Time	sec	5	9	11
Capital Cost of Etching Equipment	Multiplier	0.5	1	2
Electricity Cost for Etching Process	\$/kWh	0.04	0.08	0.12
Etching Rate	microns/min	10	13.33	20
Cost of Stainless Steel Material for Flow Fields	\$/kg	3.07	3.93	4.5
Ionomer Cost Multiplier	Multiplier	0.5	1	2
Gore Humidifier Mylar Backer reuse cycles	cycles	1	5	10
Gore Humidifier membrane dwell time multiplier	multiplier	0.5	1	2
Gore Humidifier Time to change out rolls	min	1	10	15
2013 Gore Humidifier System Cost (500,000 systems per year)			\$94.49	

Figure 148. Single-variable sensitivity limits for plate frame membrane humidifier Tornado Chart.

In comparison to the tubular membrane humidifier previously used in the 2012 analysis, the 2013 plate frame humidifier is projected to be higher cost. However, in retrospect, the 2012 tubular membrane humidifier is now viewed as undersized for the flow conditions (even at 3.8m² of membrane area) and thus a direct comparison of the two systems is not valid. In general, plate frame humidifiers will require less membrane area than tubular designs since their membranes may be thinner, (by virtue of being supported on ePTFE). However, the cost of the ePTFE support is a significant fraction of the total plate frame humidifier cost, and manufacturing (particularly of the etched plates) also adds considerably to cost (see Figure 149).

As shown by the sensitivity analysis, membrane area is an extremely important parameter in determination of humidifier cost. Uncertainty exists related to the required membrane area. Consequently, an optimistic value of 0.5m²/system was included in the sensitivity analysis based on ANL modeling projections and a pessimistic value of 2.6m² was included to reflect a large allowance for performance degradation. Further testing is required to confidently determine the membrane area requirement.

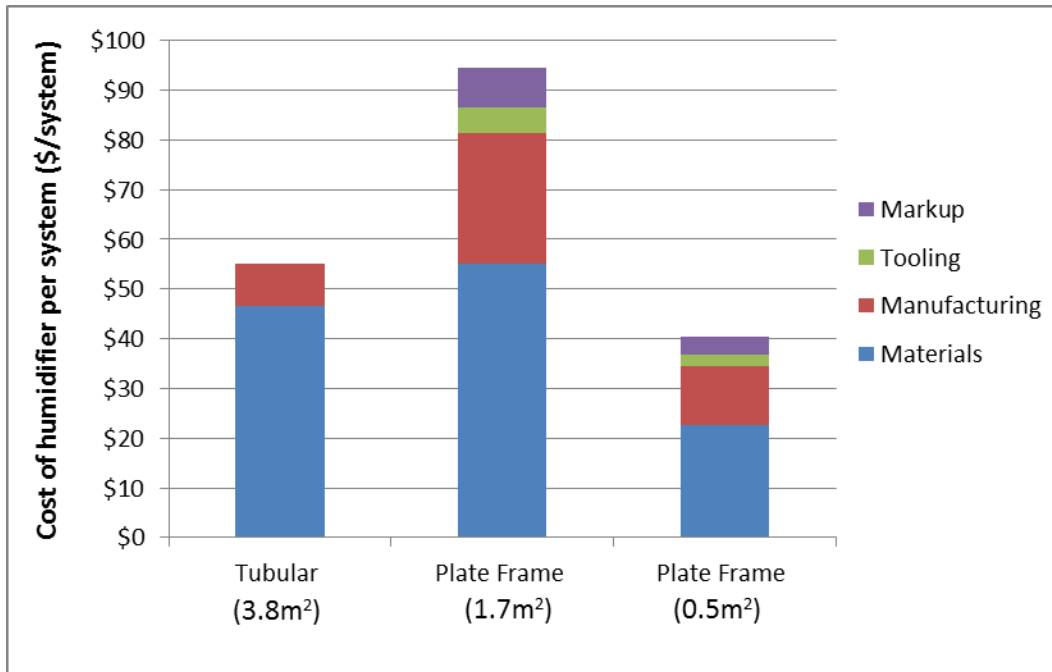


Figure 149. Graph showing the cost (at 500k sys/yr) comparison between a tubular membrane humidifier and two plate frame membrane humidifiers with different membrane area requirements.

7.2.3 Coolant Loops

The 2013 system has two coolant loops, a high-temperature loop to cool the fuel cell stacks and a low-temperature loop to cool electronic components. The low temperature loop is also used to cool the CEM motor and in the precooler (to cool the compressed intake air prior to going into the membrane humidifier).

7.2.3.1 High-Temperature Coolant Loop

Coolant Reservoir: The cost is based on a molded plastic water tank.

Coolant Pump: Small pumps to provide this flow are commercially available in large quantities at approximately \$97 per pump at quantities of 1,000, dropping to \$74 at high quantity.

Coolant DI Filter: The cost is based on a resin deionizer bed in a plastic housing.

Thermostat & Valve: The cost is based on standard automotive components.

Radiator: The heat dissipation requirements of the fuel cell system are similar to those of today's standard passenger cars. Consequently, costs for the high and low-temperature loop radiators are aligned with those of appropriately sized radiators used in contemporary automotive applications.

Radiator Fan: The cost is based on a standard automotive radiator fan and sized based on the cooling load.

Coolant Piping: Cost is based on 2” diameter rubber pipe from McMaster Carr and set at a constant \$6.93/ft.

High-temperature coolant loop cost results are shown in Figure 150.

Annual Production Rate	1,000	10,000	30,000	80,000	100,000	500,000
Coolant Reservoir (\$/system)	\$14	\$11	\$11	\$8	\$8	\$6
Coolant Pump (\$/system)	\$97	\$86	\$86	\$78	\$75	\$74
Coolant DI Filter (\$/system)	\$81	\$65	\$65	\$49	\$45	\$39
Thermostat & Valve (\$/system)	\$11	\$9	\$9	\$6	\$6	\$5
Radiator (\$/system)	\$196	\$158	\$158	\$150	\$141	\$132
Radiator Fan (\$/system)	\$89	\$68	\$68	\$52	\$50	\$47
Coolant Piping (\$/system)	\$24	\$23	\$23	\$22	\$21	\$20
Total Cost (\$/system)	\$512	\$420	\$420	\$365	\$345	\$323
Total Cost (\$/kW_{net})	\$6.40	\$5.25	\$5.25	\$4.56	\$4.32	\$4.04

Figure 150. Cost breakdown for high-temperature coolant loop

7.2.3.2 Low-Temperature Coolant Loop

In the 2012 analysis, the low-temperature loop previously cooled components both within the fuel cell system (precooler, CEM motor) and the drive train system (main traction motor inverter (TIM) electronics). Consequently, the cost of the 2012 low-temperature coolant loop was apportioned between these systems and only the cost of the loop associated with the fuel cell system was tabulated in the fuel cell cost summary. Based on the expected duties of the components, 67% of the low-temperature coolant loop cost was attributable to the fuel cell system.

As mentioned in Section 6.11, the low-temperature loop for the 2013 analysis is modeled as a dedicated fuel cell system cooling loop and thus only cools components within the fuel cell system (precooler, CEM motor). Drive train components have been removed from the cooling loop: thus 100% of the coolant loop cost is charged to the fuel cell system. This change was made in order to simplify the analysis and to be in closer alignment with Argonne National Laboratory modeling methodology.

Coolant Reservoir: The cost is based on a molded plastic water tank.

Coolant Pump: The low and high-temperature loops require similar flow rates, so the same type of pump is used in each.

Thermostat & Valve: The cost is based on standard automotive components.

Radiator: As with the radiator for the high-temperature coolant loop, the exhaust loop uses a radiator similar to those used in conventional automotive applications. It does not need to be as large as the one for the coolant loop however, so it is scaled down in cost.

Radiator Fan: It is assumed that the radiators for the high and low-temperature loops are installed together such that the air flow exiting the low-temperature radiator immediately enters the high-temperature radiator, and as such, there is a single fan for both radiators, which is accounted for in the high-temperature coolant loop (Reason why radiator fan cost is \$0 in Figure 151).

Coolant Piping: Assumed 2” diameter rubber pipe from McMaster Carr, at \$6.93/ft.

Low-temperature coolant loop cost results are shown in Figure 151.

Annual Production Rate	1,000	10,000	30,000	80,000	100,000	500,000
Coolant Reservoir (\$/system)	\$2	\$130	\$130	\$130	\$130	\$130
Coolant Pump (\$/system)	\$26	\$2	\$2	\$2	\$2	\$2
Thermostat & Valve (\$/system)	\$4	\$2,092	\$2,092	\$2,092	\$2,092	\$2,092
Radiator (\$/system)	\$45	\$68	\$68	\$52	\$50	\$47
Radiator Fan (\$/system)	\$0	\$0	\$0	\$0	\$0	\$0
Coolant Piping (\$/system)	\$20	\$530	\$530	\$530	\$530	\$530
Total Cost (\$/system)	\$97	\$88	\$88	\$78	\$74	\$70
Total Cost (\$/kW_{net})	\$1.22	\$173.58	\$173.58	\$153.71	\$145.85	\$138.19

Figure 151. Cost breakdown for low-temperature coolant loop

7.2.4 Fuel Loop

Per DOE system analysis guidelines, the hydrogen tank, the hydrogen pressure-relief device & regulator, hydrogen fueling receptacle, proportional valve, and pressure transducer are not included in the fuel cell power system cost analysis as they are considered part of the hydrogen storage system.

Inline Filter for Gas Purity Excursions: This filter ensures that any contaminants that may have gotten into the fuel lines do not damage the stack.

Flow Diverter Valve: The flow diverter valve routes hydrogen to either the low-flow or the high-flow ejector, depending on the pressure.

Over-Pressure Cut-Off (OPCO) Valve: The over-pressure cut-off valve is included as a safety precaution to prevent inadvertent stack pressurization from the high pressure (>5000psi) in the hydrogen storage tank.

Low-Flow and High-Flow Ejectors: Dual static ejectors are employed to re-circulate hydrogen from the anode exhaust to the anode inlet to achieve target flow rates and hence high stack performance. The ejectors operate on the Bernoulli Principle wherein high-pressure hydrogen gas from the fuel tank (>250 psi) flows through a converging-diverging nozzle to entrain lower-pressure anode exhaust gas. Two ejectors (high-flow and low-flow) are operated in parallel to achieve a wide turn-down range. The design of the ejectors is based on concepts from Graham Manufacturing and the patent literature (US Patent 5,441,821). The fabrication of each ejector consists of stainless steel investment casting of a two-part assembly, followed by machining, welding, and polishing. Ejectors with variable geometry are a possible design improvement for future systems. While ANL modeling suggests that a hydrogen recirculation blower is needed during very low part-power system operation to ensure proper gas flow, only the ejector system is included in the analysis.

Check Valves: The check valves ensure that no hydrogen may flow backwards from the ejectors

Purge Valve: The purge valve allows for periodic purging of the hydrogen in the fuel loop.

Hydrogen Piping: The hydrogen flow lines are modeled as 1/2" SS316 schedule 10 pipe and are priced between \$90 and \$100/system based on estimate provided by Ford.

Fuel loop cost results are shown in Figure 152.

Annual Production Rate	1,000	10,000	30,000	80,000	100,000	500,000
Inline Filter for GPE (\$/system)	\$19	\$19	\$19	\$19	\$19	\$19
Flow Diverter Valve (\$/system)	\$16	\$16	\$16	\$16	\$16	\$16
Over-Pressure Cut-Off Valve (\$/system)	\$25	\$22	\$20	\$15	\$14	\$12
Hydrogen High-Flow Ejector (\$/system)	\$51	\$36	\$36	\$33	\$31	\$31
Hydrogen Low-Flow Ejector (\$/system)	\$44	\$29	\$29	\$26	\$25	\$24
Check Valves (\$/system)	\$10	\$10	\$10	\$10	\$10	\$10
Purge Valves (\$/system)	\$80	\$70	\$64	\$48	\$45	\$38
Hydrogen Piping (\$/system)	\$106	\$104	\$103	\$99	\$96	\$92
Total Cost (\$/system)	\$350	\$304	\$295	\$265	\$255	\$241
Total Cost (\$/kW_{net})	\$4.37	\$0.44	\$0.43	\$0.38	\$0.37	\$0.35

Figure 152. Cost breakdown for fuel loop

7.2.5 System Controller

Conventional electronic engine controllers (EEC's) are assumed to control the fuel cell power system. These programmable circuit boards are currently mass-produced for all conventional gasoline engines and are readily adaptable for fuel cell use. Prototype fuel cell vehicles may use four or more controllers out of convenience, so that each subsystem is able to have a separate controller. However, even at 1,000 vehicles per year, the system will be refined enough to minimize controller use on the rationale of simplicity of cost and design. A single EEC is judged adequate for control and sensor leads to the power plant.

Controller cost is assessed by a bottom-up analysis of the system controller which breaks the controller into 17 input and output circuits, as listed in Figure 153.

For each input or output circuit, it is estimated that approximately 50 cents in electronic components (referencing catalog prices) would be needed. The costs of input and output connectors, an embedded controller, and the housing are also estimated by catalog pricing. A price quote forms the basis for the assumed dual-layer 6.5" x 4.5" circuit board. Assembly of 50 parts is based on robotic pick-and-place methods. A 10% cost contingency is added to cover any unforeseen cost increases.

Name	Signal
Inputs	
Air Mass Flow Sensor	Analog
H ₂ Pressure Sensor (upstream of ejector)	Analog
H ₂ Pressure Sensor (stack inlet manifold)	Analog
Air Pressure Sensor (after compressor)	Analog
Stack Voltage (DC bus)	Analog
Throttle Request	Analog
Current Sensors (drawn from motor)	Analog
Current Sensors (output from stack)	Analog
Signal for Coolant Temperature	Analog
H ₂ Leak Detector	Digital
Outputs	
Signal to TIM	Analog
Signal to CEM	Analog
Signal to Ejector 1	PWM
Signal to Ejector 2	PWM
High Voltage System Relay	Digital
Signal to Coolant Pump	PWM
Signal to H ₂ Purge Valve	Digital
Total Analog	11
Total Digital	3
Total PWM	3
Total Inputs/Outputs	17

Figure 153. System controller input & output requirements

Figure 154 and Figure 155 detail estimated system controller costs.

Component	Description	Cost at 500k systems/year	Cost Basis
Main Circuit Board	2 layer punchboard	\$8.01	\$5.34 for single layer of 6.5"x4.5" punchboard, Q=500, Assume 25% discount for Q=500k
Input Connector	Wire connector for inputs	\$0.18	\$0.23 each in Q=10k, reduced ~20% for Q=500k
Output Connector	Wire connector for outputs	\$0.20	\$0.23 each in Q=10k, reduced ~20% for Q=500k
Embedded Controller	25 MHz, 25 channel microprocessor board	\$32.50	Digi-Key Part No. 336-1489-ND, \$50@Q=1, assumed 35% reduction for Q=500k
MOSFETs (17 total, 1 each per I/O)	P-channel, 2W, 49MOhm @5A, 10V	\$3.74	Digi-Key Part No. 785-1047-2-ND, \$0.2352@Q=3k,\$0.2184@Q=12k
Misc. Board Elements	Capacitor, resistors, etc.	\$4.25	Estimate based on \$0.25 component for each input/output
Housing	Shielded plastic housing, watertight	\$5.00	Estimate based on comparable shielded, electronic enclosures. Includes fasteners.
Assembly	Assembly of boards/housing	\$5.83	Robotic assembly of approx. 50 parts at 3.5 sec each, \$2/min assembly cost.
Contingency	10% of all components	\$5.97	Standard DFMA additional cost to capture un-enumerated elements/activities.
Markup	25% of all Components	\$16.42	Manufacturer's Markup
Total		\$82.11	

Figure 154. System controller component costs

Annual Production Rate	1,000	10,000	30,000	80,000	100,000	500,000
System Controller	\$171	\$151	\$137	\$103	\$96	\$82
Total Cost (\$/system)	\$171	\$151	\$137	\$103	\$96	\$82
Total Cost (\$/kW _{net})	\$2.14	\$1.88	\$1.71	\$1.28	\$1.20	\$1.03

Figure 155. Cost breakdown for system controller

7.2.6 Sensors

Aside from the air mass flow sensor (which is book-kept as part of the air loop), there are three types of sensors in the fuel cell system: current sensors, voltage sensors, and hydrogen sensors. The basic sensor descriptions and their costs are listed in Figure 156 and Figure 157.

Component	Description	Cost at 500k systems/year	Cost Basis
Current Sensor (for stack current)	~400A, Hall Effect transducer	10	Based on LEM Automotive Current Transducer HAH1BV S/06, 400A
Current Sensor (for CEM motor current)	~400A, Hall Effect transducer	10	Based on LEM Automotive Current Transducer HAH1BV S/06, 400A
Voltage Sensor	225-335 V	8	Rough estimate based on a small Hall Effect sensor in series with a resistor
H ₂ Sensor	Dual-sensor unit for large and small H ₂ concentrations	101.40	Makel Engineering
H ₂ Sensor	Dual-sensor unit for large and small H ₂ concentrations	101.40	Makel Engineering
Total		\$230.80	

Figure 156. Sensor details

Annual Production Rate	1,000	10,000	30,000	80,000	100,000	500,000
Current Sensors (\$/system)	\$20	\$20	\$20	\$20	\$20	\$20
Voltage Sensors (\$/system)	\$8	\$8	\$8	\$8	\$8	\$8
Hydrogen Sensors (\$/system)	\$1,727	\$1,162	\$893	\$652	\$597	\$203
Total Cost (\$/system)	\$1,755	\$1,190	\$921	\$680	\$625	\$231
Total Cost (\$/kW_{net})	\$21.93	\$14.87	\$11.51	\$8.50	\$7.82	\$2.88

Figure 157. Cost breakdown for sensors

7.2.6.1 Current Sensors

The current sensors are located on the stack, and allow the system controller to monitor the current being produced.

7.2.6.2 Voltage Sensors

The voltage sensors are located on the stack, and allow the system controller to monitor the voltage being produced.

7.2.6.3 Hydrogen Sensors

The vehicle will require a hydrogen sensing system to guard against hydrogen leakage accumulation and fire. It is postulated that a declining number of hydrogen sensors will be used within the fuel cell power system as a function of time and as real-world safety data is accumulated. Consequently, it is estimated that two sensors would initially be used in the engine compartment, eventually dropping to zero. Additional sensors may be necessary for the passenger compartment and the fuel storage subsystem but these are not in the defined boundary of our fuel cell power system assessment.

The hydrogen sensor system specified is from Makel Engineering, based on the technology used in Ford's Model-U Hydrogen Powered Vehicle prototype. Each sensor unit (see Figure 158) is roughly the size of a quarter and contains two sensors: one for detecting large concentrations of hydrogen, and another for small concentrations. Each unit is accompanied by a control electronics box (also pictured in Figure 158).

Hydrogen sensors are currently quite expensive. 2010 discussion with Makel Engineering reveals that the specified hydrogen sensors are currently hand built and cost approximately \$850 each. Jeffrey Stroh

from Makel estimates that such units would cost approximately \$100 each if mass-produced at 500,000 per year. With further technology and manufacturing improvements, including a move to integrated circuitry, he estimates that the unit cost could drop to only \$20 per sensor. Figure 159 lists the estimated hydrogen sensor costs.

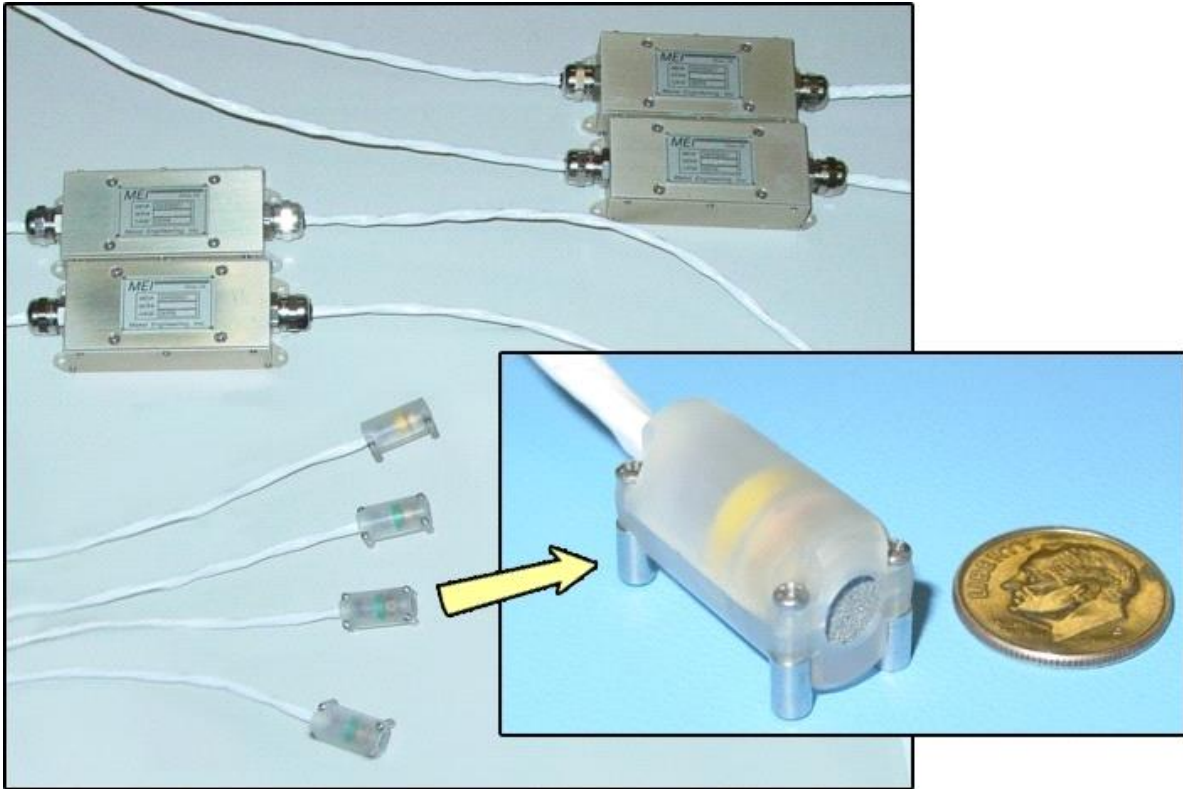


Figure 158. Hydrogen sensors & associated control electronics (Images courtesy of Makel Engineering⁸¹)

Annual Production Rate	1,000	10,000	30,000	80,000	100,000	500,000
Sensors per system	2	2	2	2	2	2
Sensor (\$)	\$863	\$581	\$446	\$326	\$299	\$101
Total Cost (\$/system)	\$1,727	\$1,162	\$893	\$652	\$597	\$203
Total Cost (\$/kW_{net})	\$21.58	\$14.52	\$11.16	\$8.15	\$7.47	\$2.53

Figure 159. Cost breakdown for hydrogen sensors

7.2.7 Miscellaneous BOP

The BOP components which do not fit into any of the other categories are listed here in the miscellaneous section.

Figure 160 shows the cost breakdown for these components.

⁸¹ <http://www.makelengineering.com/dir/Technologies/Overview/Overview.htm>

Annual Production Rate	1,000	10,000	30,000	80,000	100,000	500,000
Belly Pan (\$/system)	\$62.66	\$10.67	\$6.82	\$5.66	\$5.36	\$4.50
Mounting Frames (\$/system)	\$100.00	\$43.00	\$43.00	\$33.00	\$30.00	\$30.00
Wiring (\$/system)	\$107.90	\$97.11	\$92.79	\$90.63	\$89.55	\$86.32
Fasteners for Wiring & Piping (\$/system)	\$21.58	\$19.42	\$18.56	\$18.13	\$17.91	\$17.26
Total Cost (\$/system)	\$292.14	\$170.20	\$161.17	\$147.42	\$142.82	\$138.08
Total Cost (\$/kW_{net})	\$3.65	\$2.13	\$2.01	\$1.84	\$1.79	\$1.73

Figure 160. Cost breakdown for miscellaneous BOP components

7.2.7.1 Belly Pan

The belly pan is modeled as a 1 x 1.5 m shallow rectangular pan, bolted to the underside of the fuel cell system to protect it from weather and stone strikes.

The belly pan manufacturing process is modeled as a vacuum thermoforming process, in which thin polypropylene sheets are softened with heat and vacuum drawn onto the top of a one-sided mold. The capital cost of the vacuum thermoforming machine is approximately \$300,000, and utilizes an optional automatic loading system, which costs another \$200,000. If manual loading is selected, the process requires one laborer per line, instead of the 1/4 laborer facilitated by the automatic loading system. The analysis shows that the automatic system is only cost effective at the 500,000 systems per year production rate. Naturally, the loading option also changes the time per part; the vacuum time is 8 seconds per part, on top of which the insertion time adds another 11.2 seconds for the manual loading, or 2 seconds for the automatic method. The process parameters are shown in Figure 161, and the machine rate parameters are shown in Figure 162.

Annual Production Rate	1,000	10,000	30,000	80,000	100,000	500,000
Equipment Lifetime (years)	8	8	8	15	15	15
Interest Rate	10%	10%	10%	10%	10%	10%
Corporate Income Tax Rate	40%	40%	40%	40%	40%	40%
Capital Recovery Factor	0.229	0.229	0.229	0.175	0.175	0.175
Equipment Installation Factor	1.4	1.4	1.4	1.4	1.4	1.4
Maintenance/Spare Parts (% of CC)	5%	5%	5%	5%	5%	5%
Miscellaneous Expenses (% of CC)	6%	6%	6%	6%	6%	6%
Power Consumption (kW)	30	30	30	35	35	40

Figure 161. Belly pan thermoforming process parameters

Annual Production Rate	1,000	10,000	30,000	80,000	100,000	500,000
Machine Selection	Vacuum Thermo-former #1	Vacuum Thermo-former #1	Vacuum Thermo-former #1	Vacuum Thermo-former #2	Vacuum Thermo-former #2	Vacuum Thermo-former #2
Assembly Type	Manual	Manual	Manual	Manual	Manual	Auto
Capital Cost (\$/line)	\$50,000	\$50,000	\$50,000	\$250,000	\$250,000	\$656,281
Costs per Tooling Set (\$)	\$96,620	\$96,620	\$96,620	\$96,620	\$96,620	\$96,620
Tooling Lifetime (years)	3	3	3	3	3	3
Cavities per platen	1	1	1	1	1	1
Total Cycle Time (s)	71.20	71.20	71.20	15.20	15.20	7.00
Simultaneous Lines	1	1	1	1	1	1
Laborers per Line	1	1	1	1	1	0.25
Line Utilization	0.6%	5.9%	17.7%	10.1%	12.6%	28.9%
Effective Total Machine Rate (\$/hr)	\$1,137	\$157	\$84	\$311	\$258	\$254
Material Cost (\$/kg)	\$1.33	\$1.33	\$1.33	\$1.33	\$1.33	\$1.33

Figure 162. Machine rate parameters for belly pan thermoforming process

Because of the extremely soft nature of the hot polypropylene and the low impact of the process, each mold (~\$85,056) will easily last the entire lifetime of the thermoforming machine. However, belly pan designs are likely to change well before the forming machine wears out, so the mold's lifetime is set at three years. This means that the tooling costs are sufficiently low to ignore at all but the 1,000 systems per year level, where they account for almost 4% of the part cost. Figure 163 shows the cost breakdown.

Annual Production Rate	1,000	10,000	30,000	80,000	100,000	500,000
Material (\$/system)	\$3.94	\$3.94	\$3.94	\$3.94	\$3.94	\$3.94
Manufacturing (\$/system)	\$22.49	\$3.10	\$1.67	\$1.31	\$1.09	\$0.49
Tooling (\$/system)	\$36.23	\$3.62	\$1.21	\$0.40	\$0.32	\$0.06
Total Cost (\$/system)	\$62.66	\$10.67	\$6.82	\$5.66	\$5.36	\$4.50
Total Cost (\$/kWnet)	\$0.78	\$0.13	\$0.09	\$0.07	\$0.07	\$0.06

Figure 163. Cost breakdown for belly pan

7.2.7.2 Mounting Frames

It is assumed that the fuel cell power system would be built as a subsystem, and then hoisted as an assembly into the automotive engine compartment. Consequently, the power system attaches to a mounting frame substructure to allow easy transport. These mounting frames are assumed to be contoured steel beams with various attachment points for power system components, facilitating attachment to the vehicle chassis. The cost is roughly estimated at \$30 at 500,000 systems/year to \$100 at 1,000 systems/year.

7.2.7.3 Wiring

Wiring costs include only wiring materials as wiring installation costs are covered under the system assembly calculations.

A conceptual fuel cell system wiring schematic (Figure 164) was created to determine where cables were needed and whether they were for transmission of data, power, or both. Cable types, detailed in Figure 165, are selected based on the maximum current required by each electrical component.

With the exception of the heavy-duty power cables attached to the current collectors, every cable is comprised of multiple wires. Each cable also requires a unique type of connector, of which two are needed for each cable.

It is assumed that the wires and connectors would be purchased rather than manufactured in-house, with high-volume pricing estimates obtained for the cable components from Waytek, Inc. Taking into account the required length of each cable, the number of wires per cable, and selecting the appropriate connectors, the component prices are applied to the wiring bill of materials and the total wiring cost is calculated for each system (see Figure 166).

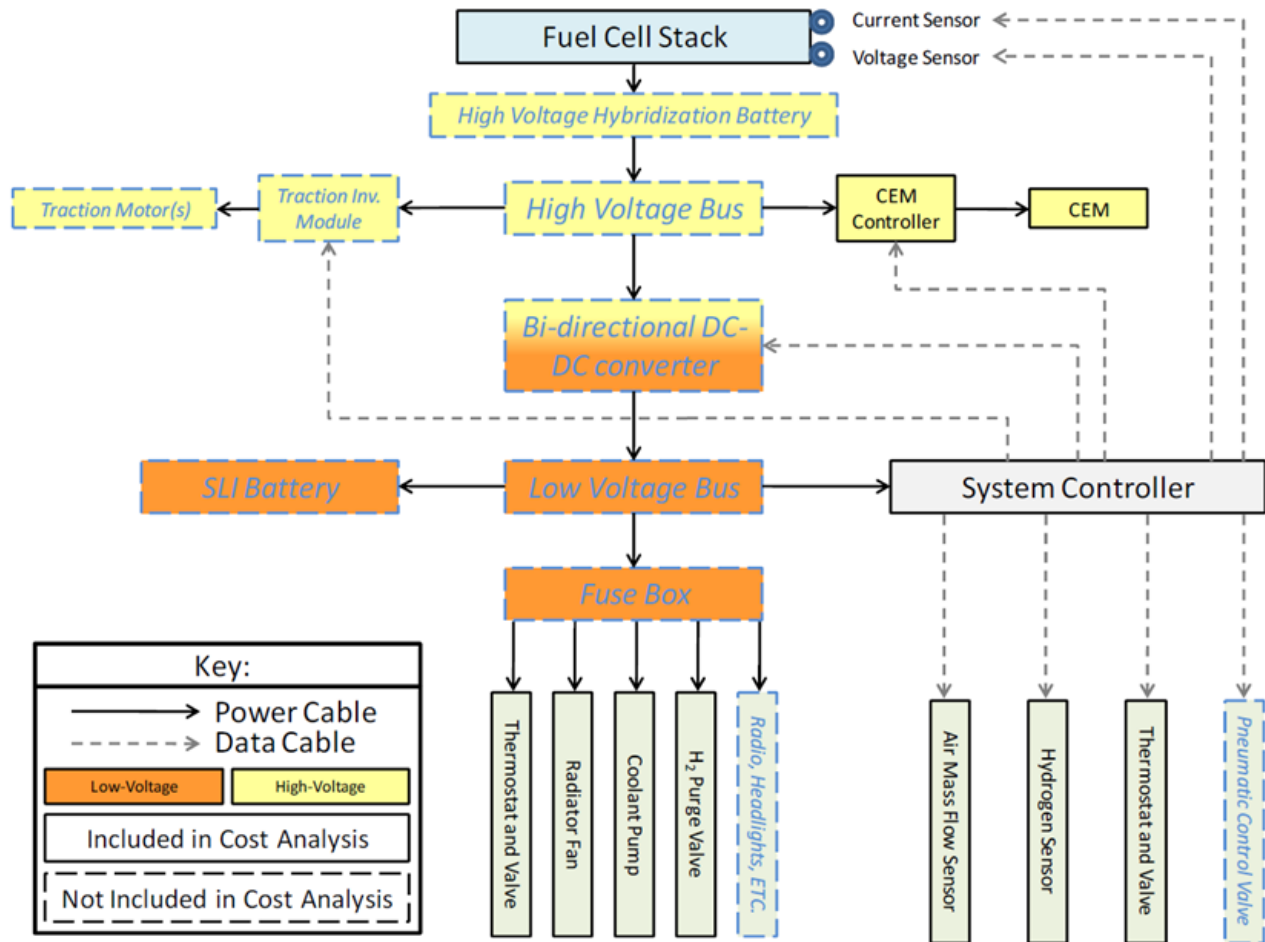


Figure 164. Fuel cell system wiring schematic

	Quantity	Length (m)
Cable Types		
Power Cable, 0000 Gauge	2	0.5
Power Cable, 6 Gauge	1	0.25
Power Cable, 7 Gauge	4	3.5
Power Cable, 12 Gauge	3	3
Power Cable, 16 Gauge	10	9
Totals	20	16.25

Figure 165. Wiring details

Annual Production Rate	1,000	10,000	30,000	80,000	100,000	500,000
Cables (\$/system)	\$35.83	\$32.25	\$30.82	\$30.10	\$29.74	\$28.67
Connectors (\$/System)	\$72.06	\$64.86	\$61.98	\$60.53	\$59.81	\$57.65
Total Cost (\$/system)	\$107.90	\$97.11	\$92.79	\$90.63	\$89.55	\$86.32
Total Cost (\$/kWnet)	\$1.35	\$1.21	\$1.16	\$1.13	\$1.12	\$1.08

Figure 166. Cost breakdown for wiring

7.2.7.4 Fasteners for Wiring & Piping

A detailed DFMA™ analysis was not conducted for these components since the level of detailed required is well outside the bounds of this project. However, these components are necessary and, in aggregate, are of appreciable cost. Cost is estimated at 20% of the wiring and piping cost.

7.2.8 System Assembly

A detailed analysis of system assembly was not conducted since that would require detailed specification of all assembly steps including identification of all screws, clips, brackets, and a definition of specific component placement within the system. Such an analysis is beyond the scope of this project. Instead, an estimate of system assembly time is obtained by breaking the system down into five categories of assembly components (major, minor, piping, hoses, wiring), estimating the number of components within each category, and then postulating a time to assemble each of those components. Specific assumptions and total estimated assembly time for manual assembly are shown in Figure 167.

	Number of Components	Component Placement Time (seconds)	Component Fixation Time (seconds)	Component Totals (minutes)
Major Components (Stack, motors, pumps, vessels, etc.)	19	45	60	33.3
Minor Components (instruments, devices, etc.)	22	30	45	27.5
Piping				
# of pipe segments		5		
bends per segment		2		
time per bend		0		
pipe placement time		30		
# welds per pipe		2		
weld time		90		
# threaded ends per pipe		0		
threading time		0		
				17.5
Hoses	21	30	105	47.3
Wiring (manual)	23	41.8	66.7	41.6
System Basic Functionality Test				10.0
Total System Assembly Time				177.1

Figure 167. Single-station system assembly assumptions

Two types of system assembly methods are examined: single-station and assembly line. In single-station assembly approach, a single workstation is used to conduct assembly of the entire fuel cell power plant. Very little custom machinery is needed to assemble the system and components and subsystems are arrayed around the workstation for easy access. For 1,000 systems per year, only one such workstation is required. Assembly process parameters are listed in Figure 168.

Annual Production Rate	1,000	10,000	30,000	80,000	100,000	500,000
Assembly Method	Assembly Line					
Index Time (min)	104.55	83.64	83.64	83.64	83.64	83.64
Capital Cost (\$/line)	\$50,000	\$100,000	\$100,000	\$100,000	\$100,000	\$100,000
Simultaneous Lines	1	1	2	5	6	27
Laborers per Line	10	10	10	10	10	10
Line Utilization	6.7%	53.2%	79.8%	85.1%	88.7%	98.5%
Effective Total Machine Rate (\$/hr)	\$664.70	\$578.12	\$568.50	\$567.30	\$566.58	\$564.85
Cost per Stack (\$)	\$148.54	\$103.36	\$101.64	\$101.42	\$101.29	\$100.98

Figure 168. System assembly process parameters

The assembly for all other annual production rates uses a ten-workstation assembly line configuration. Each fuel cell system flows through the assembly line sequentially. The line reduces the total cumulative time required for system assembly because workers at each workstation on the line have their tools and components closer at hand than they do under the single workstation approach, and because tool changes are minimized due to the higher repetitive nature of an assembly line. This method is approximately 20% faster than the single-workstation approach, with an assembly line index time⁸² of only 14.2 minutes. The system assembly cost is detailed in Figure 169.

Annual Production Rate	1,000	10,000	30,000	80,000	100,000	500,000
System Assembly & Testing (\$/System)	\$148.54	\$103.36	\$101.64	\$101.42	\$101.29	\$100.98
Total Cost (\$/system)	\$148.54	\$103.36	\$101.64	\$101.42	\$101.29	\$100.98
Total Cost (\$/kWnet)	\$1.86	\$1.29	\$1.27	\$1.27	\$1.27	\$1.26

Figure 169. Cost breakdown for system assembly & testing

7.2.9 System Testing

A ten-minute system functionality and performance test is included in the system assembly process. Each stack has separately undergone multiple hours of testing as part of stack conditioning and thus there is high confidence in the stack performance. System testing is only needed to ensure that the peripheral systems are functioning properly and adequately supporting the stack. Typically, the only testing of gasoline engines contained within automobiles is a simple engine startup as the vehicles are driven off the assembly line. Corresponding, the fuel cell “engines” are only minimally tested for functionality. Cost for this system testing is reported under system assembly.

7.2.10 Cost Contingency

It is common practice in the automotive industry to include a 10% cost contingency to cover the cost of procedures or materials not already explicitly included in the analysis. This serves as a guard against an underestimation of cost which can derail a cost estimator’s career within the automotive industry. However, no such cost contingency has been included in this cost analysis upon the request of the DOE.

⁸² Assembly line index time is defined as the time interval each system spends at a given workstation.

8 Bus Fuel Cell Power System

In addition to the annual cost updated of the automotive fuel cell power system, a 40' transit bus fuel cell power system is analyzed for the 2013 cost report. The bus fuel cell system was cost analyzed for the first time in 2012, thus the 2013 analysis represents an annual update to last year's bus study.

Primary differences between the 2012 bus and the 2013 bus include:

- all of the above listed changes between the 2012 and 2013 auto technology systems,
- widespread use of a lower tier vendor ("job-shop") to produce stack components thereby lowering component cost through better utilization of manufacturing equipment (as opposed to in-house production of parts as assumed in the 2012 bus analysis), and
- assumption of a non-vertically integrated business structure to better match expected bus market practices.

The 2013 automotive and bus power plants are very similar in operation but possess key differences in:

- power level, operating pressure, and catalyst loading,
- manufacturing rate, and
- level of vertical integration.

Section 8.1 below details the key differences between auto and bus power systems. If no difference is documented in this section, then details of material selection, manufacturing processes, and system design are assumed not to differ from that of the automotive system.

8.1 Bus Power System Overview and Comparison with Automotive Power System

Figure 170 below is a basic comparison summary of the 2013 auto and bus systems. As shown, most stack mechanical construction and system design features are identical between the bus and automotive power plants. Primary system differences include:

- Use of two $\sim 90\text{kW}_{\text{gross}}$ fuel cell stacks to achieve a net system power of $160\text{kW}_{\text{net}}$ (instead of one $\sim 90\text{kW}_{\text{net}}$ stack for an 80kW_{net} power level as used in the automotive system)
- Higher cell platinum loading ($0.4\text{mgPt}/\text{cm}^2$ instead of $0.153\text{ mgPt}/\text{cm}^2$ as used in the automotive system)
- Differences in cell active area and number of active cells per stack
- Higher system voltage (reflecting two stacks electrically in series and the desire to keep current below 400 amps)
- Operation at 1.8 atm (instead of 2.5 atm as used in the automotive system)
- Use of a multi-lobe air compressor (based on an Eaton-style design) without an exhaust gas expander (instead of a centrifugal-compressor/radial-inflow-expander based on a Honeywell-style design as used in the automotive system)
- Reduced stack operating temperature (74°C instead of 92°C as used in the auto system)
- Increased size of balance of plant components to reflect higher system gross power

	2013 Auto Technology System	2013 Bus Technology System
Power Density (mW/cm ²)	692	601
Total Pt loading (mgPt/cm ²)	0.153	0.4
Net Power (kW _{net})	80	160
Gross Power (kW _{gross})	89.4	186.2
Cell Voltage (V)	0.695	0.676
Operating Pressure (atm)	2.5	1.8
Stack Temp. (Coolant Exit Temp) (°C)	92.3	74
Q/ΔT (kW/°C)	1.45	4.65
Active Cells	359	739
Membrane Material	Nafion on 25-micron ePTFE	Nafion on 25-micron ePTFE
Radiator/ Cooling System	Aluminum Radiator, Water/Glycol Coolant, DI Filter, Air Precooler	Aluminum Radiator, Water/Glycol Coolant, DI Filter, Air Precooler
Bipolar Plates	Stamped SS 316L with TreadStone Coating	Stamped SS 316L with TreadStone Litecell™ Coating
Air Compression	Centrifugal Compressor, Radial-Inflow Expander	Eaton-Style Multi-Lobe Compressor, Without Expander
Gas Diffusion Layers	Carbon Paper Macroporous Layer with Microporous Layer (Ballard Cost)	Carbon Paper Macroporous Layer with Microporous Layer (Ballard Cost)
Catalyst Application	3M Nanostructured Thin Film (NSTF™)	3M Nanostructured Thin Film (NSTF™)
Air Humidification	Plate Frame Membrane Humidifier	Plate Frame Membrane Humidifier
Hydrogen Humidification	None	None
Exhaust Water Recovery	None	None
MEA Containment	Screen Printed Seal on MEA Subgaskets, GDL crimped to CCM	Screen Printed Seal on MEA Subgaskets, GDL crimped to CCM
Coolant & End Gaskets	Laser Welded(Cooling)/ Screen-Printed Adhesive Resin (End)	Laser Welded (Cooling), Screen-Printed Adhesive Resin (End)
Freeze Protection	Drain Water at Shutdown	Drain Water at Shutdown
Hydrogen Sensors	2 for FC System 1 for Passenger Cabin (not in cost estimate) 1 for Fuel System (not in cost estimate)	2 for FC System 1 for Passenger Cabin (not in cost estimate) 1 for Fuel System (not in cost estimate)
End Plates/ Compression System	Composite Molded End Plates with Compression Bands	Composite Molded End Plates with Compression Bands
Stack Conditioning (hours)	5	5

Figure 170: Comparison table between 2013 auto and 2013 bus technology systems

8.2 Bus System Performance Parameters

The bus and automotive power systems function in nearly identical fashion but have different power levels, flow rates, and pressure levels. The following sections describe the sizing methodology and values for key parameters of the bus power system.

8.2.1 Power Level

To provide sufficient power, two 80 kW_{net} stacks are used, for a total net electrical power of 160 kW. This power level was chosen as an intermediate point in existing bus FC power systems, which nominally range from 140 kW_{net} to 190 kW_{net} electrical. Modeling a system which is an even multiple of 80 kW has the additional advantage of allowing a comparison between a dedicated bus system and a pair of automotive systems.

8.2.2 Polarization Performance Basis

Stack performance within the bus system is based on Argonne National Laboratory modeling of 3M nanostructured thin film catalyst membrane electrode assembly (MEA) performance. The polarization

curve model used for the bus stacks is the same as used for the automotive system with modification for different operating conditions and catalyst loading (as discussed below). As understood by the authors, the two main bus fuel cell power plant suppliers, Ballard Power Systems and UTC Power, use the same stack construction and MEA composition within their bus power system stacks as they do for their light-duty vehicle stacks. Consequently, the same is assumed for this report with the exception of catalyst loading.

Beginning-of-life (BOL) stack design conditions at peak power selected for the 2013 bus power system are shown in Figure 171 compared to the 2012 analysis values.

	2012 Bus Analysis	2013 Bus Analysis
Cell Voltage	0.676 volts/cell	0.676 volts/cell
Current Density	1,060 mA/cm ²	889 mA/cm ²
Power Density	716 mW/cm ²	601 mW/cm ²
Stack Pressure	1.8 atm	1.8 atm
Stack Temperature (outlet coolant temperature)	74°C	74°C
Air Stoichiometry	1.5	2.1
Total Catalyst Loading	0.4 mgPt/cm ²	0.4 mgPt/cm ²

Figure 171: Bus fuel cell power system stack operating parameters

Past discussions with Ballard⁸³ regarding their latest generation⁸⁴ (HD7) fuel cell stacks suggests an anticipated bus application design peak power operating point of ~0.69 volts/cell at ~1,100 mA/cm² yielding a power density of 759mW/cm² at a stack pressure of 1.8 atm and a ~0.4mgPt/cm² total catalyst loading. This operating point is significantly higher than the selected 2013 bus design point and is primarily a consequence of the 2013 polarization curve.

As seen in Figure 172, the selected power density is noted to be modestly lower than the design point chosen for the automotive systems (692 vs. 601mW/cm²) and consequently results in a correspondingly larger bus fuel cell stack.

⁸³ Personal communication, Peter Bach, Ballard Power Systems, October 2012.

⁸⁴ Ballard FCvelocity[®] HD6 stacks are currently used in Ballard bus fleets. The HD7 stack is the next generation stack, has been extensively tested at Ballard, and is expected to be used in both automotive and bus vehicle power systems next year.

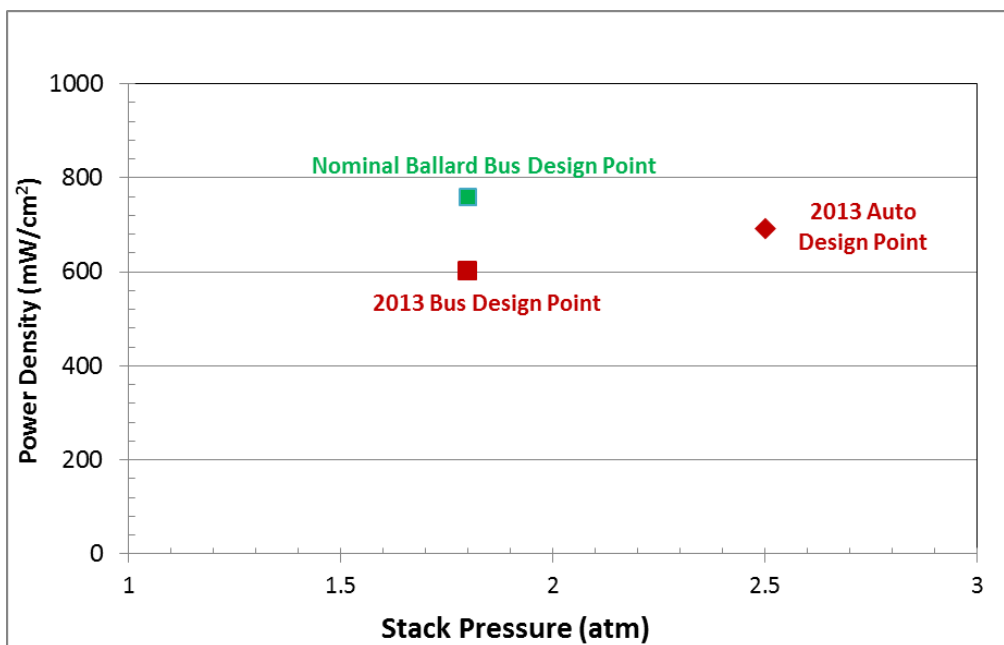


Figure 172: 2013 Bus peak power design point: Based on 2013 ANL Modeling data, 0.4mgPt/cm² total catalyst loading, 2.1 air stoic, 0.676v/cell

8.2.3 Catalyst Loading

Catalyst loading is a key driver of system cost and significant effort on the part of fuel cell suppliers has gone towards its reduction. In general, bus applications are less cost-sensitive and have longer lifetime requirements than automotive systems. Consequently, bus fuel cell stacks are more likely to have high catalyst loading since there is a general correlation between platinum loading and stack durability⁸⁵. Examination of the 3M NSTF cell performance as represented by ANL modeling results and through discussion with 3M researchers reveals that increases in catalyst cathode loading past ~0.2mgPt/cm² result in declining polarization performance due to a catalyst crowding⁸⁶ effect. It is expected that alterations of the length or thickness of the fibrous substrate used within the NSTF system would allow higher catalyst loading without performance decline. Consequently, for the bus application, we model MEA performance as if it corresponds to the 0.20mgPt/cm² loading but attribute a loading of 0.4mgPt/cm² for cost computation. This is meant to represent the performance of a bus application NSTF system that has the thin film catalyst layer optimized for both high polarization performance and higher catalyst loading (for durability). This level of catalyst loading is also approximately consistent with the levels used in Ballard fuel cell stacks.

⁸⁵ Many factors affect stack lifetime and degradation rate. But to the extent that degradation is caused by platinum catalyst poisoning, reduction in surface area, and/or reduced utilization, high catalyst loading tends to correlate with longer lifetime.

⁸⁶ The term “catalyst crowding” is meant to represent the situation where the catalyst layer on the substrate whiskers of the NSTF catalyst layer becomes so thick that it blocks gas flow or otherwise adversely affects performance.

8.2.4 Operating Pressure

As previously stated, the two main fuel cell bus power plant developers are Ballard Power Systems and UTC Power/US Hybrid⁸⁷. Recent Ballard buses, using their FCvelocity[®] HD6 fuel cell stacks, typically operating at a stack pressure of ~1.8 atm (at rated power) and do not employ an exhaust gas expander. Recent UTC Power fuel cell bus power plants, using their porous carbon bipolar plates, typically operate near ambient pressure. The UTC Power porous carbon plates allow water management within the cell (both humidification and product water removal) and are a key element of their ability to achieve high polarization performance at low pressure. The porous carbon bipolar plate construction has not been cost-modeled under this effort and it would be inappropriate to postulate the combination of stamped metal bipolar plate construction with performance of NSTF catalyst MEA at near ambient pressure⁸⁸. Consequently, ambient pressure operation is not selected for bus application cost modeling at this time, although it could be considered in future analysis tasks.

A stack pressure of 1.8 atm is selected as the bus system baseline operating stack pressure at rated power to reflect the typical operating conditions used by Ballard. An exhaust gas expander is not used as there is a limited power available from the expansion of gas at this moderate pressure. This operating point of 1.8 atm without expander is in contrast to the optimized automotive system operating conditions of 2.5 atm with expander. A system level cost optimization (i.e. varying stack operating conditions to determine the combination of parameters leading to lowest system cost) was not conducted as polarization performance is not available at the higher catalyst loadings expected to be employed to ensure durability.

8.2.5 Stack Operating Temperature

In the 2012 bus analysis, design stack temperature⁸⁹ at rated (peak) power was determined by an ANL correlation with stack operating pressure and was set at 74°C to be consistent with 1.8 atm. This was a significant reduction from the 87°C temperature of the 2012 automotive system at 2.5 atm. For the 2013 analysis, ANL has added temperature as an independent variable in their polarization model, thereby potentially allowing an optimization of operating temperature for lowest system cost. However, for a variety of non-polarization curve related reasons (as discussed below), bus fuel cell systems tend to operate at cooler temperatures. Thus rather than estimating stack performance on an optimal (high) temperature as determined by polarization data, it is more realistic to base performance on the temperature most likely to be experienced with the bus stacks. For this reason, a broader system level cost optimization is not conducted and the 74°C stack temperature is retained for the 2013 analysis. Future analysis is planned to more fully explore the impact of bus stack temperature on performance and cost.

⁸⁷ In January 2014, UTC announced the execution of a global technology and patent licensing agreement with US Hybrid Corporation for the commercialization of UTC's Proton Exchange Membrane (PEM) fuel cell technologies for the medium and heavy duty commercial vehicle sectors.

⁸⁸ This combination is theoretically possible but experimental data is not readily available nor, to the author's knowledge, have NSTF catalyst MEA parameters been optimized for ambient pressure operation.

⁸⁹ For modeling purposes, stack operating temperature is defined as the stack exit coolant temperature. Modeling suggests approximately a 10°C temperature difference between coolant inlet and outlet temperatures and the cathode exhaust temperature to be approximately 5°C higher than coolant exit temperature.

It is noted that Ballard reports their fuel cell bus stack temperatures at only 60°C. The reasons for this are several-fold. First, the system may not typically operate at rated power for long enough times for stack temperature to rise to its nominal value. This is particularly true for a bus power plant for which, depending on the bus route, maximum power may be demanded only a low fraction of the time. Second, various stack and membrane failure mode mechanisms are associated with high temperature. Thus it may be desirable to deliberately limit stack peak temperature as a means to achieving the stack lifetime goal of >12,000 hours (this is less of a concern for auto applications with lower lifetime requirements). Thirdly, higher stack temperature reduces the size of the heat rejection temperature since it increases the temperature difference with the ambient air. For an automobile, volume and frontal area are at a premium under the hood. Minimizing the size of the radiator is important for the auto application but is less important for the bus application where radiators may be placed on the roof. Thus, there are several good reasons—and fewer disadvantages—in selecting a low operating temperature for the bus compared to the auto application.

8.2.6 Q/ΔT Radiator Constraint

A Q/ΔT radiator constraint of <1.45 kW/°C was applied to the automotive system for the first time in 2013. However, such a radiator constraint is not applied to the bus fuel cell system because 1) buses are larger vehicles and have generally larger frontal areas to accommodate radiators, and 2) an appropriate numerical Q/ΔT constraint is not obvious⁹⁰. Additional analysis to determine the appropriate Q/ΔT constraint is needed before it can be imposed.

8.2.7 Cell Active Area and System Voltage

Because the system consists of two stacks electrically in series, system voltage has been set to 500V at design conditions⁹¹. This bus voltage represents a doubling relative to the automotive system and is necessary to maintain the total electrical current below 400 amps. These values are broadly consistent with the Ballard fuel cell bus voltage range⁹² of 465 to 730V. Specific cell and system parameters are detailed in Figure 173 for beginning-of-life (BOL) conditions.

Parameter	Value
Cell Voltage (BOL at rated power)	0.676 V/cell
System Voltage (BOL at rated power)	500 V
Number of Stacks	2
Active Cells per Stack	370
Total Cells per System	740
Active Area per Cell	419 cm ²
Stack Gross Power at Rated Power Conditions (BOL)	186 kW

Figure 173: Bus stack parameters

⁹⁰ The automotive Q/ΔT constraint of <=1.45 kW/°C was set by DOE per suggestion of the Fuel Cell Technical Team (FCTT). Neither the DOE nor the FCTT has set a comparable constraint for the bus application.

⁹¹ For purposed of the system cost analysis, design conditions correlate to rated maximum power at beginning of life.

⁹² Ballard FCvelocity®-HD6 Spec Sheet. <http://www.ballard.com/fuel-cell-products/fc-velocity-hd6.aspx> Accessed 9 October 2012.

8.3 Eaton-style Multi-Lobe Air Compressor-Motor (CM) Unit

8.3.1 Design and Operational Overview

An Eaton-style twin vortex, Roots-type air compressor such as that currently used in Ballard fuel cell buses is used for the 2013 bus cost analysis. A complete DFMATM analysis of the Eaton-style air compressor has been conducted and the bus air compressor unit (including motor and motor controller) is estimated at \$4,760 at 1,000 units per year. As discussed in Section 6.7, the baseline compressor is SA's interpretation of a unit using Eaton technology and is modeled on Eaton's R340 supercharger (part of Eaton's Twin Vortices Series (TVS)) and Eaton's DOE program⁹³.

Parameter	Value
Compressor Type	Roots (twin vortices)
Compression Ratio at Design Point	1.96
Air Flow Rate at Design Point	732 kg/hour (203 g/s)
Compression Efficiency ⁹⁴ at Design Point	71%
Expander Type	Not used
Combined Motor and Motor Controller Efficiency ⁹⁵	80%

Figure 174: Details of the baseline bus air compressor. Section 6.10 contains details on compressor and motor efficiency assumptions.

8.3.2 Compressor Manufacturing Process

The compressor/motor unit modeled as part of the bus DFMATM analysis consists of several components including the motor, motor controller, compressor rotors, drive shafts, couplings, bearings, housing, and other components. A schematic of the SA conceptual design used for the cost analysis (derived from Eaton R340 supercharger design) is shown in Figure 175. The motor shaft is attached to a torsional coupling that fits onto one of the compressor drive shafts with multiple dowels for alignment. Two timing gears drive the second compressor shaft at the same rotation speed as the electric motor. Each shaft has a key slot where the rotor slides on and attaches. Each rotor-shaft assembly has both ball bearings and needle bearings that hold it in place against a bearing plate and the compressor housing. Shaft seals are required so as to isolate any oil within the gear housing and to maintain pressure within the compressor. A complete list of the compressor/motor unit components is shown in Figure 176 along with selected material, type of manufacturing process used in the analysis, dimensions, quantity, and mass.

The compressor/motor system efficiency is based on the DOE 2012 MYRD&D plan target values: 71% for compressor and a combined 80% for the motor and motor controller (based on an individual efficiency of 89.5% for each the motor and motor controller). Within the DFMATM model, compressor/motor system parameters are adjusted to match requirements from the fuel cell system. Thus as stack efficiency and gross power change, the compressor/motor system is resized to the altered air flow

⁹³ Eaton/DOE Contract Number DE-EE0005665.

⁹⁴ Compression efficiency is defined as isentropic efficiency.

⁹⁵ Combined efficiency is defined as the product of motor efficiency and motor controller efficiency.

requirement, dimensions (rotors, compressor wheel, motor size), and power level (of motor and controller). Compressor/motor system cost is correspondingly updated.

Cost of the compressor/motor system components were estimated by use of Boothroyd Dewhurst Inc. (BDI) software (housings), vendor cost quotes (electric motor and most small purchased items such as bearings, seals, nuts, etc.), or by DFMA™ analysis (compressor rotors and timing drive gears).

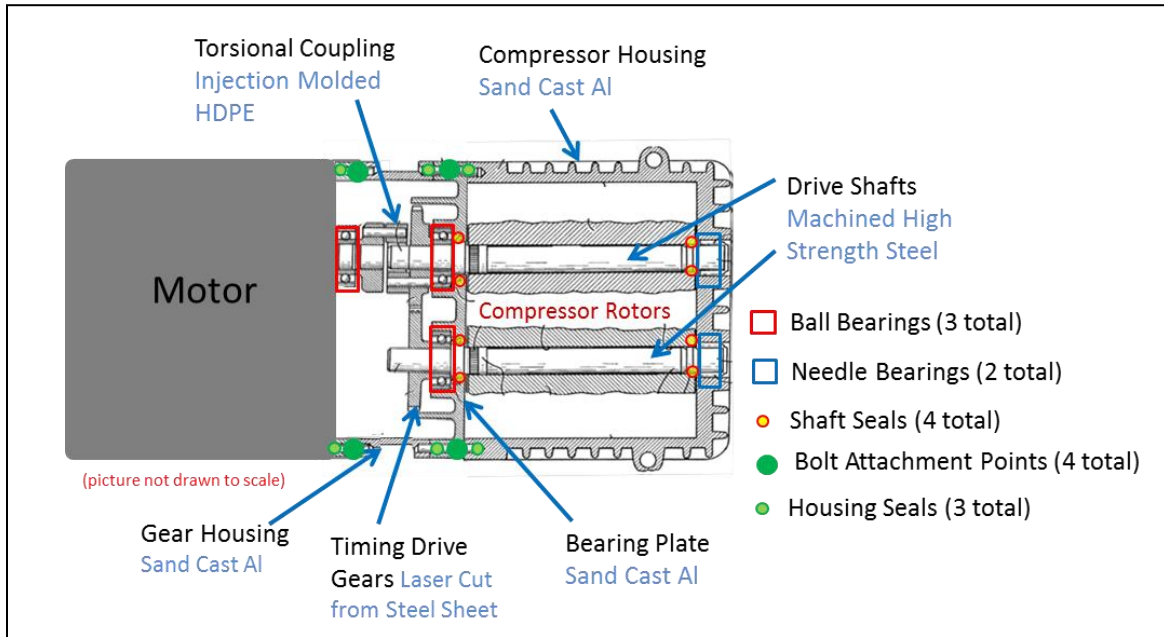


Figure 175. Schematic of cross-section of compressor/motor unit used in the DFMA™ cost analysis (Source: Drawing derivation from US patent 4,828,467: Richard J. Brown, Marshall, Mich. “Supercharger and Rotor and Shaft Arrangement Therefor”, Eaton Corporation, Cleveland, Ohio, May 9, 1989)

The compressor rotors were modeled as hot extrusions of aluminum 6061-T1. Aluminum billets are assumed to be fed to an aluminum extrusion machine, such as that shown in Figure 177, using a custom stainless steel die to add twist to the extruded rotor billet. Extrusion rates are estimated at approximately 3 cm/sec⁹⁶ plus 30 seconds setup time (total 0.62min/rotor). At this extrusion rate and for only 1,000 systems per year, the machinery is highly underutilized. Consequently, the rotors are assumed to be fabricated by a vendor who can pool orders to more highly utilize his machinery and thereby lower fabrication cost. A 30% markup is added to the projected vendor costs to reflect his G&A, scrap, R&D, and profit and thereby translate the vendor cost into a sales price to the compressor manufacturer/assembler. Cost for extra precision machinery and quality control using a conjugate pair measuring machine⁹⁷ is included in the cost.

⁹⁶ Khalifa, N. B., Tekkaya, A.E., “Newest Developments on the Manufacture of Helical Profiles by Hot Extrusion”, Journal of Manufacturing Science and Engineering, ASME, December 2011, Vol 133, 061010-1 to 8.

⁹⁷ “Inspection of Screw Compressor Rotors for the Prediction of Performance, Reliability, and Noise” International Compressor Engineering Conference at Purdue University, School of Mechanical Engineering, July 12-15,2004. <http://docs.lib.purdue.edu/cgi/viewcontent.cgi?article=2691&context=icec>

Summary of Components for SA Compressor/Motor Unit for Bus (Based on Eaton Design)							Annual Production Rate (systems/year)		
							200	1,000	
	Material	Manufacturing Method	Qty/sys	Dimensions	kg/part	kg/sys	\$/system		
Compressor Components									
Compressor Rotor	6061-T1 Aluminum	Extrusion w/twist	2	21cm x 9cm Max OD	4.96	9.92	\$135.54	\$131.66	
Compressor Housing	6061 Aluminum	Sand Casting	1	26cm x 17cm x 22cm x 1cm (aver. Thickness)	2.33	2.33	\$96.31	\$53.41	
Compressor Bearing Plate	6061-T1 Aluminum	Sand casting	1	17cm (width) x 22cm (height) x 1cm (aver. Thickness)	0.43	0.43	\$51.10	\$17.30	
Compressor Shaft Seals	O-ring seal, polymer	Purchased	4	1.9cm (ID), 5cm (OD)	0.005	0.02	\$11.17	\$10.92	
Timing Drive Gears (compressor: steel)	Stainless Steel	Laser cut from sheet	2	6cm max OD, 1cm thick	0.447	0.894	\$34.18	\$33.43	
Total						13.59	\$328.30	\$246.72	
Other Components									
Housing/Motor Seals	O-ring seal, PET	Injection molded	3	17cm x 22cm x 0.2cm (diameter round X-section)	0.07	0.21	\$93.51	\$20.38	
Housing Screws	SS 316	Purchased	4		0.005	0.02	\$2.23	\$2.18	
Front Bearing	steel ball bearings, self lubricated	Purchased	3	5cm (diameter), 1.9cm (ID)	0.322	0.966	\$9.05	\$8.85	
Rear Bearing	steel needle bearings, self lubricated	Purchased	2	5cm (diameter), 1.9cm (ID)	0.322	0.644	\$8.71	\$8.52	
Rotor Drive Shafts	High carbon Steel Alloy	Rod, machined	2	1.9cm (diameter) x 23cm (length)	0.769	1.538	\$20.24	\$18.99	
Torsionally Flexed Coupling	Fiberglass filled HDPE	Injection molded	1	3cm max OD, 1cm thick	0.004	0.004	\$37.02	\$9.24	
Coupling Dowels	Steel	Rod, machined	3	0.25cm diameter, 3cm length	0.001	0.003	\$1.73	\$1.70	
Gear Housing/motor end plates	6061-T1 Aluminum	Sand casting	1	17cm x 22cm x (height) x 7cm (length) x 1cm (aver. Thickness)	1.08	1.08	\$59.09	\$24.10	
Contingency (5% of total cost to account of any missing parts or errors in cost assumptions)								\$292.22	\$226.18
Assembly								\$11.55	\$11.16
Total						4.47	\$535.36	\$331.30	
Motor Components									
Motor		Purchased	1		est 30	est 30	\$3,295.02	\$2,373.74	
Motor Shaft Seal	formed seal	Purchased	1		0.01	0.01	\$3.49	\$3.41	
Total						30.01	\$3,298.51	\$2,377.16	
Motor Controller Components									
Controller		Purchased	1		2.00	2.00	\$1,986.06	\$1,805.76	
Total						2.00	\$1,986.06	\$1,805.76	
Total Cost for 160kW Bus Fuel Cell System (including assembly and markup*)							> 51	\$6,148.22	\$4,760.94

*Each cost per system includes either a manufacturer markup (25% @ 1ksys/yr and 29% at 200sys/yr) or a pass-through markup (18%@1ksys/yr and 20%@200 sys/yr)

Figure 176. List of components for compressor, motor, and motor controller unit for the bus DFMA™ analysis.

The timing drive gears are laser cut from a stainless steel sheet 1cm thick. The assumed laser cutting speed is approximately 0.6 cm per second (generously slower to account for intricate details in the driving gear geometry). The drive shafts for the compressor are made of a high carbon steel material and machined with a precision surface finish.



Figure 177. Medium hot extrusion press (HEP-112/72)⁹⁸

The motor used in the analysis is considered to be a purchased component. Estimates obtained by Eaton through their DOE program suggest the cost of the motor for an automotive system to be ~\$340 at 10,000 systems per year, \$190 at 200,000 systems per year, and \$160 at 500,000 systems per year. Cost of the compressor/motor drive motor for the bus system was scaled with air compressor motor power and adjusted for lower manufacturing rates. The projected cost for the motor is shown in Figure 178 and is the most expensive component in the system other than the motor controller. The motor controller is about half the cost of the compressor/motor bus unit. The DFMATM analysis of the motor controller was completed in the previous 2012 bus analysis and re-used for the 2013 analysis, after scaling for controller input power. The motor controller was also adjusted for lower manufacturing rates. Motor controller costs can also be viewed in Figure 178.

⁹⁸ Image from <http://www.hydronline.com/machines/hep-medium.htm>

2013 Bus Compressor/Motor System Cost						
Annual Production Rate	systems/year	200	400	800	1,000	
Compressor/Motor Components						
Compressor Rotor	\$/sys	\$135.54	\$133.10	\$131.84	\$131.66	
Compressor Housing	\$/sys	\$96.31	\$69.57	\$56.13	\$53.41	
Compressor Bearing Plate	\$/sys	\$51.10	\$29.60	\$19.35	\$17.30	
Compressor Shaft Seals	\$/sys	\$11.17	\$11.06	\$10.96	\$10.92	
Compressor Timing Drive Gears	\$/sys	\$34.18	\$33.86	\$33.54	\$33.43	
Housing/Motor Seals	\$/sys	\$93.51	\$47.66	\$24.19	\$20.38	
Housing Screws	\$/sys	\$2.23	\$2.21	\$2.19	\$2.18	
Front Bearing	\$/sys	\$9.05	\$8.96	\$8.87	\$8.85	
Rear Bearing	\$/sys	\$8.71	\$8.63	\$8.55	\$8.52	
Rotor Drive Shaft	\$/sys	\$20.24	\$19.53	\$19.09	\$18.99	
Torsionally Flexed Coupling	\$/sys	\$37.02	\$19.62	\$10.97	\$9.24	
Coupling Dowels	\$/sys	\$1.73	\$1.72	\$1.70	\$1.70	
Gear Housing/Motor End Plates	\$/sys	\$59.09	\$38.06	\$26.41	\$24.10	
Contingency (5% of total)	\$/sys	\$292.22	\$259.78	\$233.59	\$226.18	
Assembly	\$/sys	\$11.55	\$11.38	\$11.21	\$11.16	
Motor	\$/sys	\$3,295.02	\$2,861.18	\$2,484.24	\$2,373.74	
Motor Shaft Seals	\$/sys	\$3.49	\$3.46	\$3.42	\$3.41	
Controller	\$/sys	\$1,986.06	\$1,907.46	\$1,830.30	\$1,805.76	
Total Eaton CEM Cost With Markup	\$/sys	\$6,148.22	\$5,466.83	\$4,916.55	\$4,760.94	
Total CEM Cost (Net)	\$/kWnet	\$38.43	\$34.17	\$30.73	\$29.76	
Total CEM Cost (Gross)	\$/kWgross	\$33.02	\$29.36	\$26.40	\$25.57	

Figure 178. Cost breakdown for bus compressor/motor unit

Figure 179 compares the cost of the 2012 bus analysis compressor system (based on a Honeywell-style centrifugal compressor system) with that of the 2013 bus analysis Eaton-style compressor system. The Eaton-style system is observed to be appreciably more expensive, owing primarily to an increased motor cost. While real differences in type of motor exist (Honeywell uses a high rpm permanent magnet motor whereas Eaton uses a much lower rpm permanent magnet motor), the motor cost difference may be significantly influenced by differences in costing methodology between the two estimates: quote based vs. DFMA™ analysis. The Eaton-style motor cost was based on quotations for automotive size motors at high manufacturing rates (10,000 to 500,000 sys/yr), with a curve fit extrapolation used to predict cost of the automotive size motors at lower manufacturing rates (200-1,000 sys/yr). This projected cost was then scaled with power to reflect the cost of a bus size unit. In contrast, the Honeywell-style motor cost was based on a detailed DFMA™ analysis. The same markup percentages were applied to both the Honeywell and Eaton-style compressor systems for the bus so as to allow a fair comparison. However, the authors feel that the resulting motor cost may not accurately represent a motor used in the Eaton type compressor/motor system and plan to investigate further in next year's analysis by applying a DFMA™ analysis. Additionally, motor controller cost was held constant for the two systems, which may not be a valid assumption given the disparate compressor speeds (165,000 rpm for the Honeywell-style unit vs. 24,000 rpm for the Eaton-style unit).

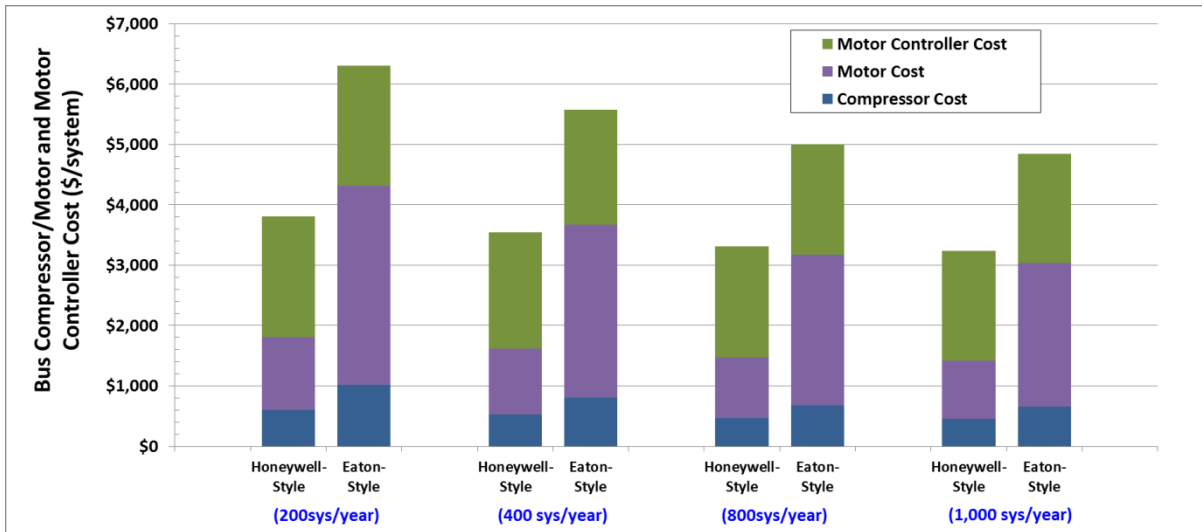


Figure 179. Comparison of cost for Honeywell-style design and the Eaton-style Compressor/Motor for a bus

8.4 Bus System Balance of Plant Components

To accommodate the increased flows and power level of a two-stack 160 kW_{net} system, many balance of plant (BOP) components had to be revised. In some cases, the previous automotive DFMATM-style analysis of the balance of plant component automatically adjusted in response to the system design change. In other cases, new quotes were obtained, part scaling was included, or individual parts were increased in number (e.g. some parts are used on each of the two stacks). The changes to BOP components to reflect a bus system are summarized in Figure 180.

Balance of Plant Item	Bus System Change
CEM & Motor Controller	DFMA TM analysis scaled to new flow and pressure ratio parameters, but switched to design without Expander
Air Mass Flow Sensor	New quote obtained for higher mass flow of bus system
Air Temperature Sensor	No change
Air Filter & Housing	New quote obtained for higher mass flow of bus system
Air Ducting	Piping and tubing diameters increased by a factor of 1.5 to adjust for higher mass flow of bus system
Air Precooler	DFMA TM analysis scaled to new mass flow and temperature parameters.
Demister	Area size scaled by ratio of bus to automotive air flows
Membrane Air Humidifier	DFMA TM analysis scaled to new gas mass flow and temperature parameters
HTL Coolant Reservoir	New quote obtained for larger expected coolant liquid volume of bus system
HTL Coolant Pump	New quote obtained for larger expected coolant flow of bus system
HTL Coolant DI Filter	Size scaled by factor of 2 to correspond to higher expected coolant flow rates of bus system
HTL Thermostat & Valve	New quote obtained for larger flow rate and pipe diameter of bus system

HTL Radiator	DFMA™ analysis scaled to new heat rejection and temperature parameters of bus system
HTL Radiator Fan	New quote obtained corresponding to larger fan diameter and air flow rate parameters of bus system
HTL Coolant piping	Piping and tubing diameters increased by a factor of 1.5 to adjust for higher coolant flow of bus system
LTL Coolant Reservoir	New quote obtained for larger expected coolant liquid volume of bus system
LTL Coolant Pump	New quote obtained for larger expected coolant flow of bus system
LTL Thermostat & Valve	New quote obtained for larger flow rate and pipe diameter of bus system
LTL Radiator	DFMA™ analysis scaled to new heat rejection and temperature parameters of bus system
LTL Radiator Fan	New quote obtained corresponding to larger fan diameter and air flow rate parameters of bus system
LTL Coolant Piping	Piping and tubing diameters increased by a factor of 1.5 to adjust for higher coolant flow of bus system
Inline Filter for Gas Purity Excursions	Size scaled by factor of 2 to correlate to increased hydrogen flow rate of bus system
Flow Diverter Valve	Quantity doubled to reflect use of two stacks in bus system
Over-Pressure Cut-Off Valve	Quantity doubled to reflect use of two stacks in bus system
Hydrogen High-Flow Ejector	Quantity doubled to reflect use of two stacks in bus system
Hydrogen Low-Flow Ejector	Quantity doubled to reflect use of two stacks in bus system
Check Valves	Quantity doubled to reflect use of two stacks in bus system
Hydrogen Purge Valve	Quantity doubled to reflect use of two stacks in bus system
Hydrogen Piping	Piping and tubing diameters increased by a factor of 1.5 to adjust for higher hydrogen flow of bus system
System Controller	Quantity doubled to reflect increased control/sensors data channels in bus system
Current Sensors	Quantity doubled to reflect use of two stacks in bus system
Voltage Sensors	Quantity doubled to reflect use of two stacks in bus system
Hydrogen Sensors	One additional sensor added to passenger cabin to reflect much large volume of cabin in bus system
Belly Pan	Excluded from bus system since a dedicated, enclosed engine compartment is expected to be used
Mounting Frames	Size increased to reflect use of two stacks and larger BOP component in bus system
Wiring	Cost doubled to reflect use of two stacks in bus system
Wiring Fasteners	Cost doubled to reflect use of two stacks in bus system

Figure 180: Explanation of BOP component scaling for bus power plant

9 Capital Equipment Cost

Figure 181 and Figure 182 display the tabulation of manufacturing/assembly processing steps along with the capital cost of each corresponding process train.⁹⁹ Multiple process trains are usually required to achieve very high manufacturing rates. The total capital cost (process train capital cost multiplied by the number of process trains) is also tabulated and shows that bipolar plate coatings is the highest capital cost process of the stack. This tabulation is meant to give an approximate cost of the uninstalled capital required for automotive stack and BOP production at 500,000 vehicles per year. Some steps are not included in the tabulation as they modeled as purchased components and thus their equipment cost is not estimated. Furthermore, the capital equipment estimates do not include installation, buildings, or support infrastructure and thus should not be used as an estimate of total capital needed for power plant fabrication. None the less, some insight may be obtained from this partial tabulation.

Stack Manufacturing Machinery Capital Costs at 500,000 sys/yr			
Step	Capital Cost per Process Train	Number of Process Trains	Total Capital Cost
Bipolar Plate Stamping	\$555,327	56	\$31,098,322
Bipolar Plate Coating	\$3,286,065	23	\$88,497,078
Membrane Production	\$35,000,000	1	\$35,000,000
NSTF Coating	\$2,008,523	17	\$34,144,898
Microporous GDL Creation	Purchased Comp.		Not Incl.
MEA Gasketing-Subgaskets	\$2,848,600	11	\$31,334,600
MEA Cutting and Slitting	\$1,266,839	2	\$2,533,678
MEA Gasketing - Screen Printed Co	\$1,460,784	16	\$23,372,541
Coolant Gaskets (Laser Welding)	\$857,562	35	\$30,014,660
End Gaskets (Screen Printing)	\$393,281	1	\$393,281
End Plates	\$503,991	3	\$1,511,973
Current Collectors	\$168,313	1	\$168,313
Stack Assembly	\$822,481	50	\$41,124,063
Stack Housing	\$656,281	1	\$656,281
Stack Conditioning	\$151,751	145	\$22,003,948
Stack Total			\$341,853,636

* Bipolar plate coating is based on a vendor-proprietary manufacturing method that consists of multiple sub-process trains. The process train quantity listed is an average of the constituent sub-trains.

Figure 181. Automotive stack manufacturing machinery capital costs at 500,000 systems/year

⁹⁹ A process train is a grouping of related manufacturing or assembly equipment, typically connected by the continuous flow of parts on a conveyor belt. For instance, the bipolar plate stamping process train consists of a sheet metal uncoiling unit, a tensioner, a 4-stage progressive stamping die, and a re-coil unit.

Balance of Plant Manufacturing Machinery Capital Costs at 500,000 sys/yr			
Step	Capital Cost per Process Train	Number of Process Trains	Total Capital Cost
Membrane Air Humidifier*	NA	1 -30	\$14,142,205
Belly Pan	656,281	1	\$656,281
Ejectors	<i>[Not Calculated]</i>	<i>N/A</i>	<i>[Not Calculated]</i>
Stack Insulation Housing	656,281	1	\$656,281
Air Precooler	<i>[Not Calculated]</i>	<i>N/A</i>	<i>[Not Calculated]</i>
Demister	288,923	1	\$288,923
CEM	<i>[Not Calculated]</i>	<i>N/A</i>	<i>[Not Calculated]</i>
(Partial) BOP Total	Does not include processes with un-calculated capital costs →		\$15,743,690

* The membrane air humidifier involves a series of processing steps, each with a distinct manufacturing Process Train. Consequently, the capital cost per Process Train and the Number of Process Trains vary in value. Capital cost for the aluminum casting step is not included in the Total Capital Cost tabulation.

Figure 182. Automotive balance of plant manufacturing machinery capital costs at 500,000 systems/year

10 Automotive Simplified Cost Model Function

A simplified cost model to estimate the total automotive power system cost at 500,000 systems/year production rate is shown in Figure 183. The simplified model splits the total system cost into five subcategories (stack cost, thermal management cost, humidification management cost, air management cost, fuel management cost, and balance of plant cost) and generates a scaling equation for each one. The scaling equations for individual cost components are based on key system parameters for that component that are likely to be of interest when studying system scaling. The curves are generated by regression analysis of many runs of the full DFMATM-style cost model over many variations of the chosen parameters. The simplified model allows a quick and convenient method to estimate system cost at off-baseline conditions.

$C_{\text{system}} = \text{Total System Cost} = C_{\text{stack}} + C_{\text{thermal}} + C_{\text{Humid}} + C_{\text{air}} + C_{\text{Fuel}} + C_{\text{BOP}}$	
C_{stack} = Total Fuel Cell Stack Cost	
<p>100 Volt, $C_{\text{stack}} = 3.7072 \times 10^{-5} \times ((0.86990 \times A - 12.52983) \times L \times PC) + (0.00750 \times A) + 177.65518$</p> <p>150 Volt, $C_{\text{stack}} = 3.7072 \times 10^{-5} \times ((0.86990 \times A - 12.52983) \times L \times PC) + (0.00671 \times A) + 278.76710$</p> <p>200 Volt, $C_{\text{stack}} = 3.7072 \times 10^{-5} \times ((0.86990 \times A - 12.52983) \times L \times PC) + (0.00649 \times A) + 325.47798$</p> <p>250 Volt, $C_{\text{stack}} = 3.7072 \times 10^{-5} \times ((0.86990 \times A - 12.52983) \times L \times PC) + (0.00600 \times A) + 427.42573$</p> <p>300 Volt, $C_{\text{stack}} = 3.7072 \times 10^{-5} \times ((0.86990 \times A - 12.52983) \times L \times PC) + (0.00620 \times A) + 444.35624$</p>	
<p>Where: A = Total active area of the stack (cm^2)</p> <p>L = Pt Loading (mg/cm^2)</p> <p>PC = Platinum cost ($\\$/\text{troy ounce}$)</p>	
C_{thermal} = Thermal Management System Cost	
$= [100.25373 \times (Q_{\text{HT}} / \Delta T_{\text{HT}}) + 190.89296]$ $+ [-0.30921 \times (Q_{\text{LT}} / \Delta T_{\text{LT}})^2 + 101.11590 \times (Q_{\text{LT}} / \Delta T_{\text{LT}}) - 4.43526 \times P^2 + 37.62812 \times P - 0.22583 \times P \times (Q_{\text{LT}} / \Delta T_{\text{LT}}) - 30.07729]$	
<p>Where: Q_{HT} = Radiator Duty ($\text{kW}_{\text{thermal}}$) of High Temperature Loop</p> <p>Q_{LT} = Radiator Duty ($\text{kW}_{\text{thermal}}$) of Low Temperature Loop</p> <p>ΔT_{HT} = Difference between coolant outlet temperature from fuel cell stack and ambient temperature ($^{\circ}\text{C}$)</p> <p>ΔT_{LT} = Difference between coolant outlet temperature from air precooler and ambient temperature ($^{\circ}\text{C}$)</p> <p>P = Stack Operating Pressure (atm)</p>	<p>*High Temperature Loop includes: coolant reservoir, coolant pump, coolant DI filter, coolant piping, thermostat & valve, radiator fan, and radiator.</p> <p>*Low Temperature Loop includes: coolant reservoir, coolant pump, coolant piping, thermostat & valve, and radiator.</p>
C_{Humid} = Humidification Management System Cost	
$= (-1.03360 \times A^2 + 48.27165 \times A + 16.58545) + (511.78879 \times (Q / \Delta T) - 1.46242)$	
<p>Where: A = Humidifier Membrane Area (m^2)</p> <p>Q = Heat Duty for Precooler (kW)</p> <p>ΔT = Delta Temp. (compr. exit air minus coolant temperature into air precooler)($^{\circ}\text{C}$)</p>	*Includes Air Precooler and Membrane Humidifier.
C_{air} = Air Management System Cost	
$= 531.63791 + (-5.16404 \times P) + (0.59331 \times P \times MF)$	
<p>Where: P = Air Peak Pressure (atm)</p> <p>MF = Air Mass Flow (kg/hr)</p>	*Includes demister, compressor, expander, motor, motor controller, air mass flow sensor, air/stack inlet manifold, air temperature sensor, air filter and housing, and air ducting.
C_{Fuel} = Fuel Management System Cost	
$= (3801.97 \times P^3 - 2967.73 \times P^2 + 1573.1 \times P - 87.807) + 241.32$	
<p>Where: P = blower power (kW)</p>	*Includes valves, ejectors, hydrogen inlet and outlet of stack manifolds, piping, and recirculation blower.
C_{BOP} = Additional Balance of Plant Cost	
<p>Where: $C_{\text{BOP}} = \\$551.97$</p>	*Includes system controllers, sensors, and miscellaneous components.

Figure 183: Simplified automotive cost model at 500,000 systems per year production rate

Because the simplified cost model equations are based upon regression analysis, there is an input parameter range outside of which the resulting cost estimates are not guaranteed to be accurate. The ranges for each parameter in each sub-equation are given in Figure 184 below.

Validity Range for Stack Cost			
Parameter	Min Value	Max Value	Units
System Power	60	120	kW _{net}
L	0.1	0.8	mg/cm ²
A	97,830	192,352	cm ²
PC	800	2,000	\$/troy ounce
Validity Range for Thermal Management System			
Parameter	Min Value	Max Value	Units
ΔT_{HT}	38	70	°C
ΔT_{LT}	25	70	°C
Q_{HT}	50	105	kW
Q_{LT}	2	17	kW
P	1.5	3.0	atm
Validity Range for Humidification Management System			
Parameter	Min Value	Max Value	Units
A	0.31	4.16	m ²
Q	6	14	kW
ΔT	29	132	°C
Validity Range for Air Management System			
Parameter	Min Value	Max Value	Units
P	1.65	3.15	atm
MF	180	370	kg/hr

Figure 184: Range of validity for simplified cost model parameters

As a check on the accuracy of the simplified regression model, the results of the full DFMATM model are compared to the calculations from the simplified model for the parameter of system net power. These results are displayed in Figure 185 indicating very good agreement between the two models within the range of validity.

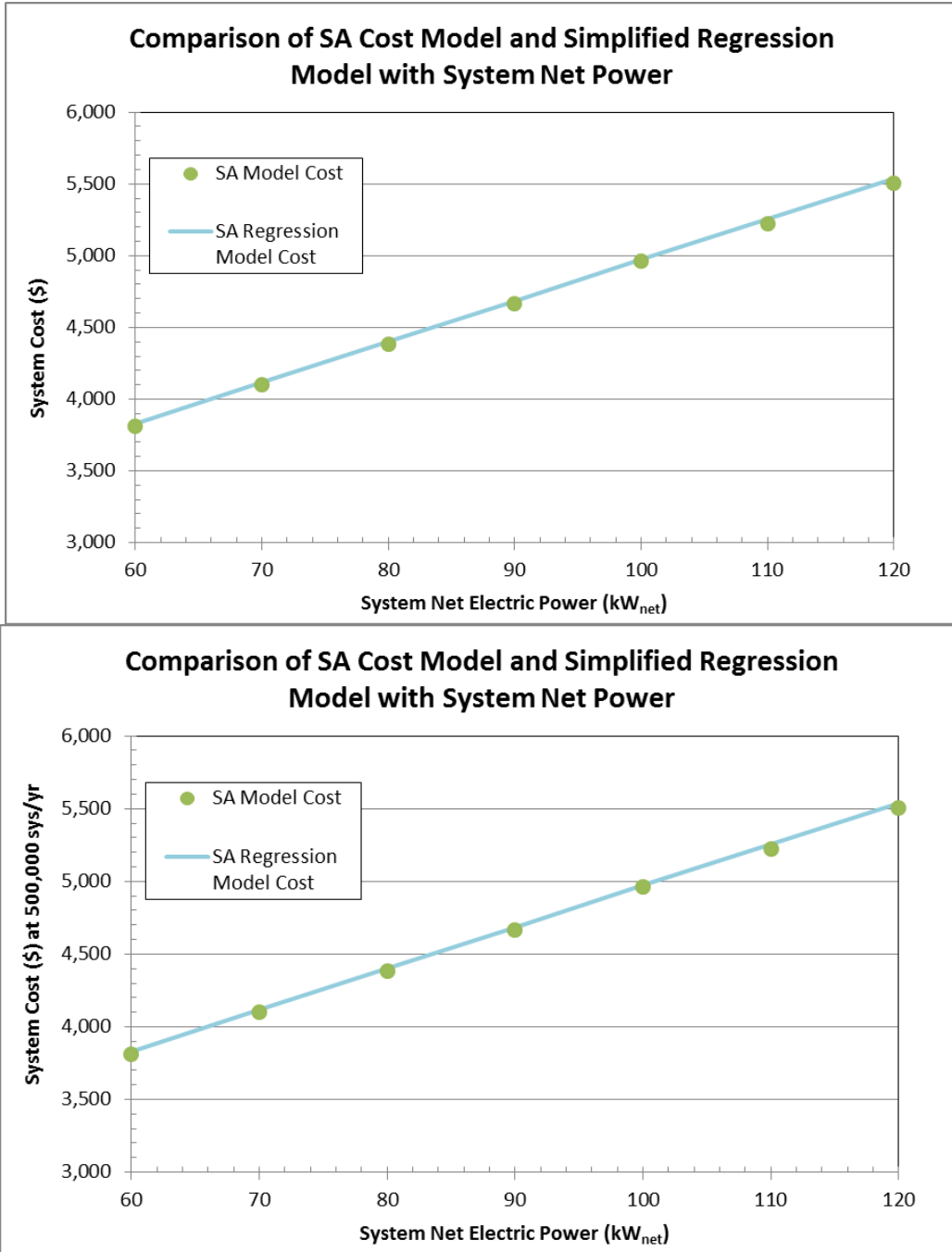


Figure 185: Comparison of SA cost model with simplified cost model at 500,000 systems per year.

11 Lifecycle Cost Analysis

Up-front cost per kW, while a useful metric and the primary focus of this report, is not the sole determining factor in market worthiness of a power system. Total lifecycle cost is an equally important consideration that takes into account the initial purchase price, cost of fuel used over the lifetime of the system, system decommissioning costs and recycle credits, and operating and maintenance expenses, all discounted to the present value using a discounted cash flow methodology. By comparing lifecycle costs, it is possible to determine whether an inexpensive but inefficient system (low initial capital cost but high operating and fuel expenses) or an expensive but efficient system (high initial capital cost but low operating and fuel expenses) is a better financial value to the customer over the entire system lifetime.

The lifecycle analysis for this report assumes a set of driving conditions and platinum recycling costs to compute the total present value cost of ownership for the lifetime of the vehicle. These assumptions are summarized in the figure below.

Lifecycle Cost Assumption	Value
Sales markup	25% of calculated system cost
Discount rate	10%
System lifetime	10 years
Distance driven annually	12,000 miles
System efficiency at rated power	51% (calculated by model)
Fuel economy	66 mpgge ¹⁰⁰
Hydrogen to gasoline lower heating value ratio	1.011 kgH ₂ /gal gasoline
Fuel cost	\$5 / kg H ₂
Total Pt loss during system lifetime and the Pt recovery process	10%
Market Pt price at end of system lifetime	\$1,500 / tr. oz.
Cost of Pt recovery	\$80 / tr. oz.
% of final salvaged Pt value charged by salvager	35%

Figure 186. Lifecycle cost assumptions

Many of the above assumptions are based upon adapting existing vehicular catalytic converter recycling parameters to expectations for a fuel cell system^{101,102}. Based on analysis of platinum recycling conducted by Mike Ulsh at the National Renewable Energy Laboratory, total platinum loss during operation and recovery is estimated at:

- a 1% loss during operational life,
- 5% loss during recycling handling, and

¹⁰⁰ Calculated from system efficiency at rated power based on formula derived from ANL modeling results: Fuel economy = 0.0028x³ - 0.3272x²+12.993x - 116.45, where x = system efficiency at rated power.

¹⁰¹ "The impact of widespread deployment of fuel cell vehicles on platinum demand and price," Yongling Sun, et. al. International Journal of Hydrogen Energy 36 (2011).

¹⁰² "Evaluation of a platinum leasing program for fuel cell vehicles," Matthew A. Kromer et. al., International Journal of Hydrogen Energy 34 (2009).

- 2%-9% loss during the recycling process itself.^{103,104}

Ten percent (10%) is chosen as the Pt loss baseline value while the low (8%) and high (15%) end are represented in the sensitivity analysis below. The cost of recycling¹⁰⁵ is expected to range between \$75 and \$90 per troy ounce of recovered platinum. However this is only the cost incurred by running the actual recycle process. In addition, there are supply chain costs as the capturer or salvager collecting the unit desires to be paid. Based on current catalyst converter practice, the salvager expects to be paid by the recycler about 70%-75% of the total value of recycled platinum¹⁰⁶ with the remaining Pt value going to the recycle as payment for the recycle process. Whether this comparatively high fraction of Pt value would continue to accrue to the supply chain salvager for fuel cell stack platinum is unclear. If it does, the owner of the fuel cell automobile effectively gets no value from the recycled Pt, just as, in general, a person selling an internal combustion vehicle for scrap doesn't separately receive payment for the catalytic converter. However, as the value of Pt in the fuel cell may be greater than that of a catalytic converter, the paradigm may be different in the future. Consequently, as a baseline for the LCC analysis, the salvager is estimated to receive 35% (half the value received for catalytic converters) of the value of the recovered Pt less recycling cost. A sensitivity analysis is conducted for cases where the salvager captures only 10% and 75% of the recovered value. Finally, due to platinum market price volatility, it is unlikely that Pt price will be exactly the same at system purchase as it is 10 years later at time of recycle. Consequently, for purposes of the baseline LCC analysis, the price of platinum is held constant at the purchase price used for the catalyst within a new vehicle (\$1,500 / tr. oz.), and sensitivity analysis is conducted for a future¹⁰⁷ higher Pt price (\$2100/tr. oz. at end of life).

Under these assumptions, a basic set of cost results is calculated and displayed in Figure 187. Note that these results are only computed for the automotive system and not for the bus system; bus drive cycle and use patterns are vastly different from the average personal vehicle. Additional modeling and research is required to develop a representative equation governing the fuel economy of transit buses.

¹⁰³ L. Shore, "Platinum Group Metal Recycling Technology Development," BASF Catalysts LLC final project report to DOE under subcontract number DE-FC36-03GO13104, 2009.

¹⁰⁴ "The impact of widespread deployment of fuel cell vehicles on platinum demand and price," Yongling Sun, et. al. *International Journal of Hydrogen Energy* 36 (2011).

¹⁰⁵ *Ibid.*

¹⁰⁶ *Ibid.*

¹⁰⁷ Platinum price is considered more likely to increase in the future rather than decrease. Consequently, the future price of Pt is based on the current Pt market price (~\$1500/tr. oz) plus a \$60/tr. oz. per year increase, resulting in a \$2100/tr. oz. price after 10 years.

2013 Auto System Life Cycle Costs						
Annual Production Rate	1,000	10,000	30,000	80,000	130,000	500,000
System Cost	\$22,426	\$8,336	\$6,706	\$5,554	\$5,335	\$4,387
System Price (After Markup)	\$28,033	\$10,420	\$8,382	\$6,942	\$6,668	\$5,483
Annual Fuel Cost	\$920	\$920	\$920	\$920	\$920	\$920
Lifecycle Fuel Cost	\$5,656	\$5,656	\$5,656	\$5,656	\$5,656	\$5,656
Net Present Value of Recoverable Pt in System at End of System Lifetime	\$314	\$314	\$314	\$314	\$314	\$314
Final Pt Net Present Value Recovered	\$204	\$204	\$204	\$204	\$204	\$204
Total Lifecycle Cost	\$33,484	\$15,872	\$13,834	\$12,394	\$12,120	\$10,935
Total Lifecycle Cost (\$/mile)	\$0.279	\$0.132	\$0.115	\$0.103	\$0.101	\$0.091

Figure 187: Auto LCC results for the baseline assumptions

The variation of lifecycle cost with system efficiency was studied in order to examine the trade-offs between low efficiency (higher operating costs but lower initial capital costs) and high efficiency (lower operating costs but higher initial capital costs) systems. Figure 188 shows the polarization curve with system efficiency at rated power.

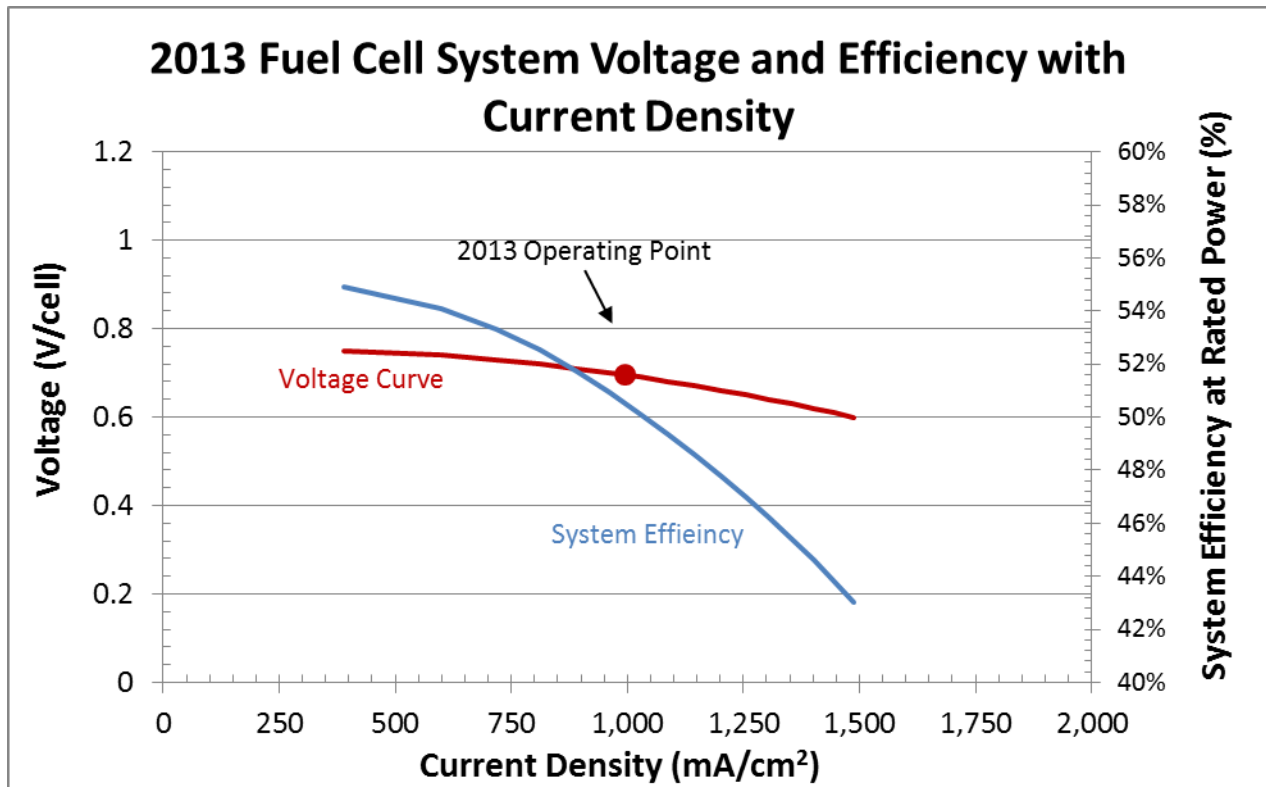


Figure 188: Polarization curves for efficiency sensitivity analysis

With this relationship, it is possible to calculate the variation in life cycle cost contributors over a range of efficiencies. These results are shown below. Figure 189 displays the results for the total lifecycle cost as well as its component costs on an absolute scale. Note that the total lifecycle cost (i.e. the present value of the 10 year expenses of the power system) is expressed as a \$/mile value for easy comparison

with internal combustion engine vehicle LCC analyses. Figure 190 shows a zoomed-in look at the total cost, indicating a minimum total life cycle cost at the baseline system value of 51% system efficiency (corresponding to 56% fuel cell stack efficiency and cell voltage of 0.695 V/cell). However, the range of LCC cost variation over the range of system efficiencies examined is quite small, indicating that LCC is generally insensitive to system efficiency.

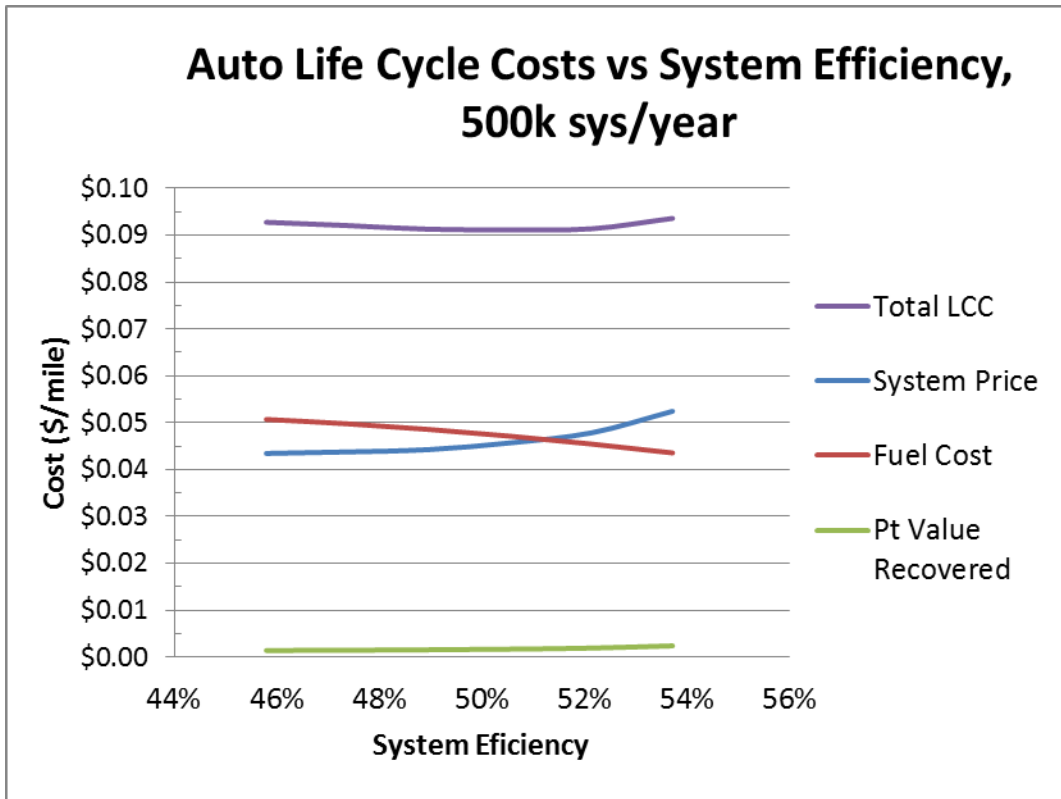


Figure 189: Life cycle cost components vs. fuel cell efficiency for 500k automobile systems/ year

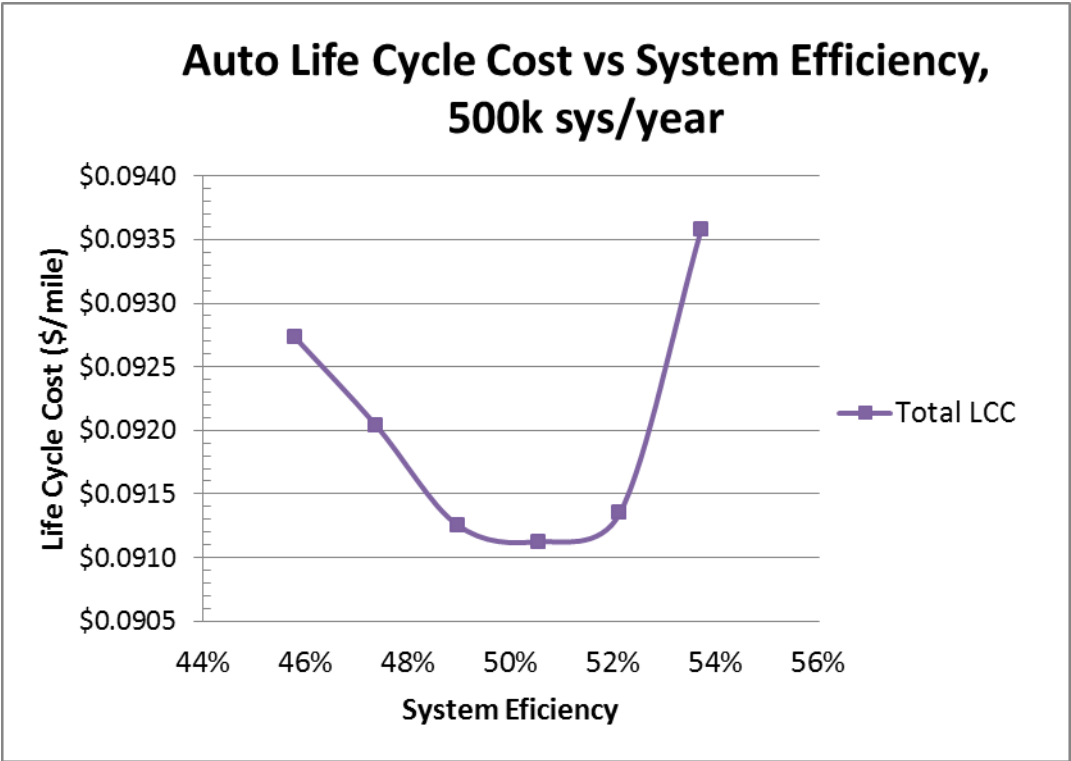


Figure 190: Life cycle cost vs. fuel cell efficiency for 500k automobile systems/year

In addition to the efficiency analysis, a simple sensitivity study was conducted on the parameters governing the platinum recycle, to determine the magnitude of the effect platinum recycling has on the lifecycle cost. Figure 191 below displays the total lifecycle cost in \$ per mile as a function of platinum price during the year of the recycle for three scenarios: the baseline case where the salvager captures 35% of the value of recovered platinum and two sensitivity cases where the salvager captures 10% of the value at the low end and 75% of the value at the high end.

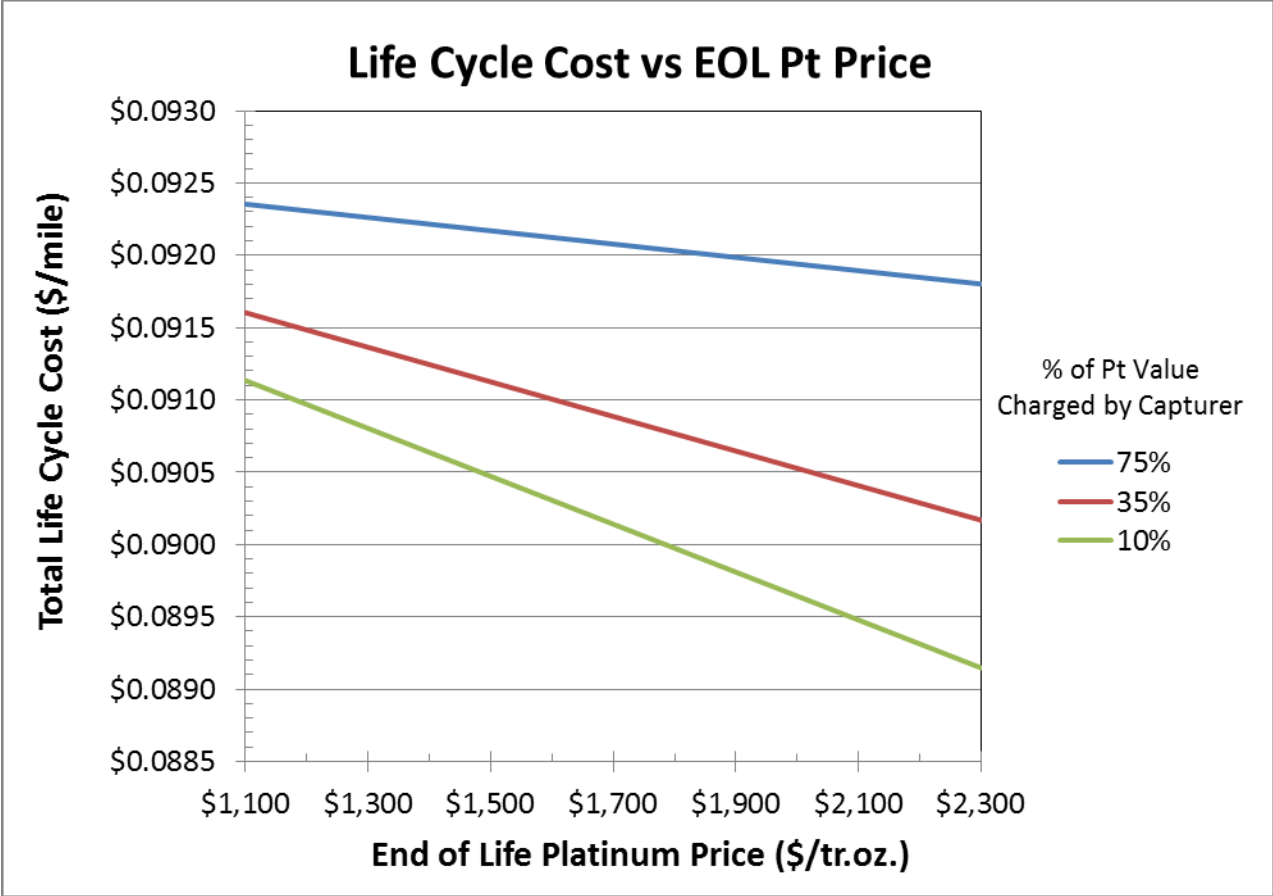


Figure 191: Life cycle cost vs. end of life platinum price (at 500k system/year)

Additional parameters were explored and are displayed as a tornado chart in Figure 192 and Figure 193. These results indicate that platinum recycle parameters do not have a large effect on the overall life cycle cost (~1%).

Life Cycle Cost (\$/mile), 500,000 systems/year				
Parameter	Units	Low Value of Variable	Base Value	High Value of Variable
Salvage Value Charged	%	10%	35%	75%
Pt Price at Recovery	\$/tr.oz.	\$1,100	\$1,500	\$2,100
Total Pt Loss	%	8%	10%	15%
Cost of Recovery	\$	\$70	\$80	\$90
2013 Auto System LLC (\$/mile)			\$0.09113	

Figure 192: Life cycle cost tornado chart parameters

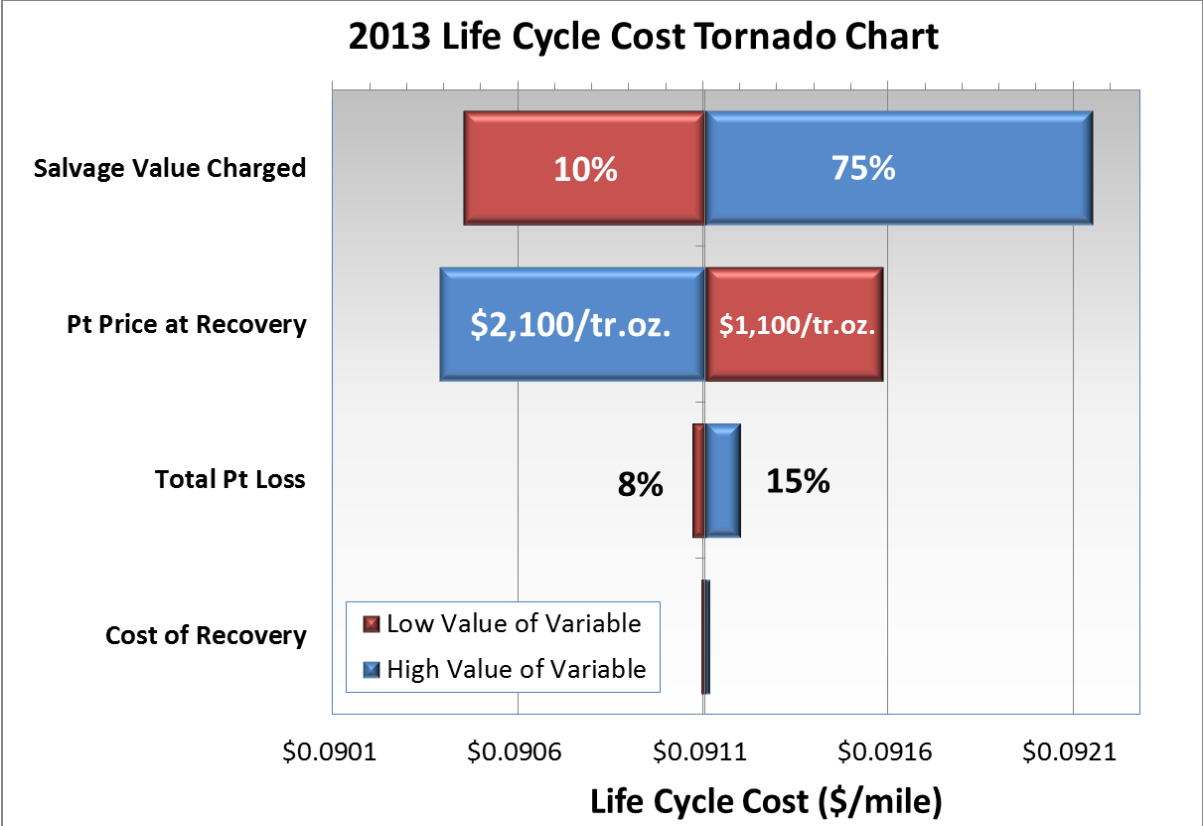


Figure 193: Life cycle cost tornado chart (at 500k systems/year)

12 Sensitivity Studies

A series of tornado and Monte Carlo sensitivity analyses were conducted to determine key parameters and assess avenues to further reduce cost.

12.1 Single Variable Analysis

12.1.1 Single Variable Automotive Analysis

A single variable analysis was performed to evaluate which parameters have the largest effect on system cost. Figure 194 shows the parameter ranges used to develop the tornado chart, while Figure 195 displays the results of the analysis.

System Cost (\$/kWnet), 500,000 sys/year				
Parameter	Units	Low Value	Base Value	High Value
Pt Loading	mgPt/cm ²	0.15	0.153	0.300
Power Density	mW/cm ²	588	692	1038
Air Compressor Cost Multiplier		0.80	1	1.20
Bipolar Plate & Coating Cost		1	1	1.5
Balance of Air Compressor Cost	\$/system	\$99.92	\$149.81	\$225
EPTFE Cost	\$/m ²	\$3.00	\$6.00	\$10.20
Compressor Effic.	%	69%	71%	75%
Motor/Controller Effic.	%	78%	80%	90%
Membrane Humidifier Cost	\$/system	\$70.77	\$94.36	\$141.53
GDL Cost	\$/m ²	\$2.79	\$3.82	\$4.97
Expander Effic.	%	71%	73%	80%
Ionomer Cost	\$/kg	\$46.63	\$77.71	\$155.43
Hydrogen Recirculation System Cost	\$/system	\$160.96	\$241.32	\$361.98
2013 Auto System Cost			\$54.83	

Figure 194: 2013 Auto results tornado chart parameter values

As shown in Figure 195, variations in operating condition parameters power density and platinum loading have the most capacity to affect system cost. For the case of power density, this affects the size and performance of the entire system, trickling down into cost changes in many components. Platinum loading's large effect is attributable to the very high price of platinum relative to the quantities used in the system.

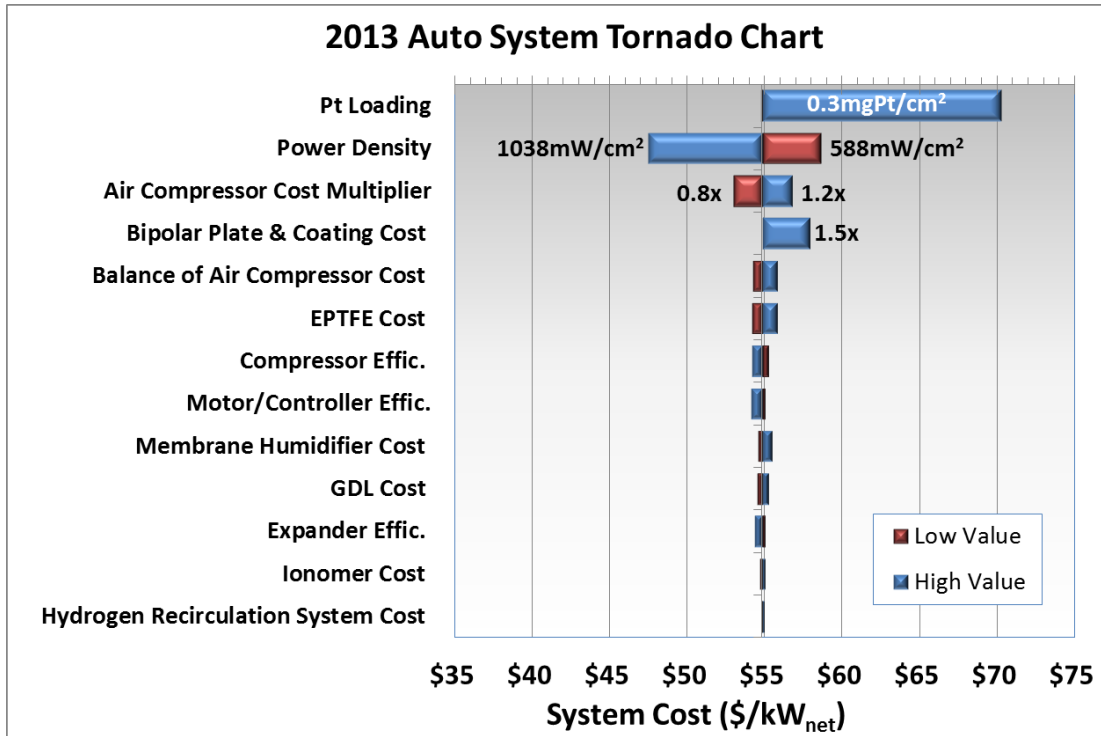


Figure 195: 2013 Auto results tornado chart

12.1.2 Automotive Analysis at a Pt price of \$1100/troy ounce

To aid in comparisons to other previous cost studies, the automotive system was also evaluated with a platinum price of \$1,100/troy ounce (instead of the baseline value of \$1,500/troy ounce). All other parameters remain the same. Results are shown in Figure 196.

		2013 Automotive System using Pt price \$1,100/tr.oz.					
Annual Production Rate	Sys/yr	1,000	10,000	30,000	80,000	100,000	500,000
System Net Electric Power (Output)	kWnet	80	80	80	80	80	80
System Gross Electric Power (Output)	kWgross	89.44	89.44	89.44	89.44	89.44	89.44
Component Costs/System							
Fuel Cell Stacks	\$/system	\$14,109	\$4,105	\$2,968	\$2,416	\$2,338	\$1,909
Balance of Plant	\$/system	\$7,909	\$3,872	\$3,380	\$2,781	\$2,640	\$2,121
System Assembly & Testing	\$/system	\$149	\$103	\$102	\$101	\$101	\$101
Cost/System	\$/system	\$22,167	\$8,080	\$6,450	\$5,298	\$5,079	\$4,131
Total System Cost	\$/kWnet	\$277.09	\$101.00	\$80.62	\$66.22	\$63.49	\$51.64
Cost/kWgross	\$/kWgross	\$247.85	\$90.34	\$72.11	\$59.24	\$56.79	\$46.19

Figure 196: Detailed system cost for the 2013 automotive technology system with a Pt price of \$1,100/troy ounce

12.1.3 Single Variable Bus Analysis

A single variable Tornado Chart analysis of the bus system was also conducted. Assumptions are shown in Figure 197 and results in Figure 198.

As with the automotive system, power density and platinum loading have the largest potential to vary system cost. Unlike the automotive system, however, there is also a large cost variation potential to be found in GDL and bipolar plate cost variations. This is because at lower manufacturing rate, the cost of

manufactured component items is high and subject to large changes in cost relative to components manufactured at high volume, as in the automotive case.

2013 Bus System Cost (\$/kWnet), 1,000 sys/year				
Parameter	Units	Low Value	Base Value	High Value
Power Density	mW/cm ²	420.7	601	823
Pt Loading	mgPt/cm ²	0.2	0.4	0.8
GDL Cost	\$/m ²	\$76.99	\$105.47	\$137.11
Bipolar Plate & Coating Cost Factor		1	1	2
Air Compressor Cost Factor		0.8	1	1.2
EPTFE Cost Multiplier		0.667	1.00	2.20
Compressor / Motor & Motor Controller Efficiencies	%	69%/78%	71%/80%	75%/90%
Ionomer Cost	\$/kg	\$47.33	\$215.12	\$527.04
Hydrogen Recirculation System Cost	\$/system	\$600.20	\$899.86	\$1,799.71
Membrane Humidifier Cost	\$/system	\$391.00	\$782.00	\$1,563.99
Balance of Air Compressor Cost	\$/system	\$248.00	\$371.81	\$743.62
Membrane Thickness	μm	15	25.4	25.4
2013 Bus System Cost			\$269.95	

Figure 197: 2013 Bus results tornado chart parameter values

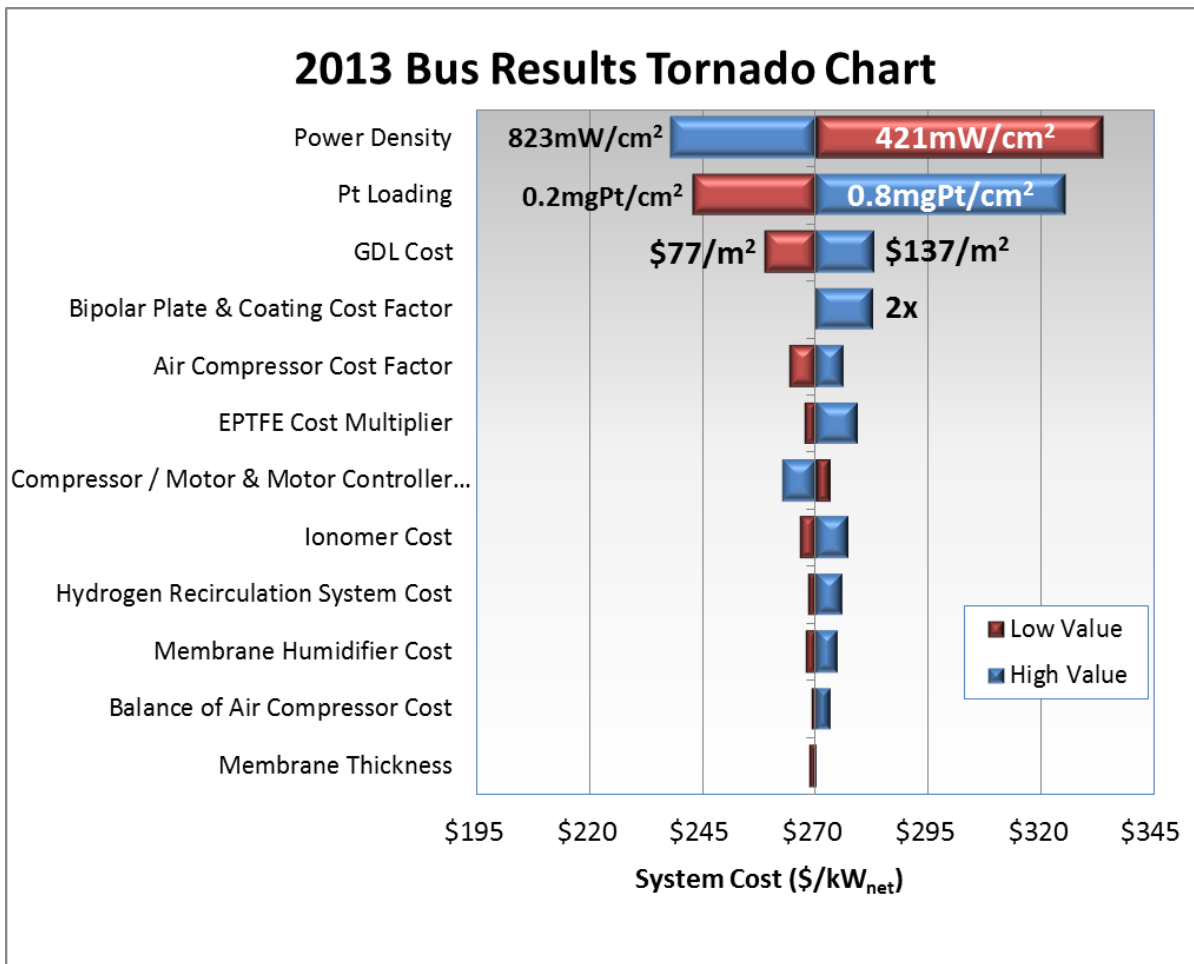


Figure 198: 2013 Bus results tornado chart

12.2 Monte Carlo Analysis

In order to evaluate the bounds for the likely variation in final results, a Monte Carlo analysis was conducted for both the automotive and bus results. With these results, it is possible to examine the probability of various model outcomes based upon assumed probability functions for selected inputs. For all inputs, triangular distributions were chosen with a minimum, maximum, and most likely value. The most likely value is the result used in the baseline cost analysis, while the maximum and minimum were chosen with the input of the Fuel Cell Tech Team to reflect likely real-world bounds for 2013.

12.2.1 Monte Carlo Automotive Analysis

Assumptions and results for the Monte Carlo analysis of the automotive system at a manufacturing rate of 500,000 systems/year are shown in Figure 199 and Figure 200.

2013 Technology Monte Carlo Analysis, 500k sys/year				
Parameter	Unit	Minimum Value	Likeliest Value	Maximum Value
Power Density	mW/cm ²	588	692	1038
Pt Loading	mgPt/cm ²	0.15	0.153	0.3
Ionomer Cost	\$/kg	\$46.63	\$77.71	\$155.43
GDL Cost	\$/m ² of GDL	\$2.79	\$3.82	\$4.97
Bipolar Plate & Coating Cost Multiplier		1	1	1.5
Membrane Humidifier Cost	\$/system	\$70.77	\$94.36	\$141.53
Compressor Effic.	%	69%	71%	75%
Expander Effic.	%	71%	73%	80%
Motor/Controller Effic.	%	78%	80%	90%
Air Compressor Cost Multiplier		0.8	1	1.2
Balance of Air Compressor Cost	\$/system	\$99.92	\$149.81	\$224.71
Hydrogen Recirculation System Cost	\$/system	\$160.96	\$241.32	\$361.98
EPTFE Cost	\$/m ² of EPTFE	\$3.00	\$6.00	\$10.20

Figure 199: 2013 automotive Monte Carlo analysis bounds

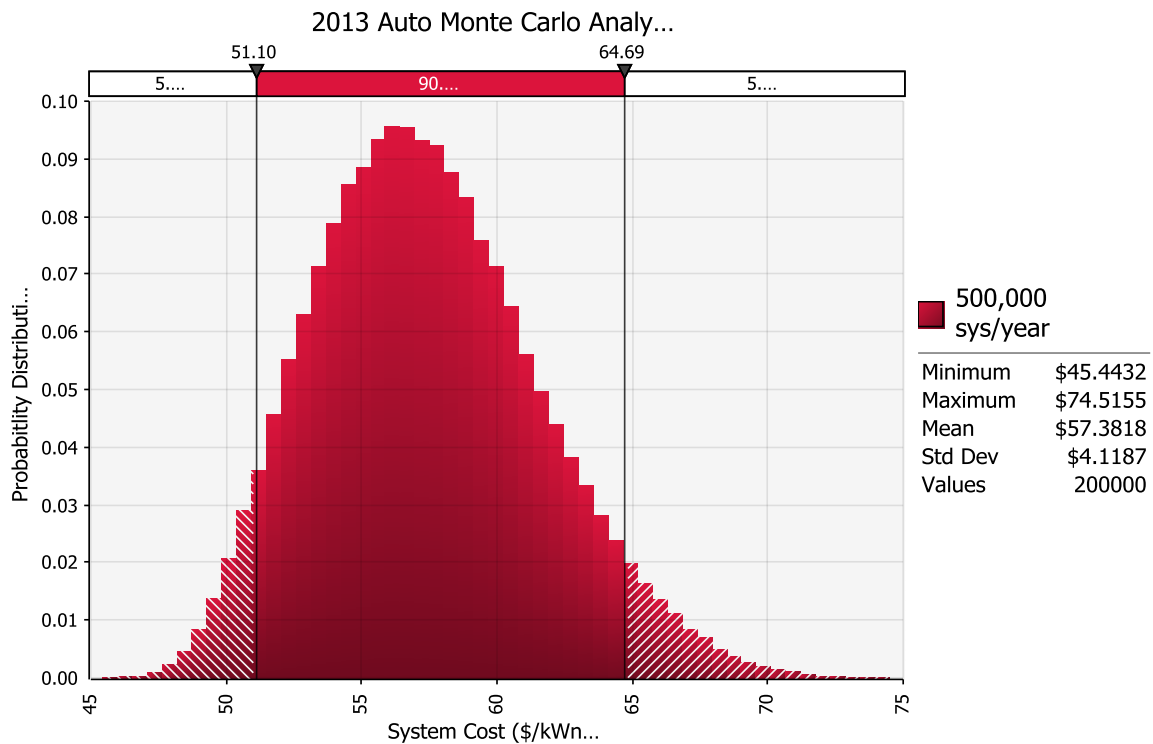


Figure 200: 2013 automotive Monte Carlo analysis results

Monte Carlo analysis indicates that the middle 90% probability range of cost is between \$51.10/kW_{net} and \$64.69/kW_{net} for the automotive system at 500,000 systems/year.

12.2.2 Monte Carlo Bus Analysis

Assumptions and results for the Monte Carlo analysis of the bus system at a manufacturing rate of 1,000 systems/year are shown in Figure 201 and Figure 202.

2013 Bus Technology Monte Carlo Analysis, 1,000 sys/year				
Parameter	Unit	Minimum Value	Likeliest Value	Maximum Value
Power Density	mW/cm ²	421	601	823.37
Pt Loading	mgPt/cm ²	0.15	0.4	0.3
Ionomer Cost	\$/kg	\$47.33	\$215.12	\$527.04
GDL Cost	\$/m ² of GDL	\$76.99	\$105.47	\$137.11
Bipolar Plate & Coating Cost Multiplier		1	1	2
Membrane Humidifier Cost	\$/system	\$375.80	\$751.61	\$1,503.22
Compressor Effic.	%	69%	71%	75%
Motor/Controller Effic.	%	78%	80%	90%
Air Compressor Cost Multiplier		0.8	1	1.2
Balance of Air Compressor Cost	\$/system	\$248.00	\$371.81	\$743.62
Hydrogen Recirculation System Cost	\$/system	\$600.20	\$899.86	\$1,799.71
EPTFE Cost	\$/m ² of EPTFE	\$9.84	\$14.75	\$32.45
Membrane Thickness	µm	15	25.4	25.4

Figure 201: 2013 bus Monte Carlo analysis bounds

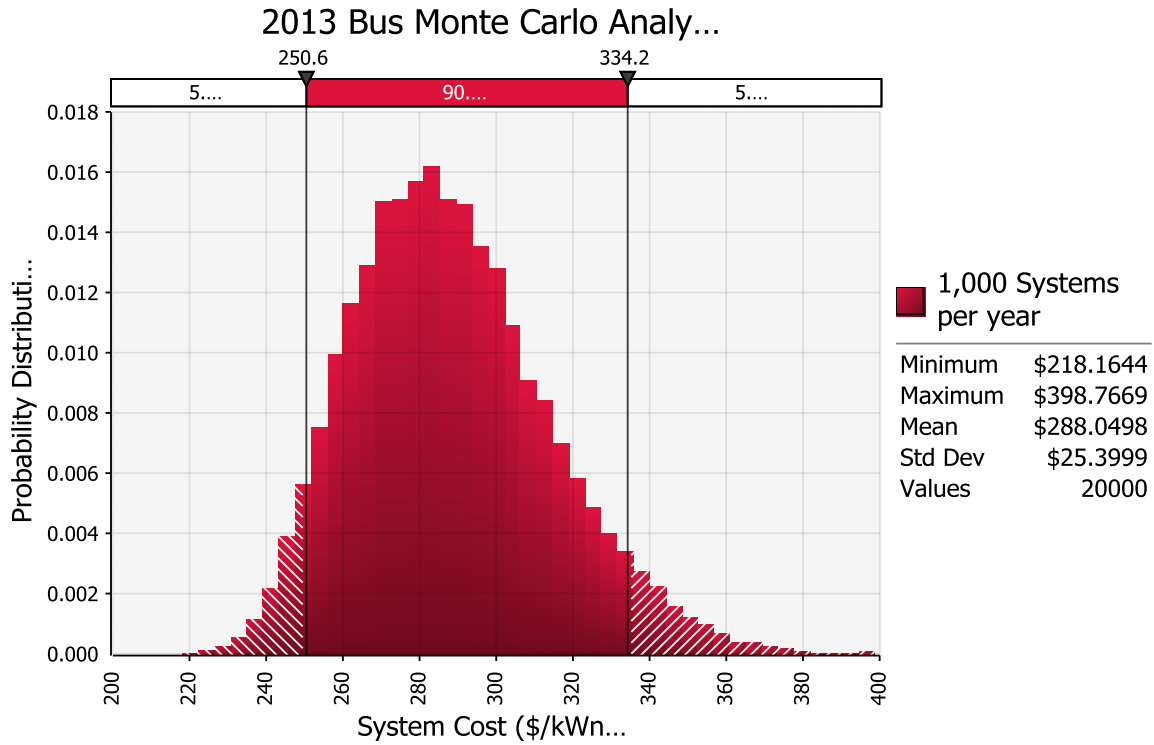


Figure 202: 2013 bus Monte Carlo analysis results

Monte Carlo analysis indicates that the middle 90% probability range of cost is between \$250.60/kW_{net} and \$334.20/kW_{net} for the bus system at 1,000 systems/year.

13 Key Progress in the 2013 Automotive and Bus Analyses

This section summarizes key progress for both the automotive and bus power systems analyses.

80 kW_{e,net} light-duty automotive fuel cell power systems:

- The 2012 DFMATM-style cost analysis was updated to reflect changes/improvements achieved in 2013.
- Performance is based on an updated 2013 stack polarization model provided by Argonne National Laboratory (based on recent 3M nanostructured thin-film catalyst test data).
- The 2013 system is optimized for low cost, and the resulting design point is shown in the Figure 203. These optimized operating conditions differ from the 2012 optimization conditions.

	2012 Design Point	2013 Design Point
Cell voltage	0.676 volts/cell	0.695 volts/cell
Power density	984 mW/cm ²	692 mW/cm ²
Pressure	2.5 atm	2.5 atm
Total catalyst loading	0.196 mgPt/cm ²	0.153 mgPt/cm ²
Stack Temp. (Coolant Exit Temp)	82°C	92.3°C
Cathode Air Stoichiometry	1.5	1.5

Figure 203. Design point comparison between 2012 and 2013.

- Other significant changes for 2013 include
 - the application of a heat loss constraint ($Q/\Delta T$) for the automotive radiator,
 - replacement of the tubular membrane air humidifier with a plate frame membrane humidifier,
 - revision of quality control procedures,
 - updates to material costs (including raising Pt price from \$1,100/tr.oz. to \$1,500/tr.oz.),
 - alignment with DOE compressor/expander/motor efficiencies,
 - markup assumptions for vertical integration, and
 - updates to sizing the low temperature coolant loop.
- Several analyses were performed to explore alternate manufacturing procedures or types of system components:
 - low-cost Gore MEA manufacturing process (Sections 6.6) and
 - Eaton-style multi-lobe air compressor-expander-motor (Section 6.7).
 - In both cases, the alternate concept was not incorporated into the baseline design for the 2013 cost analysis due to a lack of experimentally validated performance data.
- The estimated fuel cell system cost for automobiles is \$54.83/kW_{net} at 500,000 systems/year and represents the “2013 Update” to previous annual estimates. (This value does not include the cost of hydrogen storage or the electric drive train.)
- A Monte Carlo analysis indicates that the fuel cell system cost is likely to be between \$51.10/kW_{net} and \$64.69/kW_{net} for the automotive system, with 90% probability.

- The 2013 automotive system balance of plant components represent approximately 48% of the overall system cost at a production rate of 500,000 systems/year.

160 kW_{net} bus fuel cell power systems:

- Primary differences between the bus and automotive power systems include
 - system power (160kW_{net} vs. 80kW_{net}),
 - number of stacks (two vs. one),
 - operating pressure (1.8 atm vs. 2.5 atm),
 - catalyst loading (0.4 mgPt/cm² vs. 0.153 mgPt/cm²),
 - use of an exhaust gas expander (no expander vs. expander), and
 - type of air compressor (twin vortex vs. centrifugal).
- Stack performance is based on a 2013 stack polarization model provided by Argonne National Laboratory (the same data set used for the automotive system) but with the total Pt loading raised from 0.153 mgPt/cm² to 0.4 mgPt/cm² to reflect the longer durability requirements of the bus application.
- Power density, voltage, pressure, and catalyst loading of the selected system design point are roughly consistent with the actual operating conditions of Ballard fuel cell buses currently in service.

	Approximate Ballard Bus Design Point	2012 Bus Design Point	2013 Bus Design Point
Cell voltage	~0.69 volts/cell	0.676 volts/cell	0.676 volts/cell
Power density	~759 mW/cm ²	716 mW/cm ²	601 mW/cm ²
Pressure	~1.8 atm	1.8 atm	1.8 atm
Total catalyst loading	~0.4 mgPt/cm ²	0.4 mgPt/cm ²	0.4 mgPt/cm ²
Stack Temperature	~60°C	74°C	74°C
Cathode Air Stoichiometry	1.5-2.0	1.5	1.5

Figure 204. Design Point Comparison for FC Bus between Ballard Bus, 2012 analysis, and 2013 analysis

- Additional changes between 2012 and 2013 bus analyses include
 - all of 2013 automotive updates (including plate frame membrane humidifier),
 - performance and cost results for an Eaton-style multi-lobe air compressor-motor unit,
 - inclusion of non-vertically integrated markup assumptions, and
 - job-shop vs. in-house manufacturing logic.
- The system schematics and stack construction are nearly identical between the bus and automobile systems.
- The final 2013 bus cost is \$269.95/kW_{net} at 1,000 systems/year.
- A Monte Carlo analysis indicates that the bus fuel cell system cost is likely to be between \$250.60/kW_{net} and \$334.00/kW_{net}, with 90% probability.

- The 2013 bus system balance of plant represented only 32% of the overall system cost at a production rate of 1,000 systems/year.
- Because fewer bus systems are produced in a year at the maximum rate consisted, bus system costs are much more sensitive than automobile system costs to variations in the cost of components such as GDL or bipolar plate manufacturing.

14 Appendix A: 2013 Transit Bus Cost Results

14.1 Fuel Cell Stack Materials, Manufacturing, and Assembly Cost Results

14.1.1 Bipolar Plates

Annual Production Rate	200	400	800	1,000
Manufacture or Job Shop	Job Shop	Job Shop	Job Shop	Job Shop
Job Shop Line Utilization (%)	42%	46%	56%	61%
Job Shop Total Machine Rate (\$/min)	\$3.71	\$3.36	\$2.85	\$2.65
Manufactured Line Utilization (%)	5%	9%	19%	24%
Manufactured Total Machine Rate (\$/min)	\$23.38	\$11.82	\$6.03	\$4.87
Line Utilization Used (%)	42%	46%	56%	61%
Total Machine Rate Used (\$/min)	\$3.71	\$3.36	\$2.85	\$2.65

Annual Production Rate	200	400	800	1,000
Material (\$/stack)	\$282.72	\$282.72	\$282.72	\$282.72
Manufacturing (\$/stack)	\$88.23	\$79.94	\$67.66	\$62.95
Tooling (\$/stack)	\$117.78	\$98.34	\$98.34	\$102.27
Secondary Operations: Coating (\$/stack)	\$333.74	\$318.87	\$293.90	\$283.28
Markup (\$/stack)	\$332.06	\$306.46	\$284.04	\$277.26
Total Cost (\$/stack)	\$1,154.53	\$1,086.33	\$1,026.66	\$1,008.49
Total Cost (\$/kWnet)	\$14.43	\$13.58	\$12.83	\$12.61

14.1.1.1 Alloy Selection and Corrosion Concerns

Annual Production Rate	200	400	800	1,000
Material (\$/stack)	\$59.84	\$59.84	\$59.84	\$59.84
Manufacturing (\$/stack)	\$273.90	\$259.03	\$234.06	\$223.44
Total Cost (\$/stack)	\$333.74	\$318.87	\$293.90	\$283.28
Total Cost (\$/kWnet)	\$4.17	\$3.99	\$3.67	\$3.54

14.1.2 Membrane

Annual Production Rate	200	400	800	1,000
Material (\$/m ²)	\$50.97	\$45.18	\$39.89	\$38.29
Manufacturing (\$/m ²)	\$361.49	\$221.17	\$137.22	\$117.97
Markup (\$/m ²)	\$166.52	\$104.66	\$67.74	\$59.25
Total Cost (\$/m² (total))	\$578.99	\$371.01	\$244.85	\$215.51
Total Cost (\$/stack)	\$10,883.59	\$6,974.08	\$4,602.54	\$4,051.08
Total Cost (\$/kWnet)	\$136.04	\$87.18	\$57.53	\$50.64

14.1.3 Nanostructured Thin Film (NSTF) Catalyst Application

14.1.4 Catalyst Cost

Annual Production Rate	200	400	800	1,000
Manufacture or Job Shop	Job Shop	Job Shop	Job Shop	Job Shop
Job Shop Line Utilization (%)	39%	41%	45%	47%
Job Shop Total Machine Rate (\$/min)	\$22.99	\$21.81	\$20.15	\$19.48
Manufactured Line Utilization (%)	2%	4%	8%	10%
Manufactured Total Machine Rate (\$/min)	\$178.75	\$94.09	\$50.14	\$41.14
Line Utilization Used (%)	39%	41%	45%	47%
Total Machine Rate Used (\$/min)	\$22.99	\$21.81	\$20.15	\$19.48

Annual Production Rate	200	400	800	1,000
Material (\$/stack)	\$3,169.92	\$3,159.52	\$3,149.38	\$3,146.18
Manufacturing (\$/stack)	\$236.29	\$217.21	\$195.41	\$187.56
Tooling (\$/stack)	\$50.30	\$25.09	\$20.88	\$20.04
Markup (\$/stack)	\$1,395.50	\$1,336.78	\$1,287.31	\$1,271.64
Total Cost (\$/stack)	\$4,852.01	\$4,738.59	\$4,652.98	\$4,625.42
Total Cost (\$/kWnet)	\$60.65	\$59.23	\$58.16	\$57.82

14.1.5 Gas Diffusion Layer

Annual Production Rate	200	400	800	1,000
GDL Cost (\$/stack)	\$4,692.71	\$3,262.37	\$2,268.00	\$2,017.50
Markup (\$/stack)	\$3,706.04	\$2,411.93	\$1,570.56	\$1,368.13
Total Cost (\$/stack)	\$8,398.75	\$5,674.31	\$3,838.57	\$3,385.64
Total Cost (\$/kWnet)	\$104.98	\$70.93	\$47.98	\$42.32

14.1.6 MEA Sub-Gaskets Total

Annual Production Rate	200	400	800	1,000
Material (\$/stack)	\$69.75	\$69.75	\$69.75	\$69.75
Manufacturing (\$/stack)	\$455.92	\$409.08	\$372.24	\$341.70
Tooling (Kapton Web) (\$/stack)	\$22.09	\$20.20	\$20.18	\$20.54
Cost/Stack	\$221.15	\$196.10	\$213.14	\$193.14
Total Cost (\$/stack)	\$768.92	\$695.13	\$675.31	\$625.12
Total Cost (\$/kWnet)	\$4.81	\$4.34	\$4.22	\$3.91

14.1.6.1 Sub-Gasket Formation

Annual Production Rate	200	400	800	1,000
Manufacture or Job Shop	Job Shop	Job Shop	Job Shop	Job Shop
Job Shop Line Utilization (%)	39%	42%	46%	49%
Job Shop Total Machine Rate (\$/min)	\$25.16	\$24.05	\$22.21	\$21.42
Manufactured Line Utilization (%)	2%	5%	9%	12%
Manufactured Total Machine Rate (\$/min)	\$250.71	\$131.18	\$69.40	\$56.77
Line Utilization Used (%)	39%	42%	46%	49%
Total Machine Rate Used (\$/min)	\$25.16	\$24.05	\$22.21	\$21.42

Annual Production Rate	200	400	800	1,000
Material (\$/stack)	\$64.68	\$64.68	\$64.68	\$64.68
Manufacturing (\$/stack)	\$312.58	\$289.74	\$260.01	\$248.63
Tooling (Kapton Web) (\$/stack)	\$22.09	\$20.20	\$20.18	\$20.54
Markup (\$/stack)	\$161.23	\$147.21	\$131.90	\$126.58
Total Cost (\$/stack)	\$560.58	\$521.83	\$476.76	\$460.43
Total Cost (\$/kWnet)	\$7.01	\$6.52	\$5.96	\$5.76

14.1.6.2 Sub-Gasket Adhesive Application (screen-printing)

Annual Production Rate	200	400	800	1,000
Manufacture or Job Shop	Job Shop	Job Shop	Manufactured	Manufactured
Job Shop Line Utilization (%)	49%	61%	48%	60%
Job Shop Total Machine Rate (\$/min)	\$2.37	\$1.97	\$2.41	\$2.00
Manufactured Line Utilization (%)	12%	24%	48%	60%
Manufactured Total Machine Rate (\$/min)	\$6.61	\$3.44	\$1.86	\$1.54
Line Utilization Used (%)	49%	61%	48%	60%
Total Machine Rate Used (\$/min)	\$2.37	\$1.97	\$1.86	\$1.54

Annual Production Rate	200	400	800	1,000
Material (\$/stack)	\$5.07	\$5.07	\$5.07	\$5.07
Manufacturing (\$/stack)	\$143.34	\$119.34	\$112.24	\$93.07
Markup (\$/stack)	\$59.92	\$48.89	\$81.24	\$66.55
Total Cost (\$/stack)	\$208.33	\$173.30	\$198.55	\$164.69
Total Cost (\$/kWnet)	\$2.60	\$2.17	\$2.48	\$2.06

14.1.7 MEA Crimping, Cutting, and Slitting

Annual Production Rate	200	400	800	1,000
Manufacture or Job Shop	Job Shop	Job Shop	Job Shop	Job Shop
Job Shop Line Utilization (%)	37%	37%	38%	38%
Job Shop Total Machine Rate (\$/min)	\$9.48	\$9.45	\$9.38	\$9.35
Manufactured Line Utilization (%)	0%	0%	1%	1%
Manufactured Total Machine Rate (\$/min)	\$1,699.95	\$912.10	\$477.74	\$386.70
Line Utilization Used (%)	37%	37%	38%	38%
Total Machine Rate Used (\$/min)	\$9.48	\$9.45	\$9.38	\$9.35

Annual Production Rate	200	400	800	1,000
Manufacturing (\$/stack)	\$7.39	\$6.86	\$6.51	\$6.41
Tooling (\$/stack)	\$2.95	\$2.46	\$2.21	\$2.36
Markup (\$/stack)	\$4.17	\$3.66	\$3.33	\$3.33
Total Cost (\$/stack)	\$14.51	\$12.98	\$12.05	\$12.09
Total Cost (\$/kWnet)	\$0.18	\$0.16	\$0.15	\$0.15

14.1.8 End Plates

Annual Production Rate	200	400	800	1,000
Manufacture or Job Shop	Job Shop	Job Shop	Job Shop	Job Shop
Job Shop Line Utilization (%)	38%	39%	41%	42%
Job Shop Total Machine Rate (\$/min)	\$2.38	\$2.33	\$2.24	\$2.20
Manufactured Line Utilization (%)	1%	2%	4%	5%
Manufactured Total Machine Rate (\$/min)	\$52.26	\$26.34	\$13.38	\$10.79
Line Utilization Used (%)	38%	39%	41%	42%
Total Machine Rate Used (\$/min)	\$2.38	\$2.33	\$2.24	\$2.20

Annual Production Rate	200	400	800	1,000
Material (\$/stack)	\$85.40	\$80.96	\$76.76	\$75.45
Manufacturing (\$/stack)	\$12.44	\$12.18	\$11.71	\$11.49
Tooling (\$/stack)	\$4.31	\$2.15	\$1.08	\$0.86
Markup (\$/stack)	\$41.24	\$37.45	\$34.25	\$33.29
Total Cost (\$/stack)	\$143.38	\$132.75	\$123.79	\$121.10
Total Cost (\$/kWnet)	\$1.79	\$1.66	\$1.55	\$1.51

14.1.9 Current Collectors

Annual Production Rate	200	400	800	1,000
Manufacture or Job Shop	Job Shop	Job Shop	Job Shop	Job Shop
Job Shop Line Utilization (%)	37%	37%	37%	37%
Job Shop Total Machine Rate (\$/min)	\$2.20	\$2.20	\$2.20	\$2.20
Manufactured Line Utilization (%)	0%	0%	0%	0%
Manufactured Total Machine Rate (\$/min)	\$1,214.59	\$703.52	\$352.15	\$291.05
Line Utilization Used (%)	37%	37%	37%	37%
Total Machine Rate Used (\$/min)	\$2.20	\$2.20	\$2.20	\$2.20

Annual Production Rate	200	400	800	1,000
Material (\$/stack)	\$9.41	\$9.39	\$9.37	\$9.36
Manufacturing (\$/stack)	\$0.30	\$0.26	\$0.26	\$0.25
Tooling (\$/stack)	\$0.35	\$0.17	\$0.09	\$0.07
Secondary Operation (\$/stack)	\$0.53	\$0.53	\$0.53	\$0.53
Markup (\$/stack)	\$4.27	\$4.07	\$3.92	\$3.87
Total Cost (\$/stack)	\$14.86	\$14.42	\$14.16	\$14.08
Total Cost (\$/kWnet)	\$0.19	\$0.18	\$0.18	\$0.18

14.1.10 Coolant Gaskets/Laser-welding

Annual Production Rate	200	400	800	1,000
Manufacture or Job Shop	Job Shop	Job Shop	Job Shop	Manufactured
Job Shop Line Utilization (%)	46%	55%	73%	45%
Job Shop Total Machine Rate (\$/min)	\$3.24	\$2.76	\$2.16	\$3.31
Manufactured Line Utilization (%)	9%	18%	36%	45%
Manufactured Total Machine Rate (\$/min)	\$11.78	\$6.01	\$3.12	\$2.54
Line Utilization Used (%)	46%	55%	73%	45%
Total Machine Rate Used (\$/min)	\$3.24	\$2.76	\$2.16	\$2.54

Annual Production Rate	200	400	800	1,000
Material (\$/stack)	\$0.00	\$0.00	\$0.00	\$0.00
Manufacturing (\$/stack)	\$147.36	\$125.50	\$97.97	\$115.52
Tooling (\$/stack)	\$0.00	\$0.00	\$0.00	\$0.00
Markup (\$/stack)	\$59.49	\$49.32	\$37.47	\$78.34
Total Cost (\$/stack)	\$206.85	\$174.82	\$135.44	\$193.86
Total Cost (\$/kWnet)	\$2.59	\$2.19	\$1.69	\$2.42

14.1.11 End Gaskets

Annual Production Rate	200	400	800	1,000
Manufacture or Job Shop	Job Shop	Job Shop	Job Shop	Job Shop
Job Shop Line Utilization (%)	37%	37%	37%	37%
Job Shop Total Machine Rate (\$/min)	\$3.02	\$3.02	\$3.01	\$3.00
Manufactured Line Utilization (%)	0%	0%	0%	0%
Manufactured Total Machine Rate (\$/min)	\$1,174.88	\$587.63	\$293.95	\$235.21
Line Utilization Used (%)	37%	37%	37%	37%
Total Machine Rate Used (\$/min)	\$3.02	\$3.02	\$3.01	\$3.00

Annual Production Rate	200	400	800	1,000
Material (\$/stack)	\$0.03	\$0.03	\$0.03	\$0.03
Manufacturing (\$/stack)	\$0.99	\$0.98	\$0.98	\$0.98
Markup (\$/stack)	\$0.41	\$0.40	\$0.39	\$0.38
Total Cost (\$/stack)	\$1.43	\$1.42	\$1.40	\$1.40
Total Cost (\$/kWnet)	\$0.02	\$0.02	\$0.02	\$0.02

14.1.12 Stack Assembly

Annual Production Rate	200	400	800	1,000
Manufacture or Job Shop	Manufactured	Manufactured	Manufactured	Manufactured
Job Shop Line Utilization (%)	56%	38%	76%	95%
Job Shop Total Machine Rate (\$/min)	\$1.31	\$1.23	\$1.05	\$1.03
Manufactured Line Utilization (%)	19%	38%	76%	95%
Manufactured Total Machine Rate (\$/min)	\$0.90	\$0.83	\$0.80	\$0.79
Line Utilization Used (%)	19%	38%	76%	95%
Total Machine Rate Used (\$/min)	\$0.90	\$0.83	\$0.80	\$0.79

Annual Production Rate	200	400	800	1,000
Compression Bands (\$/stack)	\$0.00	\$0.00	\$0.00	\$0.00
Assembly (\$/stack)	\$86.38	\$79.73	\$76.40	\$75.74
Markup (\$/stack)	\$68.22	\$58.94	\$52.91	\$51.36
Total Cost (\$/stack)	\$154.60	\$138.67	\$129.31	\$127.10
Total Cost (\$/kWnet)	\$1.93	\$1.73	\$1.62	\$1.59

14.1.13 Stack Housing

Annual Production Rate	200	400	800	1,000
Manufacture or Job Shop	Job Shop	Job Shop	Job Shop	Job Shop
Job Shop Line Utilization (%)	37%	37%	38%	38%
Job Shop Total Machine Rate (\$/min)	\$1.41	\$1.41	\$1.41	\$1.41
Manufactured Line Utilization (%)	0%	0%	1%	1%
Manufactured Total Machine Rate (\$/min)	\$46.17	\$23.49	\$12.14	\$9.87
Line Utilization Used (%)	37%	37%	38%	38%
Total Machine Rate Used (\$/min)	\$1.41	\$1.41	\$1.41	\$1.41

Annual Production Rate	200	400	800	1,000
Material (\$/stack)	\$10.32	\$10.32	\$10.32	\$10.32
Manufacturing (\$/stack)	\$3.36	\$3.35	\$3.34	\$3.33
Tooling (\$/stack)	\$181.16	\$90.58	\$45.29	\$36.23
Markup (\$/stack)	\$78.66	\$40.97	\$22.55	\$18.92
Total Cost (\$/stack)	\$273.50	\$145.22	\$81.50	\$68.80
Total Cost (\$/kWnet)	\$1.71	\$0.91	\$0.51	\$0.43

14.1.14 Stack Conditioning and Testing

Annual Production Rate	200	400	800	1,000
Capital Cost (\$/line)	\$462,359	\$451,945	\$441,531	\$438,178
Simultaneous Lines	1	1	2	2
Laborers per Line	0.1	0.1	0.1	0.1
Test Duration (hrs/stack)	5	5	5	5
Line Utilization Used (%)	12%	23%	23%	29%
Total Machine Rate Used (\$/min)	\$4.45	\$2.24	\$2.19	\$1.76

Annual Production Rate	200	400	800	1,000
Conditioning/Testing (\$/stack)	\$445.22	\$223.86	\$218.98	\$176.38
Markup (\$/stack)	\$351.61	\$165.50	\$151.64	\$119.61
Total Cost (\$/stack)	\$796.83	\$389.36	\$370.63	\$295.99
Total Cost (\$/kWnet)	\$9.96	\$4.87	\$4.63	\$3.70

14.2 2013 Transit Bus Balance of Plant (BOP) Cost Results

14.2.1 Air Loop

Annual Production Rate	200	400	800	1,000
Filter and Housing (\$/system)	\$75.30	\$74.55	\$73.80	\$73.56
Compressor, Expander & Motor (\$/system)	\$6,148.22	\$5,466.83	\$4,916.55	\$4,760.94
Mass Flow Sensor (\$/system)	\$101.87	\$100.85	\$99.84	\$99.52
Air Ducting (\$/system)	\$197.48	\$193.81	\$190.14	\$188.96
Air Temperature Sensor (\$/system)	\$10.75	\$10.32	\$9.90	\$9.77
Markup on Purchased Components (\$/system)	\$155.59	\$149.14	\$142.93	\$140.98
Total Cost (\$/system)	\$6,689.21	\$5,995.49	\$5,433.16	\$5,273.73
Total Cost (\$/kW _{net})	\$41.81	\$37.47	\$33.96	\$32.96

14.2.2 Humidifier & Water Recovery Loop

Annual Production Rate	200	400	800	1,000
Air Precooler (\$/system)	\$163.19	\$158.59	\$154.32	\$153.01
Demister (\$/system)	\$105.64	\$79.43	\$64.66	\$61.30
Membrane Air Humidifier (\$/system)	\$1,151.41	\$931.92	\$788.49	\$751.61
Total Cost (\$/system)	\$1,420.24	\$1,169.93	\$1,007.47	\$965.91
Total Cost (\$/kW_{net})	\$8.88	\$7.31	\$6.30	\$6.04

14.2.2.1 Air Precooler

Annual Production Rate	200	400	800	1,000
Material (\$/system)	\$45.59	\$45.59	\$45.59	\$45.59
Manufacturing (\$/system)	\$45.59	\$45.59	\$45.59	\$45.59
Markup (\$/system)	\$72.01	\$67.41	\$63.14	\$61.83
Total Cost (\$/system)	\$163.19	\$158.59	\$154.32	\$153.01
Total Cost (\$/kW_{net})	\$1.02	\$0.99	\$0.96	\$0.96

14.2.2.2 Demister

Annual Production Rate	200	400	800	1,000
Manufacture or Job Shop	Job Shop	Job Shop	Job Shop	Job Shop
Job Shop Line Utilization (%)	37%	37%	37%	37%
Job Shop Total Machine Rate (\$/min)	\$3.12	\$3.12	\$3.12	\$3.12
Manufactured Line Utilization (%)	0%	0%	0%	0%
Manufactured Total Machine Rate (\$/min)	\$829.12	\$712.82	\$556.71	\$501.79
Line Utilization Used (%)	37%	37%	37%	37%
Total Machine Rate Used (\$/min)	\$3.12	\$3.12	\$3.12	\$3.12

Annual Production Rate	200	400	800	1,000
Material (\$/system)	\$42.96	\$40.69	\$38.42	\$37.69
Manufacturing (\$/system)	\$2.24	\$1.30	\$0.83	\$0.74
Tooling (\$/system)	\$30.06	\$15.03	\$7.52	\$6.01
Markup (\$/system)	\$30.38	\$22.41	\$17.89	\$16.85
Total Cost (\$/system)	\$105.64	\$79.43	\$64.66	\$61.30
Total Cost (\$/kW_{net})	\$0.66	\$0.50	\$0.40	\$0.38

14.2.2.3 Membrane Humidifier

14.2.2.3.1 Membrane Humidifier Manufacturing Process

Station 1: Fabrication of Composite Humidifier Membranes

Annual Production Rate	200	400	800	1,000
Manufacture or Job Shop	Job Shop	Job Shop	Job Shop	Job Shop
Job Shop Line Utilization (%)	37%	37%	37%	37%
Job Shop Total Machine Rate (\$/min)	\$24.79	\$24.44	\$24.04	\$23.90
Manufactured Line Utilization (%)	0.1%	0.2%	0.3%	0.4%
Manufactured Total Machine Rate (\$/min)	\$5,760.29	\$3,218.17	\$1,728.52	\$1,407.69
Line Utilization Used (%)	37.1%	37.2%	37.3%	37.4%
Total Machine Rate Used (\$/min)	\$24.79	\$24.44	\$24.04	\$23.90

Annual Production Rate	200	400	800	1,000
Material (\$/stack)	\$317.44	\$288.75	\$261.51	\$253.03
Manufacturing (\$/stack)	\$131.49	\$75.76	\$47.50	\$41.74
Tooling (\$/stack)	\$0.50	\$0.50	\$0.50	\$0.50
Markup (\$/stack)	\$177.94	\$139.71	\$114.39	\$107.88
Total Cost (\$/stack)	\$627.36	\$504.72	\$423.89	\$403.14
Total Cost (\$/kWnet)	\$3.92	\$3.15	\$2.65	\$2.52

Station 2: Fabrication of Etched Stainless Steel Flow Fields

Annual Production Rate	200	400	800	1,000
Manufacture or Job Shop	Job Shop	Job Shop	Job Shop	Job Shop
Job Shop Line Utilization (%)	38%	38%	40%	40%
Job Shop Total Machine Rate (\$/min)	\$7.99	\$7.88	\$7.66	\$7.56
Manufactured Line Utilization (%)	1%	1%	3%	3%
Manufactured Total Machine Rate (\$/min)	\$295.41	\$149.69	\$76.82	\$62.65
Line Utilization Used (%)	38%	38%	40%	40%
Total Machine Rate Used (\$/min)	\$7.99	\$7.88	\$7.66	\$7.56

Annual Production Rate	200	400	800	1,000
Material (\$/stack)	\$47.15	\$47.15	\$47.15	\$47.15
Manufacturing (\$/stack)	\$55.13	\$54.33	\$52.82	\$51.78
Markup (\$/stack)	\$40.49	\$38.84	\$36.95	\$36.14
Total Cost (\$/stack)	\$142.77	\$140.32	\$136.92	\$135.07
Total Cost (\$/kWnet)	\$0.89	\$0.88	\$0.86	\$0.84

Station 3: Pouch Formation

Annual Production Rate	200	400	800	1,000
Manufacture or Job Shop	Job Shop	Job Shop	Job Shop	Job Shop
Job Shop Line Utilization (%)	37%	38%	38%	39%
Job Shop Total Machine Rate (\$/min)	\$3.25	\$3.22	\$3.16	\$3.13
Manufactured Line Utilization (%)	0%	1%	1%	2%
Manufactured Total Machine Rate (\$/min)	\$224.59	\$113.21	\$56.94	\$45.63
Line Utilization Used (%)	37%	38%	38%	39%
Total Machine Rate Used (\$/min)	\$3.25	\$3.22	\$3.16	\$3.13

Annual Production Rate	200	400	800	1,000
Material (\$/stack)	\$1.38	\$1.38	\$1.38	\$1.38
Manufacturing (\$/stack)	\$12.40	\$12.20	\$11.94	\$11.82
Tooling (\$/stack)	\$0.33	\$0.33	\$0.33	\$0.33
Markup (\$/stack)	\$5.59	\$5.32	\$5.04	\$4.95
Total Cost (\$/stack)	\$19.70	\$19.23	\$18.69	\$18.48
Total Cost (\$/kWnet)	\$0.12	\$0.12	\$0.12	\$0.12

Station 4: Stainless Steel Rib Formation

Annual Production Rate	200	400	800	1,000
Manufacture or Job Shop	Job Shop	Job Shop	Job Shop	Job Shop
Job Shop Line Utilization (%)	38%	39%	40%	41%
Job Shop Total Machine Rate (\$/min)	\$1.35	\$1.32	\$1.28	\$1.26
Manufactured Line Utilization (%)	1%	2%	3%	4%
Manufactured Total Machine Rate (\$/min)	\$37.65	\$19.02	\$9.64	\$7.76
Line Utilization Used (%)	38%	39%	40%	41%
Total Machine Rate Used (\$/min)	\$1.35	\$1.32	\$1.28	\$1.26

Annual Production Rate	200	400	800	1,000
Material (\$/stack)	\$3.71	\$3.71	\$3.71	\$3.71
Manufacturing (\$/stack)	\$11.26	\$11.02	\$10.63	\$10.46
Tooling (\$/stack)	\$12.00	\$12.00	\$11.50	\$11.60
Markup (\$/system)	\$10.68	\$10.23	\$9.55	\$9.42
Total Cost (\$/stack)	\$37.65	\$36.96	\$35.40	\$35.19
Total Cost (\$/kWnet)	\$0.24	\$0.23	\$0.22	\$0.22

Station 5: Stack Formation

Annual Production Rate	200	400	800	1,000
Manufacture or Job Shop	Job Shop	Job Shop	Job Shop	Job Shop
Job Shop Line Utilization (%)	41%	44%	52%	56%
Job Shop Total Machine Rate (\$/min)	\$1.50	\$1.40	\$1.24	\$1.17
Manufactured Line Utilization (%)	4%	7%	15%	19%
Manufactured Total Machine Rate (\$/min)	\$10.44	\$5.33	\$2.78	\$2.26
Line Utilization Used (%)	41%	44%	52%	56%
Total Machine Rate Used (\$/min)	\$1.50	\$1.40	\$1.24	\$1.17

Annual Production Rate	200	400	800	1,000
Material (\$/stack)	\$13.54	\$13.54	\$13.54	\$13.54
Manufacturing (\$/stack)	\$56.24	\$52.43	\$46.44	\$44.05
Markup (\$/system)	\$27.63	\$25.25	\$22.17	\$21.04
Total Cost (\$/stack)	\$97.40	\$91.21	\$82.15	\$78.63
Total Cost (\$/kWnet)	\$0.61	\$0.57	\$0.51	\$0.49

Station 6: Formation of the Housing

Annual Production Rate	200	400	800	1,000
Material (\$/stack)	\$12.75	\$12.75	\$12.75	\$12.75
Manufacturing (\$/stack)	\$48.10	\$27.75	\$17.40	\$15.30
Tooling (\$/stack)	\$97.32	\$56.24	\$32.51	\$27.25
Markup (\$/system)	\$62.62	\$37.03	\$23.16	\$20.20
Total Cost (\$/stack)	\$220.79	\$133.78	\$85.82	\$75.50
Total Cost (\$/kWnet)	\$1.38	\$0.84	\$0.54	\$0.47

Station 7: Assembly of the Composite Membrane and Flow Fields into the Housing

Annual Production Rate	200	400	800	1,000
Manufacture or Job Shop	Job Shop	Job Shop	Job Shop	Job Shop
Job Shop Line Utilization (%)	37%	37%	38%	38%
Job Shop Total Machine Rate (\$/min)	\$1.24	\$1.24	\$1.24	\$1.24
Manufactured Line Utilization (%)	0%	0%	1%	1%
Manufactured Total Machine Rate (\$/min)	\$32.68	\$16.73	\$8.76	\$7.16
Line Utilization Used (%)	37%	37%	38%	38%
Total Machine Rate Used (\$/min)	\$1.24	\$1.24	\$1.24	\$1.24

Annual Production Rate	200	400	800	1,000
Manufacturing (\$/stack)	\$2.48	\$2.48	\$2.48	\$2.48
Markup (\$/system)	\$0.98	\$0.95	\$0.92	\$0.90
Total Cost (\$/stack)	\$3.47	\$3.43	\$3.39	\$3.38
Total Cost (\$/kWnet)	\$0.02	\$0.02	\$0.02	\$0.02

Station 8: Humidifier System Testing

Annual Production Rate	200	400	800	1,000
Manufacture or Job Shop	Job Shop	Job Shop	Job Shop	Job Shop
Job Shop Line Utilization (%)	37%	38%	38%	38%
Job Shop Total Machine Rate (\$/min)	\$1.17	\$1.17	\$1.17	\$1.17
Manufactured Line Utilization (%)	0%	1%	1%	1%
Manufactured Total Machine Rate (\$/min)	\$19.36	\$10.06	\$5.41	\$4.48
Line Utilization Used (%)	37%	38%	38%	38%
Total Machine Rate Used (\$/min)	\$1.17	\$1.17	\$1.17	\$1.17

Annual Production Rate	200	400	800	1,000
Manufacturing (\$/stack)	\$1.63	\$1.63	\$1.62	\$1.62
Markup (\$/system)	\$0.65	\$0.62	\$0.60	\$0.59
Total Cost (\$/stack)	\$2.28	\$2.25	\$2.23	\$2.22
Total Cost (\$/kWnet)	\$0.03	\$0.03	\$0.03	\$0.03

14.2.2.3.2 Combined Cost Results for Plate Frame Membrane Humidifier

Annual Production Rate	200	400	800	1,000
Material (\$/stack)	\$395.96	\$367.28	\$340.04	\$331.56
Manufacturings (\$/stack)	\$318.72	\$237.60	\$190.84	\$179.25
Tooling (\$/stack)	\$110.15	\$69.07	\$44.84	\$39.68
Markup (\$/stack)	\$326.58	\$257.96	\$212.78	\$201.12
Total Cost (\$/stack)	\$1,151.41	\$931.92	\$788.49	\$751.61
Total Cost (\$/kWnet)	\$7.20	\$5.82	\$4.93	\$4.70

14.2.3 Coolant Loops

14.2.3.1 High-Temperature Coolant Loop

Annual Production Rate	200	400	800	1,000
Coolant Reservoir (\$/system)	\$15.96	\$15.80	\$15.64	\$15.59
Coolant Pump (\$/system)	\$140.66	\$138.55	\$136.48	\$135.81
Coolant DI Filter (\$/system)	\$174.19	\$167.22	\$160.53	\$158.43
Thermostat & Valve (\$/system)	\$20.43	\$20.22	\$20.02	\$19.96
Radiator (\$/system)	\$646.25	\$629.48	\$612.71	\$607.31
Radiator Fan (\$/system)	\$133.63	\$131.62	\$129.65	\$129.02
Coolant Piping (\$/system)	\$109.12	\$107.09	\$105.07	\$104.41
Markup (\$/system)	\$500.72	\$475.48	\$451.36	\$443.83
Total Cost (\$/system)	\$1,740.96	\$1,685.47	\$1,631.45	\$1,614.36
Total Cost (\$/kW_{net})	\$10.88	\$10.53	\$10.20	\$10.09

14.2.3.2 Low-Temperature Coolant Loop

Annual Production Rate	200	400	800	1,000
Coolant Reservoir (\$/system)	\$2.06	\$2.04	\$2.02	\$2.01
Coolant Pump (\$/system)	\$35.95	\$35.41	\$34.88	\$34.71
Thermostat & Valve (\$/system)	\$8.23	\$8.15	\$8.06	\$8.04
Radiator (\$/system)	\$90.46	\$88.12	\$85.77	\$85.01
Radiator Fan (\$/system)	\$0.00	\$0.00	\$0.00	\$0.00
Coolant Piping (\$/system)	\$15.28	\$14.99	\$14.71	\$14.62
Markup (\$/system)	\$61.36	\$58.44	\$55.63	\$54.75
Total Cost (\$/system)	\$213.34	\$207.14	\$201.07	\$199.14
Total Cost (\$/kW_{net})	\$1.33	\$1.29	\$1.26	\$1.24

14.2.4 Fuel Loop

Annual Production Rate	200	400	800	1,000
Inline Filter for GPE (\$/system)	\$33.39	\$32.45	\$31.57	\$31.31
Flow Diverter Valve (\$/system)	\$31.26	\$31.26	\$31.26	\$31.26
Over-Pressure Cut-Off Valve (\$/system)	\$53.73	\$51.58	\$49.52	\$48.87
Hydrogen High-Flow Ejector (\$/system)	\$118.20	\$110.50	\$102.94	\$100.54
Hydrogen Low-Flow Ejector (\$/system)	\$103.34	\$95.81	\$88.43	\$86.09
Check Valves (\$/system)	\$20.00	\$20.00	\$20.00	\$20.00
Purge Valves (\$/system)	\$170.89	\$164.06	\$157.49	\$155.44
Hydrogen Piping (\$/system)	\$185.95	\$182.94	\$179.93	\$178.96
Markup (\$/system)	\$289.38	\$270.59	\$252.88	\$247.39
Total Cost (\$/system)	\$1,006.14	\$959.18	\$914.02	\$899.86
Total Cost (\$/kW_{net})	\$6.29	\$5.99	\$5.71	\$5.62

14.2.5 System Controller

Annual Production Rate	200	400	800	1,000
System Controller	\$415.78	\$382.94	\$352.68	\$343.46
Markup (\$/system)	\$167.86	\$150.48	\$134.90	\$130.23
Total Cost (\$/system)	\$583.65	\$533.42	\$487.58	\$473.69
Total Cost (\$/kW_{net})	\$3.65	\$3.33	\$3.05	\$2.96

14.2.6 Sensors

Annual Production Rate	200	400	800	1,000
Current Sensors (\$/system)	\$40.00	\$40.00	\$40.00	\$40.00
Voltage Sensors (\$/system)	\$16.00	\$16.00	\$16.00	\$16.00
Hydrogen Sensors (\$/system)	\$3,181.77	\$2,926.84	\$2,671.91	\$2,589.84
Markup (\$/system)	\$1,307.19	\$1,172.14	\$1,043.38	\$1,003.22
Total Cost (\$/system)	\$4,544.95	\$4,154.98	\$3,771.28	\$3,649.06
Total Cost (\$/kW_{net})	\$28.41	\$25.97	\$23.57	\$22.81

14.2.6.1 Hydrogen Sensors

Annual Production Rate	200	400	800	1,000
Sensors per system	3	3	3	3
Sensor (\$)	\$1,060.59	\$975.61	\$890.64	\$863.28
Total Cost (\$/system)	\$3,181.77	\$2,926.84	\$2,671.91	\$2,589.84
Total Cost (\$/kW_{net})	\$19.89	\$18.29	\$16.70	\$16.19

14.2.7 Miscellaneous BOP

Annual Production Rate	200	400	800	1,000
Belly Pan (\$/system)	\$262.20	\$134.01	\$70.38	\$57.72
Mounting Frames (\$/system)	\$249.31	\$239.34	\$229.77	\$226.77
Wiring (\$/system)	\$237.13	\$232.06	\$226.99	\$225.36
Fasteners for Wiring & Piping (\$/system)	\$47.43	\$46.41	\$45.40	\$45.07
Markup (\$/system)	\$321.40	\$256.14	\$218.99	\$210.41
Total Cost (\$/system)	\$1,117.47	\$907.97	\$791.52	\$765.32
Total Cost (\$/kW_{net})	\$6.98	\$5.67	\$4.95	\$4.78

14.2.7.1 Belly Pan

Annual Production Rate	200	400	800	1,000
Manufacture or Job Shop	Job Shop	Job Shop	Job Shop	Job Shop
Job Shop Line Utilization (%)	37%	37%	37%	38%
Job Shop Total Machine Rate (\$/min)	\$1.42	\$1.41	\$1.41	\$1.41
Manufactured Line Utilization (%)	0.1%	0.2%	0.5%	0.6%
Manufactured Total Machine Rate (\$/min)	\$91.54	\$46.17	\$23.49	\$18.95
Line Utilization Used (%)	37.1%	37.2%	37.5%	37.6%
Total Machine Rate Used (\$/min)	\$1.42	\$1.41	\$1.41	\$1.41

14.2.7.2 Wiring

Annual Production Rate	200	400	800	1,000
Cables (\$/system)	\$78.60	\$76.92	\$75.24	\$74.70
Connectors (\$/System)	\$158.53	\$155.14	\$151.75	\$150.66
Total Cost (\$/system)	\$237.13	\$232.06	\$226.99	\$225.36
Total Cost (\$/kW_{net})	\$1.48	\$1.45	\$1.42	\$1.41

14.2.8 System Assembly

Annual Production Rate	200	400	800	1,000
Assembly Method	Assembly Line	Assembly Line	Assembly Line	Assembly Line
Index Time (min)	111.25	111.25	111.25	111.25
Capital Cost (\$/line)	\$50,000	\$50,000	\$50,000	\$50,000
Simultaneous Lines	1	1	1	1
Laborers per Line	12	12	12	12
Cost per Stack (\$)	\$231.90	\$169.28	\$137.44	\$130.86
Line Utilization Used (%)	1%	3%	6%	7%
Total Machine Rate Used (\$/min)	\$18.23	\$13.69	\$11.42	\$10.97

Annual Production Rate	200	400	800	1,000
System Assembly & Testing (\$/System)	\$259.15	\$194.65	\$162.41	\$155.96
Markup (\$/system)	\$204.66	\$143.91	\$112.46	\$105.76
Total Cost (\$/system)	\$463.81	\$338.56	\$274.87	\$261.72
Total Cost (\$/kWnet)	\$2.90	\$2.12	\$1.72	\$1.64